



**Escola Nacional
de Saúde Pública**

UNIVERSIDADE NOVA DE LISBOA

***In vitro* genotoxic and epigenotoxic effects of occupational
exposure to nanofibres**

Doctor of Philosophy in Public Health

Célia Cristina Barbosa Ventura

March, 2019



**Escola Nacional
de Saúde Pública**

UNIVERSIDADE NOVA DE LISBOA

***In vitro* genotoxic and epigenotoxic effects of occupational
exposure to nanofibres**

Thesis submitted in fulfilment of the requirements necessary for the degree of Doctor of
Philosophy in Public Health in the specialty of Environmental and Occupational Health,
under the supervision of:

António Neves Pires de Sousa Uva, MD, PhD

Full Professor, Head of the Department of Occupational and Environmental Health
National School of Public Health, NOVA University of Lisbon

Maria João Silva, PhD

Leader of the Genetic Toxicology Research Group
Department of Human Genetics
National Institute of Health Doutor Ricardo Jorge, Lisbon

March, 2019

Acknowledgments

I will always be grateful to José Rueff who started this adventure with his friendship, kindly support and motivation for changing my professional life.

My truthful thanks to Glória Isidro for being understanding and helping me with my need to change from work environment and routines, and to João Lavinha for receiving me in his research unit, gladdening and enriching my days.

My special gratitude to Maria João Silva who made me feel very welcome to her lab and gave me the support and wise advices needed to fulfil this work, and particularly for being an example of intelligence, constant energy and good mood.

My sincere thanks to António Sousa Uva for giving me the pleasure of being my supervisor, with friendship and care.

I must thank to Henriqueta Louro for being such a great colleague and a friend, and to all my other colleagues of the Department of Human Genetics that were always there to help me with all the things I needed. There is no space for so many names in this page, but they know they are in my heart.

My gratitude to my family, including my longing companion Sebastião, for their support during these years.

My devoted gratefulness to Luís for his constant motivation, endless love, dedication and patience throughout our truly happy life together.

Last, but not least, my apologies to my loves Ricardo e Gonçalo for the time they gave up of their mother to work and for my constant head in the clouds.

ABSTRACT

In recent years, human exposure to nanofibres (i.e., fibres with diameters < 100 nm) has considerably increased due to their incorporation in a wide range of consumer products. As such, there is a growing concern that the distinctive physicochemical characteristics of nanofibres may lead to adverse human health effects, mainly by their inhalation in occupational settings. Several toxicological studies have indicated that some nanofibres, such as the MWCNT-7, display *in vitro* toxicity and induce pulmonary inflammation, fibrosis, granulomas and carcinogenesis *in vivo*. Others, like cellulose nanofibrills (CNF), seem biocompatible and promising for biomedical applications. Thus, the genotoxic effects of nanofibres must be deeply studied to identify their possible hazard, and new “omics” methodologies can uncover their underlying mechanisms of action. Moreover, distinctive genomic or epigenomic expression profiles may be biomarkers of occupational exposure to nanofibres. In this work, the two above-mentioned nanofibres are analyzed *in vitro*, and the toxic effects of MWCNT-7 compared to those of crocidolite asbestos. Cytotoxicity and genotoxicity were investigated through conventional assays, and the differentially expressed microRNA (DE miRNA) in alveolar epithelial cells exposed to MWCNT-7 or crocidolite identified by next-generation sequencing. The overall results demonstrate that MWCNT-7 is cytotoxic, genotoxic and immunotoxic. Notably, it induced nucleoplasmic bridges in alveolar cells, possibly due to its resemblance with the microtubules and physical interference with the mitotic spindle. Different viabilities and micronucleus frequencies were observed in alveolar cells when using a conventional monoculture or a co-culture of these cells with macrophages, which may be related to their epithelial-mesenchymal transition and consequent increase of cell resistance to apoptosis. Regarding CNF, at low concentrations it stimulates cell proliferation, whereas at higher ones it is moderately toxic. Although no immunotoxicity and no significant DNA damage were detected, low CNF doses induced micronucleus. Concerning the epigenotoxic study, several DE miRNA were identified in alveolar cells exposed to MWCNT-7 or crocidolite, and a unique set was identified for each exposure. Both materials caused common changes in pathways related to cell metabolism, cell growth and death, cell-to-cell communication, protein processing, and signal transduction. Other functional pathways were distinctively identified for each material that suggest particular mechanisms of action. Since most are cancer related, a network of DE miRNA and target cancer genes was constructed, highlighting the carcinogenic potential of both materials.

Keywords: Occupational exposure, *in vitro* genotoxicity, carbon nanotubes, nanocellulose, miRNA expression.

RESUMO

Nos últimos anos, a exposição humana a nanofibras (i.e., fibras com diâmetros <100 nm) tem vindo a aumentar, devido à sua incorporação em vários produtos para consumo humano. Como tal, a preocupação de que as características singulares das nanofibras possam ter efeitos adversos na saúde humana tem-se intensificado, particularmente por inalação em contexto ocupacional. Diversos estudos toxicológicos indicam que certas nanofibras, como o MWCNT-7, têm toxicidade *in vitro* e induzem inflamação pulmonar, fibrose, granulomas e carcinogénese *in vivo*. Outras, como a celulose nanofibrilar (CNF), aparentam biocompatibilidade e são prometedoras para aplicações biomédicas. Desta forma, é essencial aprofundar o estudo sobre a sua genotoxicidade para conhecer a sua perigosidade. Neste contexto, as metodologias “ómicas” permitem compreender os mecanismos de ação das nanofibras e, além disso, os perfis genómicos ou epigenómicos podem ser úteis como biomarcadores de exposição ocupacional. Neste trabalho, as nanofibras acima citadas são analisadas *in vitro*, sendo o MWCNT-7 comparado à crocidolite (amianto). A citotoxicidade e genotoxicidade são analisadas pelos ensaios convencionais, sendo ainda identificados quais os microRNA diferencialmente expressos (miRNA DE) nas células alveolares expostas ao MWCNT-7 ou à crocidolite, por sequenciação de nova geração. Os resultados globais indicam que o MWCNT-7 é citotóxico, genotóxico e imunotóxico. De realçar a indução de pontes nucleoplásmicas nas células alveolares, provavelmente relacionadas com a semelhança do MWCNT-7 aos microtúbulos e interferência com o fuso mitótico. A diferente viabilidade e frequência de micronúcleos nas células alveolares em monocultura ou co-cultura com macrófagos pode estar relacionada com a sua transição epitelial-mesenquimal e aumento da resistência à apoptose. Quanto à CNF, observou-se proliferação celular nas doses baixas e citotoxicidade moderada nas doses mais elevadas. Embora não se tenham detetado danos significativos no DNA ou imunotoxicidade, foram induzidos micronúcleos nas doses baixas. No que respeita ao estudo de epigenotoxicidade, foi identificado um conjunto único de miRNA DE nas células expostas ao MWCNT-7 ou à crocidolite. Ambos os materiais causaram as mesmas alterações em vias de metabolismo celular, crescimento e morte celular, comunicação célula-a-célula, processamento proteico e transdução de sinal. Outras vias distintamente alteradas sugerem mecanismos de acção específicos. Uma vez que a maioria está associada a cancro, foi construída uma rede entre miRNAs DE e genes alvo associados a cancro que realça o potencial carcinogénico de ambos os materiais.

Palavras-chave: Exposição ocupacional, genotoxicidade *in vitro*, nanotubos de carbono, nanocelulose, expressão de miRNAs.

Table of contents

Acknowledgments.....	iii
Abstract.....	v
Resumo.....	vii
List of abbreviations and acronyms.....	xi
1. Background	13
1.1. Occupational exposure to nanomaterials.....	15
1.1.1 Carbon nanotubes and cellulose nanofibrils	17
1.1.2. Biomarkers of exposure to nanofibres.....	20
1.2. Assessment of nanofibres toxicity	21
1.3. Research objectives	23
1.4. Experimental approach used in this research	24
1.4.1. Implementation of a co-culture cell model.....	25
1.4.2. Nanofibres and crocidolite characterization.....	26
1.4.3. Cytotoxicity and genotoxicity assessment.....	26
1.4.4. Next-generation sequencing of microRNAs.....	28
1.4.5. Differentially expressed microRNAs and functional pathway analysis..	28
1.4.6. Network of differentially expressed miRNA and target cancer genes...	30
14.7. References.....	30
2. Conventional and novel "omics"-based approaches to the study of carbon nanotubes pulmonary toxicity.....	37
3. Evaluating the genotoxicity of cellulose nanofibrils in a co-culture of human lung epithelial cells and monocyte-derived macrophages.	69
4. Cytotoxicity and genotoxicity of MWCNT-7 and crocidolite: assessment in alveolar epithelial cells versus their co-culture with monocyte-derived macrophages	83
5. Functional effects of differentially expressed microRNAs in alveolar epithelial cells exposed to MWCNT-7 or crocidolite.....	115
6. Final Conclusions	147
7. Future Perspectives.....	151

List of abbreviations and acronyms

AFM	atomic force microscopy	MWCNT	multi-walled carbon nanotube
AMPK	AMP-activated protein kinase	NGS	next-generation sequencing
ANOVA	analysis of variance	NIOSH	National Institute for Occupational Safety and Health
APF	assigned protection factor	NM	nanomaterial
ATCC	American Type Culture Collection	nm	nanometer
CBMN	cytokinesis-block micronucleus	NSCLC	non-small-cell lung cancer
CNF	cellulose nanofibrils	OEL	occupational exposure limits
CNT	carbon nanotube	OSHA	Occupational Safety and Health Administration
DAPI	4',6-diamidino-2-phenylindole	PBS	phosphate buffered saline
DE miRNA	differentially-expressed miRNA	PCNA	proliferating cell nuclear antigen
DLS	dynamic light scattering	PI3K/Akt	phosphatidylinositol 3-kinase/serine-threonine kinase
DNA	deoxyribonucleic acid	qPCR	quantitative polymerase chain reaction
DP	degree of polymerization	REL	recommended exposure limit
DS	degree of substitution	RI	replication index
ECM	extracellular matrix	RNA	ribonucleic acid
EGFR	epidermal growth factor receptor	ROS	reactive oxygen species
EMS	ethyl methanesulphonate	RT	reverse transcription
EMT	epithelial-mesenchymal transition	SE	standard deviation
FBS	foetal bovine serum	SWCNT	single-walled carbon nanotube
FDR	false discovery rate	TEMPO	2,2,6,6-tetramethylpiperidine-1-oxyl radical
FE-SEM	field emission-scanning electron microscopy	TGF-β1	transforming growth factor beta 1
FISH	fluorescence in situ hybridisation	TLR	Toll-like receptor
FoxO	forkhead box O	TNF-α	tumour necrosis factor α
FpG	formamidopyrimidine DNA glycosylase	TPA	12-O-tetradecanoylphorbol-13-acetate
GO	gene ontology	TWA	time-weighted average
IARC	International Agency for Research on Cancer	UICC	Union for International Cancer Control
IL-1β	interleukin 1 β	UTR	untranslated region
IL-6	interleukin 6	WHO	World Health Organization
IRSST	Institut de Recherche Robert-Sauvé en Santé et en Sécurité du Travail		
ISO	International Standardization Organization		
KEGG	Kyoto Encyclopedia of Genes and Genomes		
KL-6	Krebs von den Lungen-6		
LDH	lactate dehydrogenase		
LPS	lipopolysaccharide		
miRNA	microRNA		
MMC	mitomycin		
MN	micronuclei		
MNBC	micronucleated binucleated cells		
mRNA	messenger RNA		
mTOR	the mammalian target of rapamycin		
MTT	3-(4,5-dimethylthiazol-2-yl)-2,5-diphenyltetrazolium bromide		

1. Background

1.1. Occupational exposure to nanomaterials

Worker safety and health is a cornerstone of an emergent technology responsible development, because workers are the first population group likely to be exposed to the products of that technology and the workplace offers the first opportunity to develop and implement responsible practices¹. Already in 2015, the *Institut de Recherche Robert-Sauvé en Santé et en Sécurité du Travail* (IRSST) of Québec has estimated that about 10% of manufacturing jobs worldwide were associated with nanotechnologies, and more than 2.000 commercial products contained nanomaterials (NM)².

Nanotechnology is a fast-evolving multidisciplinary field that comprises the production of materials in the nanoscale, i.e., with a size range from approximately 1 to 100 nm³. Below 100 nm, the ratio between the particle surface area and its mass increases exponentially, exerting a strong reactive effect on the adjacent materials⁴. Nanotechnology has been producing different types of manufactured NM that hold unique interesting electrical, mechanical and thermal properties for applications in science, technology, medicine and industry. These include carbon-based NM (e.g., fullerenes and carbon nanotubes), metal NM (e.g., Au), oxide NM (e.g., TiO₂), organic NM (e.g., dendrimers), among others. NM can be grouped according to their external dimensions (figure 1).

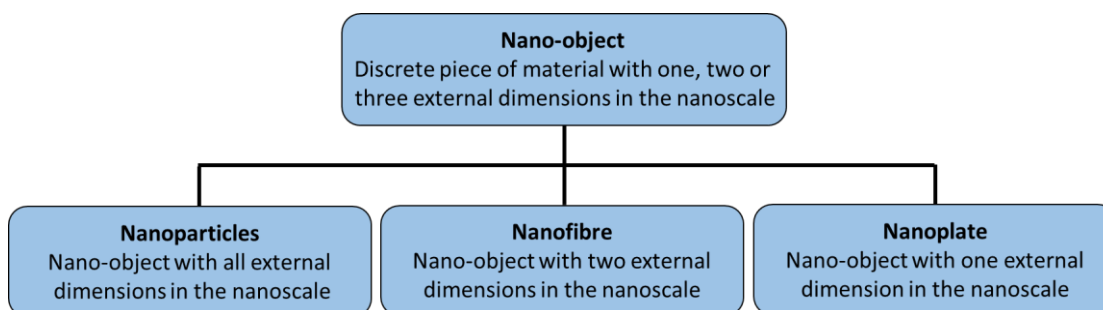


Figure 1. Hierarchy of terms related to nano-objects (from ISO/DRT12885:2017)

Occupational exposure to NM, during their production or incorporation into products, is more likely to happen when they are dispersed in the environment, particularly in the air or in liquid suspensions that may form aerosols, and, consequently, inhalation is the most probable route of exposure. In the workplace, this can happen during several stages: (i) production of solid NM in open or poorly sealed enclosures; (ii) handling of nanometric powders or liquid suspensions; (iii) packaging, storing or transport; (iv) incorporation into matrices; (v) mechanical work on products containing NMs; (vi) aerosol application; (vii) leaning of equipment, work areas and ventilation systems; (viii) repair and maintenance

of equipment; (ix) leaks, accidental spills, equipment malfunction, and (x) waste management².

Previous studies on human exposure to ultrafine aerosols, atmospheric pollution and manufactured mineral fibres have demonstrated the association between small-scale material exposure and respiratory disease^{5,6,7,8}. Concerning manufactured NM, several *in vitro* and *in vivo* toxicological studies have shown that the very same properties of NM that are intentionally exploited may have detrimental biological effects. These are associated with their physicochemical properties, including chemistry, size, shape, surface area, solubility, surface reactivity, charge, functional groups at the surface, crystalline structure, tendency to agglomerate and the presence of impurities⁹. One group of NM that has been a cause of concern about their potential hazard to human health is nanofibres, which refer to nano-objects with two similar dimensions in the nanoscale and the third dimension significantly larger³.

The IRSST has published a best practices guide for handling NM, recommending a preventive approach designed to minimize occupational exposure on a case-by-case basis, taking into account the risk assessment of each workstation². The recommended measures for preventing workplace exposure to nanofibres are listed in table I.

Table I. Summary of the measurement operations and recommendations for fibrous nanoparticles of the Institut de Recherche Robert-Sauvé en Santé et en Sécurité du Travail (IRSST).

NM type	Type of Enterprise	Potential Exposure	Airborne particle size (nm)	Controls	Specific recommendations based on emission readings at workstations
Nano cellulose	Research/ Production	Grinding Production Sieving Cleaning	[5–40]	Fume hood	Capture NMs at source Repair and maintain general ventilation Follow recommendations for fume hood use Modify work practices Set up a respiratory protection program
Single-walled carbon nanotubes	Producer	Collection Cleaning	[200–10,000]	Fume hood Contained production room Locker room adjoining work area Respiratory protection (APF=100)	Follow recommendations for fume hood use Revise respiratory protection program and Conduct airtightness tests
Multiwalled carbon nanotubes	Research/ Integration	Homogenization Thermal analysis Milling	[24–500]	Glove box Respiratory protection (APF=10)	Change gloves in glove box Do the homogenization under a fume hood Modify polishing and sawing practices Maintain respiratory protection program
Carbon nanofibres	Research/ Integration	Collection Cleaning	[100–400]	Contained area Double locker room adjoining work area Fume hood General ventilation (20 air changes/h) Respiratory protection (APF=25-1,000)	Follow recommendations for fume hood use Modify locker room exit sequence Maintain respiratory protection program

APF: assigned protection factor.

1.1.1. Carbon nanotubes and cellulose nanofibrils

Carbon nanotubes (CNT) are one of the most promising and widespread class of NM. CNT consist of graphite sheets with a cylindrical arrangement, displaying various lengths, and a diameter within the nanoscale. They can have a single wall (SWCNT) or multiple walls (MWCNT) assembled in concentric layers, and can be functionalized by the introduction of specific elements, other than carbon, on the pristine CNT (figure 2).

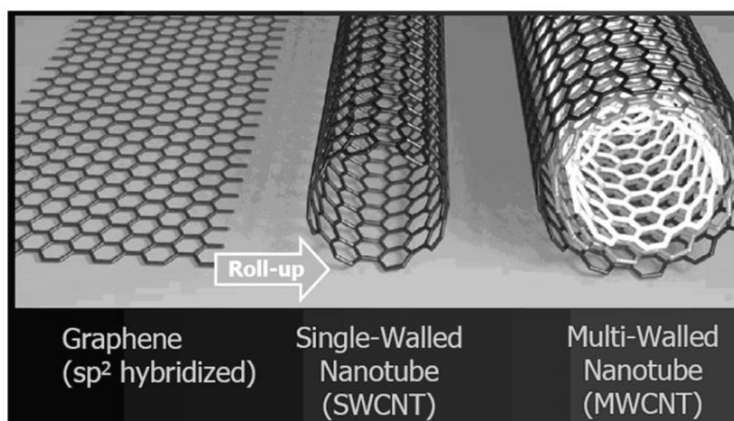


Figure 2. A scheme showing how graphene could be ideally rolled-up to form single- or multi-walled carbon nanotubes¹⁰.

Only in relation to SWCNTs, more than 50,000 potential combinations existed in 2012, depending on structural types, length, manufacturing and purification processes, and surface coatings¹¹. According to the ISO/TS 80004-4:2011, CNTs are hollow nanofibres, although the National Institute for Occupational Safety and Health (NIOSH) distinguishes between a carbon nanofibre and a CNT depending on the graphene plane alignment (if the graphene plane and fibre axis do not align the structure is defined as carbon nanofibre; when they are parallel, it is a CNT).

CNT display unique physicochemical properties: they are mechanically strong, flexible, lightweight, heat resistant, and have high electrical conductivity. Currently, they have several industrial and biomedical applications, including electronics, lithium-ion batteries, solar cells, super capacitors, thermoplastics, polymer composites, coatings, adhesives, biosensors, enhanced electron-scanning microscopy imaging techniques, inks, as well as in pharmaceutical/biomedical devices for bone grafting, tissue repair, drug delivery, and medical diagnostics¹ (figure 3).

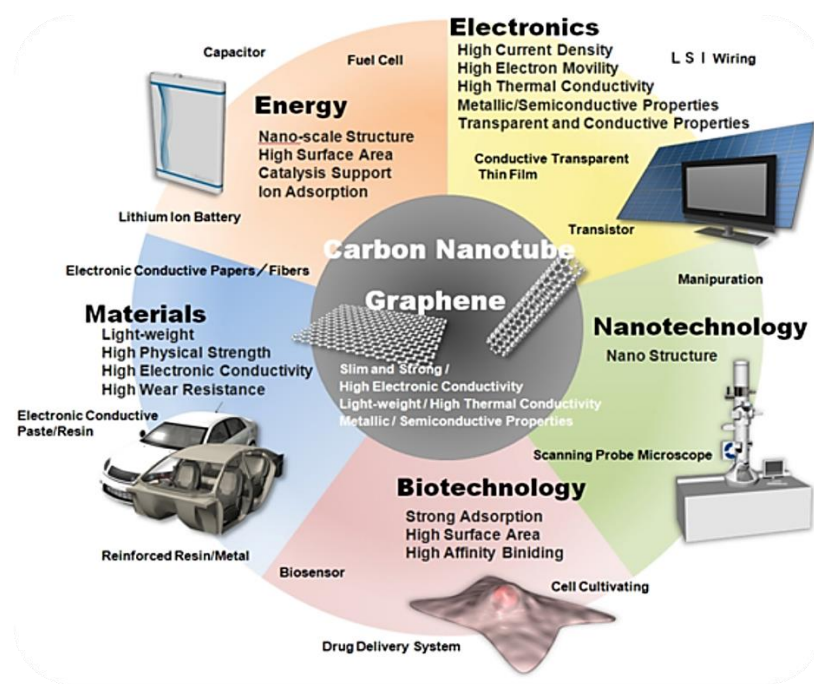


Figure 3. Carbon nanotubes applications (available at <http://www.meijo-nano.com/en/applications/use.html>).

The highest release of CNT has been detected during their production and handling, and cleaning of the production reactors, and ranged from 0.68 to 38 $\mu\text{g}/\text{m}^3$ in the personal breathing zone of workers that performed key work operations and procedures in 11 on-site exposure studies in different workplaces¹². To date, several professional and scientific organizations assumed a precautionary approach and agreed in that there is sufficient information for CNT to be regarded as an occupational hazard¹³. NIOSH set a recommended exposure limit (REL) of 1 $\mu\text{g}/\text{m}^3$ elemental carbon as a respirable mass 8-hour time-weighted average (TWA) concentration¹, even if this limit seems lower than some values that have been measured on-site¹².

Another emergent-engineered nanofibre is nanocellulose. Nanocellulose exhibits unique characteristics that include high tensile strength and stiffness, besides being renewable and biodegradable in nature^{14,15,16}. Nanocelluloses can be divided in different categories, according to the source, methodology and final characteristics. These are bacterial nanocellulose, nanocrystalline cellulose - also known as cellulose nanocrystals or nanowhiskers - and cellulose nanofibrils (CNF) - also referred to as cellulose nanofibres or nanofibrillated cellulose. CNF are usually obtained from wood, cotton, hemp, flax, sugar beet or potato tuber. Depending on the source and on the production method, the size of the fibrils can vary significantly, but usually nanofibrils are defined as materials with diameters inferior to 100 nm and lengths in the micrometre scale (TAPPI standard

proposal WI3021)^{17,18}. CNF have exceptional high mechanical resistance and low density, being a prime candidate for strength-enhancement of the mechanical properties of other composite materials, such as paper, carton and packaging materials. They also have a wide array of applications in the form of gels or emulsions, e.g., as a rheology modifier. Due to its likely biocompatibility, CNF have been investigated in regenerative medicine as scaffolds for tissue-engineered meniscus, blood vessels, ligaments or tendons^{19,20,21,22}. Other biomedical applications of CNF are on wound healing^{23,24,25,26,27}, stem cell decorated threads for surgical suturing²⁸, haemodialysis membranes²⁹, long-lasting sustained drug delivery systems³⁰ or 3D cell culture scaffolds^{31,32,33} (figure 4).



Figure 4. Nanocellulose potential applications (available at https://www.researchgate.net/publication/313618565_Cellulosic_Biocomposites_Potential_Materials_for_Future).

Currently, there are no occupational exposure limits (OEL) or recommended exposure limits (REL) for nanocellulose. The NIOSH REL for bulk cellulose particles is 10 mg/m³ for total dust and 5 mg/m³ as a respirable fraction, both expressed as a TWA. The Occupational Safety and Health Administration (OSHA) permissible exposure limits are 15 mg/m³ and 5 mg/m³, both as TWA. However, based on previous knowledge about the adverse effects of other nanofibres, e.g., CNT, it is expected that the high aspect ratio of CNF and its biodurability in the human lungs³⁴ increases its toxicity compared to that of bulk cellulose.

A study by Vartiainen et al. (2011) concluded that workers' exposure to particles in the air during grinding and spray drying of birch cellulose was low or non-existent with the implementation of appropriate protection equipment and proper handling³⁵. The NIOSH in partnership with the Forest Products Laboratory conducted two exposure characterization studies to evaluate the potential for occupational exposure to cellulose nanocrystals and CNF. The results indicated that nanocellulose is aerosolized during centrifugation, handling of dry product, and production and manipulation of nanocellulose polymer composites, but none of these measures exceeded the applicable OEL for cellulose^{36,37}.

1.1.2. Biomarkers of exposure to nanofibres

Biological monitoring assesses human exposure to occupational hazardous substances through biomarkers. A biomarker is a chemical, its metabolite, or the product of an interaction between a chemical and some target molecule or cell that is measured in the human body³⁸. In addition to exposure biomarkers, the consequent biological effects and the individual susceptibility to the risk factor are characterized by biomarkers of early biological effect and biomarkers of susceptibility, respectively³⁹. At present, biomarkers suitable for routine biomonitoring of occupational exposure to nanofibres are not available, representing a challenging task of extreme importance in occupational health research. The evaluation of early biological effects associated to human exposure to NM has been based on the evaluation of oxidative stress markers, antioxidant enzyme activity, expression of acute phase proteins or alterations in the distribution of lymphocyte subclasses⁴⁰. These effect biomarkers, although highly sensitive, are influenced by other non-occupational factors and are not specific for NM-induced damage, although their validity may improve through their combined use⁴¹.

According to a 2013 NIOSH guideline, the health surveillance and medical monitoring of workers exposed to CNT should include: i) a nonspecific initial evaluation of the medical and occupational history of the worker, with emphasis on the respiratory system (including the use of a standardized questionnaire for respiratory symptoms); ii) a physical examination that may include spirometry testing and iii) a baseline chest X-ray, and iv) other tests deemed appropriate for each case. Then, an annual update of the occupational and medical history, and a spirometry test at least every 3 years should be performed¹. These are useful medical procedures to detect illness, but it would be more valuable to detect early adverse effects before they are noticeable, in order to prevent further exposure and the clinical manifestation of disease.

One of the few published studies on workers exposed to MWCNT described a significant increase in interleukin 1 β (IL-1 β), interleukin 6 (IL-6), tumour necrosis factor α (TNF- α), inflammatory cytokines, and Krebs von den Lungen-6 (KL-6), a serological biomarker for interstitial lung disease, in the sputum of these workers. Moreover, transforming growth factor beta 1 (TGF- β 1), a known regulator of fibrosis, was increased in the serum from the youngest exposed workers⁴². Besides providing possible biomarkers, this study confirmed the adverse health effects from human occupational exposure to MWCNT.

1.2. Assessment of nanofibres toxicity

Toxicological studies aim to predict the health effects caused by exposure to a given substance or agent, thus reducing the risk to humans associated with its hazard. *In vitro* toxicological studies are typically conducted prior to *in vivo* studies with the objective of evaluating if the tested compound interacts with the cellular components or its functions, leading to alteration or disruption of cellular homeostasis. *In vitro* conventional toxicological assays evaluate, among other endpoints, the substance effect on cell viability (cytotoxicity) leading to cell death through apoptosis or necrosis, and the direct or indirect damaging effects on DNA or chromosomes, such as gene mutations and chromosomal aberrations, respectively (genotoxicity) that can ultimately lead to carcinogenicity. To date, several *in vitro* and *in vivo* studies have characterized the toxic effects of CNT; a literature review is presented in Chapter 2, as well as the limitations of *in vitro* and *in vivo* studies to predict human adverse effects. On the contrary, few studies have assessed CNF toxicity, and they are summarised in Chapter 3, where the genotoxicity assessment of a CNF is reported.

Large-scale gene expression studies and epigenomic studies are increasingly being used in toxicology as a promising new area of research. Through the identification of the differentially expressed genes following exposure to a toxicant, a global overview of all molecular pathways that are modified in the cell, tissue or organism is achieved in a time- and dose-dependent manner. An example of the potential of these new approaches to generate more comprehensive data is presented in Chapter 2, where a functional pathway and gene ontology analysis were performed from transcriptomic data available in the literature.

Regarding epigenotoxicity, there is evidence that NM possibly cause epigenetic alterations^{43,44}, i.e., histone modifications, changes in DNA methylation and changes in microRNA (miRNA) expression (figure 5).

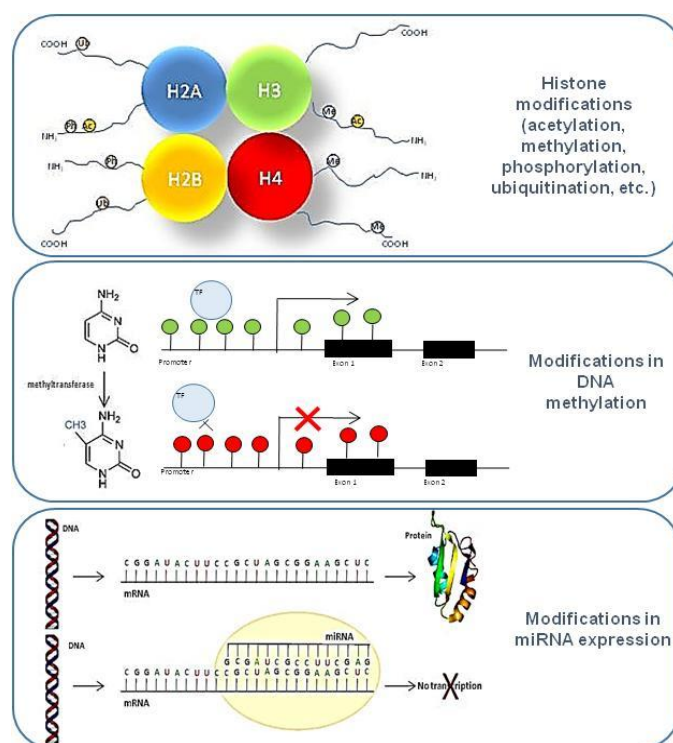


Figure 5. Different epigenetic mechanisms for regulating gene expression: histone tail modifications, changes in DNA methylation and different miRNA expression.

Concerning miRNAs, they are small non-coding RNAs involved in nearly all key biological processes⁴⁵, usually acting as endogenous repressors of gene activity via transcriptional repression and degradation of mRNA (figure 6). Lung has a specific miRNA expression profile, and several pulmonary diseases such as chronic obstructive pulmonary disease, asthma, cystic fibrosis, pulmonary hypertension and lung cancer have been associated with alterations in the expression of lung related miRNAs^{46,47,48}.

Moreover, miRNAs are highly sensitive, reproducible, specific and stable in serum⁴⁹ and its expression patterns have been successfully evaluated in a wide range of solid cancers as promising biomarkers of early disease onset or relapse⁵⁰. Differential expression of cell-free circulating miRNAs after exposure to a toxicant has been considered a promising area of research to identify biomarkers suitable for monitoring human exposure. For example, in mouse, serum miR-122 demonstrated a sensitivity at least as good as alanine aminotransferase and aspartate aminotransferase to predict liver adverse effects induced by silica⁵¹ and miR-103 has been suggested as a possible biomarker for mesothelioma using the cellular fraction of human peripheral blood⁵².

Chapter 2 presents an extensive review of the transcriptomic and epigenomic studies of CNT exposure, performed *in vitro* and in rodents. In addition, the results of the functional

analysis of differentially expressed miRNA in cells exposed to a MWCNT or crocidolite are displayed in chapter 4. As to CNF, no such studies were found in the literature.

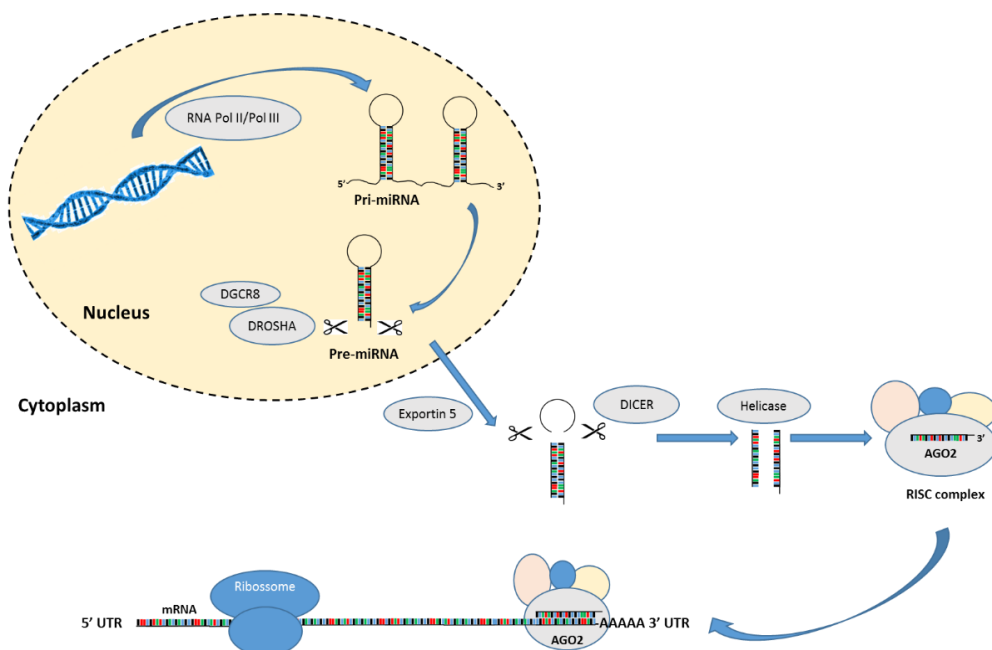


Figure 6. In the nucleus, DNA is transcribed by the RNA polymerase II (Pol II) or Pol III enzyme into the primary miRNA (pri-miRNA). The pri-miRNA transcript folds into a single or a cluster of multiple hairpin structures that are cleaved by the complex formed by the enzyme Drosha, a nuclear RNase III, and the RNA binding protein cofactor DGCR8 (also known as Pasha). This 60–70 nucleotides stem-loop structure, the precursor miRNA (pre-miRNA), is transported across the nuclear membrane by Exportin 5. In the cytoplasm, the hairpin loop of the pre-miRNA is cropped off by Dicer, a second RNase enzyme, leaving a miRNA duplex that is unwound by a helicase. This single-stranded miRNA is cleaved into a mature miRNA (18–25 nucleotides), and integrated into an RNA-induced silencing complex (RISC). RISC incorporates an Argonaute protein that cleaves the target mRNA strand in the 3' untranslated region (UTR) complementary to their bound miRNA, inhibiting protein translation or degrading the mRNA itself.

1.3. Research objectives

As the number of nanofibres produced and the spectrum of their application grow, also the number of workers exposed to nanofibers, e.g., the MWCNT-7, has been greatly increasing. Consequently, there is a huge demand for accurate and rapid testing of NM safety *in vitro*, in order to infer their potential impact on human health. For this purpose, it is not only important to deepen their *in vitro* toxicological characterization, but also to investigate the mechanisms behind their biological effects at molecular, cellular and organismal levels, particularly through the application of innovative high throughput methodologies. In view of the stated above, this research has two general aims: i) to contribute to the assessment of the potential impact of occupational exposure to nanofibres on the health of exposed workers, and ii) to discover new biomarkers of

exposure to MWCNT-7 and its early biological adverse effects, based on an epigenomic approach. To this end, the specific goals to be achieved are:

- i) Gathering background information about the CNT pulmonary toxicity and identify gaps in knowledge that need to be investigated, particularly, using new approaches;
- ii) Characterization of the *in vitro* pulmonary cytotoxicity and genotoxicity of MWCNT-7 comparatively to that of crocidolite, a well characterized asbestos fibre;
- iii) Characterization of the *in vitro* pulmonary cytotoxicity and genotoxicity of CNF;
- iv) Application of novel “omics” approaches to identify miRNAs that can represent possible biomarkers of respiratory exposure to MWCNT-7 and also the cellular pathways that are altered by the up- or down-regulation of their target genes, as compared to crocidolite.

1.4 Experimental approaches used in this research

To achieve the specific above-mentioned goals, the experimental design used in this research, which will be presented in the next chapters, is shown in figure 7.

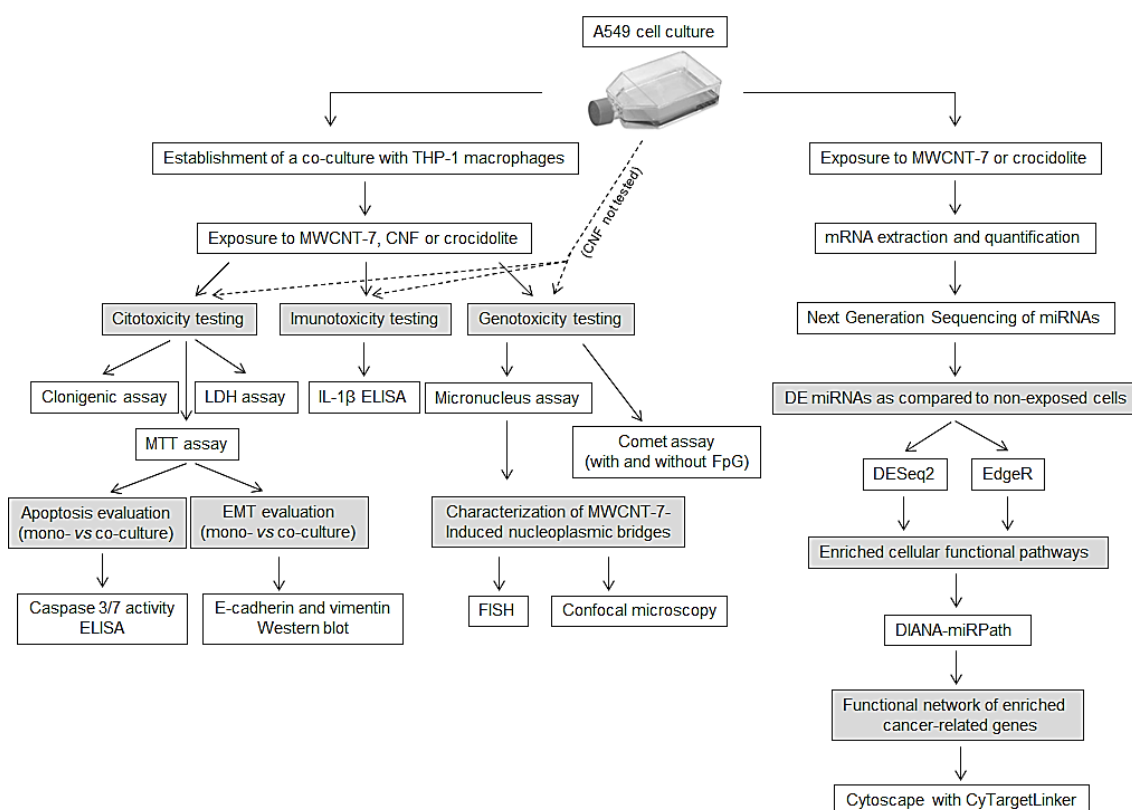


Figure 7. Schematic representation of the workflow developed in the following chapters of this thesis. DE - differentially expressed. White boxes represent the techniques used while grey boxes represent the objectives for their use.

1.4.1. Implementation of a co-culture cell model

A co-culture of alveolar epithelial cells (A549) and macrophages (THP-1) was implemented in an attempt to better mimic the human lung epithelium, as detailed in the “Materials and Methods” section of the following chapters 3 and 4.

The A549 cell line (ATCC, Manassas, VA, USA, CCL-185) is a human alveolar type II epithelial cell line derived from a human lung adenocarcinoma⁵³, and the human monocytic cell line THP-1 (ATCC, TIB-202) is derived from the blood of a boy with acute monocytic leukemia⁵⁴.

A first step to optimize the differentiation of monocytes to macrophages was to evaluate the 12-O-tetradecanoylphorbol-13-acetate (TPA) concentration that resulted in macrophages that better resembled the phenotype of human monocyte-derived macrophages. For this purpose, THP-1 cells were incubated with 10, 20, 50 and 100 ng/mL of TPA for 24 h and 48 h. Some of the macrophages features are: adherence to surfaces, altered morphology into flat and amoeboid cells with increased cytoplasmic volume, enhanced cytoplasmic granularity with well-developed Golgi apparatus, rough endoplasmic reticula and many ribosomes, and increased auto-fluorescence⁵⁵. Based on the cells adherence capacity and morphology (figure 8), the condition chosen consisted of a TPA concentration of 100 ng/mL during 48 h, followed by a resting period of 48 h in serum-free medium.

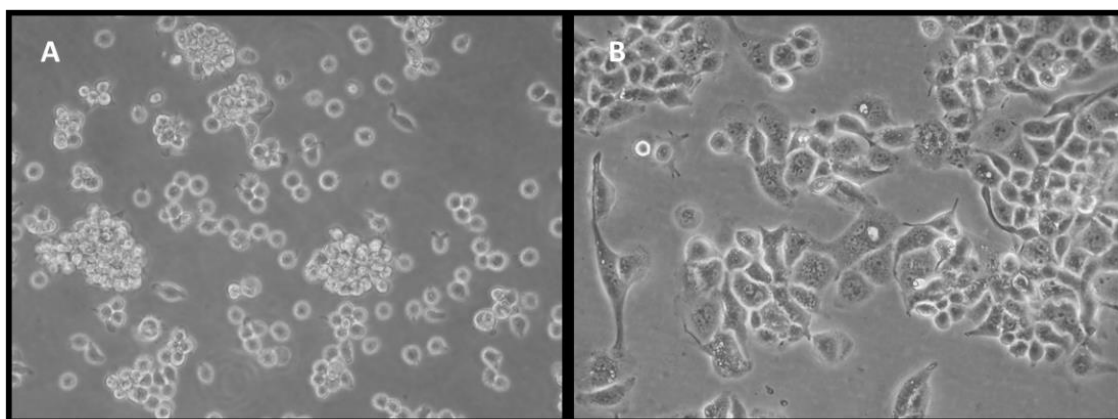


Figure 8. THP-1 cells after 48 h incubation in culture medium only (A) and supplemented with 100 ng/mL TPA (B), followed by a resting period of 48 h in serum-free medium without TPA.

To set up the co-culture, A549 cells were cultured on 12-well plates at a density of 0.5×10^5 cells/mL. THP-1 cells were cultured in transwell inserts with a nominal pore size of $0.4 \mu\text{m}$ at a density of 0.2×10^5 cells/mL and, following differentiation, they were placed

on top of the A549 cells. Both cultures were grown in RPMI 1640 medium supplemented with 10% heat-inactivated foetal bovine serum, 1% penicillin/ streptomycin and 1% fungizone at 37 °C in 5% CO₂. The resulting co-culture presented a proportion of one macrophage per five epithelial cells, which mimic the normal proportion of these cells in human lungs⁵⁶.

1.4.2. Nanofibres and crocidolite characterization

The MWCNT-7 (Mitsui-7) used in this work was provided as a sub-sample (NRCWE-006) by the National Research Centre for the Working and Environment (http://ihcp.jrc.ec.europa.eu/our_activities/nanotechnology/nanomaterials-repository/list_materials_JRC_rep_oct_2011.pdf) in the context of the European NANOGENOTOX project (www.nanogenotox.eu). Its physicochemical characteristics are listed in detail in table I, included in the Materials and Methods section of Chapter 4.

The cellulose nanofibrills were produced and characterized by the Department of Chemical Engineering of the University of Coimbra, and their physicochemical properties are described in Chapter 3.

The crocidolite standard reference material was obtained from the Union for International Cancer Control (UICC, Geneva, Switzerland) and was kindly provided by the Department of Environmental Health of the INSA. Their preparation and characterization was described in detail in several publications^{57,58,59,60}.

1.4.3. Cytotoxicity and genotoxicity assessment

Three different cytotoxicity assays were applied in this study, as shown in figure 7:

- The MTT assay, which is based on the ability of metabolically active viable cells to use NAD(P)H-dependent cellular oxidoreductase enzymes to reduce the tetrazolium dye MTT (3-(4,5-dimethylthiazol-2-yl)-2,5-diphenyltetrazolium bromide) to insoluble formazan. This is a purple coloured product whose absorbance is spectrophotometrically read at 570 nm, being its intensity directly related to the number of viable cells⁶¹;
- Determination of the lactate dehydrogenase (LDH), a cytosolic enzyme that is released into the culture medium from cells with a damage membrane (non-viable cells). The LDH released into the culture medium is measured with an enzymatic assay that converts resazurin into a fluorescent resorufin product. The amount of fluorescence produced is proportional to the number of lysed cells⁶².

- The clonogenic assay, also called colony forming efficiency, a cell-surviving assay that measures the retained ability of a single cell to form a large number of progeny after exposure to xenobiotics⁶³.

The evaluation of the genotoxicity of nanofibres and crocidolite was performed by the comet assay and its modified form, and the cytokinesis-block micronucleus (CBMN) assay:

- The comet assay allows the quantification of DNA single and double strand breaks and alkali-labile sites that, under alkaline electrophoresis conditions (pH > 13) of previously lysed cells that are embedded in low melting point agarose and spread on agarose-precoated microscope slides, migrate further towards the anode than the cell nucleoid, appearing as “comets” on a fluorescence microscope. Scoring of DNA damage is done by measuring the percentage of DNA in the tail of the nucleoids, previously stained with ethidium bromide⁶⁴.
- In the CBMN assay, micronuclei that remain in the cytoplasm of cytokinesis-blocked (binucleated) cells after mitosis are scored under bright field or fluorescence microscopy. Cytokinesis is blocked with cytochalasin-B, an inhibitor of microfilament ring assembly required for the completion of cytokinesis. Micronuclei originate from chromosome fragments or whole chromosomes that lag behind at anaphase during nuclear division, nucleoplasmic bridges correspond mainly to dicentric chromosomes resulting from telomere end-fusions or DNA misrepair, and nuclear buds are a biomarker of gene amplification⁶⁵. Afterwards, the cells can be scored for its viability status (necrosis, apoptosis), its mitotic status (mononucleated, binucleated, multinucleated) and its chromosomal damage or instability status (presence of micronuclei, nucleoplasmic bridges and nuclear buds).

Apoptosis was also analysed through the determination of caspase-3 and -7 activities, which are apoptotic executioner caspases (cysteine-aspartic acid-specific proteases), i.e., they are the final endonucleases of the caspase activation signalling cascade with the role of degrading cellular compounds to initiate apoptosis⁶⁶. Apo-ONE® Homogeneous Caspase-3/7 Assay Kit (Promega) was used, in which the caspase-3/7 substrate rhodamine 110, bis-(N-CBZ-Laspartyl-L-glutamyl-L-valyl-L-aspartic acid amide; Z-DEVD-R110) exists as a profluorescent substrate. Cells are lysed and upon sequential cleavage and removal of the DEVD peptides by caspase-3/7 activity and excitation at 499 nm, the rhodamine 110 leaving group becomes intensely fluorescent. The amount of fluorescent product generated is proportional to the amount of caspase-3/7 cleavage activity present in the sample.

Other complementary assays and methodologies were applied as necessary to elucidate the results obtained by the above-mentioned assays, e.g., fluorescence *in situ* hybridisation (FISH), confocal microscopy and western blotting. These techniques are described in chapter 4.

1.4.4. Next-generation sequencing of miRNA

The identification of the differently expressed miRNAs in the exposed A549 cells, as compared with non-exposed cells, was accomplished by next-generation sequencing (NGS), also called massively parallel or deep sequencing. NGS consist of a set of technologies that allow rapid sequencing of a large number of DNA segments simultaneously, including the entire human genome or exome, as opposed to the Sanger sequencing technique in which one fragment of DNA was sequenced at a time. In this work, Illumina NGS technology was applied (figure 9) to sequence all the miRNA of A549 cells expressed after exposed to Mitsui-7 or crocidolite during 24 h, and in the non exposed cell cultures performed simultaneously. Further analytical details can be found in Chapter 5.

1.4.5. Differentially expressed miRNAs and functional pathway analysis

NGS data analysis for identifying the differently expressed miRNA in the exposed alveolar cells, and the corresponding functional cellular pathways that are activated or repressed as a consequence of gene expression modifications, is a complex task that requires bioinformatics resources and skills. The bioinformatics analyses were performed in collaboration with the Technology and Innovation Unit of INSA.

Two different R software packages were used to identify the differently expressed miRNAs, in order to verify data concordance and obtain an improved consistency, namely DESeq2 v1.18.168⁶⁷ and RNASeqGUI v1.1.269⁶⁸. The latter was used for performing differential expression analysis with the EdgeR Exact Test⁷⁰. This methodology allowed the identification of unique differentially expressed miRNA profiles in alveolar epithelial cells exposed 24 h to MWCNT-7 or crocidolite. Further details are given in Chapter 5.

The over or under-expressed miRNAs were then used as input in DIANA-miRPath (<http://www.microrna.gr/miRPathv2>). This software performs an enrichment analysis of the predicted target genes of the multiple miRNAs and compares each set to the KEGG (Kyoto Encyclopedia of Genes and Genomes) pathways⁷⁰.

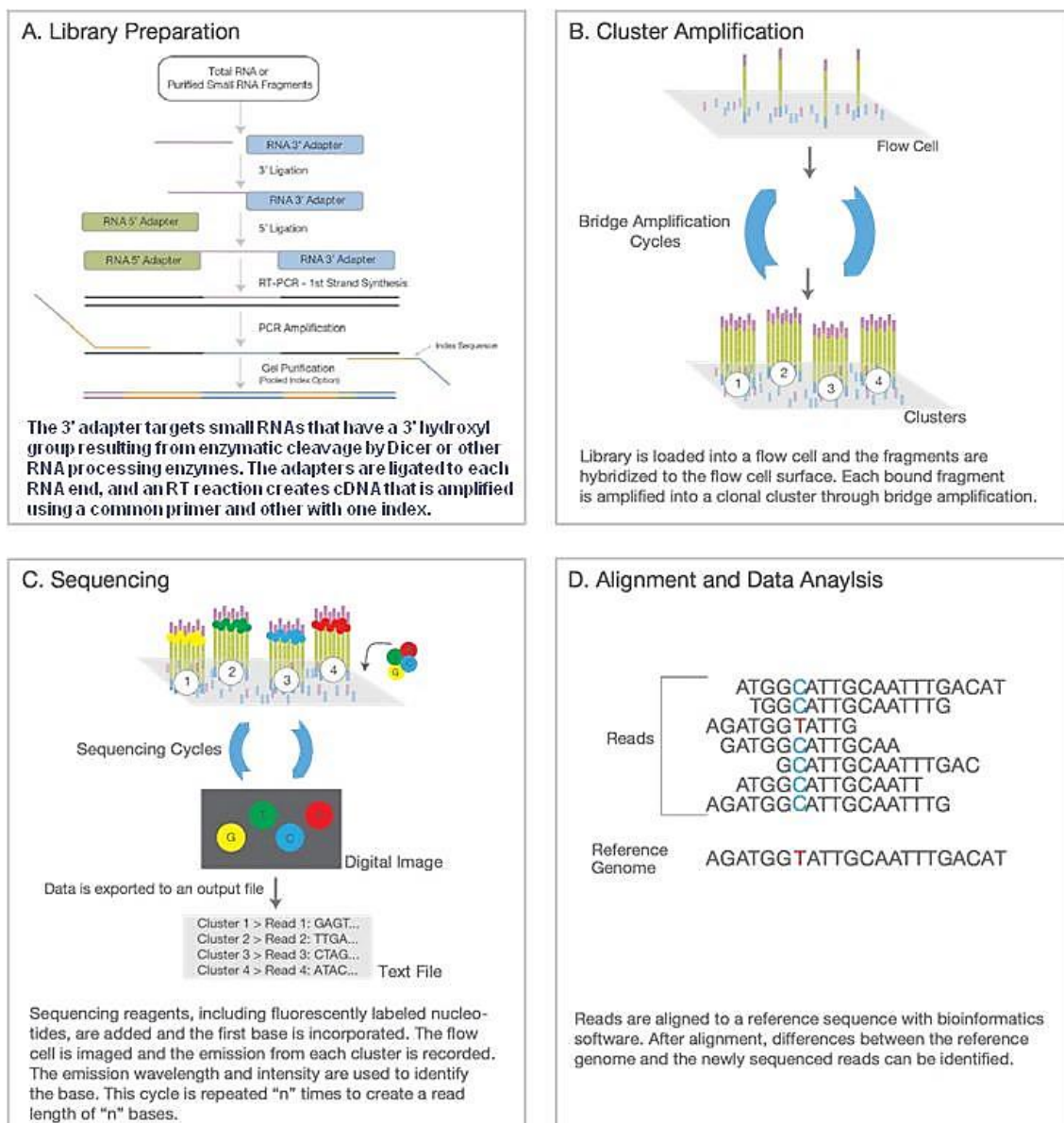


Figure 9. Summary of the four steps of Illumina next-generation sequencing of miRNA. Image adapted from "An introduction to Next-Generation Sequencing Technology" (available at https://www.illumina.com/documents/products/illumina_sequencing_introduction.pdf).

KEGG pathway (<https://www.genome.jp/kegg/>) is a database resource of pathway maps that represent the current knowledge on the molecular interaction, reaction and relation networks about metabolism, genetic information processing, environmental information processing, cellular processes, organismal systems, human diseases and drug development⁷¹.

In addition to investigating the KEGG pathways altered after exposure to MWCNT-7 and crocidolite, the potential gene targets of the differentially expressed miRNA were also

classified according to gene ontology (GO) terms, e.g., to concepts/classes that describe biological functions and their relationships to one another. This comprehensive computational model of biological systems concerning gene function (molecular function of the gene products, the cellular component where they are active, and the biological process made up of the activities of multiple gene products), is provided by the Gene Ontology Consortium (<http://www.geneontology.org/>)^{72, 73}.

1.4.6. Network of differentially expressed miRNAs and target cancer genes

Given the over-representation of functional pathways related to cancer in the above-mentioned cellular pathways affected by exposure to MWCNT-7 and crocidolite, a network analysis of the differentially expressed miRNAs and their target cancer genes, included in the KEGG subcategory “pathways in cancer”, was constructed. Cytoscape version 3.7.0⁷⁴ was used for network extension using CyTargetLinker 4.0.1⁷⁵. Detailed information on this bioinformatics analysis is given in Chapter 5.

The comparison of all results obtained for MWCNT-7 and crocidolite will provide further knowledge of the differences and similarities of the molecular modes of action of both materials, and the hazard of MWCNT-7 for occupational human exposure.

1.4.7. References

1. NIOSH. Occupational Exposure to Carbon Nanotubes and Nanofibers. 2013.
2. Ostiguy C, Debia M, Roberge B, Dufresne A. Best Practices Guidance for nanomaterial Risk Management in the Workplace. Québec; 2015. Report No.: R-899.
3. ISO (International Standardization Organization). ISO/TS 80004-4: 2011 Nanotechnologies - Vocabulary - Part 4: Nanostructured Materials. Geneva, Switzerland; 2011. Report No.: ISO/TS 80004-4:2011.
4. Oberdörster G, Oberdörster E, Oberdörster J. Nanotoxicology: An emerging discipline evolving from studies of ultrafine particles. *Environ Health Perspect.* 2005;113(7):823–39.
5. Donaldson K, Stone V, Tran CL, Kreyling W, Borm PJA. Nanotoxicology. *Occup Environ Med.* 2004;61(9):727–8.

6. Oberdörster G, Maynard AA, Donaldson K, Castranova V, Fitzpatrick J, Ausman KK, et al. Principles for characterizing the potential human health effects from exposure to nanomaterials: elements of a screening strategy. *Part Fibre Toxicol.* 2005;2(1):8.
7. Borm PJA, Robbins D, Haubold S, Kuhlbusch T, Fissan H, Donaldson K, et al. The potential risks of nanomaterials: a review carried out for ECETOC. *Part Fibre Toxicol.* 2006;3:11.
8. Oberdörster G. Safety assessment for nanotechnology and nanomedicine: Concepts of nanotoxicology. *J Intern Med.* 2010;267(1):89–105.
9. Lanone S, Andujar P, Kermanizadeh A, Boczkowski J. Determinants of carbon nanotube toxicity. *Adv Drug Deliv Rev.* 2013;65(15):2063–9.
10. Hammond JL, Formisano N, Estrela P, Carrara S, Tkac J. Electrochemical biosensors and nanobiosensors. *Essays Biochem.* 2016;60(1):69–80.
11. WHO. Nanotechnology and human health: Scientific evidence and risk governance. Bonn; 2012.
12. IARC working group on the evaluation of carcinogenic risks to humans. Some nanomaterials and some fibres. Lyon, France: World Health Organization; 2017. p. 325.
13. Trout DB, Schulte PA. Medical surveillance, exposure registries, and epidemiologic research for workers exposed to nanomaterials. *Toxicology* 2010;269(2–3):128–35.
14. Eichhorn SJ, Dufresne A, Aranguren M, Marcovich NE, Capadona JR, Rowan SJ, et al. Review: current international research into cellulose nanofibres and nanocomposites. *J Mater Sci.* 2010;45(1):1–33.
15. Abdul Khalil HPS, Davoudpour Y, Islam MN, Mustapha A, Sudesh K, Dungani R, et al. Production and modification of nanofibrillated cellulose using various mechanical processes: A review. *Carbohydr Polym.* 2014;99:649–65.
16. Nechyporchuk O, Belgacem MN, Bras J. Production of cellulose nanofibrils: A review of recent advances. *Ind Crops Prod*; 2016;93:2–25.
17. Chinga-Carrasco G, Miettinen A, Hendriks CLL, Gamstedt EK, Kataja M. Structural characterisation of kraft pulp fibres and their nanofibrillated materials for biodegradable composite applications. *Nanocomposites Polym with Anal Methods.* 2011;243–60.

18. Kangas H, Lahtinen P, Sneek A, Saariaho AM, Laitinen O, Hellen E. Characterization of fibrillated celluloses. A short review and evaluation of characteristics with a combination of methods. *Nord Pulp Pap Res J*. 2014;29(01):129–43.
19. Jia B, Li Y, Yang B, Xiao D, Zhang S, Rajulu AV, et al. Effect of microcrystal cellulose and cellulose whisker on biocompatibility of cellulose-based electrospun scaffolds. *Cellulose*. 2013;20(4):1911–23.
20. Lin N, Dufresne A. Nanocellulose in biomedicine: Current status and future prospect. *Eur Polym J*. 2014;59:302–25.
21. Mathew AP, Oksman K, Pierron D, Harmand MF. Fibrous cellulose nanocomposite scaffolds prepared by partial dissolution for potential use as ligament or tendon substitutes. *Carbohydr Polym*. 2012;87(3):2291–8.
22. Mathew AP, Oksman K, Pierron D, Harmand MF. Biocompatible fibrous networks of cellulose nanofibres and collagen crosslinked using genipin: potential as artificial ligament/tendons. *Macromol Biosci*. 2013;13(3):289–98.
23. Basu A, Lindh J, Ålander E, Strømme M, Ferraz N. On the use of ion-crosslinked nanocellulose hydrogels for wound healing solutions: Physicochemical properties and application-oriented biocompatibility studies. *Carbohydr Polym*. 2017;174:299–308.
24. Hakkarainen T, Koivuniemi R, Kosonen M, Escobedo-Lucea C, Sanz-Garcia A, Vuola J, et al. Nanofibrillar cellulose wound dressing in skin graft donor site treatment. *J Control Release* 2016;244:292–301.
25. Jack AA, Nordli HR, Powell LC, Powell KA, Kishnani H, Johnsen PO, et al. The interaction of wood nanocellulose dressings and the wound pathogen *P. aeruginosa*. *Carbohydr Polym*. 2017;157:1955–62.
26. Sun F, Nordli HR, Pukstad B, Kristofer Gamstedt E, Chinga-Carrasco G. Mechanical characteristics of nanocellulose-PEG bionanocomposite wound dressings in wet conditions. *J Mech Behav Biomed Mater*. 2017;69:377–84.
27. Syverud K, Kirsebom H, Hajizadeh S, Chinga-Carrasco G. Cross-linking cellulose nanofibrils for potential elastic cryo-structured gels. *Nanoscale Res Lett*. 2011;6:1–6.
28. Mertaniemi H, Escobedo-Lucea C, Sanz-Garcia A, Gandía C, Mäkitie A, Partanen J, et al. Human stem cell decorated nanocellulose threads for biomedical applications. *Biomaterials*. 2016;82:208–20.

29. Ferraz N, Leschinskaya A, Toomadj F, Fellström B, Strømme M, Mihranyan A. Membrane characterization and solute diffusion in porous composite nanocellulose membranes for hemodialysis. *Cellulose*. 2013;20(6):2959–70.
30. Kolakovic R, Peltonen L, Laukkanen A, Hirvonen J, Laaksonen T. Nanofibrillar cellulose films for controlled drug delivery. *Eur J Pharm Biopharm*. 2012;82(2):308–15.
31. Bhattacharya M, Malinen MM, Lauren P, Lou YR, Kuisma SW, Kanninen L, et al. Nanofibrillar cellulose hydrogel promotes three-dimensional liver cell culture. *J Control Release* 2012;164(3):291–8.
32. Lou Y-R, Kanninen L, Kuisma T, Niklander J, Noon LA, Burks D, et al. The use of nanofibrillar cellulose hydrogel as a flexible three-dimensional model to culture human pluripotent stem cells. *Stem Cells Dev*. 2014;23(4):380–92.
33. Malinen MM, Kanninen LK, Corlu A, Isoniemi HM, Lou YR, Yliperttula ML, et al. Differentiation of liver progenitor cell line to functional organotypic cultures in 3D nanofibrillar cellulose and hyaluronan-gelatin hydrogels. *Biomaterials* 2014;35(19):5110–21.
34. Stefaniak AB, Seehra MS, Fix NR, Leonard SS. Lung biodegradability and free radical production of cellulose nanomaterials. *Inhal Toxicol*. 2014;26(12):733–49.
35. Vartiainen J, Pöhler T, Sirola K, Pylkkänen L, Alenius H, Hokkinen J, et al. Health and environmental safety aspects of friction grinding and spray drying of microfibrillated cellulose. *Cellulose*. 2011;18(3):775–86.
36. Martinez, Kenneth F; Eastlake, Adrienne; Rudie, Alan; Geraci C. Occupational exposure characterization during the manufacture of cellulose nanomaterials. *Prod Appl Cellul Nanomater*. 2013;61–4.
37. Eastlake A, Rudie A, Geraci C. Nanocellulose – Evaluation of the full spectrum of workplace health and safety. *NSTI- Nanotech*. 2014;3(3):105–8.
38. Damstra T, Díaz- F. Environmental Health Criteria 237 principles for evaluating health risks in children associated with exposure. WHO 2006.
39. Sousa-Uva A. Trabalhadores saudáveis e seguros em locais de trabalho saudáveis e seguros. Editores P, editor. Lisboa; 2011.
40. Iavicoli I, Leso V, Manno M, Schulte PA. Biomarkers of nanomaterial exposure and effect: Current status. *J Nanoparticle Res*. 2014;16(3).

41. Higashisaka K, Yoshioka Y, Yamashita K, Morishita Y, Fujimura M, Nabeshi H, et al. Acute phase proteins as biomarkers for predicting the exposure and toxicity of nanomaterials. *Biomaterials* 2011;32(1):3–9.
42. Fatkhutdinova LM, Khaliullin TO, Vasil OL, Zalyalov RR, Musta IG, Kisin ER, et al. Fibrosis biomarkers in workers exposed to MWCNTs. *Toxicol Appl Pharmacol.* 2016;299:125–31.
43. Stocco A, Karlsson HL, Coppedè F, Migliore L. Epigenetic effects of nano-sized materials. *Toxicology* 2013;313(1):3–14.
44. Lu X, Miousse IR, Pirela S V., Melnyk S, Koturbash I, Demokritou P. Short-term exposure to engineered nanomaterials affects cellular epigenome. *Nanotoxicology.* 2016;10(2):140–50.
45. Ha M, Kim VN. Regulation of microRNA biogenesis. *Nat Rev Mol Cell Biol.* 2014;15:509–24.
46. Yanaihara N, Caplen N, Bowman E, Seike M, Kumamoto K, Yi M, et al. Unique microRNA molecular profiles in lung cancer diagnosis and prognosis. *Cancer Cell.* 2006;9(3):189–98.
47. Rupani H, Sanchez-elsner T, Howarth P. MicroRNAs and respiratory diseases. *Eur Respir J.* 2013;41:695–705.
48. Sessa R, Hata A. Role of microRNAs in lung development and pulmonary diseases. *Pulm Circ.* 2013;3(2):315–28.
49. Chen X, Ba Y, Ma L, Cai X, Yin Y, Wang K, et al. Characterization of microRNAs in serum : a novel class of biomarkers for diagnosis of cancer and other diseases. *Cell Reseach.* 2008;18:997–1006.
50. Redova M, Sana J, Slaby O. Circulating miRNAs as new blood-based biomarkers for solid cancers. *Futur Oncology.* 2013;9:387–402.
51. Nagano T, Higashisaka K, Kunieda A. Liver-specific microRNAs as biomarkers of nanomaterial-induced liver damage. *Nanotechnology.* 2013;24(405172).
52. Bru T, Weber DG, Johnen G, Bryk O, Jo K. Identification of miRNA-103 in the Cellular Fraction of Human Peripheral Blood as a Potential Biomarker for Malignant Mesothelioma – A Pilot Study. *PLoS One.* 2012;7(1):1–9.
53. Foster KA, Oster CG, Mayer MM, Avery ML, Audus KL. Characterization of the A549 Cell Line as a Type II Pulmonary Epithelial Cell Model for Drug Metabolism. *Exp Cell Res.* 1998;243(2):359–66.

54. Tsuchiya S, Yamabe M, Yamaguchi Y, Kobayashi Y, Konno T, Tada K. Establishment and characterization of a human acute monocytic leukemia cell line (THP-1). *Int J Cancer*. 1980;26(2):171–6.
55. Daigneault M, Preston JA, Marriott HM, Whyte MKB, Dockrell DH. The identification of markers of macrophage differentiation in PMA-stimulated THP-1 cells and monocyte-derived macrophages. *PLoS One*. 2010;5(1).
56. Pinkerton K, Gehn P, Crapo J. Comparative Biology of Normal Lung. Treatise on Pulmonary Toxicology, Volume 1. Boca raton, FL: CRC Press; 1992.
57. Timbrell V, Rendall R. Preparation of the UICC* Standard Reference Samples of Asbestos. *Powder Technol*. 1972;5:279–87.
58. Rendall R. The data sheets on the chemical and physical properties of the UICC standard reference samples. In: Shapiro H., editor. Pneumoconiosis proceedings of the international conference, 1969, Johannesburg. Oxford: Oxford University Press; 1970. p. 23–7.
59. Timbrell V. Characteristics of the International Union Against Cancer standard reference samples of asbestos. In: Shapiro H., editor. Pneumoconiosis proceedings of the international conference, 1969, Johannesburg. Oxford: Oxford University Press; 1970. p. 28–36.
60. Kohyama N, Shinohara Y, Suzuki Y. Mineral phases and some reexamined characteristics of the International Union against cancer standard asbestos samples. *Am J Ind Med*. 1996;30(5):515–28.
61. Mosmann T. Rapid colorimetric assay for cellular growth and survival: Application to proliferation and cytotoxicity assays. *J Immunol Methods*. 1983;65(1–2):55–63.
62. Riss T, Moravec R. Introducing the cytotox-one tm homogeneous membrane integrity Assay. *Cell notes*. 2002;(4):6–9.
63. Herzog E, Casey A, Lyng FM, Chambers G, Byrne HJ, Davoren M. A new approach to the toxicity testing of carbon-based nanomaterials-The clonogenic assay. *Toxicol Lett*. 2007;174(1–3):49–60.
64. Tice RR, Agurell E, Anderson D, Burlinson B, Hartmann A, Kobayashi H, et al. Single cell gel/comet assay: guidelines for in vitro and in vivo genetic toxicology testing. *Environ Mol Mutagen*. 2000;35(3):206-21
65. Fenech M. Cytokinesis-block micronucleus cytome assay. *Nat Protoc*. 2007;2(5):1084–104.

66. McIlwain DR, Berger T, Mak TW. Caspase functions in cell death and disease. *Cold Spring Harb Perspect Biol.* 2013;5(4):1–28.
67. Love MI, Huber W, Anders S. Moderated estimation of fold change and dispersion for RNA-seq data with DESeq2. *Genome Biol.* 2014;15:550.
68. Russo F, Angelini C. Bioinformatics applications note RNASeqGUI : a GUI for analysing RNA-Seq data. *Bioinformatics.* 2014;30(17):2514–6.
69. Robinson MD, McCarthy DJ, Smyth GK. edgeR : a Bioconductor package for differential expression analysis of digital gene expression data. *Bioinformatics.* 2010;26(1):139–40.
70. Vlachos IS, Zagganas K, Paraskevopoulou MD, Georgakilas G, Karagkouni D, Vergoulis T, et al. DIANA-miRPath v3.0 : deciphering microRNA function with experimental support. *Nucleic Acids Res.* 2015;43(May):460–6.
71. Kanehisa M, Sato Y, Furumichi M, Morishima K, Tanabe M. New approach for understanding genome variations in KEGG. *Nucleic Acids Res.* 2019;47(D1):D590–5.
72. Ashburner M, Ball CA, Blake JA, Botstein D, Butler H, Cherry JM, et al. Gene ontology: tool for the unification of biology. *Nat Genet.* 2000;25(1):25-9.
73. The Gene Ontology Consortium. The Gene Ontology Resource: 20 years and still GOing strong. *Nucleic Acids Res.* Jan 2019;47(D1):D330-D338.
74. Shannon P, Markiel A, Ozier O, Baliga NS, Wang JT, Ramage D, et al.. “Cytoscape : A Software Environment for Integrated Models of Biomolecular Interaction Networks.” *Genome Res.* 2003;13: 2498–2504.
75. Kutmon M, Evelo CT, Ehrhart F, Coort SL, Willighagen EL, Morris JH. 2019. “CyTargetLinker App Update : A Flexible Solution for Network Extension in Cytoscape” *F1000Research* 7: 743–54.

2. Conventional and novel "omics"-based approaches to the study of carbon nanotubes pulmonary toxicity.

Article published in:

Ventura C, Sousa-Uva A, Lavinha J, Silva MJ. (2018). *Environmental and Molecular Mutagenesis*. 59(4):334-362. doi: 10.1002/em.22177. Epub 2018 Feb 26.

Review

Conventional and Novel “Omics”-Based Approaches to the Study of Carbon Nanotubes Pulmonary Toxicity

Célia Ventura,^{1,2,3} António Sousa-Uva,^{2,4} João Lavinha,¹ and Maria João Silva^{1,3*}¹Departamento de Genética Humana, Instituto Nacional de Saúde Doutor Ricardo Jorge (INSA), Lisboa, Portugal²Departamento de Saúde Ocupacional e Ambiental, Escola Nacional de Saúde Pública, Universidade NOVA de Lisboa (UNL), Lisboa, Portugal³Center for Toxicogenomics and Human Health (ToxOmics), NOVA Medical School-FCM, UNL, Lisboa, Portugal⁴CISP – Public Health Research Center, Lisboa, Portugal

The widespread application of carbon nanotubes (CNT) on industrial, biomedical, and consumer products can represent an emerging respiratory occupational hazard. Particularly, their similarity with the fiber-like shape of asbestos have raised a strong concern about their carcinogenic potential. Several *in vitro* and *in vivo* studies have been supporting this view by pointing to immunotoxic, cytotoxic and genotoxic effects of some CNT that may conduct to pulmonary inflammation, fibrosis, and bronchioalveolar hyperplasia in rodents. Recently, high throughput molecular methodologies have been applied to obtain more insightful information on CNT toxicity, through the identification of the affected biological and molecular pathways. Toxicogenomic approaches are expected to identify unique gene expression profiles that, besides providing mechanistic information and guiding new research, have also the potential

to be used as biomarkers for biomonitoring purposes. In this review, the potential of genomic data analysis is illustrated by gene network and gene ontology enrichment analysis of a set of 41 differentially expressed genes selected from a literature search focused on studies of C57BL/6 mice exposed to the multiwalled CNT Mitsui-7. The majority of the biological processes annotated in the network are regulatory processes and the molecular functions are related to receptor-binding signalling. Accordingly, the network-annotated pathways are cell receptor-induced pathways. A single enriched molecular function and one biological process were identified. The relevance of specific epigenomic effects triggered by CNT exposure, for example, alteration of the miRNA expression profile is also discussed in light of its use as biomarkers in occupational health studies. Environ. Mol. Mutagen. 59:334–362, 2018. © 2018 Wiley Periodicals, Inc.

Key words: toxicogenomics; toxicoepigenomics; carbon nanotubes; gene expression; miRNA; nanotoxicology

INTRODUCTION

Nanotechnology is a fast-evolving field and carbon nanotubes (CNT) are one of the most promising and widespread classes of manufactured nanomaterials. According to the ISO/TS 80004-4:2011, CNT are nanofibers, that is, nano-objects with two similar dimensions in the nanoscale (size range from approximately 1 to 100 nm) and the third dimension significantly larger (ISO, 2011). They consist of graphite sheets with a cylindrical arrangement, and can have a single wall (SWCNT), double wall (DWCNT) or multiple walls (MWCNT) assembled in concentric layers, and can be functionalized by the introduction of specific elements on the pristine CNT other than carbon. Only in relation to SWCNT,

more than 50,000 potential combinations may exist depending on structural types, length, manufacturing and purification processes, and surface coatings (WHO, 2012).

Grant sponsor: Fundação para a Ciência e a Tecnologia;; Grant number: UID/BIM/00009/2013.

*Correspondence to: Maria João Silva, Departamento de Genética Humana, Instituto Nacional de Saúde Doutor Ricardo Jorge, Av. Padre Cruz, 1649-016 Lisboa, Portugal. E-mail: m.joao.silva@insa.min-saude.pt

Received 20 July 2017; provisionally accepted 5 January 2018; and in final form 21 January 2018

DOI 10.1002/em.22177

Published online 26 February 2018 in Wiley Online Library (wileyonlinelibrary.com).

CNT display unique physicochemical properties: they are mechanically strong, flexible, lightweight, heat resistant, and have high electrical conductivity (nanowires). They currently have several industrial and biomedical applications, including electronics, lithium-ion batteries, solar cells, super capacitors, thermoplastics, polymer composites, coatings, adhesives, biosensors, enhanced electron-scanning microscopy imaging techniques, inks, as well as in pharmaceutical/biomedical devices for bone grafting, tissue repair, drug delivery, and medical diagnostics (NIOSH, 2013). Many novel applications of CNT are expected to be developed in the coming years and their commercial market is expected to grow fast (WHO, 2012).

Although great societal and economic benefits are expected from CNT usage, the very same properties which are intentionally exploited and are responsible for their success, may have detrimental effects. Those effects may raise some concern, especially in occupational settings where, upon unintentional exposure and interaction with the biological systems CNT have the potential to impact on workers' health (WHO, 2012). Previous studies on human exposure to fine aerosols, atmospheric pollution and manufactured mineral fibers have already demonstrated the association between small-scale material exposure and respiratory disease (Donaldson et al., 2004; Oberdörster et al., 2005a; Borm et al., 2006; Oberdörster, 2010). Regarding manufactured nanomaterials, several *in vitro* and *in vivo* studies have already established that they can also lead to adverse biological responses. These responses are associated with the nanomaterial intrinsic physicochemical properties, including chemistry, size, shape, surface area, solubility, surface reactivity, charge, functional groups, crystalline structure, tendency to agglomerate and the presence of contaminants (Lanone et al., 2013). Baytubes, for example, are entangled agglomerated macro-sized MWCNT with high physical stability and chemical purity (Wirnitzer et al., 2009). They will probably induce a very different biological effect as compared to straight, needle-like MWCNT, for example, MWCNT-7. Biopersistence is an important aspect because lung injury caused by nanomaterials with low biopersistence is less severe than the burden caused by nanomaterials with high biopersistence, even if the former have higher toxicity, due to the protracted adverse effects on lung tissue that result in chronic inflammation (Landsiedel et al., 2014). The dimension, durability and dose (the so-called three D's) of CNT are well known key parameters for their hazard (Donaldson et al., 2013), and their high aspect ratio (length to width ratio) is a characteristic very relevant to their toxicity.

The present work intends to critically review the knowledge about the pulmonary adverse effects of CNT particularly related with occupational exposure, with a

special emphasis on the information gathered from toxicogenomic and toxicopigenomic studies using high throughput technologies. These new “omics” paradigm best fits the next generation testing strategy based on the identification of CNT adverse outcome pathways and derived points of departure for risk assessment of genomic damage (Dearfield et al., 2017). In addition, a critical analysis of the “omics” data allowed a network analysis and gene ontology enrichment analysis to be performed on a set of 41 differentially expressed genes identified in the literature. The utility of the toxicological findings that are herein reviewed envisaging their potential use as biomarkers for biomonitoring studies in occupational settings are also discussed.

OCCUPATIONAL EXPOSURE TO CNT

The human health risk from exposure to CNT is probably more relevant when they are dispersed in the environment or in suspensions, which is more likely to occur in an occupational setting. The highest release of CNT has been observed during their production and handling, as well as during cleaning of the production reactors, and ranged from 0.68 to 38 $\mu\text{g}/\text{m}^3$ in the personal breathing zone of workers performing key work operations and procedures in 11 on-site exposure studies in different workplaces (IARC, 2014). In the USA, a 2013 survey identified 43 companies with an estimated total number of 375 workers engaged in CNT manufacturing, but when extending the workforce to the fabrication or handling of nanofiber-enabled materials and composites this number, although unknown, is likely to be significantly higher (NIOSH, 2013). Adopting a precautionary approach, several professional and scientific organizations agreed that there is sufficient information for CNT to be regarded as an occupational hazard (Trout and Schulte, 2010). Although the National Institute for Occupational Safety and Health (NIOSH) distinguishes between carbon nanofiber (CNF) and CNT depending on the graphene plane alignment (if the graphene plane and fiber axis do not align, the structure is defined as CNF; when they are parallel, it is considered a CNT), the recommended exposure limit (REL) for both is 1 $\mu\text{g}/\text{m}^3$ elemental carbon as a respirable mass 8-hr time-weighted average (TWA) concentration (NIOSH 2013). This limit seems to be lower than some values that have been measured on-site (IARC 2014), even though it is difficult to extrapolate the values relative to key work events performed within minutes to an 8-hr TWA.

In the occupational setting, inhalation is most likely to occur and gastrointestinal absorption can result from the mucociliary transport of inhaled CNT in case of accidents or when hygiene standards are not met (Iavicoli et al., 2014). According to NIOSH guidelines, health surveillance

and medical monitoring of workers exposed to CNF and CNT should include a nonspecific initial evaluation of the medical and occupational history of the worker, with emphasis on the respiratory system (including the use of a standardized questionnaire for respiratory symptoms), a physical examination that may include spirometry testing and a baseline chest X-ray, followed by other tests deemed appropriate for each case. Then, an annual update of the occupational and medical history, and a spirometry test at least every 3 years should be performed (NIOSH, 2013).

The deposition of ultrafine particles in the respiratory system (the first site of contact of the particle after inhalation) is predominantly determined by diffusion that redirects the particles of inhaled and exhaled air currents towards the airway walls and its subsequent impaction and sedimentation. This movement is affected by (i) the particle size, shape, and possible dynamical change during breathing, (ii) the geometry of the respiratory tract and alveolar structures, (iii) the pattern of breathing (including breathing through the nose or mouth) that determines the speed of the air stream, and (iv) the residence time in the respiratory system (Kreyling et al., 2006). Depending on the inhaled particles diameter, which may result from the aggregation or agglomeration state of the individual particles, their regional deposition in the lungs will vary from the extra-thoracic regions (larger particles) to the alveoli (smaller particles; Kreyling et al., 2006). Under real-life conditions, the majority of airborne nanomaterials are in an agglomerated form, and their deposition in the lungs follows the pattern of larger particles (Laux et al., 2017). Furthermore, particle agglomerate volume may better explain the effects of repeated dosing leading to inflammation, as opposed to surface area that may be the dose metric applied to describe the acute effects of instilled or inhaled particles. In addition to agglomeration, particle dissolution is also fundamental to the toxicity of inhaled particles, due to the reduction of their size and related changes of dissolution kinetics (Laux et al., 2017). It is considered that particles as CNT, which are not dissolved in the epithelial lining fluid, may be phagocytized by the alveolar macrophages and be cleared by mucociliary transport, be transported across the epithelial barrier and be stored in interstitial tissue or be carried for storage in tracheobronchial and bifurcational lymph nodes (Kreyling, 1990). In mouse models, it was observed that the lung burden of a MWCNT at 56 days post-exposure by pharyngeal aspiration was about 68.7%, 7.5%, and 22% in the alveolar macrophages, alveolar tissue and granulomatous lesions, respectively, demonstrating its potential to reach the alveolar region (Mercer et al., 2011). In this microenvironment, nanoparticles may possibly be translocated to distant organs and systems or interact with the cells of the immune system. The translocation of MWCNT from the lungs to the liver, kidney, heart, brain,

tracheobronchial lymph nodes, parietal pleura and the diaphragm has been documented on male C57BL/6J mice exposed in a whole-body inhalation system for 5 hr/day for 12 days (lung burden 28.1 $\mu\text{g}/\text{lung}$; Mercer et al., 2013b). One day after the exposure ended, most of the extrapulmonary MWCNT fibers were found in the tracheobronchial lymph nodes (1.08% of lung burden). At 336 days post-exposure, the extrapulmonary burden of MWCNT was significantly higher than at 1 day post-exposure, that is, the lymph nodes accumulated 7.34% of the lung burden, while the levels in extrapulmonary organs as a whole increased approximately in the same proportion, that is, 6–7-fold (Mercer et al., 2013b). Other toxicological studies have shown that inhaled MWCNT are able to reach the pleura (Porter et al., 2010; Donaldson et al., 2010; Donaldson et al., 2013). The route of translocation of nanofibers from the lungs to the visceral pleura, into the pleural space, and to the parietal pleura is unknown. It is postulated that translocation to the lung interstitium and visceral pleura can occur either by a paracellular route or by direct penetration across injured alveolar epithelial cells, and translocation to the pleural space via the lymphatic and blood vessels (by themselves or within macrophages) or passively in the same manner as interstitial fluid (Broaddus et al., 2011). Given the fiber-like shape similarity of MWCNT with asbestos fibers, there are concerns about their fibrogenic and carcinogenic potential to the mesothelium (Pacurari et al., 2010), which will be further discussed along the text.

An important acquired property of CNT that it is thought to influence its pharmacokinetics and pharmacodynamics is the *corona*, that is, the biomolecules that nanomaterials, due to their high surface energy, adsorb from their biological environment. This interaction transforms bare nanomaterials into nanomaterials with a biological coating (Westmeier et al., 2016). Plasmatic proteins can possibly form a corona around CNT, altering their physicochemical properties and biological effects, for example, inflammatory effects. This highly relevant and less consensual issue as been already reviewed elsewhere (Monopoli et al., 2012).

Although occupational studies of CNT exposure are still missing, much information regarding the toxicological potential of CNT has been gathered in the last years from *in vitro* and rodent studies.

TOXICOLOGICAL STUDIES IN VITRO

Cytotoxicity and Genotoxicity Assessment

Several studies have demonstrated the ability of CNT to induce cytotoxic, genotoxic effects, or even epigenotoxic effects (the last two categories of effects are further developed in Fig. 1), even though some studies have also reported negative results. Whereas genotoxicity relates to

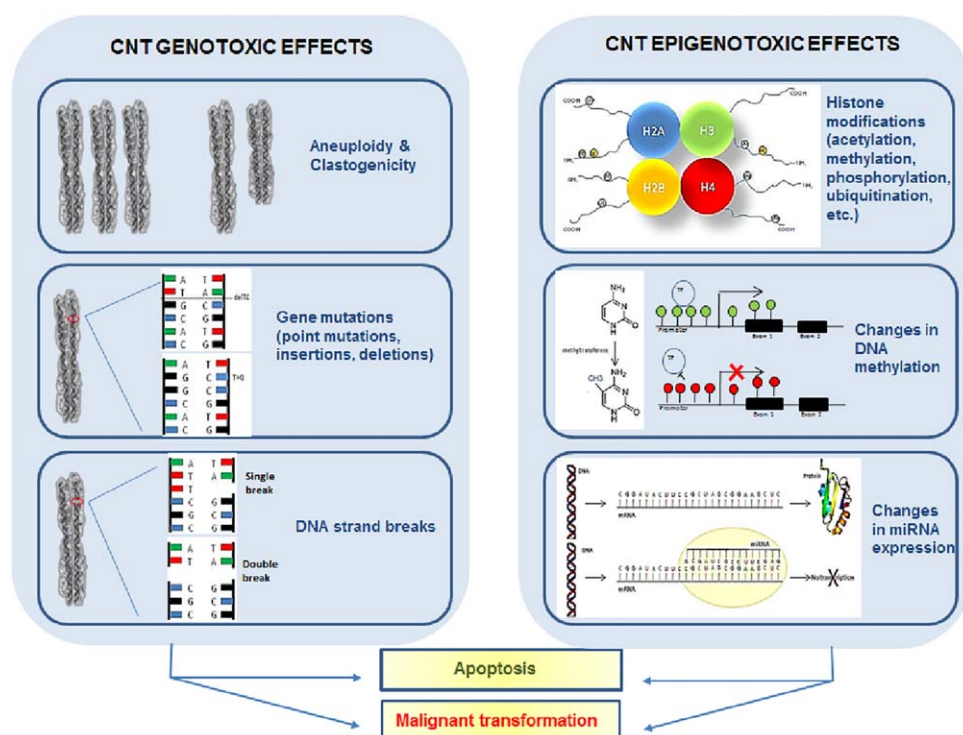


Fig. 1. Possible genotoxic and epigenotoxic effects from exposure to CNT. The genotoxicity of CNT can be caused by direct action of the CNT on the DNA molecule, or due to indirect mechanisms, for example, mediated by ROS generation or secondary to inflammation. Epigenotoxic effects are changes in the regulation of gene expression in response to CNT exposure: methylation of DNA, histone tail alterations and differential microRNA (miRNA) expression.

DNA or chromosome damage and may lead to genetic instability, epigenotoxicity comprises mechanisms that change gene expression through transcription inhibition, chromatin remodeling or degradation of RNA, in response to environmental stimuli. Both genotoxic and epigenotoxic effects can trigger cell death by apoptosis or lead to malignant transformation and eventually to cancer development.

When comparing the cytotoxicity of asbestos (crocidolite), MWCNT, and SWCNT (up to 48 $\mu\text{g}/\text{cm}^2$) in Chinese hamster lung fibroblasts (V79 cell line), Kisin et al. (2011) reported a concentration- and time-dependent loss of viability for all tested materials, the magnitude of the effect being asbestos > MWCNT > SWCNT. Additionally, all tested materials revealed genotoxicity with the strongest effect seen for the MWCNT (Kisin et al., 2011). Previously, in another study from the same authors performed using lung fibroblasts, SWCNT exposure caused (i) loss of cell viability in a concentration- and time-dependent manner and (ii) an increase in the level of DNA damage in a concentration-dependent manner (Kisin et al., 2007). It should be emphasized that a major factor of the cyto-genotoxic potential of asbestos is ROS generation mainly induced by the mobilizable surface iron of its fibers (Srivastava et al., 2010). In fact, only Fe-rich MWCNT at concentrations of 50 and 100 $\mu\text{g}/\text{cm}^2$ were

significantly cytotoxic and genotoxic and induced oxidative stress in murine alveolar macrophages, while Fe-free MWCNT did not exert any of these adverse effects, supporting the view that iron content represents an important key constituent in promoting MWCNT-induced toxicity (Aldieri et al., 2013). Nevertheless, very high levels of ROS and decreased metabolic activity were observed in A549 cells after exposure to pristine MWCNT (Thurnherr et al., 2011). Noteworthy, another study reported that agglomerated MWCNT decreased human epithelial and mesothelial cell viability without being internalized or producing oxidative stress, contrasting to asbestos (Tabet et al., 2008).

In another study, dispersed SWCNT stimulated fibroblast proliferation, induced collagen production without cell damage, and increased the activity of MMP-9, one of the major matrix metalloproteinases involved in lung fibrosis (Wang et al., 2010). *In vitro* exposure of mesothelial cells to SWCNT increased oxidative stress, cell death, enhanced DNA damage, including histone H2AX phosphorylation, and activated poly(ADP-ribose) polymerase 1 (PARP-1), activator protein-1 (AP-1), nuclear factor κB (NF- κB), protein p38, and protein serine-threonine kinase (Akt). However, the tested SWCNT had metal contamination, a characteristic already suggested to mediate CNT toxicity, that could have induced the observed effects

(Pacurari et al., 2008). In fact, a more recent study showed that SWCNT and MWCNT caused a low level of DNA damage on mesothelial cells as assessed by the comet assay, in some cases only at relatively high doses (48-hr exposure to 80 $\mu\text{g}/\text{cm}^2$), and little or no effect was observed on bronchial epithelial cells. No evidence of chromosomal damage was found in both cell lines (Lindberg et al., 2013). These observations suggest that mesothelial cells are more sensitive to the CNT-associated DNA damaging effects than bronchial epithelial cells. The low γ -glutamylcysteine synthetase reactivity in pleural mesothelium may be associated with the highest sensitivity of mesothelial cells to fiber-induced toxicity due to glutathione depletion (Puhakka et al., 2002). In a more recent study using a human lung adenocarcinoma epithelial cell line, the A549 cell line and the human-derived bronchial epithelial cell line BEAS-2B, there was no induction of DNA single or double DNA strand breaks (comet assay) by any of the four benchmark MWCNT tested. However, discrepant results were observed in the two cell lines: cytotoxic effects were detected only in A549 cells with the IC_{50} values varying from approximately 8 to 61 $\mu\text{g}/\text{cm}^2$ and the two longest MWCNT significantly raised the micronucleus frequency in A549 cells at the highest tested concentrations (64 and 128 $\mu\text{g}/\text{cm}^2$), whereas in BEAS-2B cells negative results were obtained for all MWCNT. This discrepancy was explained by the different size-distribution of MWCNT in the cell culture medium, rather than by the cell line specificities (Louro et al., 2016). In another study, the rigid MWCNT-7 (2.5 and 15 $\mu\text{g}/\text{ml}$) was able to induce micronuclei formation in human lymphocytes exposed *ex vivo*, supporting the chromosome damaging effect of some MWCNT with the potential to mediate a tumorigenic effect in humans (Tavares et al., 2014). It should be noted that also a lower MWCNT specific surface area, and therefore, a larger diameter, has been associated with increased genotoxicity (Poulsen et al., 2016).

As to the type of genetic lesions that MWCNT have been able to induce, the majority of positive results have been associated with chromosome damage rather than to DNA strand breaks. In fact, a 11.3-nm diameter and 0.7 μm length MWCNT (10–50 $\mu\text{g}/\text{ml}$) with traces of cobalt and iron catalysts displayed a dose-dependent increase in the micronucleus frequency in the human breast epithelial cell line MCF-7 due to clastogenic and aneugenic events (Muller et al., 2008). MWCNT, at occupationally relevant exposure levels (0.024–24 $\mu\text{g}/\text{cm}^2$), also induced a dose-related increase in the frequency of disrupted centrosomes, abnormal mitotic spindles and aneuploid chromosome number in BEAS-2B cells (Siegrist et al., 2014). Noteworthy, the study showed that CNT were integrated into microtubules, DNA and centrosome structure. In addition, a G1/S block of the cell cycle was observed, probably as a consequence of the CNT

integration into the centrosome structure and interaction with the microtubules as well as a potential to pass the genetic damage to daughter cells. The mechanical interaction of MWCNT with the mitotic spindle microtubules and its adjacent structures may explain their ability to induce micronuclei by an aneugenic mechanism of action. This mechanism also supports the moderate to null ability of MWCNT to generate positive results in the comet assay that detects primary DNA lesions (Azqueta et al., 2014). However, this mode of action may not be inherent to all MWCNT, given that for instance Baytubes (2.5–10 $\mu\text{g}/\text{ml}$, 4 and 18 hr exposure), induced neither cytotoxic nor clastogenic effects in the chromosome aberration test using Chinese hamster lung fibroblasts (Wirnitzer et al., 2009).

A more recent analysis of 15 MWCNT with different physicochemical characteristics in rat epithelial lung cells showed no significant cytotoxicity and only a weak genotoxicity at a concentration-range of 12.5–200 $\mu\text{g}/\text{ml}$. Nevertheless, cell proliferation decreased at the highest doses of some MWCNT, this effect being associated with a higher CNT surface area and ROS production (Jackson et al., 2015). Oxidative stress was also reported in rat lung epithelial cells exposed to 0.5–10 $\mu\text{g}/\text{ml}$ MWCNT, which stimulated the apoptosis signaling pathway through caspase activation (Ravichandran et al., 2009).

Immunotoxicity Assessment

Inflammasomes comprise a group of large intracellular multiprotein signaling complexes that can respond to exogenous stimuli and control the proteolytic activation of IL-1 β and IL-18. Lung inflammation is probably caused by the induction of NLRP3 inflammasome activation in the airway epithelial cells (Fig. 2), a mechanism already linked to several pulmonary diseases (Birrell and Eltom, 2011; Im and Ammit, 2013; Nardo et al., 2014) and to exposure to nanomaterials (Yazdi et al., 2010; Sun et al., 2013), including MWCNT (Hussain et al., 2014). The NLRP3 inflammasome can assemble through a wide range of stimuli including pathogen-associated molecular patterns (PAMPs), damage-associated molecular patterns (DAMPs), fibers/particles, metabolic products, environmental hazards, and engineered nanomaterials (Sun et al., 2013). Long, needle-like CNT activation of the NLRP3 inflammasome depends on ROS production, cathepsin B activity, P2X7 receptor, and Src and Syk tyrosine kinases, inducing IL-1 β secretion (Palomaki et al., 2011). Noteworthy, pyroptosis, a highly inflammatory form of programmed cell death, was observed in primary human bronchial epithelial (HBE) cells exposed to 1.5–24 $\mu\text{g}/\text{ml}$, due to NLRP3 activation (Hussain et al., 2014).

Macrophages are alveolar cells that play a key role in the alveolar tissue indirect response to nanomaterials, especially for poorly soluble nanomaterials, as CNT. It

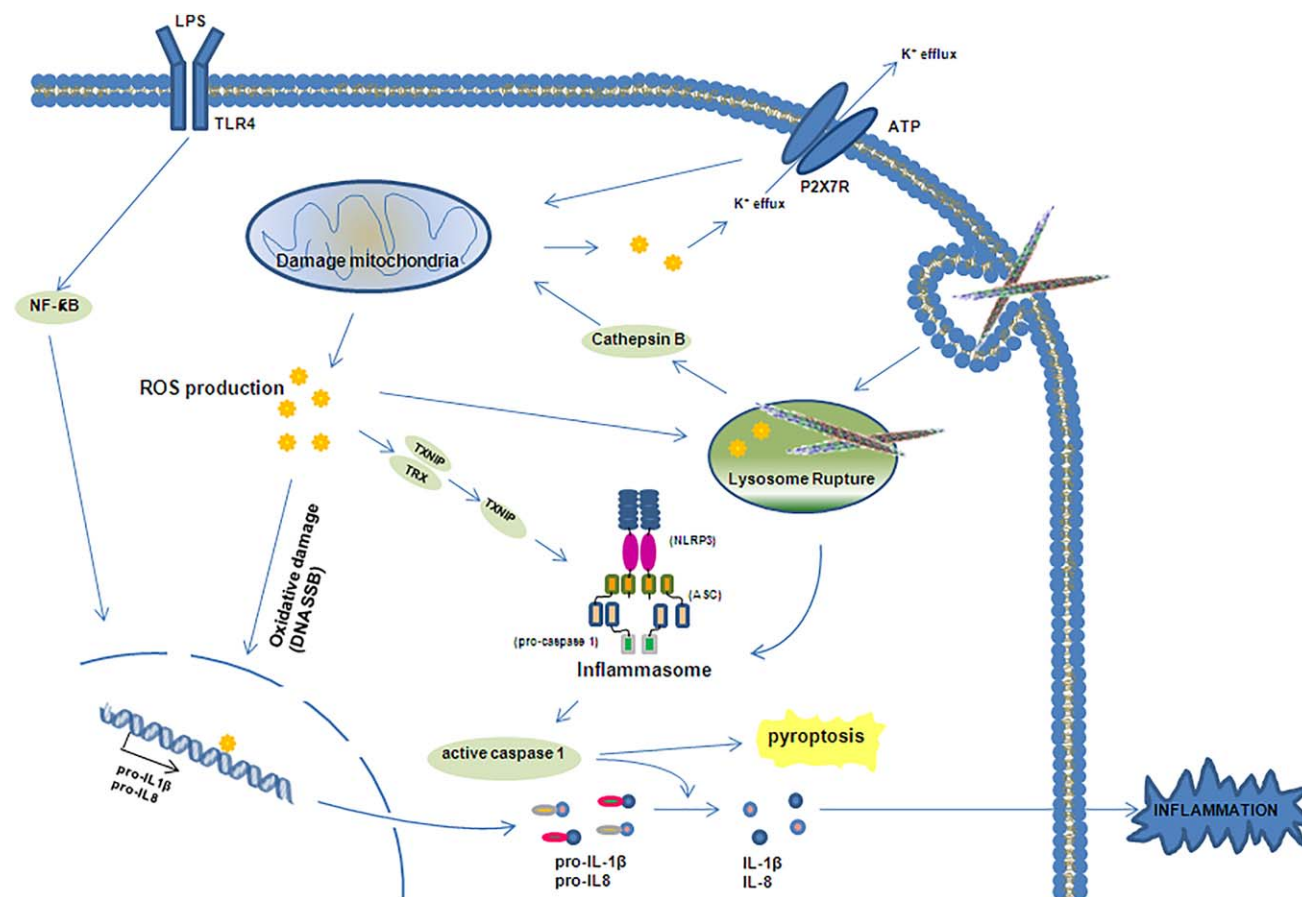


Fig. 2. Schematic representation of the mechanisms involved in NLRP3 inflammasome activation in lung macrophages and epithelial cells. The mechanisms of inflammasome activation by nanofibers are not completely understood. Phagocytosis of nanofibers results in mitochondrial damage leading to the production of reactive oxygen species (ROS). ROS production can induce a direct genotoxic effect, namely DNA single-strand breaks (SSB). ROS can also cause lysosome destabilization and consequent cathepsin B release and further mitochondrial damage. Furthermore, high aspect-ratio nanomaterials can cause lysosomal rupture and release of cathepsin B to the cytosol. ROS generation leads to the oxidation of the redox-active thioredoxin (TXN) dissociating it from thioredoxin-

interacting protein (TXNIP). In its free form, TXNIP can activate NLRP3. NLRP3 inflammasome activation causes caspase-1 proteolysis of the precursor forms of cytokines IL-1 β and IL-18 into their active forms, which are powerful inflammation inducers. Caspase-1 activation can also induce cell pyroptosis. The production of the pro-cytokines is under the control of the NF- κ B signaling pathway via activation of the Toll-like receptor 4. In addition, K⁺ efflux may be a common trigger of NLRP3 inflammasome activation, causing mitochondrial membrane potential disruption. The increase of extracellular ATP from damaged cells binds to the P2X purinoreceptor 7 (P2X7) activating this ion channel, contributing to the K⁺ efflux.

has been proposed that neutrophils begin the process of nanoparticle degradation, converting long particles into shorter ones, thus facilitating their uptake by the activated macrophages present in the lungs for complete degradation with peroxynitrite generated by superoxide anion radicals and nitrogen oxides produced via the NADPH oxidase pathway (Kagan et al., 2014). If these oxidative species formation is excessive, injury to the neighbor cells and tissue can occur, especially for biopersistent particles as CNT. Following macrophage activation, phagocytosis of CNT also leads to the release of proinflammatory cytokines and chemokines (e.g., TNF α , IL-1 β , IL-6, IL-10, and MCP1) and transcription factors associated with inflammation (NF- κ B and AP-1; He et al., 2012; Oberdörster et al., 2005b).

Long, straight, and well-dispersed nanofilaments produced significantly more TNF- α and ROS in monocytic cells (15.625–62.5 μ /ml, 4 hr exposure) as compared to highly curved and entangled materials, confirming that fiber morphology and state of aggregation are important factors in the immunotoxicity of CNT (Brown et al., 2007). In addition, it was suggested that when nanofiber length exceeds the pleural macrophages length, it triggers an inflammatory response in the pleural cavity due to “frustrated phagocytosis”, which in turn stimulates a cytokine proinflammatory response from adjacent mesothelial cells (Brown et al., 2007; Murphy et al., 2012; Landsiedel et al., 2014).

Moreover, it was observed that MWCNT (30 μ g/ml) directly promote the fibroblast to myofibroblast and

epithelial to mesenchymal transitions through the activation of the TGF- β /Smad2 signaling pathway (Wang et al., 2015). SWCNT also stimulate TGF- β 1 production in BEAS-2B cells and macrophages promoting fibroblast to myofibroblast transformation (He et al., 2012). These findings corroborate the evidence from the rodent studies that indicated the pro-fibrotic potential of CNT.

Much of the described cytotoxic, genotoxic and immunotoxic effects of CNT that were identified *in vitro* have been also documented in the rodent studies presented in the next section, allowing linking them to *in vivo* adverse health effects. One of the most relevant questions stands on whether the concentration-ranges of CNT tested *in vitro* are somehow comparable to the ones used in rodent studies, which, in turn, should ideally mimic real human exposure. Considering the peak airborne concentrations of MWCNT in an occupational setting, and the difference between the surface area of the lung alveoli of humans and rodents, Porter et al. (2010) concluded that a 10 μg MWCNT exposure to a mouse would correspond to approximately one month of exposure to a human performing light work in an environment with aerosol concentrations of 400 $\mu\text{g}/\text{m}^3$ MWCNT. Thus, if the human average daily MWCNT aerosol exposure was of 4–40 $\mu\text{g}/\text{m}^3$, the 10 μg MWCNT exposure in mouse would approximate a person performing light work for approximately 9 months to 7.5 years (Porter et al., 2010). If this concentration is extrapolated for use during *in vitro* studies, a concentration lower than 1 $\mu\text{g}/\text{ml}$ (or generally lower than 0.5 $\mu\text{g}/\text{cm}^2$) in standard tissue culture protocols is obtained. As described above, however, many *in vitro* MWCNT pulmonary toxicity studies use exposure concentrations much higher than that, although this may be admissible in toxicological *in vitro* studies that typically use very short exposure lengths, for example, 4–72 hr (Snyder-Talkington et al., 2012).

TOXICOLOGICAL STUDIES IN RODENTS

In recent years, experimental intratracheal instillation or pharyngeal aspiration of CNT liquid suspensions in rodents resulted in the development of acute or persistent pulmonary inflammation and persistent interstitial fibrosis with granuloma formation, and bronchiolar or bronchioalveolar hyperplasia (Fig. 3; NIOSH, 2013; Landsiedel et al., 2014).

Already in the first rodent studies performed by intratracheal instillation of CNT in mice (Lam et al., 2004) and rats (Warheit et al., 2004), multifocal granulomas were a major finding. Another study performed in C57BL/6 mice exposed to SWCNT through pharyngeal aspiration demonstrated the induction of dose-dependent acute inflammation with early onset progressive fibrosis and granulomatous bronchial interstitial pneumonia

(Shvedova et al., 2005). Granuloma was mainly associated with hypertrophic epithelial cells around SWCNT dense aggregates, whereas the diffuse interstitial fibrosis and thickening of the alveolar wall was probably linked with dispersed SWCNT. A sequential increase in neutrophil, lymphocyte and macrophage counts was also observed at day 1, 3, and 7, respectively, accompanied by an elevation of proinflammatory cytokines (day 1) and TGF- β 1 (day 7). Another study from the same group demonstrated that inhalation exposure to respirable SWCNT was more potent in inducing oxidative stress, inflammatory response, collagen deposition and fibrosis than aspiration of an equivalent mass of SWCNT, probably due to the exposure to less agglomerated and smaller SWCNT structures (Shvedova et al., 2008). The same conclusion was observed later, that is, inhalation exposure to SWCNT in mice showed significantly greater inflammatory, fibrotic, and genotoxic effects than bolus pharyngeal aspiration. Nevertheless, even one year after a single pharyngeal aspiration, CNT, similarly to asbestos, could still be visualized in mouse lungs, inducing chronic bronchopneumonia and lymphadenitis, accompanied by pulmonary fibrosis (Shvedova et al., 2014). These observations are in agreement with the evidence that exposure to dispersed SWCNT triggers a more potent interstitial fibrotic reaction with an increase in collagen deposition and without granuloma formation, than the exposure to less dispersed material (Mercer et al., 2008). Furthermore, not only CNT dispersion but also their clearance from the lungs are related to their hydrophilicity and hydrophobicity. The latter depends on the CNT preparation method and the use of their pristine versus functionalized form (Kim et al., 2010).

It has been suggested that direct stimulation of fibroblasts, the lung cells that produce the collagen matrix, may play a significant role in lung fibrosis. SWCNT seem to be more fibrogenic than MWCNT or asbestos, that have a stronger inflammatory effect (Shvedova et al., 2014). However, despite the relatively low fraction of MWCNT delivered to the alveolar tissue, a progressive and persistent fibrotic response was observed 336 days post-exposure reflected by up to 73% increase in the average thickness of connective tissue and a time- and dose-dependent increase in its collagen content (Mercer et al., 2011, 2013).

Concerning mesothelial cells, direct instillation of CNT into the mouse pleural cavity resulted in a similar acute inflammatory and progressive fibrosis response in the parietal pleura as compared to asbestos. It was also observed that the pathogenicity of long fibers is greater, probably due to its length-dependent retention in the parietal pleura *stomata* (Donaldson et al., 2010; Murphy et al., 2011).

In vivo studies also demonstrated cytotoxic effects associated with exposure to DWCNT and MWCNT, as

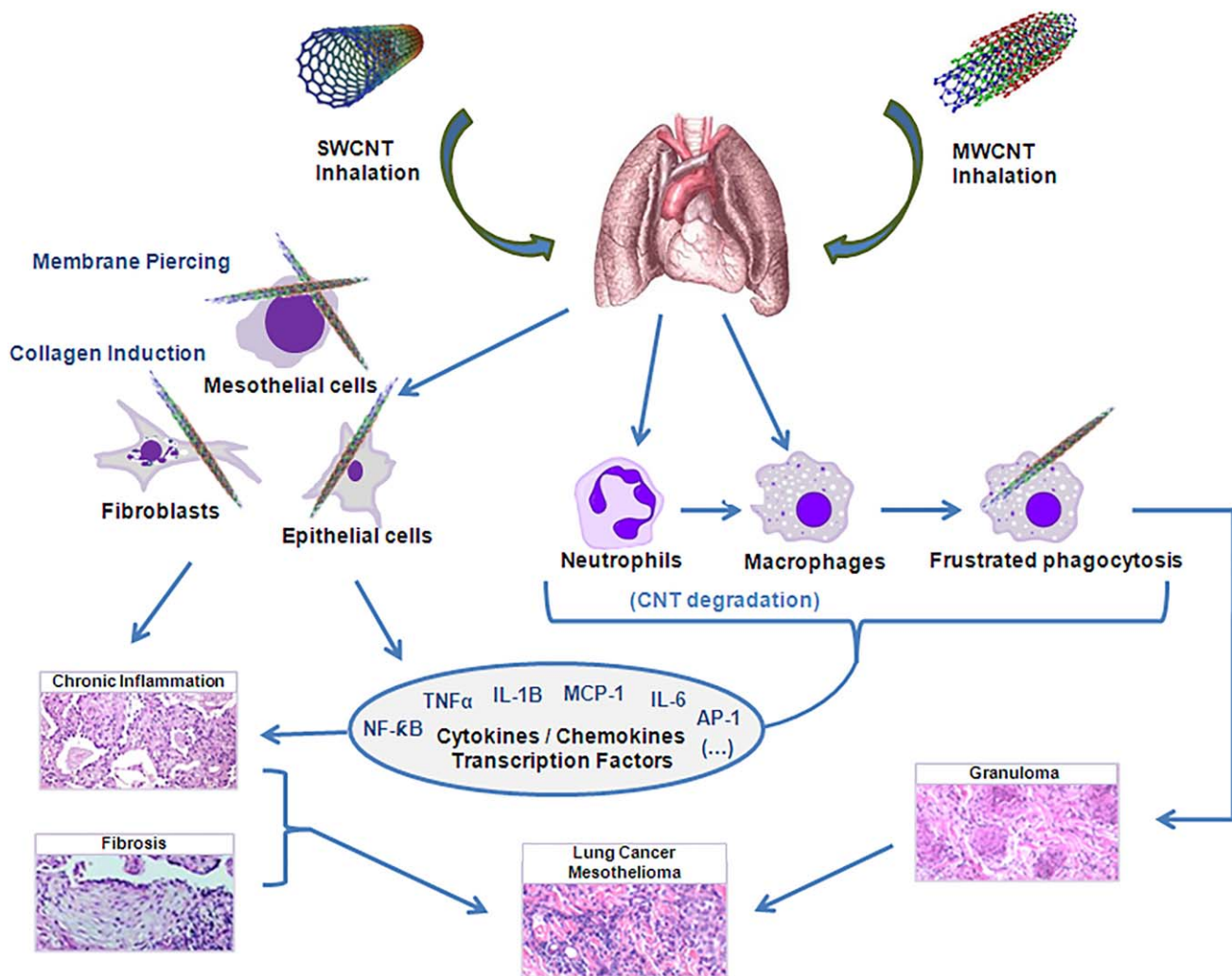


Fig. 3. Lung adverse effects of inhalatory exposure to CNTs. Although all CNT can lead to inflammation, fibrosis, granuloma and cancer, SWCNT in the aggregated form are related to granuloma, but when well dispersed are usually associated with lung fibrosis due to an increase in the collagen content. MWCNT are commonly related with chronic inflammation due to cell membrane piercing and frustrated phagocytosis. Ultimately, this adverse affects can culminate in lung cancer.

evidenced by the dose-dependent elevation in lactate dehydrogenase activity in bronchoalveolar lavage fluid of rats (Muller et al., 2008; Sager et al., 2013; Snyder-Talkington et al., 2016a). Albumin levels were also increased in bronchoalveolar lavage fluid of rats exposed to DWCNT, indicating loss of the integrity of the blood–gas barrier in the lung (Sager et al., 2013). Genotoxic effects as well as hyperplasia and dysplasia (mitotic figures, binucleated cells, anisocytosis, and anisokaryosis) were reported in bronchial epithelial cells of mice exposed to MWCNT by tracheal instillation (Kim et al., 2010). MWCNT induced a significant and dose-dependent increase in the micronucleus frequency in rat type II pneumocytes (Muller et al., 2008). Furthermore, SWCNT exposure induced cytogenetic alterations reflected as micronucleus formation and nuclear protrusions and

increased the incidence of *K-ras* oncogene mutations, similarly to MWCNT, but not to asbestos exposure (Shvedova et al., 2014).

Regarding possible carcinogenic effects of CNT, the discordant evidence obtained for different CNT led the International Agency for Research on Cancer (IARC) to categorize all SWCNT and MWCNT, except MWCNT-7, as not classifiable as to their carcinogenicity to humans (Group 3). On the contrary, MWCNT-7 was classified as possibly carcinogenic to humans (Group 2B; IARC, 2014). In fact, MWCNT-7 has been shown to induce peritoneal mesothelioma after a single intraperitoneal injection in mice (0.003–3 mg/animal; Takagi et al., 2008, 2012), after two intraperitoneal injections with a one-week interval in rats (0.5–5 mg/animal; Nagai et al., 2011), after intrascrotal injection (1 mg/animal) in rats

(Sakamoto et al., 2009) and lung carcinomas after whole-body inhalation exposure of male rats ($0.2\text{--}2\text{ mg/m}^3$) and female rats (2 mg/m^3 ; Kasai et al., 2016). Moreover, it promoted growth and neoplastic progression of lung cells of B6C3F1 mice previously exposed to methylcholanthrene, leading to lung bronchioloalveolar adenomas and adenocarcinomas at doses similar to the ones that can be achieved in human occupational exposure (Sargent et al., 2014). In another study, Mitsui-7 injection in the peritoneal cavity of rats induced, like asbestos, an early and selective sustained immunosuppressive response characterized by the accumulation of monocytic Myeloid Derived Suppressor Cells (CD11b/cint and His48hi). These cells possess the ability to suppress polyclonal activation of T lymphocytes and correspond to M-MDSC, counteracting the effective immune surveillance of tumor cells (Huaux et al., 2016).

Several MWCNT demonstrated carcinogenic effects. For example, the administration of 1 mg MWCNT/rat by trans-tracheal intrapulmonary spraying during the initial 2 weeks of the experiment, using three groups of animals—MWCNT before filtration ($4.2\text{ }\mu\text{m}$ average length), flow-through fraction after filtration ($2.6\text{ }\mu\text{m}$ average length) and retained fraction (length not determined)—caused malignant mesothelioma (6/38) and lung tumors (14/38). All malignant mesotheliomas were localized in the pericardial pleural cavity (Suzui et al., 2016).

The malignant mesotheliomas induced by intraperitoneal injection of MWCNT in rats had a histopathology and immunohistochemistry analogous to that of the mesotheliomas induced by asbestos, suggesting similar pathogenesis (Rittinghausen et al., 2014). Interestingly, mesotheliomas induced by thin (diameter $\sim 50\text{ nm}$) and highly crystalline MWCNT share a homozygous deletion of the tumour suppressor genes *Cdkn2a/2b*, similar to mesotheliomas induced by asbestos (Nagai et al., 2011). In this latter study, it was proposed that thin and crystalline MWCNT might have a piercing effect in the mesothelial cell membrane causing *in vitro* cytotoxicity, and *in vivo* inflammatory and carcinogenic effects. Aggregative and thick MWCNT do not penetrate mesothelial cells and cause no direct cell injury, the observed carcinogenicity being likely mediated by indirect effects (Nagai et al., 2011).

PITFALLS AND CHALLENGES IN CNT HAZARD ASSESSMENT

As seen in the studies reviewed above, toxicological studies of CNT can sometimes generate conflicting results mostly due to different methodological approaches (Lanone et al., 2013; Landsiedel et al., 2014), which hinders the comprehension of their relevance in terms of exposure to humans. Moreover, many of these studies use different

concentration metrics (rarely, fiber number, but frequently, weight/unit volume of medium or weight/unit area of cells), which makes comparisons between studies more laborious and frequently impossible. To ensure that the observed effects are due to the CNT characteristics and to be able to compare the results from different laboratories it is essential to harmonize the experimental protocols, such as the nanofiber preparation, exposure conditions (biological model, route and mode of administration, dose, and exposure duration) and endpoints. Even so, other factors can influence the results, for instance, the dispersing agent used for keep the nanofibers dispersed in the cells culture medium in *in vitro* studies, crucial for the protein corona formation and consequent nanofiber biokinetics, or the interaction of the CNT with the culture media components, assay reagents or detection molecules (Casey et al., 2008; Lanone et al., 2013; Landsiedel et al., 2014).

In this regard, the use of reference well characterized CNT can contribute to improve inter-laboratory comparability. In addition, in rodent studies, CNT/CNF aerosol characterization of size distribution, mass, number concentration, agglomeration/aggregation state, density, and other physicochemical characteristics (surface properties, impurities, length, diameter, dissolution, and leaching) is recommended (Oberdörster et al., 2015).

CNT surface functionalization is extremely diverse and can thus modify the biological effects, for example, acid-treated MWCNT induce a less severe inflammatory response than pristine MWCNT and are less tumorigenic (Kim et al., 2010; Yu et al., 2013); carboxylated (COOH) MWCNT are more cytotoxic and genotoxic than hydroxylated-oxygenated (O+), aminated (NH₂) and pristine MWCNT (Chatterjee et al., 2014). Another example is the thin film coating of MWCNT through an atomic layer deposition of Al₂O₃; it alters cytokine production by human mononuclear cells *in vitro* and cytokine expression in mouse lungs, reducing fibrosis (Taylor et al., 2014). Therefore, the identification of the properties that are critical to determine the CNT hazard can allow the design of safer and sustainable products, a concept known as “safer-by-design”. Thus, the uniqueness of each CNT makes it necessary to assess its individual hazard(s), though it is foreseeable that some concepts can be shared by applying a grouping approach (Oberdörster, 2010). Indeed, the categorization of nanomaterials in hazard groups, the so-called *grouping strategy* depending on their intrinsic characteristics, lifecycle, biokinetics and effects is useful for risk assessment, and can prevent unnecessary laborious testing (Braakhuis et al., 2016; Dekkers et al., 2106).

Moreover, if the aim is to identify and characterize the hazard through the establishment of a dose-effect (or exposure-adverse effect) curve, the experimental design often does not reflect the reality. Much criticism has thus

emerged from the high CNT mass doses commonly used in toxicity studies, since real life human airway deposition can take weeks to reach a dose that is administered instantaneously in the experimental setting. Bearing those criticisms in mind, various calculation models of the effective dose metrics have been developed (Oberdörster, 2010; Klein et al., 2012; Landsiedel et al., 2014).

It is now anticipated that more useful toxicological information can be gathered from low-dose studies examining multiple endpoints, than from a single acute exposure. In addition, in rodent studies, intratracheal instillation and pharyngeal aspiration were also criticized for not reproducing the real deposition pattern of exposure, and inhalation has been the recommended exposure route to obtain data necessary for the risk assessment of CNT and CNF following pulmonary exposure (Oberdörster, 2010). Nevertheless, some studies suggested that pharyngeal aspiration of a well-dispersed suspension of MWCNT result in a pulmonary distribution and inflammatory response that closely simulates the inhalation exposure (Snyder-Talkington et al., 2016a). Other recommendations have recently been provided for rodent inhalation studies, for example, (i) the preference of 90-day inhalation studies in rats using whole-body exposure to pristine material (with no treatment with dispersant or sonication) (ii) using aerosols produced by dry powder generator methods with (iii) a minimum of three concentrations that include a no observed adverse effect level (NOAEL) and a maximum tolerated dose, (iv) using positive and negative benchmark controls and (v) preceding the 90-day inhalation study by an acute 1- to 10-day inhalation study followed by a post-exposure observation/recovery period (Oberdörster et al., 2015). The same authors recommend the endpoints (e.g., lung weight changes) and the minimal data set to be gathered and analyzed (e.g., specific bronchoalveolar lavage parameters, and determination of retained lung burden). All these concerns have to take into consideration that there are significant differences in the lung structure and function between rodents and humans, for instance, in the branching patterns of the tracheobronchial tree that affects the deposition of inhaled materials (Miller et al., 1993), and in the thickness of the interstitium and pulmonary capillary endothelium (Crapo et al., 1983).

Actually, both the initial transport rate of nanoparticles from the lungs to the gastrointestinal tract, as the decay of the transport rate, vary considerably between species. Generally, in humans and large animals, the particle initial transport rate is an order of magnitude less than in rodents. This can be a consequence of the shorter distance from the alveolus to the terminal bronchiolus in rodents, compared to dogs, monkeys, and humans (Kreyling, 1990). Dosimetric risk extrapolation from animals to humans has to consider other species differences related to the biokinetics of inhaled particulate materials, for example the greater interstitial compartmentalization of

retained particles in primates *versus* rodents (Laux et al., 2017). However, despite these differences, the distribution of cells in the alveolar tissue and their average volume and surface area seem to be constant among rats, dogs, baboons, and humans (Crapo et al., 1983).

In the last decades, there has been an effort to replace animal testing by *in vitro* studies for ethical reasons. However, a modest correlation has been found between toxicological results obtained *in vitro* and those obtained *in vivo*. Therefore, there has been an attempt to improve conventional monoculture cell systems through the co-culture of various cell types present in the target organ to better mimic *in vitro*, the *in vivo* model and to provide more reliable information on nanoparticles' toxicity (Snyder-Talkington et al., 2012). For example, an *in vitro* co-culture model of human small airway epithelial cells (SAEC) and human microvascular endothelial cells (HMVEC) has correlated better than the two cell monoculture models with the *in vivo* mouse lung transcriptomic profile following MWCNT exposure (Snyder-Talkington et al., 2015) confirming the utility of these more complex cell systems. Nonetheless, even the use of more sophisticated cellular models and more realistic exposure systems will not overcome the lack of other important factors that affect a whole organism response, for instance, the complexity of the immune system response. Moreover, if an air-liquid interface exposure or the use of 3D cell cultures would be more realistic for inhalation exposure or animal studies replacement, their use is not yet generalized in most laboratories.

NEW PERSPECTIVES IN CNT TOXICOLOGY

Toxicogenomics

Genomic studies begin to have a significant impact on toxicology, as they allow a global overview to be made of all molecular pathways that are modified in the cell, tissue or organism in response to a toxic insult. For instance, it was demonstrated that the accuracy of predicting acetaminophen (paracetamol, APAP) toxic effects based on blood cell gene expression patterns was significantly better than that based on conventional clinical parameters such as clinical chemistry, hematology, or histopathology (Bushel et al., 2007). For this reason, large-scale gene expression studies are increasingly being used leading to the emergence of "toxicogenomics" (Nuwaysir et al., 1999; Aardema and Macgregor, 2002; Newton, Aardema, and Aubrecht, 2004).

Through the identification of the differentially expressed genes following a CNT exposure, a detailed assessment of their potential health hazards, in a time- and dose-dependent manner, can be achieved. Microarrays and, more recently, high throughput next generation sequencing (NGS), are techniques that provide a massive

amount of toxicogenomics data. The objective of finding a gene signature for each mechanism of toxicity from an initial set of thousands of up- or down-regulated genes can be cumbersome, and it is only feasible with the help of sophisticated bioinformatics tools. This is obvious when considering the number of differentially expressed genes and the complexity of related pathways that have been identified in each CNT toxicogenomic *in vitro* and rodent study listed in Table I. They include apoptosis, inflammation, oxidative stress, fibrosis, cell cycle and proliferation, among others.

The objective of finding a particular set of genes that could be related with nanofiber exposure often relies on their previously known participation in cellular pathways suspected to be critical for the observed toxic effects, as seen in Table I for cancer. The selection of genes to be further analysed, from the original gene sets, based on their foreseen participation in processes like inflammation or fibrosis can simplify the data analysis (Guo et al., 2012; Dymacek et al., 2015; Snyder-Talkington et al., 2016a). Nevertheless, this biased approach (the so-called candidate gene approach) can let unlooked other important pathways leading to the toxicity of the stressor. Some examples are given below.

In Vitro Studies

Cancer-related gene expression and signaling pathway alterations following exposure to CNT are frequent endpoints of toxicological studies. There is compelling evidence that human lung epithelial cells chronically exposed to SWCNT, that is, continuously exposed to low, physiologically relevant concentrations of SWCNT for a prolonged period of 6 months, leads to carcinogenesis by the acquisition of cancer stem cells (CSC) subpopulations, which possess high tumorigenic potential. These CSC have characteristics similar to those observed in the cells of non-small cell lung cancer and chronic asbestos-exposed lung cells and display aberrant stem cell markers, notably Nanog, SOX-2, SOX-17, and E-cadherin, and the specific stem cell surface markers CD24^{low} and CD133^{high} (Luanpitpong et al., 2014).

Long-term *in vitro* exposure of normal lung epithelia to SWCNT showed malignant cell transformation with altered expression of several genes involved in apoptosis, cell cycle control and oncogenic progression (activation of pAkt/p53/Bcl-2 signaling axis, increased expression of the *Ras* family involved in cell cycle control, Dsh-mediated Notch 1, and down-regulation of the apoptotic genes *BAX* and *PMAIP1*). Activated immune responses were among the major changes of biological function (Chen et al., 2015). Moreover, SWCNT exposure of primary normal human bronchial epithelial and alveolar cells resulted in down-regulation of the mRNA expression and consequent enzymatic activity of the drug-metabolizing

enzymes CYP1A1 and CYP1B1, as a consequence of preventing the binding of activated aryl hydrocarbon receptor (AhR) to the enhancer region of the corresponding genes. Down-regulation of these enzymes may affect detoxification of xenobiotics, may reduce the procarcinogen bioactivation in the lungs and alter the metabolism of drugs in this organ (Hitoshi et al., 2012).

Regarding MWCNT exposure, the comparative analysis of asbestos- and MWCNT-induced effects in epithelial lung cells revealed that both materials triggered changes in 12 mesothelioma related genes and 22 lung cancer genes (Kim et al., 2012).

Furthermore, both MWCNT and asbestos seem to decrease mitochondrial membrane potential in human bronchial epithelial BEAS-2B cells at a dose of 0.25 and 2 $\mu\text{g}/\text{cm}^2$, respectively. This decrease was associated with a 330-gene signature; 49 of those genes show highly similar expression patterns over time and are regulated by two transcription factors, *APP* and *NRF-1* (Nymark et al., 2015).

Studies in Rodents

When analyzing the relationship between MWCNT and carcinogenesis using mice exposed by pharyngeal aspiration, 7 and 11 biomarker genes showed significant expression changes at 7 and 56 days post-exposure, respectively. In particular *Ccdc99*, *Msx2*, *NOS2*, and *Wif1*, were differentially expressed at both time points. These gene signatures were suggested as of possible utility for medical surveillance of MWCNT exposed workers (Pacurari et al., 2011). In another genome-wide study performed in C57BL/6J mice exposed to MWCNT, a 35-gene signature identified at 56 days post-exposure and a further set of 16 consistently differentially expressed genes was found to be potentially useful to predict lung cancer risk in humans (Guo et al., 2012). Nevertheless, even using the same experimental model, different MWCNT can have dissimilar genomic responses. A long/thick MWCNT (NM-401) and a small/thin curled MWCNT (NRCWE-026) showed overall similar changes in gene expression, but a subset of 14 genes was specifically associated with the long MWCNT, possibly linked to the increased fibrotic response at day 28 post-exposure, observed *in vivo* only for this MWCNT (Poulsen et al., 2015). When comparing MWCNT and asbestos toxicity, although similar outcomes are observed (inflammation and fibrosis), they may be mediated by the activation of different cellular signaling pathways through a different gene expression profile. The exposure to MWCNT tends to favor pathways involved in immune responses, namely, canonical interleukin and B- and T-cell signaling, whereas asbestos exposure tends to favor pathways involved in ROS production, electron transport, and cancer (Snyder-Talkington et al., 2016a).

TABLE I. *In vivo* and *in vitro* toxicogenomic studies on the effects of carbon nanotubes (CNT) on the lungs

Reference	CNT tested (manufac-turer)	Biological Model	No. of differentially expressed genes	Methodology	Bioinformatic Approach	Major Molecular and Biological Functions, Processes and Pathways
Alazzam et al. (2010)	SWCNT (Sigma- Aldrich; Oakville, Ontario, Canada)	Normal human bron- chial epithelial cells	Up-regulated: 7,029 Down-regulated: 7,265	Microarray; RT-PCR	FlexArray software (Affymetrix)	Cell apoptosis, signalling, growth and structure Transcription regulator Adhesion and signaling Extracellular matrix Cell motility and survival Cell cycle
Pacurari et al. (2011)	MWCNT-7 (Mitsui- &-Company)	Male C57BL/6J mice	7 at day 7 11 at day 56	qRT-PCR	IPA	Major Canonical Pathways: Basal Cell Carcinoma signaling Corticotropin releasing hormone signaling HIF1 signaling IL-12 signaling and production in macrophages IL-17 signaling LXR/RXR activation MIF regulation of innate immunity MSP-RON signaling pathway Relaxin signaling Role of macrophages, fibroblasts and endothelial cells in rheumatoid arthritis Sonic hedgehog signaling Type I diabetes mellitus signaling Major Biological Functions/Disorders: Organismal injury and abnormalities Developmental disorder Genetic disorder Antimicrobial response Cancer Immunological disease Neurological disease Pathways: Regulation of actin cytoskeleton Wnt signaling pathway MAPK signaling pathway Major Biological Processes: Metabolic Process Cell proliferation Cell-cell signaling Intracellular transport Protein transport Only cancer related genes were selected
Li et al. (2011)	MWCNT	NIH/3T3 cells	up-regulated: 266 down-regulated: 217	miRNA SOLiD sequencing; qRT-PCR	KEGG and GO	
Guo et al. (2012)	MWCNT-7 (Mitsui & Company)	Male C57BL/6J mice	Total no.? 24 with significant changes at least in two time	microarray	IPA	

TABLE I. (continued).

Reference	CNT tested (manufac-turer)	Biological Model	No. of differentially expressed genes	Methodology	Bioinformatic Approach	Major Molecular and Biological Functions, Processes and Pathways
Hsieh et al. (2012)	SWCNT (CarboLex, Inc.)	Male ICR mice	points, a more than 1.5-fold change at all doses and signifi- cant in the linear model for the dose or the interaction of time and dose. 330 at day 56 729	Microarray qPCR	Self-developed com- posite regulatory signature database	Pathways: Cytokine–cytokine receptor interaction ECM–receptor interaction Antigen processing and presentation Adipocytokine signaling pathway Glycolysis gluconeogenesis Complement and coagulation cascades Focal adhesion B-cell receptor signaling pathway Huntington's disease Type I diabetes mellitus PPAR signaling pathway Leukocyte transendothelial migration Jak-STAT signaling pathway Hematopoietic cell lineage Major Biological Processes: Cell morphogenesis Protein complex assembly Enzyme linked receptor protein signaling pathway Protein targeting Microtubule-based process Nucleocytoplasmic transport Nuclear transport Angiogenesis Protein import into nucleus Striated muscle contraction Regulation of angiogenesis Major Canonical Pathways: Regulation of actin cytoskeleton Melanogenesis Apoptosis Glycine, serine and threonine metabolism Type I diabetes mellitus Selenoamino acid metabolism Toll-like receptor signaling pathway
Kim et al. (2012)	MWCNT (Hanwha Nanotech; Incheon, Korea)	Normal human bron- chial epithelial cells	up-regulated: 1,201 (6 hr) and 1,252 (24 hr), down-regulated: 1,977 (6 hr) and 1,542 (24 hr)	microarray	GO and IPA	

TABLE I. (continued).

Reference	CNT tested (manufac-turer)	Biological Model	No. of differentially expressed genes	Methodology	Bioinformatic Approach	Major Molecular and Biological Functions, Processes and Pathways
Poulsen et al. (2013)	MWCNT- XNRI-7 (Hadoga Chemical industry)	C57BL/6 mice and Muta Mouse lung epithelial cell line (FE1)	<i>in vivo</i> : low dose - 580 medium dose - 1,333 high dose - 113 in common - 46 <i>in vitro</i> : low dose - 706 medium dose - 1,259 high dose - 3,559 in common - 1,147	Microarray; qRT- PCR	GO and IPA	Colorectal cancer Hematopoietic cell lineage Type II diabetes mellitus Histidine metabolism Cyanoaminoacid metabolism Major Biological Processes: <i>In vivo</i> : Immune response Oxidation reduction Behavior Inflammatory response Chemotaxis <i>In vitro</i> : Regulation of cell proliferation Vasculature development ncRNA metabolic process Steroid biosynthetic process Response to protein stimulus Major Canonical Pathways: Pyrimidine ribonucleotides de novo biosynthesis Aryl hydrocarbon receptor signaling LPS/IL-1 mediated inhibition of RXR function Estrogen-mediated S-phase entry LXR/RXR activation Glutathione-mediated detoxification Acute phase response signaling Chemokine signaling IL-17 signaling Retinoate biosynthesis I Retinol biosynthesis Neuregulin signaling Role of tissue factor in cancer Aldosterone signaling in epithelial cells Glucocorticoid receptor signaling Major Biological Functions/Disorders: Cellular movement Cellular growth and proliferation Cell death and survival Cancer Inflammatory response Lipid metabolism Cell-to-cell signaling and interaction Cell cycle

TABLE I. (continued).

Reference	CNT tested (manufac-turer)	Biological Model	No. of differentially expressed genes	Methodology	Bioinformatic Approach	Major Molecular and Biological Functions, Processes and Pathways
Snyder-Talkington et al. (2013)	MWCNT-7 (Mitsui & Company)	Male C57BL/6J mice	2,996 (773 related to inflammation and 890 related to fibrosis)	Microarray	IPA	Only inflammation and fibrosis related genes were selected
Dymacek et al. (2015)	MWCNT-7 (Mitsui & Company)	Male C57BL/6J mice	123 genes and 92 miRNAs related to fibrosis and inflammation	Microarray	MEGPath NMF algorithm miRTarBase miRe- cords TargetScan IPA	Major Canonical Pathways (NMF algorithm) Axonal Guidance Signaling IL-6 Signaling Corticotropin Releasing Hormone Signaling Ovarian Cancer Signaling Hepatic Fibrosis/Hepatic Stellate Cell Activation Role of Osteoblasts, Osteoclasts, and Chon- drocytes in Rheumatoid Arthritis NF-κB Signaling Role of Macrophages, Fibroblasts, and Endo- thelial Cells in Rheumatoid Arthritis HMGB1 Signaling Major Canonical Pathways (IPA) Hepatic Fibrosis/Hepatic Stellate Cell Activation Role of Osteoblasts, Osteoclasts, and Chon- drocytes in Rheumatoid Arthritis Colorectal Cancer Metastasis Signaling ILK Signaling Granulocyte Adhesion and Diapedesis Major Biological Processes: Response to metal ion Antigen processing and presentation of pep- tide antigen via MHC class I Regulation of circadian rhythm Antigen processing and presentation Positive regulation of microtubule depolymerization Regulation of phagocytosis Interspecies interaction between organisms Cellular chloride ion homeostasis Vacuolar transport Rhythmic process Major Molecular Functions: MHC class I receptor activity Flavonol 3-sulfotransferase activity Aryl sulfotransferase activity G-protein coupled photoreceptor activity SH3 domain binding Ubiquitin-specific protease activity
Chen et al (2015)	SWCNT (CNI, Houston, TX, USA)	BEAS-2B cells	?	Microarray; western- blot	GO and IPA	

TABLE I. (continued).

Reference	CNT tested (manufac-turer)	Biological Model	No. of differentially expressed genes	Methodology	Bioinformatic Approach	Major Molecular and Biological Functions, Processes and Pathways
Nymark et al. (2015)	MWCNT-XXNRI-7 (Mitsui & Co Ltd.)	BEAS-2B cells	Total no.? 330 genes related to decrease mitochon- drial membrane potential	Microarray	Chipster ConsensusPathDB STEM DTW4Omics	Photoreceptor activity Protein binding Ubiquitin thiolesterase activity Cysteine-type endopeptidase activity Major Biological Functions/Disorders: Cellular growth and proliferation, hematolog- ical system development and function, humoral immune response Connective tissue disorders, inflammatory disease, skeletal and muscular disorders Cell death and survival, embryonic develop- ment, organismal development Cellular compromise, skeletal and muscular system development and function, post- translational modification Cell morphology, cellular assembly and orga- nization, cellular development Respiratory system development and func- tion, tissue morphology, cell cycle Cancer, gastrointestinal disease, hepatic sys- tem disease Cell morphology, cell-to-cell signaling and interaction, nervous system development and function DNA replication, recombination, and repair, cellular compromise, cell death and survival Lipid metabolism, molecular transport, small molecule biochemistry Only mitochondrial membrane potential related genes and miRNAs were selected Major molecular pathways (GO): Gluconeogenesis Glucose metabolism Metabolism of carbohydrates Myoclonic epilepsy of Lafora Glycogen storage disease Mitochondrial LC-fatty acid β -oxidation Monosaccharide metabolism process Cellular amino acid biosynthetic process Tetrahydrofolate interconversion Major Biological Processes: Cell cycle Microtubule-based process DNA metabolic process
Poulsen et al. (2015)	NRCWE-026 (Nanocyl 7000)	Female C57BL/6 mice	NRCWE-026: Day 1 – 1546 Day 3 – 4252 Day 28 – 111	Microarray; qRT- PCR	GO and IPA	

TABLE I. (continued).

Reference	CNT tested (manufac-turer)	Biological Model	No. of differentially expressed genes	Methodology	Bioinformatic Approach	Major Molecular and Biological Functions, Processes and Pathways
Snyder-Talkington et al. (2015a)	NM-401 (IO-LE- TECNano-materials CP-0006-SG)	Male C57BL/6J mice Mono- or co-culture of human small air- way epithelial cells (SAEC) and human microvascular endo- thelial cells (HMVEC)	NM-401: Day 1 – 1609 Day 3 – 4020 Day 28 – 372	Microarray	IPA	Immune response Response to wounding Major Canonical Pathways: LXR/RXR activation Atherosclerosis signaling Oxidative ethanol degradation III Hepatic fibrosis/hepatic stellate cell activation Pyrimidine ribonucleotides interconversion Acute phase response signaling Aryl hydrocarbon receptor signaling Antigen presentation pathway Dendritic cell maturation Crosstalk between dendritic cells and natural killer cells Hematopoiesis from pluripotent stem cells Primary immunodeficiency signaling B cell development Calcium-induced T lymphocyte apoptosis Retinol biosynthesis IL-10 signaling Pyrimidine deoxyribonucleotides <i>de novo</i> biosynthesis I Hypoxia signaling in the cardiovascular system IL-8 signaling Major Biological Functions/Disorders: Cancer Cellular growth and proliferation Cell death and survival Cellular movement Hematological system, development and function Inflammatory response
						Major Canonical Pathways related to those concordant genes significantly changed in SAEC mono- and co-culture: Airway inflammation in asthma Inhibition of matrix metalloproteases LXR/RXR activation Communication between innate and adaptive immune cells Hematopoiesis from multipotent stem cells Major Canonical Pathways related to those concordant genes

TABLE I. (continued).

Reference	CNT tested (manufac-turer)	Biological Model	No. of differentially expressed genes	Methodology	Bioinformatic Approach	Major Molecular and Biological Functions, Processes and Pathways
Snyder-Talkington et al. (2015b)	MWCNT-7 (Hodo- gaya Chemical Company)	Male B6C3F1 mice	Total no.? 19 mRNA and 17 miRNA related to hyperplasia, fibrosis, bronchiolo-alveolar adenoma and bronchiolo-alveolar adenocarcinoma	Microarray	IPA	<p>significantly changed in HMVEC mono- and co-culture:</p> <p>PTEN signaling Actin nucleation by ARP-WASP complex ATM signaling Cardiomyocyte differentiation via BMP receptors ERK5 signaling</p> <p>Major Canonical Pathways:</p> <p>Wound repair Fibrosis and tumorigenesis Cell growth, proliferation and invasion Cell apoptosis owing to stress to the endo- plasmic reticulum</p> <p>Major Diseases and Functions:</p> <p>Pulmonary fibrosis Inflammation of respiratory system Fibrosis of lung Lung cancer</p> <p>Non-small cell lung adenocarcinoma</p>
Snyder-Talkington et al. (2016a)	MWCNT-7 (Hodo- gaya Chemical Company)	Male C57BL/6J mice	1 µg: 90 10 µg: 293 40 µg: 301 80 µg: 254	Microarray	IPA	<p>Major Canonical Pathways:</p> <p>Parkinson's signaling Mitochondrial dysfunction Oxidative phosphorylation Hematopoiesis from pluripotent stem cells Protein ubiquitination pathway CD27 signaling in lymphocytes Communication between innate and adaptive immune cells T-cell receptor signaling TCA cycle II (eukaryotic) Primary immunodeficiency signaling</p> <p>Major Biological Functions/Disorders:</p> <p>Cell-mediated immune response Cellular development Cellular function and maintenance Hematological system development and function Hematopoiesis Cell-to-cell signaling and interaction Cell death and survival Cancer Organ morphology Tissue development</p>

KEGG- Kyoto encyclopedia of genes and genomes (<http://genome.ad.jp/kegg/>); GO- Gene Ontology (<http://geneontology.org/>); IPA- Ingenuity Pathway Analysis (<http://ingenuity.com>).

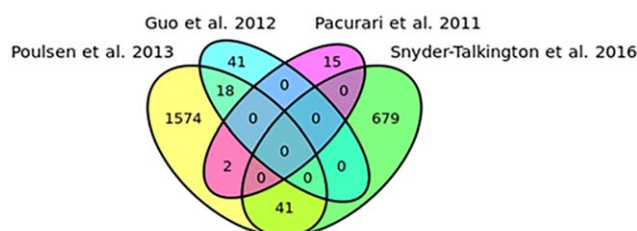


Fig. 4. Venn diagram showing the overlapping differentially expressed genes in the available transcriptomic datasets on the effect of Mitsui-7 on C57BL/6J mice. Guo et al. (2012), Pacurari et al. (2011) and Snyder-Talkington et al. (2016a) studies do not have any gene in common among them, but all these three studies share some genes with the Poulsen et al. (2013) study, which has the largest gene set. Therefore, all studies together have no common altered gene expression. Nevertheless, there are 41-shared genes between the Poulsen et al. (2013) and the Snyder-Talkington et al. (2016a) study. The Guo et al. (2012) study does not present the complete gene set, but only the genes selected for further analysis. All these toxicogenomic studies were performed using microarray technology, except Pacurari et al. (2011) that used RT-PCR.

Similar biological responses through different molecular mechanisms are well known findings between *in vivo* and *in vitro* systems. In fact, although most of the altered pathways that were identified are shared between the two experimental models, the specific genes that are involved are different (Poulsen et al., 2013). Moreover, although differences in gene expression exist between *in vivo* and *in vitro* exposure to CNT, *in vitro* exposures can efficiently recapitulate the significantly altered molecular functions *in vivo* (Kinaret et al., 2017).

In a near future, the meta-analysis of the large transcriptomic datasets that are becoming available in the literature will possibly allow the validation of the proposed up- or down-regulated genes to be made. Noteworthy is the fact that the comparison of gene expression profiles from the lungs of mice exposed to three different MWCNT within the framework of an adverse outcome pathway (AOP) for lung fibrosis, permitted the calculation of transcriptional benchmark doses (BMD) for MWCNT-induced lung fibrosis (Labib et al., 2016). These transcriptional BMD were comparable to the apical BMD derived by NIOSH for MWCNT-induced lung fibrotic lesions, suggesting that they could be used to establish acceptable levels of exposure applicable to human health risk assessment. Nevertheless, the comparative analysis of the transcriptomic results available in the literature is still a challenging task.

A Representative Functional Network and Gene Ontology Enrichment Analysis

In this section of the review, a simple comparison of the altered gene sets presented in the four studies listed in Table I that share the same animal model (C57BL/6J mice), exposed to a similar CNT (Mitsui-7) is presented, in order to evaluate the consistency of the “omics”

findings among them. It should be noted that in the study by Guo et al. (2012) only 59 differentially expressed genes were accounted for, because the full list was not available. The result of this comparison is shown in Figure 4 that highlights the limited concordance among the published data.

The reduced number of overlapping genes among the four studies may be due to several factors: different exposure methods and doses, different time points of analysis, different RNA quantitation (RT-PCR or microarray) or even different selection of microarray probe sets. Moreover, an important number of commonly expressed genes was uniquely identified between the Poulsen et al. (2013) and the Snyder-Talkington et al. (2016a) studies, probably because they were the ones with the largest transcriptomic dataset, that is, 1,635 and 720 genes, respectively. This fact supports the need of analyzing a large number of genes in order to reach sufficient statistical power. Nonetheless, the same significant gene expression changes observed in both studies occurred at exposure doses that differ by up to two orders of magnitude (Table II). This can possibly be explained by the different experimental setup: in the Snyder-Talkington et al. (2016a) study, the animals were sacrificed 1 year after a single pharyngeal aspiration whereas in the Poulsen et al. (2013) study, the animals were sacrificed 24 hr after a single intratracheal instillation and a higher acute dose was needed to reach the same transcriptional alteration. Nevertheless, when the overlapping gene list was filtered for genes related to inflammation and fibrosis using the IPA analysis in these two reports, their number was reduced to four genes related to inflammation (*Ccl19*, *Ccl5*, *Cd14*, and *Myd88*) and none related to fibrosis. Since inflammation and fibrosis are the two main pulmonary adverse effects associated with CNT exposure, the lack of overlapping fibrosis-related genes was an unexpected finding. It should be noted that these differentially expressed genes have to be confirmed by independent studies, as it is usually done, for instance, in all genome-wide association studies, to validate the positive findings.

In view of the fact that the genes listed in Table II represent the largest set of overlapping genes found in the various studies, a network analysis of the possible existing interactions among them was additionally performed. The obtained functional interaction (FI) network consists of 32 genes structured according to four different modules of highly-interacting groups of genes and 17 linker genes, that is, genes included to connect the input genes in the network (Fig. 5).

The pathway enrichment results are showed in Table III. This set of 41 genes was also analysed using PANTHER Overrepresentation Test annotation version 11.0 (release 2016-07-15) with the Bonferroni correction and a *P* value ≤ 0.05 . Gene Ontology enrichment analysis identified helicase activity (GO:0004386) as the single enriched molecular function (*P* value = 1.27E-02) and the

TABLE II. Limited concordance of the transcriptomic published data. Overlapping differentially expressed genes identified in the publicly available gene sets from Poulsen et al. (2013) and Snyder-Talkington et al. (2016a) following mouse exposure to different doses of the MWCNT Mitsui-7

	Dose (µg/animal)	Poulsen et al. (2013; intratracheal instillation; 24 hr)		
		18 µg	54 µg	162 µg
Snyder-Talkington et al. 2016a (pharyngeal aspiration; one year)	1 µg	Ddx21		Ddx21 Gzma Nudt8 Sp110
	10 µg	Kcna6 Spcs3 Sprr1a Wdr74	H2afv	Brix1 Ccl19 Cd72 Fam188a H2afv Kcna6 Myd88 Npc2 Nubp2 P2rx4 Sprr1a Wdr74
	40 µg	Cdc14a Emp3 Mcm5 Wdr74		Blnk Brix1 Ccl5 Cd14 Cd19 Cd2 Cd72 Cdc14a Cirbp Hexb Ltb Ly6a Ly6d Mrps18b Nt5e Pinx1 Rnase6 Rps8 Spib Ufd11 Wdr74
	80 µg	Emp3 Wdr74	H2afv	Blnk Ccl5 Cd19 Cd2 Cd72 D130062J21Rik Ddx5 H2afv Irf1 Ltb Mthfd11 P2rx4 Pinx1 Ufd11 Wdr74

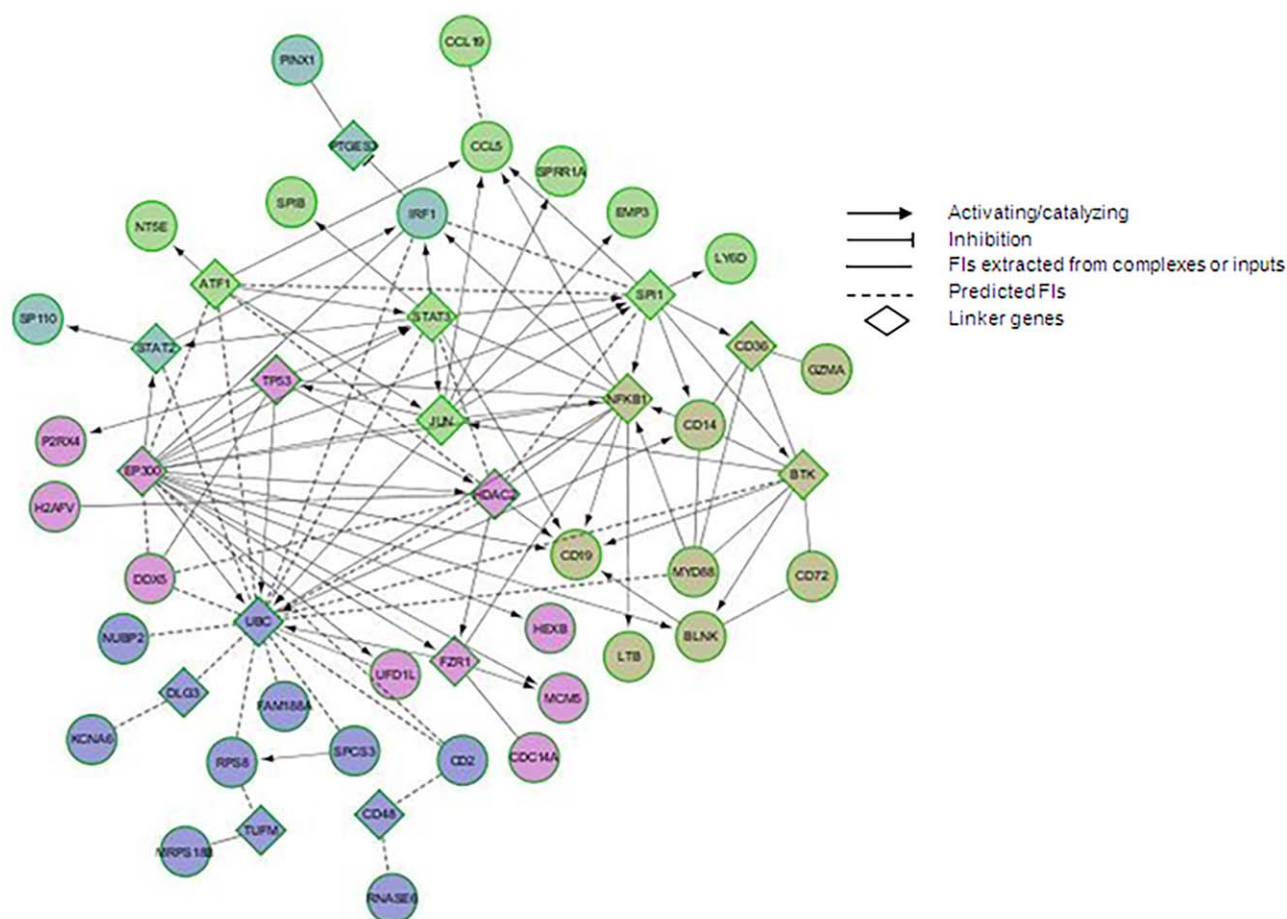


Fig. 5. Functional interaction network analysis of the 41 shared differentially expressed genes. Different colors indicate sub-networks of functionally related genes. The network was constructed using the ReactomeFIViz app (Wu et al., 2014) from Reactome (Croft et al., 2013; Fabregat et al., 2016) and Cytoscape v3.3.0 (Shannon et al., 2003). This app accesses the Reactome functional interaction network to reveal the interactions of a group of genes.

response to interferon-gamma (GO:0034341) as the only enriched biological process (P value = 4.55E-02) among the set of 41 genes.

As can be observed in Table III, most biological processes annotated in the network are regulatory processes (e.g., the positive regulation of endocytosis, presumably involved in the nanofiber uptake by the cells). The molecular functions are related to receptor binding signaling. Accordingly, the annotated pathways include cell receptor induced pathways (e.g., B cell receptor signaling and Toll-like receptor signaling), and their downstream pathways (e.g., NF- κ B signaling).

The results obtained suggest that the activation of the innate immune cells, including macrophages and other cells contributing to immunity (epithelial cells, endothelial cells, and fibroblasts) depends on the nanofiber recognition by Toll-like receptors (TLR) as already described for other PAMPs (Takeuchi and Akira, 2010). The binding to TLR up-regulates the transcription of genes that encode

proinflammatory cytokines, type I interferons, and chemokines, through the nuclear translocation of transcription factors such as NF- κ B. As seen above, NF- κ B activation was observed in a dose-dependent manner in normal and malignant mesothelial cells and RAW264.7 macrophages exposed to SWCNT (Pacurari et al., 2008; He et al., 2012), and in A549 epithelial lung cells exposed to MWCNT (Ye et al., 2009). TLR stimulation also up-regulates the expression of hundreds of genes in macrophages, and induces the expression of noncoding RNAs (Takeuchi and Akira, 2010). Helicase activity is required for the transcriptional regulation of all these pathways and, consequently, it is expected to be predominantly present in the network. The enrichment of the response to interferon gamma (IFN- γ) is also expected, as IFN- γ is a potent endogenous inducer of the pro-inflammatory type-1 phenotype in tissue macrophages via signal transducer and activator of transcription 1 (STAT1). STAT1 amplifies the signal of cytokines and enhances macrophage

TABLE III. KEGG pathways, 10 major GO biological processes and molecular functions identified in the 41-gene interaction network using Cytoscape, with a false discovery rate (FDR) of 0.1

Pathways in Network (KEGG)	<i>P</i> value	Nodes
NF-kappa B signaling pathway	8,07E-04	MYD88,LTB,BLNK,CCL19,CD14
B cell receptor signaling pathway	9,07E-04	CD72,BLNK,CD19
Pertussis	1,39E-03	MYD88,IRF1,CD14
Hematopoietic cell lineage	2,43E-03	CD2,CD19,CD14
Toll-like receptor signaling pathway	3,82E-03	CCL5,MYD88,CD14
Primary immunodeficiency	3,82E-03	BLNK,CD19
Top 10 Biological Processes (GO)	<i>P</i> value	Nodes
Positive regulation of interleukin-12 biosynthetic process	1,23E-04	LTB,IRF1
Positive regulation of tumor necrosis factor production	2,26E-04	CD2,CCL19,CD14
Positive regulation of endocytosis	6,60E-04	CCL19,CD14
Dendritic cell chemotaxis	7,56E-04	CCL5,CCL19
Cellular calcium ion homeostasis	8,32E-04	HEXB,CCL5,CCL19
Leukocyte cell-cell adhesion	1,33E-03	CCL5,NT5E
Positive regulation of calcium ion transport	1,75E-03	CCL5,P2RX4
Lymphocyte chemotaxis	2,07E-03	CCL5,CCL19
Regulation of chronic inflammatory response	2,66E-03	CCL5
Adenosine biosynthetic process	2,66E-03	NT5E
Top 10 Molecular Functions (GO)	<i>P</i> value	Nodes
Chemokine receptor binding	2,17E-04	CCL5,CCL19
Receptor binding	7,26E-04	CD72,CD2,LTB,UFD1L,P2RX4
Receptor signaling protein tyrosine kinase activator activity	2,66E-03	CCL5
Opsonin receptor activity	2,66E-03	CD14
Peptidoglycan receptor activity	2,66E-03	CD14
Chemokine receptor antagonist activity	2,66E-03	CCL5
TIR domain binding	2,66E-03	MYD88
Beta-N-acetylhexosaminidase activity	5,32E-03	HEXB
Chemokine activity	7,02E-03	CCL5,CCL19
5'-nucleotidase activity	7,96E-03	NT5E

responses to TLR ligands. IFN- γ can also inactivate feedback inhibitory loops, such as those mediated by IL-10 and STAT3. IFN- γ may be particularly important in early immune responses when the low IFN- γ concentrations transiently induce expression of a small subset of IFN- γ -inducible genes, including STAT1 that accumulates in primed macrophages, with concomitant activation of downstream STAT1-dependent genes and inflammatory functions (Boehm et al., 1997; Hu et al., 2008; Su et al., 2015).

All these results are compatible with the immunotoxic adverse effects that were reviewed above, and represent pathways that should be further investigated to test their relevance to the pulmonary toxicity of Mitsui-7. In this context, it should be recalled that Rimbach et al. (2000) reported that macrophages stimulated by IFN- γ increased NF- κ B transactivation in primary human endothelial cells, accompanied by an increase in the monocyte chemoattractant protein (MCP-1) mRNA, which in turn stimulates the monocyte recruitment into the arterial wall. It was suggested that the influx of stimulated monocytes into the subendothelial space could lead to endothelial dysfunction. Moreover, IFN- γ upregulates the expression of

TLR2–5 mRNA and accelerates the up-regulation the NF- κ B activation induced by PAMPs in biliary epithelial cells (Harada et al., 2006). It would be pertinent to investigate the relevance of these observed biological effects in the epithelial lung tissue.

In conclusion, the herein bioinformatics analysis of the transcriptomic data available in the literature has the potential of unveiling the molecular pathways of Mitsui-7 pathogenesis in the lungs, indicating future targets for investigating its mode of action. Conversely, the annotated pathways identified in this exercise, when considered in isolation from each other, may not allow differentiating Mitsui-7 exposure from that of other inhaled toxicants. In fact, the identification of a molecular signature of CNT exposure that could be useful as a specific biomarker would benefit from the comparison between these gene expression profiles and the ones produced by other inhaled materials, such as asbestos or carbon black, using a similar strategy. Snyder-Talkington et al. (2016a), using a transcriptomic approach, showed that MWCNT and asbestos affected different gene sets and related pathways, suggesting dissimilar modes of action, even though they produce similar major outcomes.

In line with the present findings, MWCNT exposure tended to impact on genes and pathways involved in immune responses (Snyder-Talkington et al., 2016a). Regarding carbon black, although the inflammatory and immune responses, or the chemokine signaling, are also among the up-regulated biological pathways identified in exposed C57/BL6 mice (intratracheal instillation), other up-regulated genes and related pathways were found, for example, those governing cholesterol and sterol metabolic processes that do not overlap the ones herein identified for Mitsui-7 (Bourdon et al., 2012). This may indicate that the above described expression profiles are globally associated with exposure to MWCNT with physicochemical properties similar to Mitsui-7, which can further contribute to a previously proposed grouping strategy (Braakhuis et al., 2016; Dekkers et al., 2016). On the other hand, the lack of reproducibility of the four supposedly similar transcriptomic studies analysed is worrying, and more studies with larger transcriptomic datasets are needed to validate these findings. Clearly, relevant doses and time points concerning human exposure should be harmonized to allow inter-comparability of the results.

Toxicoepigenomics

Several nanomaterials seem to cause epigenetic alterations (Stocco et al., 2013; Lu et al., 2016), and CNT have been shown to contribute to global DNA hypermethylation in A549 cells (Li et al., 2016). miRNA expression profiling is a frequent epigenetic research area. miRNAs are small non-coding RNAs (19–25 nucleotides) involved in nearly all key biological processes (Ha and Kim, 2014). They represent one of the oldest and broadest mechanisms of gene regulation, usually acting as endogenous repressors of gene activity via transcriptional repression and degradation of mRNA. Lung has a very specific miRNA expression profile, essential in its development and homeostasis. Several pulmonary diseases such as chronic obstructive pulmonary disease, asthma, cystic fibrosis, pulmonary hypertension and lung cancer have been associated with alterations in the expression of lung related miRNAs (Yanaihara et al., 2006; Rupani et al., 2013; Sessa and Hata, 2013). Effectively, serum and plasma miRNAs have been successfully evaluated in a wide range of solid cancers as promising biomarkers of early disease onset or relapse (Redova et al., 2013). For instance, several up- or down-regulated miRNAs have been reported in malignant mesothelioma tumors, and some of them have been suggested as potential biomarkers for histopathological subtyping of tumors (Guled et al., 2009; Busacca et al., 2010; Kubo et al., 2011; Ak et al., 2015) or as potential regulators of the adenoma to adenocarcinoma transition (Snyder-Talkington et al., 2016b). miRNA differential expression was also related to asbestos exposure, with 13 asbestos-related differentially-expressed miRNAs and corresponding target genes

identified, including over-expression of the squamous cell carcinoma-associated miR-205, linked to down-regulation of the *DOK4* gene (Nymark et al., 2011).

Few studies have been performed on the expression of miRNAs following exposure to CNT (Li et al., 2011; Dymacek et al., 2015; Snyder-Talkington et al., 2016b; Nymark et al., 2015). One of those studies applied SOLiD sequencing, a high-throughput deep sequencing method, to mouse embryo-derived NIH/3T3 cell small RNAs. After filtering the sequencing reads and comparing with miRBase database, the research ended up with 172 altered miRNAs (Li et al., 2011). In another study, the chosen technique was a microarray containing 704 mouse miRNA probes covering 714 mature miRNAs (Dymacek et al., 2015).

When the results of one-day exposure to MWCNT obtained in the Dymacek et al. (2015) study are compared with those of the Li et al. (2011) study for 100 and 80 µg, respectively, the microarray technique identified only eight miRNAs *versus* the 172 miRNAs identified in the SOLiD sequencing study. From these eight miRNAs, only five were shared by both studies (miR-125b, miR-223, miR-296, miR-29b, and miR-382). Nevertheless, Li et al. (2011) used an *in vitro* system with NIH/3T3 cells, whereas Dymacek et al. (2015) performed an *in vivo* study with total RNA extracted from frozen mouse lung tissue. Thus, the discrepant miRNAs can be related to cell/tissue specificity. Furthermore, although miR-1275 is a possible key regulator of the BEAS-2B cells mitochondrial membrane potential decrease after exposure to MWCNT and asbestos fibers (Nymark et al., 2015), it was not identified in the two other referred studies. Moreover, from the three other differently expressed miRNA of the Nymark et al. (2015) study (miR-1225-5p, miR-29b-1-5p, and miR-4672) only one is in the above-mentioned five shared miRNAs.

miRNAs are highly sensitive, reproducible, specific and stable in serum (Chen et al., 2008). Therefore, epigenomic studies targeting miRNAs are a promising area of research aiming to identify biomarkers suitable for monitoring human exposure, especially in occupational settings. For example, in mouse, serum miR-122 demonstrated a sensitivity at least as good as alanine aminotransferase and aspartate aminotransferase to predict liver adverse effects induced by silica (nSP70; Nagano, Higashisaka, and Kunieda, 2013) and miR-103 has been already suggested as a possible biomarker for mesothelioma using the cellular fraction of human peripheral blood (Bru et al., 2012). Cancer-specific miRNA expression profiles in whole blood samples are not determined by a single cell type, for example, leukocytes of lung cancer patients show a cancer-specific miRNA expression profile, including the up-regulation of miR-21, which is associated with poor lung cancer prognosis (Leidinger et al., 2014).

Regarding MWCNT, the study of whole blood collected from mice after inhalation exposure has correlated the *FCRL5* gene and miR-122-5p to the presence of hyperplasia, the *MTHFD2* gene and miR-206-3p to the presence of fibrosis, the *FAM178A* gene and miR-130a-3p to the presence of bronchiolo-alveolar adenoma, and the *IL7R* gene and miR-210-3p to the presence of bronchiolo-alveolar adenocarcinoma, among others (Snyder-Talkington et al., 2016b). These miRNA changes are potential blood biomarkers for MWCNT-induced lung pathological changes.

In the near future, miRNA profiling in biological samples may become a tool to identify exposure to individual, or to groups of similar toxicants. As the above-mentioned studies seem to point out, for example, the Li et al. (2011) study, CNT exposure apparently causes up- or down-regulation of cellular pathways through differential miRNA expression. If these cellular pathways are specific, individually or as a whole, these miRNA profiles can be useful as biomarkers of exposure to individual CNT or to CNT with similar physicochemical properties. In addition, bioinformatics tools are being continuously developed to facilitate the establishment of a linkage between the miRNAs identified, the mRNAs they regulate, and the corresponding genes. Therefore, the molecular and biological pathways that are involved in the response to xenobiotics can be elucidated through miRNA research. In fact, the relationship between specific miRNAs and adverse outcomes has already been established in lung cancer, as discussed above, although in many cases, the precise mechanisms underlying miRNA up- or down-regulation remain unknown.

CONCLUSIONS AND PROSPECTS

Toxicological data from *in vitro* and *in vivo* studies have suggested that some CNT represent a risk factor for respiratory disease that may parallel that of asbestos. Current knowledge of the high morbidity and mortality associated with the past occupational exposure to asbestos prompts the need for a thorough risk assessment of CNT to allow risk management by regulatory authorities. Furthermore, the lack of molecular biomarkers suitable for exposure and biological effects assessment, before the onset of potential disease, makes CNT biomonitoring evenly difficult, particularly in the context of occupational exposure. New hopes have arisen with the development of genomic high-throughput technologies, although the "omics" data presently available are still complex and hard to interpret. Nevertheless, in this review it is shown that their meta-analysis can prove to be a valuable tool to discover unique expression patterns, and to identify consistent molecular and biological pathways involved in lung pathology from CNT exposure. Furthermore, in

terms of mechanistic investigation, it will be important to further elucidate how the molecular pathways identified in this analysis contribute to the pulmonary toxicity of CNT, for example, provide new insights on the relevance of Toll-like receptor signaling, NF- κ B activation, or response to IFN- γ to the adverse effects of CNT. This knowledge can allow grouping approaches towards CNT clustering according to their similar mode of action, and contribute to a safer CNT design through the modification of the properties identified as more critical to their toxicity, for example, their surface area or functionalization. Although the epigenomic data are still scarce, CNT have been shown to contribute to global DNA hypermethylation, and the differentially expressed miRNA can have a potential role in the identification of affected regulatory pathways and even as biomarkers for occupational health studies. However, if the difficulty to compare the "omics" findings from *in vitro* studies and *in vivo* studies has been highlighted, other difficulty to overcome is the extrapolation of results between species. Another pertinent topic for research would be to find out the role of polymorphisms in genes involved in DNA damage repair pathways as modifiers of the individual susceptibility to the adverse effects of CNT exposure. However, it should not be forgotten that this potential usefulness of biomarkers for risk management and health protection in the workplace can be misused for worker selection and discrimination. Thus, an appropriate ethical framework should be put in place before its application, ensuring personal data confidentiality.

Nevertheless, all genomic and epigenomic information will need to be first validated through data gathered from workers with known levels of exposure to CNT. Only then, the most needed development of reliable omics-based biomarkers to allow an early detection of potential health impacts and the implementation of preventive or mitigating strategies will be achievable. This reinforces the need for biomonitoring studies in occupational settings.

STATEMENT OF AUTHOR CONTRIBUTIONS

All authors contributed to the literature review and manuscript writing. In addition, Célia Ventura performed the critical analysis of the toxicogenomics data herein reviewed and the functional gene network and gene ontology enrichment analysis.

ACKNOWLEDGMENTS

The authors acknowledge Dr. Luís Vieira from the Technology and Innovation Unit of INSA for the support on the bioinformatics. This research was co-funded by the Centre for Toxicogenomics and Human Health (ToxOmics) and the Foundation for Science and Technology (UID/BIM/00009/2013).

CONFLICTS OF INTEREST

The authors declare that there are no conflicts of interest.

REFERENCES

- Aardema MJ, Macgregor JT. 2002. Toxicology and genetic toxicology in the new era of 'toxicogenomics': Impact of '-omics' technologies. *Mutat Res* 499:13–25.
- Ak G, Tomaszek SC, Kosari F, Metintas M, Jett JR, Metintas S, Yildirim H, Dundar E, Dong J, Aubry MC, et al. 2015. Micro-RNA and mRNA features of malignant pleural mesothelioma and benign asbestos-related pleural effusion. *Biomed Res Int* 635748: 1–8.
- Alazzam A, Mfoumou E, Stiharu I, Kassab A, Darnel A, Yasmeen A, Sivakumar N, Bhat R, Al Moustafa A. 2010. Identification of deregulated genes by single wall carbon-nanotubes in human normal bronchial epithelial cells. *Nanomedicine* 6:563–569.
- Aldieri E, Fenoglio I, Cesano F, Gazzano E, Gulino G, Scarano D, Mazzucco G, Ghigo D, Fubini B. 2013. The role of iron impurities in the toxic effects exerted by short multiwalled carbon nanotubes (MWCNT) in murine alveolar macrophages. *J Toxicol Env Heal A* 76:1056–1071.
- Azqueta A, Slyskova J, Langie SAS, Gaivão IO, Collins A. 2014. Comet assay to measure DNA repair: Approach and applications. *Front Genet* 5:288.
- Birrell MA, Eltom S. 2011. The role of the NLRP3 inflammasome in the pathogenesis of airway disease. *Pharmacol Ther* 130:364–370.
- Boehm U, Klamp T, Groot M, Howard JC. 1997. Cellular responses to interferon- γ . *Annu Rev Immunol* 15:749–795.
- Borm PJA, Robbins D, Haubold S, Kuhlbusch T, Fissan H, Donaldson K, Schins R, Stone V, Kreyling W, Lademann J, et al. 2006. The potential risks of nanomaterials: A review carried out for ECE-TOC. *Part Fibre Toxicol* 3:11.
- Bourdon JA, Halappanavar S, Saber AT, Jacobsen NR, Williams A, Wallin H, Vogel U, Yauk CL. 2012. Hepatic and pulmonary toxicogenomic profiles in mice intratracheally instilled with carbon black nanoparticles reveal pulmonary inflammation, acute phase response, and alterations in lipid homeostasis. *Toxicol Sci* 127: 474–484.
- Braakhuis HM, Oomen AG, Cassee FR. 2016. Grouping nanomaterials to predict their potential to induce pulmonary inflammation. *Toxicol Appl Pharm* 299:3–7.
- Broadbush VC, Everitt JI, Black B, Kane AB. 2011. Non-neoplastic and neoplastic pleural endpoints following fiber exposure. *J Toxicol Env Heal B* 14:153–178.
- Brown DM, Kinloch IA, Bangert U, Windle AH, Walters DM, Walker GS, Scotchford CA, Donaldson K, Stone V. 2007. An in vitro study of the potential of carbon nanotubes and nanofibres to induce inflammation mediators and frustrated phagocytosis. *Carbon* 45:1743–1756.
- Bru T, Weber DG, JohnenBryk GO, Jo K. 2012. Identification of miRNA-103 in the cellular fraction of human peripheral blood as a potential biomarker for malignant mesothelioma – A pilot study. *PLOS One* 7:1–9.
- Busacca S, Germano S, De Cecco L, Rinaldi M, Comoglio F, Favero F, Murer B, Mutti L, Pierotti M, Gaudino G. 2010. MicroRNA signature of malignant mesothelioma with potential diagnostic and prognostic implications. *Am J Resp Cell Mol* 42:312–319.
- Bushel PR, Heinloth AN, Li J, Huang L, Chou JW, Boorman GA, Malarkey DE, Houle CD, Ward SM, Wilson RE, et al. 2007. Blood gene expression signatures predict exposure levels. *P Natl Acad Sci USA* 104:18211–18216.
- Casey A, Herzog E, Lyng FM, Byrne HJ, Chambers G, Davoren M. 2008. Single walled carbon nanotubes induce indirect cytotoxicity by medium depletion in A549 lung cells. *Toxicol Lett* 179:78–84.
- Chatterjee N, Yang J, Kim H, Jo E, Kim P, Choi K, Choi J. 2014. Potential toxicity of differential functionalized multiwalled carbon nanotubes (MWCNT) in human cell line (BEAS2B) and *Caenorhabditis Elegans*. *J Toxicol Env Heal A* 77:1399–1408.
- Chen D, Stueckle TA, Luanpitpong S, Rojanasakul Y, Lu Y, Wang L. 2015. Gene expression profile of human lung epithelial cells chronically exposed to single-walled carbon nanotubes. *Nanoscale Res Lett* 10:12.
- Chen X, Ba Y, Ma L, Cai X, Yin Y, Wang K, Guo J, Zhang Y, Guo X, Li Q, et al. 2008. Characterization of microRNAs in serum: A novel class of biomarkers for diagnosis of cancer and other diseases. *Cell Res* 18:997–1006.
- Crapo JD, Young SL, Fram EK, Pinkerton KE, Barry BE, Crapo RO. 1983. Morphometric Characteristics of Cells in the Alveolar Region of Mammalian Lungs. *Am Rev Respir Dis* 128:S42–S46.
- Croft D, Mundo AF, Haw R, Milacic M, Weiser J, Wu G, Caudy M, Garapati P, Gillespie M, Kamdar MR, Jassal B, Jupe S, Matthews L, May B, Palatnik S, Rothfels K, Shamovsky V, Song H, Williams M, Birney E, Hermjakob H, Stein L, D'Eustachio P. 2014. The reactome pathway knowledgebase. *Nucleic Acids Res* 42:D472–D477.
- Dearfield KL, Gollapudi BB, Bemis JC, Benz RD, Douglas GR, Elespuru RK, Johnson GE, Kirkland DJ, LeBaron MJ, Li AP, Marchetti F, Pottenger LH, Rorie E, Tanir JY, Thybaud V, van Benthem J, Yauk CL, Zeiger E, Luijten M. 2017. Next generation testing strategy for assessment of genomic damage: A conceptual framework and considerations. *Environ Mol Mutagen* 58: 264–283.
- Dekkers S, Oomen AG, Bleeker EAJ, Vandebriel RJ, Micheletti C, Cabellos J, Janer G, Fuentes N, Vázquez-Campos S, Borges T, Silva MJ, Prina-mello A, Movia D, Nesslany F, Ribeiro AR, Leite PE, Groenewold M, Cassee FR, Sips AJAM, Dijkzeul A, van Teunenbroek T, Wijnhoven SWP. 2016. Towards a nanospecific approach for risk assessment. *Regul Toxicol Pharmacol* 80: 46–59.
- Donaldson K, Stone V, Tran CL, Kreyling W, Borm PJA. 2004. Nanotoxicology. *Occup Env Med* 61:727–728.
- Donaldson K, Murphy FA, Duffin R, Poland CA. 2010. Asbestos, carbon nanotubes and the pleural mesothelium: A review of the hypothesis regarding the role of long fibre retention in the parietal pleura, inflammation and mesothelioma. *Part Fibre Toxicol* 7:5.
- Donaldson K, Poland CA, Murphy FA, MacFarlane M, Chernova T, Schinwald A. 2013. Pulmonary toxicity of carbon nanotubes and asbestos – Similarities and differences. *Adv Drug Deliver Rev* 65:2078–2086.
- Dymacek J, Snyder-Talkington BN, Porter DW, Mercer RR, Wolfarth MG, Castranova V, Qian Y, Guo NL, Virginia W. 2015. mRNA and miRNA regulatory networks reflective of multi-walled carbon nanotube-induced lung inflammatory and fibrotic pathologies in mice. *Toxicol Sci* 144:51–64.
- Fabregat A, Sidiropoulos K, Garapati P, Gillespie M, Hausmann K, Haw R, Jassal B, Jupe S, Korninger F, McKay S, et al. 2016. The reactome pathway knowledgebase. *Nucleic Acids Res* 44:D481–D487.
- Guled M, Lahti L, Lindholm PM, Salmenkivi K, Bagwan I, Nicholson AG, Knuutila S. 2009. CDKN2A, NF2, and JUN are dysregulated among other genes by miRNAs in malignant mesothelioma – A miRNA microarray analysis. *Genes Chromosomes Cancer* 48:615–623.
- Guo NL, Wan Y, Denvir J, Porter DW, Pacurari M, Wolfarth MG, Castranova V, Qian Y. 2012. Multiwalled carbon nanotube-

- induced gene signatures in the mouse lung: Potential predictive value for human lung cancer risk and prognosis. *J Toxicol Env Heal A* 75:1129–1153.
- Ha M, Kim VN. 2014. Regulation of microRNA biogenesis. *Nat Rev Mol Cell Bio* 15:509–524.
- Harada K, Isse K, Nakanuma Y. 2006. Interferon gamma accelerates NF-Kappa B activation of biliary epithelial cells induced by Toll-like receptor and ligand interaction. *J Clin Pathol* 59:184–190.
- He X, Young S, Fernback JE, Ma Q. 2012. Single-walled carbon nanotubes induce fibrogenic effect by disturbing mitochondrial oxidative stress and activating NF- κ B signaling. *J Clin Toxicol Suppl* 5.
- Hitoshi K, Katoh M, Suzuki T, Ando Y, Nadai M. 2012. Changes in expression of drug-metabolizing enzymes by single-walled carbon nanotubes in human respiratory tract cells. *Drug Metab Dispos* 40:579–587.
- Hsieh WY, Chou CC, Ho CC, Yu SL, Chen HY, Chou HY, Chou HY, Chen J, Chen HW, Yang PC. 2012. Single-walled carbon nanotubes induce airway hyperreactivity and parenchymal injury in mice. *Am J Respir Cell Mol Biol* 46:257–267.
- Hu X, Chakravarty SD, Ivashkiv LB. 2008. Regulation of IFN and TLR signalling during macrophage activation by opposing feed-forward and feedback inhibition mechanisms. *Immunol Rev* 226:41–56.
- Huax F, d'Ursel de Bousies V, Parent MA, Orsi M, Uwambayinema F, Devosse R, Ibouaadaten S, Yakoub Y, Panin N, Palmi-Pallag M, et al. 2016. Mesothelioma response to carbon nanotubes is associated with an early and selective accumulation of immunosuppressive monocytic cells. *Part Fibre Toxicol* 13:46.
- Hussain S, Sangtian S, Anderson SM, Snyder RJ, Marshburn JD, Rice AB, Bonner JC, Garantzios S. 2014. Inflammasome activation in airway epithelial cells after multi-walled carbon nanotube exposure mediates a profibrotic response in lung fibroblasts. *Part Fibre Toxicol* 11:28.
- IARC (International Agency for Research on Cancer). IARC monographs vol. 111 (2014) Some nanomaterials and some fibres. IARC working group on the evaluation of carcinogenic risks to humans. Lyon; France.
- Iavicoli I, Leso V, Manno M, Schulte PA. 2014. Biomarkers of nanomaterial exposure and effect: Current status. *J Nanopart Res* 16:2302.
- Im H, Ammit AJ. (2014) The NLRP3 inflammasome: role in airway inflammation. *Clin Exp Allergy* 44:160–172.
- ISO (International Standardization Organization) (2011) ISO/TS 80004-4: 2011 Nanotechnologies – Vocabulary – Part 4: Nanostructured Materials. ISO/TS 80004-4:2011. Geneva, Switzerland.
- Jackson P, Kling K, Jensen KA, Clausen PA, Madsen AM, Wallin H, Vogel U. 2015. Characterization of genotoxic response to 15 multiwalled carbon nanotubes with variable physicochemical properties including surface functionalizations in the FE1-Muta(TM) mouse lung epithelial cell line. *Environ Mol Mutagen* 56:183–203.
- Kagan VE, Kapralov AA, St. Croix CM, Watkins SC, Kisin ER, Kotchey GP, Balasubramanian K, Vlasova II, Yu J, Kim K, et al. 2014. Lung macrophages digest carbon nanotubes using a superoxide/peroxynitrite oxidative pathway. *ACS Nano* 8:5610–5621.
- Kasai T, Umeda Y, Ohnishi M, Mine T, Kondo H, Takeuchi T, Matsumoto M, Fukushima S. 2016. Lung carcinogenicity of inhaled multiwalled carbon nanotube in rats. *Part Fibre Toxicol* 13:53.
- Kim J, Lim H, Minai-tehrani A, Kwon J, Woo C, Choi M, Baek J, Jeong DH, Ha Y, Chae C, et al. 2010. Toxicity and clearance of intratracheally administered multiwalled carbon nanotubes from murine lung. *J Toxicol Env Heal A* 73:1530–1543.
- Kim JS, Choi YC, Yu IJ, Song KS, Bang IS, Lee JK, Kang CS. 2012. Toxicogenomic comparison of multi-wall carbon nanotubes (MWCNTs) and asbestos. *Arch Toxicol* 86:553–562.
- Kinaret P, Marwah V, Fortino V, Ilves M, Wolff H, Ruokolainen L, Auvinen P, Savolainen K, Alenius H, Greco D. 2017. Network analysis reveals similar transcriptomic responses to intrinsic properties of carbon nanomaterials in vitro and in vivo. *ACS Nano* 11:3786–3796.
- Kisin ER, Murray AR, Sargent L, Lowry D, Chirila M, Siegrist KJ, Schwegler-berry D, Leonard S, Castranova V, Fadeel B, et al. 2011. Genotoxicity of carbon nano fibers: Are they potentially more or less dangerous than carbon nanotubes or asbestos? *Toxicol Appl Pharm* 252:1–10.
- Kisin ER, Murray AR, Keane MJ, Shi X, Gorelik O, Arepalli S, Castranova V, Wallace WE, Kagan VE, Shvedova AA. 2007. Single-walled carbon nanotubes: Geno- and cytotoxic effects in lung fibroblast V79 cells. *J Toxicol Env Heal A* 70:2071–2079.
- Klein CL, Wiench K, Wiemann M, Ma-Hock L, Van Ravenzwaay B, Landsiedel R. 2012. Hazard identification of inhaled nanomaterials: Making use of short-term inhalation studies. *Arch Toxicol* 86:1137–1151.
- Kreyling WG, Semmler-Behnke M, Möller W. 2006. Health implications of nanoparticles. *J Nanopart Res* 8:543–562.
- Kreyling WG. 1990. Interspecies Comparison of Lung Clearance of "Insoluble" Particles. *J Aerosol Med* 3:S-93–S-110.
- Kubo T, Toyooka S, Tsukuda K, Sakaguchi M, Fukazawa T, Soh J, Asano H, Ueno T, Muraoka T. 2011. Epigenetic silencing of microRNA-34b/c plays an important role in the pathogenesis of malignant pleural mesothelioma. *Clin Cancer Res* 17:4965–4975.
- Labib S, Williams A, Yauk CL, Nikota JK, Wallin H, Vogel U, Halappanavar S. 2016. Nano-risk science: Application of toxicogenomics in an adverse outcome pathway framework for risk assessment of multi-walled carbon nanotubes. *Part Fibre Toxicol* 13:15.
- Lam CW, James JT, McCluskey R, Hunter RL. 2004. Pulmonary toxicity of single-wall carbon nanotubes in mice 7 and 90 days after intratracheal instillation. *Toxicol Sci* 77:126–134.
- Landsiedel R, Sauer UG, Ma-hock L, Schneckeburger J, Wiemann M. 2014. Pulmonary toxicity of nanomaterials: A critical comparison of published in vitro assays and in vivo inhalation or instillation studies. *Nanomedicine (London)* 9:2557–2585.
- Lanone S, Andujar P, Kermandizadeh A, Boczkowski J. 2013. Determinants of carbon nanotube toxicity. *Adv Drug Deliv Rev* 65:2063–2069.
- Laux P, Riebeling C, Booth AM, Brain JD, Brunner J, Cerrillo C, Creutzenberg O, Estrela-Lopis I, Gebel T, Johanson G, Jungnickel H, Kock H, Tentschert J, Tlili A, Schäffer A, Sips AJAM Yokel RA, Luch A. 2017. Biokinetics of nanomaterials: The role of biopersistence. *NanoImpact* 6:69–80.
- Leidinger P, Backes C, Dahmke IN, Galata V, Huwer H, Stehle I, Bals R, Keller A, Meese E. 2014. What makes a blood cell based miRNA expression pattern disease specific? - A miRNome analysis of blood cell subsets in lung cancer patients and healthy controls. *Oncotarget* 5:9484–9497.
- Li S, Wang H, Qi Y, Tu J, Bai Y, Tian T, Huang N, Wang Y, Xiong F, Lu Z, Xiao Z. 2011. Biomaterials assessment of nanomaterial cytotoxicity with SOLiD sequencing-based microRNA expression profiling. *Biomaterials* 32:9021–9030.
- Li J, Tian M, Cui L, Dwyer J, Fullwood NJ, Shen H, Martin LF. 2016. Low-dose carbon-based nanoparticle-induced effects in A549 lung cells determined by biospectroscopy are associated with increases in genomic methylation. *Sci Rep* 6:20207.
- Lindberg HK, Falck GC, Singh R, Suhonen S, Järventaus H, Vanhala E, Catalán J, Farmer PB, Savolainen KM, Norppa H. 2013.

- Genotoxicity of short single-wall and multi-wall carbon nanotubes in human bronchial epithelial and mesothelial cells in vitro. *Toxicology* 313:24–37.
- Louro H, Pinhão M, Santos J, Tavares A, Vital N, Silva MJ. 2016. Evaluation of the cytotoxic and genotoxic effects of benchmark multi-walled carbon nanotubes in relation to their physicochemical properties. *Toxicol Lett* 262:123–134.
- Lu X, Miousse IR, Pirela SV, Melnyk S, Koturbash I, Demokritou P. 2016. Short-term exposure to engineered nanomaterials affects cellular epigenome. *Nanotoxicology* 10:140–150.
- Luanpitpong S, Wang L, Castranova V, Rojanasakul Y. 2014. Induction of stem-like cells with malignant properties by chronic exposure of human lung epithelial cells to single-walled carbon nanotubes. *Part Fibre Toxicol* 11:22.
- Mercer RR, Scabilloni J, Wang L, Kisin E, Murray AR, Schwegler-Berry D, Shvedova AA, Castranova V. 2008. Alteration of deposition pattern and pulmonary response as a result of improved dispersion of aspirated single-walled carbon nanotubes in a mouse model. *Am J Physiol - Lung C* 294:87–97.
- Mercer RR, Hubbs AF, Scabilloni JF, Wang L, Battelli LA, Friend S, Castranova V, Porter DW. 2011. Pulmonary fibrotic response to aspiration of multi-walled carbon nanotubes. *Part Fibre Toxicol* 8:1–11.
- Mercer RR, Scabilloni JF, Hubbs AF, Battelli LA, McKinney W, Friend S, Wolfarth MG, Andrew M, Castranova V, Porter DW. 2013. Distribution and fibrotic response following inhalation exposure to multi-walled carbon nanotubes. *Part Fibre Toxicol* 10:33–47.
- Mercer RR, Scabilloni JF, Hubbs AF, Wang L, Battelli LA, McKinney W, Castranova V, Porter DW. 2013b. Extrapulmonary transport of MWCNT following inhalation exposure. *Part Fibre Toxicol* 10:38.
- Miller FJ, Mercer RR, Crapo JD. 1993. Lower respiratory tract structure of laboratory animals and humans: Dosimetry implications. *Aerosol Sci Technol* 18:257–271.
- Monopoli MP, Åberg C, Salvati A, Dawson KA. 2012. Biomolecular coronas provide the biological identity of nanosized materials. *Nat Nanotechnol* 7:779–786.
- Muller J, Decordier I, Hoet PH, Thomassen L, Lison D, Kirsch-volders M. 2008. Clastogenic and aneugenic effects of multi-wall carbon nanotubes in epithelial cells. *Carcinogenesis* 29:427–433.
- Murphy FA, Schinwald A, Poland CA, Donaldson K. 2012. The mechanism of pleural inflammation by long carbon nanotubes: Interaction of long fibres with macrophages stimulates them to amplify pro-inflammatory responses in mesothelial cells. *Part Fibre Toxicol* 9:8.
- Murphy FA, Poland CA, Duffin R, Al-Jamal KT, Ali-Boucetta H, Nunes A, Byrne F, Prina-Mello A, Volkov Y, Li S, et al. 2011. Length-dependent retention of carbon nanotubes in the pleural space of mice initiates sustained inflammation and progressive fibrosis on the parietal pleura. *Am J Pathol* 178:2587–2600.
- Nagai H, Okazaki Y, Chew S, Misawa N, Yamashita Y, Akatsuka S, Ishihara T, Yamashita K, Yoshikawa Y, Yasuic H, et al. 2011. Diameter and rigidity of multiwalled carbon nanotubes are critical factors in mesothelial injury and carcinogenesis. *Proc Natl Acad Sci Usa* 108:E1330–E1338.
- Nagano T, Higashisaka K, Kunieda A. 2013. Liver-specific micRNAs as biomarkers of nanomaterial-induced liver damage. *Nanotechnology* 24:405102.
- Nardo DD, Nardo CMD, Latz E. 2014. New insights into mechanisms controlling the NLRP3 inflammasome and its role in lung disease. *Am J Pathol* 184:42–54.
- Newton RK, Aardema M, Aubrecht J. 2004. The utility of DNA microarrays for characterizing genotoxicity. *Environ Health Persp* 112:420–422.
- NIOSH (National Institute for Occupational Safety and Health). 2013. NIOSH publication 2013-145. CIB 65: Occupational Exposure to Carbon Nanotubes and Nanofibers.
- Nymark P, Guled M, Borze I, Faisal A, Lahti L, Salmenkivi K. 2011. Integrative analysis of microRNA, mRNA and aCGH data reveals asbestos- and histology-related changes in lung cancer. *Gene Chromosome Canc* 50:585–597.
- Nymark P, Wijshoff P, Cavill R, van Herwijnen M, Coonen MLJ, Claessen S, Catalán J, Norppa H, Kleinjans JCS, Briedé JJ. 2015. Extensive temporal transcriptome and microRNA analysis identify molecular mechanisms underlying mitochondrial dysfunction induced by multi-walled carbon nanotubes in human lung cells. *Nanotoxicology* 9:624–635.
- Nuwaysir EF, Bittner M, Trent J, Barrett JC, Afshari CA. 1999. Microarrays and toxicology: The advent of toxicogenomics. *Mol Carcinog* 24:153–159.
- Oberdörster G, Castranova V, Asgharian B, Sayre P. 2015. Inhalation exposure to carbon nanotubes (CNT) and carbon CNT (CNF): Methodology and dosimetry. *J Toxicol Env Heal B* 18:121–212.
- Oberdörster G. 2010. Safety assessment for nanotechnology and nanomedicine: Concepts of nanotoxicology. *J Intern Med* 267:89–105.
- Oberdörster G, Maynard A, Donaldson K, Castranova V, Fitzpatrick J, Ausman K, Carter J, Karn B, Kreyling W, Lai D, Olin S, Monteiro-Riviere N, Warheit D, Yang H, and A Report from the ILSI Research Foundation/Risk Science Institute Nanomaterial Toxicity Screening Working Group. 2005b. Principles for characterizing the potential human health effects from exposure to nanomaterials: Elements of a screening strategy. *Part Fibre Toxicol* 2:8.
- Oberdörster G, Oberdörster E, Oberdörster J. 2005a. Nanotoxicology: An emerging discipline evolving from studies of ultrafine particles. *Environ Health Persp* 113:823–839.
- Pacurari M, Qian Y, Porter DW, Wolfarth M, Wan Y, Luo D, Ding M, Castranova V, Guo NL. 2011. Multi-walled carbon nanotube-induced gene expression in the mouse lung: Association with lung pathology. *Toxicol Appl Pharm* 255:18–31.
- Pacurari M, Castranova V, Vallyathan V. 2010. Single- and multi-wall carbon nanotubes versus asbestos: Are the carbon nanotubes a new health risk to humans? *J Toxicol Env Heal A* 73:378–395.
- Pacurari M, Yin XJ, Zhao J, Ding M, Leonard SS, Schwegler-Berry D, Ducatman B, Sbarra SD, Hoover MD, Castranova V, Vallyathan V. 2008. Raw single-wall carbon nanotubes induce oxidative stress and activate MAPKs, AP-1, NF- κ B, and Akt in normal and malignant human mesothelial cells. *Environ Health Persp* 116:1211–1217.
- Palomaki J, Valimäki E, Sund J, Vippola M, Clausen PA, Jensen KA, Savolainen K, Matikainen S, Alenius H. 2011. Long, needle-like carbon nanotubes and asbestos activate the NLRP3 inflammasome through a similar mechanism. *ACS Nano* 5:6861–6870.
- Porter DW, Hubbs AF, Mercer RR, Wu N, Wolfarth MG, Sriram K, Leonard S, Battelli L, Schwegler-Berry D, Friend S, et al. 2010. Mouse pulmonary dose- and time course-responses induced by exposure to multi-walled carbon nanotubes. *Toxicology* 269:136–147.
- Poulsen SS, Jackson P, Kling K, Knudsen KB, Kyjovska ZO, Thomsen BL, Clausen PA, Atluri R, Berthing T, Bengtson S, et al. 2016. Multi-walled carbon nanotube physicochemical properties predict pulmonary inflammation and genotoxicity. *Nanotoxicology* 7:1–13.
- Poulsen SS, Saber AT, Williams A, Andersen O, Købler C, Atluri R, Pozzebon ME, Mucelli SP, Simion M, Rickerby D, et al. 2015. MWCNTs of different physicochemical properties cause similar inflammatory responses, but differences in transcriptional and histological markers of fibrosis in mouse lungs. *Toxicol Appl Pharm* 284:16–32.

- Poulsen SS, Jacobsen NR, Labib S, Wu D, Husain M, Bøgelund JP, Andersen O, Købler C, Møhlave K, Kyjovska ZO, et al. 2013. Transcriptomic analysis reveals novel mechanistic insight into murine biological responses to multi-walled carbon nanotubes in lungs and cultured lung epithelial cells. *PLOS One* 8:1–25.
- Puhakka A, Ollikainen T, Soini Y, Kahlos K, Säily M. 2002. Modulation of DNA single-strand breaks by intracellular glutathione in human lung cells exposed to asbestos fibers. *Mutat Res* 514:7–17.
- Ravichandran P, Periyakaruppan A, Sadanandan B, Ramesh V, Hall JC, Jejelowo O, Ramesh GT. 2009. Induction of apoptosis in rat lung epithelial cells by multiwalled carbon nanotubes. *J Biochem Mol Toxicol* 23:333–344.
- Redova M, Sana J, Slaby O. 2013. Circulating miRNAs as new blood-based biomarkers for solid cancers. *Future Oncol* 9:387–402.
- Rimbach G, Valacchi G, Caneli R, Virgili F. 2000. Macrophages stimulated with IFN-gamma activate NF-kappa B and induce MCP-1 gene expression in primary human endothelial cells. *Mol Cell Biol Res Commun* 3:238–242.
- Rittinghausen S, Hackbarth A, Creutzenberg O, Ernst H, Heinrich U, Leonhardt A, Schaudien D. 2014. The carcinogenic effect of various multi-walled carbon nanotubes (MWCNTs) after intraperitoneal injection in rats. *Part Fibre Toxicol* 11:59–77.
- Rupani H, Sanchez-elsner T, Howarth P. 2013. MicroRNAs and respiratory diseases. *Eur Respir J* 41:695–705.
- Sager TM, Wolfarth MW, Battelli LA, Leonard SS, Andrew M, Steinbach T, Endo M, Tsuruoka S, Porter DW, Castranova V. 2013. Investigation of the pulmonary bioactivity of double-walled carbon nanotubes. *J Toxicol Env Heal A* 76:922–936.
- Sakamoto Y, Nakae D, Fukumori N, Tayama K. 2009. Induction of mesothelioma by a single intrascrotal administration of multi-wall carbon nanotube in intact male Fischer 344 rats. *J Toxicol Sci* 34:65–76.
- Sargent LM, Porter DW, Staska LM, Hubbs AF, Lowry DT, Battelli L, Siegrist KJ, Kashon ML, Mercer RR, Bauer AK, et al. 2014. Promotion of lung adenocarcinoma following inhalation exposure to multi-walled carbon nanotubes. *Part Fibre Toxicol* 11:1–18.
- Sessa R, Hata A. 2013. Role of microRNAs in lung development and pulmonary diseases. *Pulm Circ* 3:315–328.
- Shannon P, Markiel A, Ozier O, Baliga NS, Wang JT, Ramage D, Amin N, Schwikowski B, Ideker T. 2003. Cytoscape: A software environment for integrated models of biomolecular interaction networks. *Genome Res* 13:2498–2504.
- Shvedova AA, Kisin E, Murray AR, Johnson VJ, Gorelik O, Arepalli S, Hubbs AF, Mercer RR, Keohavong P, Sussman N, et al. 2008. Inhalation vs aspiration of single-walled carbon nanotubes in C57BL/6 mice: Inflammation, fibrosis, oxidative stress, and mutagenesis. *Am J Physiol - Lung C* 295:552–565.
- Shvedova AA, Kisin ER, Mercer R, Murray AR, Johnson VJ, Potapovich AI, Tyurina YY, Gorelik O, Arepalli S, Schwegler-Berry D, et al. 2005. Unusual inflammatory and fibrogenic pulmonary responses to single-walled carbon nanotubes in mice. *Am J Physiol - Lung C* 289:L698–L708.
- Shvedova AA, Yanamala N, Kisin ER, Tkach AV, Murray AR, Hubbs A, Chirila MM, Keohavong P, Sycheva LP, Kagan VE, Castranova V. 2014. Long-term effects of carbon containing engineered nanomaterials and asbestos in the lung: One-year postexposure comparisons. *Am J Physiol - Lung C* 306:170–182.
- Siegrist KJ, Reynolds SH, Kashon ML, Lowry DT, Dong C, Hubbs AF, Young S, Salisbury JL, Porter DW, Benkovic SA, et al. 2014. Genotoxicity of multi-walled carbon nanotubes at occupationally relevant doses. *Part Fibre Toxicol* 11:6–21.
- Snyder-Talkington BN, Dong C, Porter DW, Ducatman B, Wolfarth MG, Andrew M, Battelli L, Raese R, Castranova V, Guo NL, Qian Y. 2016a. Multiwalled carbon nanotube-induced pulmonary inflammatory and fibrotic responses and genomic changes following aspiration exposure in mice: A 1-year postexposure study. *J Toxicol Env Heal A* 79:352–366.
- Snyder-Talkington BN, Dong C, Sargent LM, Porter DW, Staska LM, Hubbs AF, Raese R, McKinney W, Chen BT, Battelli L, et al. 2016b. mRNAs and miRNAs in whole blood associated with lung hyperplasia, fibrosis, and bronchiolo-alveolar adenoma and adenocarcinoma after multi-walled carbon nanotube inhalation exposure in mice. *J Appl Toxicol* 36:161–174.
- Snyder-Talkington BN, Dong C, Zhao X, Dymacek J, Porter DW, Wolfarth MG, Castranova V, Qian Y, Guo NL. 2015. Multi-walled carbon nanotube-induced gene expression in vitro: Concordance with in vivo studies. *Toxicology* 328:66–74.
- Snyder-Talkington BN, Dymacek J, Porter DW, Wolfarth MG, Mercer RR, Pacurari M, Denvir J, Castranova V, Qiana Y, Guo NL. 2013. System-based identification of toxicity pathways associated with multi-walled carbon nanotube-induced pathological responses. *Toxicol Appl Pharm* 272: 476–489.
- Snyder-Talkington BN, Qian Y, Castranova V, Guo NL. 2012. New perspectives for in vitro risk assessment of multiwalled carbon nanotubes: Application of coculture and bioinformatics. *J Toxicol Env Heal B* 15:468–492.
- Srivastava RK, Lohani M, Pant AB, Rahman Q. 2010. Cyto-genotoxicity of amphibole asbestos fibers in cultured human lung epithelial cell line: Role of surface iron. *Toxicol Ind Health* 26:575–582.
- Stocco A, Karlsson HL, Coppède F, Migliore L. 2013. Epigenetic effects of nano-sized materials. *Toxicology* 313:3–14.
- Su X, Yu Y, Zhong Y, Giannopoulou EG, Hu X, Lui H, Cross JR, Ratsch G, Rice CM, Ivashkiv LB. 2015. Interferon- γ regulates cellular metabolism and mRNA translation to potentiate macrophage activation. *Nat Immunol* 16:838–849.
- Sun B, Wang X, Ji Z, Li R, Xia T. 2013. NLRP3 inflammasome activation induced by engineered nanomaterials. *Small* 9:1595–1607.
- Suzui M, Futakuchi M, Fukamachi K, Numano T, Abdelgied M, Takahashi S, Ohnishi M, Omori T, Tsuruoka S, Hirose A, et al. 2016. Multiwalled carbon nanotubes intratracheally instilled into the rat lung induce development of pleural malignant mesothelioma and lung tumors. *Cancer Sci* 107:924–935.
- Tabet L, Bussy C, Amara N, Setyan A, Grodet A, MJ, Pairon J, Boczkowski J, Lanone S. 2008. Adverse effects of industrial multiwalled carbon nanotubes on human pulmonary cells. *J Toxicol Env Heal A* 72:60–73.
- Takagi A, Hirose A, Nishimura T, Fukumori N, Ogata A, Ohashi N, Kitajima S, Kanno J. 2008. Induction of mesothelioma in p53 +/– mouse by intraperitoneal application of multi-wall carbon nanotube. *J Toxicol Sci* 33:105–116.
- Takagi A, Hirose A, Futakuchi M, Tsuda H, Kanno J. 2012. Dose-dependent mesothelioma induction by intraperitoneal administration of multi-wall carbon nanotubes in p53 heterozygous mice. *Cancer Sci* 103:1440–1444.
- Takeuchi O, Akira S. 2010. Pattern recognition receptors and inflammation. *Cell* 140:Elsevier Inc.:805–820.
- Tavares AM, Louro H, Antunes S, Quarré S, Simar S, De Temmerman P, Verleysen E, Mast J, Jensen KA, Norppa H. 2014. Genotoxicity evaluation of nanosized titanium dioxide, synthetic amorphous silica and multi-walled carbon nanotubes in human lymphocytes. *Toxicol in Vitro* 28:60–69.
- Taylor AJ, McClure CD, Shipkowski KA, Thompson EA, Hussain S, Garantzotis S, Parsons GN, Bonner JC. 2014. Atomic layer deposition coating of carbon nanotubes with aluminum oxide alters pro-fibrogenic cytokine expression by human mononuclear phagocytes in vitro and reduces lung fibrosis in mice in vivo. *PLOS One* 9:e106870.
- Trout DB, Schulte PA. 2010. Medical surveillance, exposure registries, and epidemiologic research for workers exposed to nanomaterials. *Toxicology* 269:128–135.

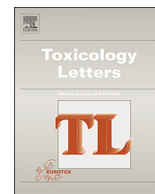
- Thurnherr T, Brandenberger C, Fischer K, Diener L, Manser P, Maeder-Althaus X, Kaiser JP, Krug HF, Rothen-Rutishauser B, Wick P. 2011. A comparison of acute and long-term effects of industrial multiwalled carbon nanotubes on human lung and immune cells in vitro. *Toxicol Lett* 200:176–186.
- Wang L, Mercer RR, Rojanasakul Y, Qiu A, Lu Y, Scabilloni JF, Wu N, Castranova V. 2010. Direct fibrogenic effects of dispersed single-walled carbon nanotubes on human lung fibroblasts. *J Toxicol Env Heal A* 73:410–422.
- Wang P, Wang Y, Nie X, Braïni C, Bai R, Chen C. 2015. Multiwall carbon nanotubes directly promote fibroblast – Myofibroblast and epithelial – Mesenchymal transitions through the activation of the TGF- β /Smad signalling pathway. *Small* 11:446–455.
- Warheit DB, Laurence BR, Reed KL, Roach DH, Reynolds GA, Webb TR. 2004. Comparative pulmonary toxicity assessment of single-wall carbon nanotubes in rats. *Toxicol Sci* 77:117–125.
- Westmeier D, Stauber RH, Docter D. 2016. The concept of bio-corona in modulating the toxicity of engineered nanomaterials (ENM). *Toxicol Appl Pharm* 299:53–57.
- WHO (World Health Organization). 2012. Nanotechnology and Human Health: Scientific Evidence and Risk Governance. Bonn.
- Wirnitzer U, Herbold B, Voetz M, Ragot J. 2009. Studies on the in vitro genotoxicity of Baytubes®, agglomerates of engineered multi-walled carbon-nanotubes (MWCNT). *Toxicol Lett* 186:160–165.
- Wu G, Dawson E, Duong A, Haw R, Stein L. 2014. ReactomeFIViz: a Cytoscape app for pathway and network-based data analysis. *F1000Research* 3:146–159.
- Yanaihara N, Caplen N, Bowman E, Seike M, Kumamoto K, Yi M, Stephens RM, et al. 2006. Unique microRNA molecular profiles in lung cancer diagnosis and prognosis. *Cancer Cell* 9: 189–198.
- Yazdi AS, Guarda G, Riteau N, Drexler SK, Tardivel A, Couillin I, Tschopp J. 2010. Nanoparticles activate the NLR pyrin domain containing 3 (Nlrp3) inflammasome and cause pulmonary inflammation through release of IL-1 α and IL-1 β . *Proc Natl Acad Sci U S A* 107:19449–19454.
- Yu K, Kim JE, Seo HW, Chae C. 2013. Differential toxic responses between pristine and functionalized multiwall nanotubes involve induction of autophagy accumulation in murine lung. *J Toxicol Env Heal A* 76:1282–1292.
- Ye SF, Wu YH, Hou ZQ, Zhang QQ. 2009. ROS and NF-kappaB are involved in upregulation of IL-8 in A549 cells exposed to multi-walled carbon nanotubes. *Biochem Biophys Res Commun* 379: 643–648.

Accepted by—
B. Gollapudi

3. Evaluating the genotoxicity of cellulose nanofibrils in a co-culture of human lung epithelial cells and monocyte-derived macrophages.

Article published article in:

Ventura C, Lourenço AF, Sousa-Uva A, Ferreira PJT, Silva MJ. (2018). *Toxicology Letters*. 291:173-183. doi: 10.1016/j.toxlet.2018.04.013. Epub 2018 Apr 18.



Evaluating the genotoxicity of cellulose nanofibrils in a co-culture of human lung epithelial cells and monocyte-derived macrophages

Célia Ventura^{a,b,c}, Ana Filipa Lourenço^d, António Sousa-Uva^{b,e}, Paulo J.T. Ferreira^d, Maria João Silva^{a,c,*}

^a Department of Human Genetics, National Institute of Health Doutor Ricardo Jorge (INSA), Lisbon, Portugal

^b Department of Occupational and Environmental Health, National School of Public Health, NOVA University of Lisbon (UNL), Lisbon, Portugal

^c Center for Toxicogenomics and Human Health (ToxOmics), NOVA Medical School-FCM, UNL, Lisbon, Portugal

^d CIEPQPF, Department of Chemical Engineering, University of Coimbra, Coimbra, Portugal

^e CISP – Public Health Research Center, Lisbon, Portugal

ARTICLE INFO

Keywords:

Cellulose nanofibrils
Safety assessment
Immunotoxicity
Comet assay
Micronucleus assay

ABSTRACT

Cellulose nanofibrils (CNF) are manufactured nanofibres that hold impressive expectations in forest, food, pharmaceutical, and biomedical industries. CNF production and applications are leading to an increased human exposure and thereby it is of utmost importance to assess its safety to health. In this study, we screened the cytotoxic, immunotoxic and genotoxic effects of a CNF produced by TEMPO-mediated oxidation of an industrial bleached *Eucalyptus globulus* kraft pulp on a co-culture of lung epithelial alveolar (A549) cells and monocyte-derived macrophages (THP-1 cells). The results indicated that low CNF concentrations can stimulate A549 cells proliferation, whereas higher concentrations are moderately toxic. Moreover, no proinflammatory cytokine IL-1 β was detected in the co-culture medium suggesting no immunotoxicity. Although CNF treatment did not induce sizable levels of DNA damage in A549 cells, it led to micronuclei formation at 1.5 and 3 $\mu\text{g}/\text{cm}^2$. These findings suggest that this type of CNF is genotoxic through aneugenic or clastogenic mechanisms. Noteworthy, cell overgrowth and genotoxicity, which are events relevant for cell malignant transformation, were observed at low CNF concentration levels, which are more realistic and relevant for human exposure, e.g., in occupational settings.

1. Introduction

Nanocellulose is an advanced material that exhibits unique characteristics, depending on the source and production method. These include high specific surface area, high aspect ratio (length to width ratio) and high tensile strength and stiffness, besides being renewable and biodegradable in nature (Eichhorn et al., 2010; Abdul Khalil et al., 2014; Nechyporchuk et al., 2016). Cellulose nanofibrils (CNF), also referred to as cellulose nanofibres or nanofibrillated cellulose, are usually obtained from wood, cotton, hemp, flax, sugar beet or potato tuber. Depending on the source and on the production method, the size of the fibrils can vary significantly, but usually nanofibrils are defined as materials with diameters inferior to 100 nm and lengths in the micrometer scale (TAPPI standard proposal W13021, Chinga-Carrasco et al., 2011; Kangas et al., 2014). CNF are produced by intensive mechanical treatment, such as in a high-pressure homogenizer (Li et al., 2012; Osong et al., 2016; Siró and Plackett, 2010), usually combined with a chemical or enzymatic pre-treatment to reduce energy

consumption. One of the most effective pre-treatments is an oxidation mediated by 2,2,6,6-tetramethylpiperidine-1-oxyl radical (TEMPO) that introduces carboxylate and aldehyde functional groups in the cellulose fibres, making them highly negative and more suitable for their deconstruction process (Isogai et al., 2011; Lourenço et al., 2017; Saito and Isogai, 2007). CNF exhibits exceptional high mechanical resistance and low density, being a prime candidate for strength-enhancement of the mechanical properties of other composite materials, such as paper, carton and packaging materials. They also have a wide array of applications in the form of gels or emulsions, e.g., as a rheology modifier. Due to its likely biocompatibility, CNF have been investigated in regenerative medicine as scaffolds for tissue-engineered meniscus, blood vessels, ligaments or tendons (Jia et al., 2013; Lin and Dufresne, 2014; Mathew et al., 2012, 2013). Other biomedical applications of CNF are on wound healing (Basu et al., 2017; Hakkarainen et al., 2016; Jack et al., 2017; Sun et al., 2017; Syverud et al., 2011), stem cell decorated threads for surgical suturing (Mertaniemi et al., 2016), haemodialysis membranes (Ferraz et al., 2013), long-lasting sustained drug delivery

* Corresponding author at: Departamento de Genética Humana, Instituto Nacional de Saúde Doutor Ricardo Jorge, Av. Padre Cruz, 1649-016, Lisboa, Portugal.
E-mail address: m.joao.silva@insa.min-saude.pt (M.J. Silva).

systems (Kolakovíc et al., 2012) or 3D cell culture scaffolds (Bhattacharya et al., 2012; Lou et al., 2014; Malinen et al., 2014).

The production of CNF at an industrial scale and its application in a multiplicity of products and biomedical devices can represent a potential hazard to workers along the lifecycle and to consumers, as well. Vartiainen et al. (2011) concluded that workers' exposure to particles in the air during grinding and spray drying of birch cellulose was low or non-existent with the implementation of appropriate protection equipment and proper handling. However, the high aspect ratio of CNF and its biodegradability in the human lungs (Stefaniak et al., 2014) resembles the fibre paradigm that has been associated to the adverse effects of other fibrous nanomaterials (e.g., carbon nanotubes, CNT). Therefore, to ensure the safety of CNF to humans prior to their large-scale commercialization, it is of utmost importance to investigate their potential toxicological properties, particularly their genotoxicity that is closely associated to carcinogenicity.

Most toxicological studies have focused on nanocellulose types with morphological and surface chemical characteristics different from the above-mentioned CNF. These include bacterial nanocellulose (Jeong et al., 2010; Lin and Dufresne, 2014; Moreira et al., 2009; Pertile et al., 2012; Saska et al., 2012; Scarel-Caminaga et al., 2014) and nanocrystalline cellulose (Catalán et al., 2015; Clift et al., 2011; Dong et al., 2012; Kovacs et al., 2010; Shvedova et al., 2016; Yanamala et al., 2014). These nanocellulose types are generally considered as nontoxic, although nanocrystalline cellulose could induce low cytotoxicity and immunotoxicity *in vitro* and *in vivo* (Clift et al., 2011; Yanamala et al., 2014). Regarding CNF, the few published studies mainly indicate no relevant cytotoxic, genotoxic or immunotoxic effects (Alexandrescu et al., 2013; Colić et al., 2015; Nordli et al., 2016; Pitkänen et al., 2014; Vartiainen et al., 2011). Nevertheless, a recent study by Catalán et al. (2017) showed that C57BL/6 mice exposure by pharyngeal aspiration to CNF produced through TEMPO oxidation led to an acute lung inflammatory response and induced DNA damage in lung cells. However, it cannot be completely excluded that the effects observed were related to the presence of LPS, given that no information about this issue is provided. Moreover, Lopes et al. (2018) reported that an unmodified CNF induced a pro-inflammatory effect in THP-1 macrophages that could be moderated by the introduction of surface modifications (Lopes et al., 2018). Thus, more investigation is clearly required to create a knowledge basis to assess the human health risk from exposure to CNF.

The present study aimed at investigating the immunotoxic and genotoxic effects of a CNF produced from industrial bleached *Eucalyptus globulus* kraft pulp fibrillated by a combination of high pressure homogenization with a preliminar oxidation mediated by TEMPO on a co-culture of A549 human lung epithelial alveolar cells and THP-1 monocyte-derived macrophages. Nowadays, it is recognized that co-culture systems best mimic the *in vivo* toxicological potential of nanomaterials and are more realistic models as compared to monocultures (Snyder-Talkington et al., 2012, 2015). Macrophages are well-recognized primary immune cells in the forefront of the defence system through the engulfment of foreign material from tissues, and alveolar macrophages can play a key role in the biological response to inhaled nanofibres. Histological analysis of mouse lung tissue has demonstrated CNF accumulation in the cytoplasm of lung macrophages (Catalán et al., 2017), and it has been suggested that the acidic pH of the macrophage phagolysosome is insufficient to degrade nanocellulose (Stefaniak et al., 2014). Thus, nanocelluloses are likely to be cleared by mechanical movement of macrophages out of the alveoli and eventually to the mucociliary escalator. This knowledge reinforces the relevance of incorporating THP-1 monocyte-derived macrophages in the A549 cell culture to reflect more realistically, in an *in vitro* system, the *in vivo* biological response to CNF exposure.

2. Materials and methods

2.1. Nanocellulose production and characterization

Nanocelluloses were produced from industrial bleached *Eucalyptus globulus* kraft pulp. In order to fibrillate the pulp, an oxidation mediated by TEMPO was applied, according to a procedure described elsewhere (Lourenço et al., 2017; Saito and Isogai, 2007), followed by mechanical treatment in a high-pressure homogenizer. For that, the pulp, previously refined at 4000 rev. PFI, was mixed with TEMPO (0.016 g/g of fibres) and NaBr (0.1 g/g of fibres) in demineralized water and, after proper mixing, a NaClO solution (9.7% active chlorine) was slowly added (5 mM/g of fibre). The reaction was carried out for 2 h with pH constant at 10 by adding NaOH 0.1 M. The resultant fibres were thoroughly washed with demineralized water until the suspension final conductivity was low (20 μ S/cm). Finally, the pre-treated fibres were passed 2 times in the homogenizer (GEA Niro Soavi Model Panther NS3006L), the first one at 500 bar and the second one at 1000 bar, to reduce the size of the fibrillated fibres to the nanoscale. The final consistency of the nanocellulose aqueous suspension was 0.83 wt% exhibiting a gel-like behaviour.

The nanocellulose was characterized for its fibrillation yield, amount of carboxylic groups, degree of substitution, degree of polymerization and size. The yield was determined in duplicate by submitting a 0.2 wt% nanocellulose suspension to centrifugation at 9000 r/min for 30 min (8965g) in a Hettich Universal 32. The yield was calculated as the percentage of supernatant material (w/w), corresponding to the nanofibrillated fraction of the sample (Gamelas et al., 2015). The concentration of carboxyl groups (C_{COOH}) was determined by a conductometric titration according to a methodology reported elsewhere (Lourenço et al., 2017): briefly, an aqueous suspension of nanocellulose (0.1 g dry weight) was well stirred and its pH was set to 3.0 with HCl. Then, a 0.01 M NaOH solution was added until pH 11. The carboxylate content was determined in triplicate from the conductivity curve and, from this value, it was possible to estimate the degree of substitution (DS), taking into account the molar masses of the anhydroglucose units and of units substituted at the C6 position by COO^-Na^+ groups, as explained elsewhere (Lourenço et al., 2017). The degree of polymerization (DP) was calculated using the Mark-Houwink equation with the parameters reported by Henriksson (2008). The intrinsic viscosity necessary for the calculations was determined by the cupri-ethylene-diamine methodology (ISO standard 5351). The structure of the fibrils was assessed by Field emission-SEM (FE-SEM) on 20 g/m² films prepared by air-drying of a 0.2% (w/v) nanocellulose suspension. The images were acquired at 500 \times magnification in a Carl Zeiss Merlin microscope, in secondary electron mode, using 1 kV voltage. Gold sputtering (3s) was previously performed. The fibrils diameter was assessed by atomic force microscopy (AFM) in a Bruker Innova microscope using the aforementioned films. The peak force-tapping mode was used with a tip radius of 8 nm. Several $2 \times 2 \mu$ m scans were acquired and a mean diameter was computed using the Gwyddion software. As a complement to this measurement, a non-operator dependent technique, providing results more representative of the whole sample, since thousands of fibrils are analysed, was used – the Dynamic Light Scattering (DLS). For that, the supernatant of the aforementioned centrifugation was analysed in a Zetasizer Nano ZS equipment (Malvern Instruments) at a scattering angle of 173° and using the CONTIN algorithm to obtain the size distribution. The value reported corresponds to the smaller peak of the distribution. However, some caution needs to be taken considering that this technique is not suitable for particles with such a high aspect ratio as that of the nanocellulose. Nevertheless, it provides information that may be used for comparison purposes, namely with samples under similar conditions. Although the CNF was not tested for LPS contamination, previous studies by Nordli et al. (2016) showed that the TEMPO-mediated oxidation performed in alkaline conditions strongly reduces the LPS content in the sample,

becoming easier to wash out from the fibres after the oxidation process. Because washing was performed exhaustively in this CNF production it is unlikely that LPS still persists in the sample.

2.2. Cell culture

The human alveolar epithelial cell line A549 (ATCC, Manassas, VA, USA, CCL-185) and the human monocytic leukaemia cell line THP-1 (ATCC, TIB-202) were both grown in RPMI 1640 medium (Gibco, Waltham, MA, USA) supplemented with 10% heat-inactivated foetal bovine serum (FBSi) (Gibco), 1% penicillin/streptomycin (1.000 U/mL penicillin and 10 mg/mL streptomycin), Gibco) and 1% fungizone (0.25 mg/mL, Gibco), at 37 °C in an atmosphere of 5% CO₂. The THP-1 monocytes were grown on transwell inserts with a nominal pore size of 0.4 µm (Greiner Bio-One GmbH, Kremsmünster, Austria) at a density of 0.2×10^5 cells/mL and differentiated into macrophages by 48 h incubation with 100 ng/mL of 12-O-tetradecanoylphorbol-13-acetate (TPA, Sigma-Aldrich). The medium was then removed and substituted by serum-free RPMI 1640 medium for further 48 h, to allow cells to recover from the TPA effect. The A549 cells were cultured on 12-well plates at a density of 0.5×10^5 cells/mL and the inserts with differentiated THP-1 cells were placed directly on the top of the A549 cells. The resulting co-culture was incubated for further 24 h in RPMI 1640 medium. To ensure that THP-1 and A549 cells were exposed to the same CNF concentrations (1.5, 3, 6, 12.5, and 25 µg/cm²) the dispersions were added to the apical and basolateral sides of the insert whenever co-cultures were used.

2.3. MTT assay

The MTT assay was performed according to [Mossmann \(1983\)](#) using three independent experiments. A549 cells were plated in 96-well plates and allowed to attach for 24 h at 37 °C and 5% CO₂. The cells were then exposed for 24 h or 48 h to 1.5, 3, 6, 12.5, and 25 µg/cm² of CNF in culture medium. These concentrations were prepared from a stock solution at 1.5 mg/mL of a 0.872% CNF gel diluted in phosphate buffered saline (PBS) and correspond to the dry weight of the CNF. SDS (1 µg/mL, Sigma), 1 h exposure, was used as a positive control. After washing twice with PBS, the cells were incubated for 2 h with fresh growth medium containing 10% of the MTT solution (5 mg/mL, Calbiochem, Darmstadt, Germany). The MTT-containing medium was discharged and DMSO (Sigma) was added for 20 min under shaking. The absorbance was recorded at 570 nm against a reference filter set at 690 nm using a Multiscan Ascent spectrophotometer (Labsystems, Helsinki, Finland). The relative cell survival of exposed cultures was expressed as the ratio between the absorbance of the exposed and unexposed cultures, assuming that the absorbance of the latter represents 100% cell survival.

2.4. Lactate dehydrogenase (LDH) assay

LDH determination was conducted in the supernatant removed from CNF-exposed cultures for 48 h, used for the MTT assay. After centrifugation of the supernatant at 4000g for 10 min, LDH concentration was measured using the CytoTox-ONE homogeneous membrane integrity assay (Promega, Madison, USA). A maximum LDH release control was performed by the addition of lysis solution to the untreated control cells before adding Cyto-tox ONE. The percentage of cytotoxicity was calculated as the ratio between the concentration of LDH in each supernatant (subtracting the culture medium background) and the maximum LDH release (subtracting the culture medium background) multiplied by 100.

2.5. Clonogenic assay

The clonogenic assay was performed as described by [Herzog et al.](#)

(2007). Briefly, a very low density of A549 cells (100 cells) was plated in each well of a 6-well plate and allowed to attach for approximately 16 h, at 37 °C and 5% CO₂. The cells were then exposed to 1.5, 3, 6, 12.5, 25, 50, and 100 µg/cm² of CNF. For each experiment, negative (non-treated cells) and positive (0.004 µg/mL mitomycin C, Sigma) controls were included. Cells were incubated for 8 days, at 37 °C and 5% CO₂ to allow colonies formation. The wells were then washed twice with PBS, fixed in absolute methanol (Sigma) and stained with 10% Giemsa (Merck, Darmstadt, Germany) in phosphate buffer, pH 6.8. The number of colonies formed was counted and the plating efficiency (CE) was determined using the following equation ([Herzog et al., 2007](#)):

$$CE = 100 \times (\text{no. colonies in negative control} / \text{no. of plated cells})$$

The surviving fraction (SF) for each CNF concentration was calculated as follows:

$$SF = \text{no. colonies formed after exposure} / (\text{no. of plated cells} \times CE / 100)$$

The cytotoxicity was determined as the decrease in the SF in relation to the negative control, based on the results from three independent experiments.

2.6. Determination of IL-1β secretion

Cell culture supernatants were collected after the 24 h treatment for the comet assay and stored at −80 °C until analysis. The IL-1β concentration in the supernatants of the 1.5, 6 and 25 µg/cm² treatment with CNF was determined using a colorimetric sandwich ELISA method (IL-1β-EASIA Kit, Source, Louvain-la-Neuve, Belgium), according to the manufacturer's protocol. A positive control was prepared adding 100 ng/µL of lipopolysaccharide (LPS; Sigma) and 5 mM adenosine 5'-triphosphate disodium salt (ATP; Sigma) to the supernatant of the cell culture in the inserts ([Park et al., 2007](#)).

2.7. Comet assay

The A549 and THP-1 cells in co-culture were equally exposed for 24 h to 1.5, 3, 6, 12.5, and 25 µg/cm² of CNF by adding the corresponding volume of the dispersion medium to both sides of the transwell inserts placed on 12-well plates. Ethyl methanesulphonate (EMS, 5 mM, Sigma-Aldrich) with an exposure time of 1 h was used as a positive control. The plates were washed with PBS and harvested after tripsinization. The comet assay was performed as described in [Louro et al. \(2016\)](#). Briefly, the cell suspensions were centrifuged (1200 r/min, 10 min, 4 °C) and the pellets resuspended and embedded in 0.8% low melting point agarose, then spread onto 1% agarose-precoated microscope slides (2 gels per slide). Slides were immersed in lysis solution (2.5 M NaCl, 100 mM EDTA, 10 mM Tris, 10% DMSO and 1% Triton X-100, pH 10) for a minimum of 1 h and washed twice with enzyme buffer (40 mM HEPES, 100 mM KCl, 0.5 mM EDTA, 0.2 mg/mL BSA, pH 8). The resultant agarose-embedded nucleoids were then treated either with enzyme buffer or with 50 µL of formamidopyrimidine DNA glycosylase (FpG, kindly provided by Dr. A. R. Collins, University of Oslo, Norway), for 30 min, at 37 °C. The slides were immersed into cold electrophoresis buffer (0.3 M NaOH, 1 mM hydrated Na₂EDTA; pH 13) for 30 min to allow DNA unwinding under alkaline conditions followed by a 25 min electrophoresis at 0.8 V/cm. Finally, after 10 min neutralization with PBS, slides were rinsed another 10 min with distilled water, dried overnight and stained with ethidium bromide (0.125 µg/µL). Three independent experiments were carried out, each with two replicates per treatment condition. In each experiment, a total of 100 randomly selected nucleoids (i.e., 50 nucleoids per gel) were analysed in FpG-treated and untreated gels for each culture, using an Axioplan2 Imaging epifluorescence microscope equipped with a high resolution camera (Carl Zeiss Microscopy, Gottingen, Germany).

Scoring was done with the Comet Imager 2.2 software (MetaSystems, Althussheim, Germany), choosing the percentage of DNA in the tail as a measure of DNA damage. The results represent the Mean \pm Standard Deviation (M \pm SD) of three independent experiments.

2.8. Micronucleus assay

The cytokinesis-blocked micronucleus assay was carried out as described by Louro et al. (2016). Following the A549/THP-1 cells co-culture exposure to 1.5, 3, 6, 12.5, and 25 $\mu\text{g}/\text{cm}^2$ of CNF for 6 h, cytochalasin B (Sigma) was added to each well at a final concentration of 6 $\mu\text{g}/\text{mL}$. For each experiment, negative (non-treated cells) and positive (50 $\mu\text{g}/\text{mL}$ mitomycin C, Sigma) controls were included. Briefly, at the end of the 48 h treatment, cells were washed twice with PBS and, following detachment with trypsin-EDTA, cells were submitted to a hypotonic shock with a RPMI 1640:DH2O:FBS (37.5:12.5:1) solution, centrifuged and the pellet spread onto microscope slides. The slides were dried, fixed in absolute methanol (Sigma), stained with 4% Giemsa (Merck, Darmstadt, Germany) and air-dried at room temperature. Slides were scored under a bright field microscope for the presence of micronuclei (MN), using the criteria described by Fenech (2007). At least 2000 binucleated cells from two independent cultures were scored per treatment condition and the results of the frequency of micronucleated binucleated cells (MNBC) are presented as the M \pm SD. In addition, nuclear buds and nucleoplasmic bridges were also scored in those binucleated cells and their mean frequency determined. The proportion of mono- (MC), bi- (BC) or multinucleated-cells (MTC) was calculated by scoring 1000 cells per treatment and the cytokinesis-blocked proliferation index (CBPI) was calculated as follows (OECD, 2010): $\text{CBPI} = (\text{MC} + 2\text{BC} + 3\text{MTC})/\text{Total cells}$. The Replication Index (RI) was calculated using the following equation:

$$\text{RI} = [(\text{BC} + 2\text{MTC})/\text{Total cells, in treated cells}]/[(\text{BC} + 2\text{MTC})/\text{Total cells, in untreated cells}]$$

2.9. Statistical analysis

Statistical comparisons of the clonogenic, MTT and comet assays data between treated and control cells were performed through a one-way analysis of variance (ANOVA) followed by Tukey's multiple comparison test, after testing for the data normality. Then, in the Comet assay, the two-tailed Student's *t*-test was used to compare the differences between the results obtained with and without FpG treatment. The same test was also used to compare the CBPI results between the treated and control cells. The 2-tailed Fisher's exact test was applied to analyse the results of the frequency of micronucleated cells. All analyses were performed with the SPSS statistical package (version 22, SPSS Inc. Chicago, IL).

3. Results

3.1. Nanocellulose characterization

The nanocellulose sample was fully characterized in order to assess the properties that could be more significant for the cytotoxicity and genotoxicity tests. For that, their chemical and physical characteristics (Table 1) were evaluated by measuring the amount of carboxylic groups

Table 1
Characterization of the nanocellulose sample.

Yield (%)	C _{COOH} ($\mu\text{eq g/g}$)	DS	DP	d _{AFM} (nm)	d _{DLS} (nm)
82.4	1177	0.19	289	25.9	18.5

C_{COOH}: Carboxyl group content; DS: Degree of substitution; DP: Degree of polymerization; d_{AFM,DLS}: Diameter (obtained by AFM or DLS).

attached to the cellulose chain after the TEMPO-mediated oxidation, as well as the obtained degree of substitution and degree of polymerization.

A FE-SEM image of low magnification is presented to show the structure organization of the cellulose nanofibrils (Fig. 1), in which agglomeration of the fibrils is observable. The size of the fibrils was assessed by AFM (Fig. 2). As visible in Fig. 2B, the sample presents a wide distribution of diameters, with the mode in the 20–25 nm range. A value for the length of the nanofibrils could not be assessed by AFM since they are several micrometers long. In fact, for nano-objects with such a high aspect ratio, this is a common limitation. In order to analyse a larger number of nanofibrils, a dynamic analyser based on light scattering was also used. Although not adequate for non-spherical particles, it provides a comparison between different samples. The result obtained in this study is of the < 50 nm magnitude.

3.2. Cytotoxic effects

Fig. 3 presents the results of the MTT assay and shows that none of the CNF concentrations tested during a 24-h exposure period induced a significant cytotoxic effect in A549 cells, as compared to controls ($p > 0.05$, one-way ANOVA). Following 48 h of exposure to the same CNF dose-range, an increase in cells viability was observed for the two lowest concentrations (1.5 and 3 $\mu\text{g}/\text{cm}^2$) and a significant decrease in cell viability was observed for the two highest concentration tested ($p = 0.003$ and $p = 0.0004$, respectively). Nevertheless, according to the ISO 10995-5, a clear cytotoxic effect was observed for the 25 $\mu\text{g}/\text{cm}^2$ concentration only ($51 \pm 1.42\%$), whereas the 12.5 $\mu\text{g}/\text{cm}^2$ concentration decreased cells viability to $72 \pm 2.13\%$, i.e., slightly above the 70% imposed by international standards. A dose-response effect was obtained following a potential function ($r^2 = 0.987$). The positive control showed a relative cell viability of 2.1% and 2.6% at 24 h and 48 h, respectively.

Regarding the results of the LDH assay following a 48-h incubation time, a statistically significant membrane integrity loss was observed only for the highest CNF concentration tested ($p = 0.03$). Nevertheless, it should be highlighted that this difference corresponds merely to a 4% increase in cytotoxicity relatively to control cells (Fig. 4).

The clonogenic assay was additionally used to assess the CNF ability to impair cell proliferation following a longer exposure period (8 days). A statistically significant increase in the number of A549 colonies formed was observed for the 1.5 $\mu\text{g}/\text{cm}^2$ of CNF, as compared to controls ($p < 0.05$, Tukey HDS), followed by a slight non-significant decrease in cell proliferation ability for higher CNF concentrations. The dose-response relationship was fitted to a sigmoidal curve ($r^2 = 0.987$, Fig. 5). The positive control produced a decrease of cells surviving fraction to 50% relatively to control.

3.3. Immunotoxic effects

Cells exposure to three CNF concentrations (1.5, 6 and 25 $\mu\text{g}/\text{cm}^2$) during 24 h did not induce the release of detectable levels of IL-1 β to the culture medium (detection limit of 0.35 pg/mL). The positive control had a determination of 57 pg/mL of IL-1 β in the cell culture supernatant.

3.4. Genotoxic effects

The genotoxic effects of the CNF under study were assessed by the comet and the micronucleus assays performed in A549 cells cultured in the above described co-culture system. The selection of the concentration-range was based on the results of the cytotoxicity tests with A549 cells monocultures, assuming that the presence of THP-1 cells would not negatively affect A549 cells viability. The results of the comet assay (without FpG treatment) revealed a significant genotoxic effect of CNF in the co-culture of A549 cells and THP-1 differentiated macrophages,

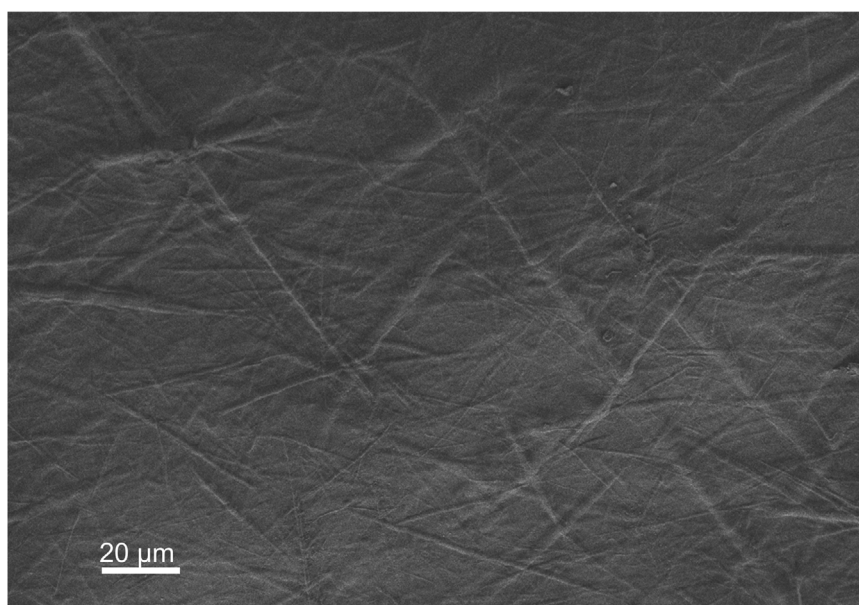


Fig. 1. Field-Emission SEM of films of cellulose nanofibrils.

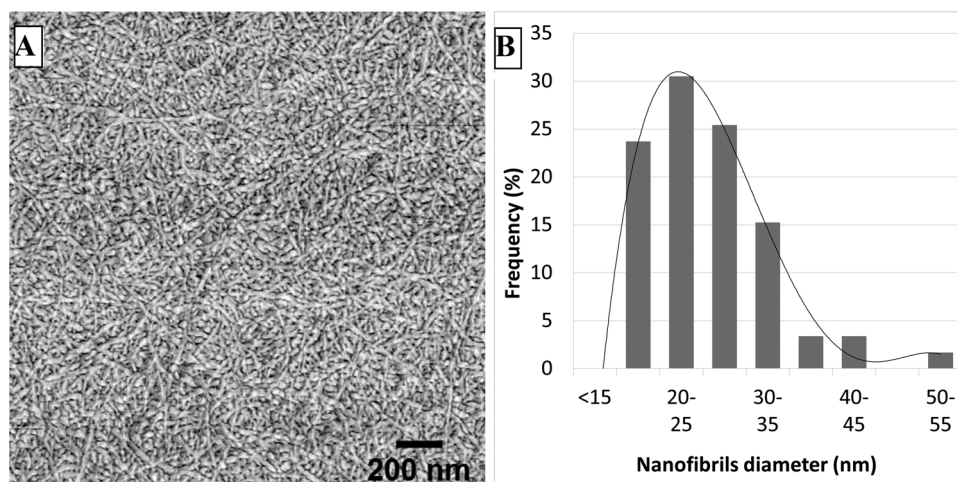


Fig. 2. Cellulose nanofibrils AFM image in phase imaging mode (A) and nanofibrils diameter distribution obtained by AFM (B).

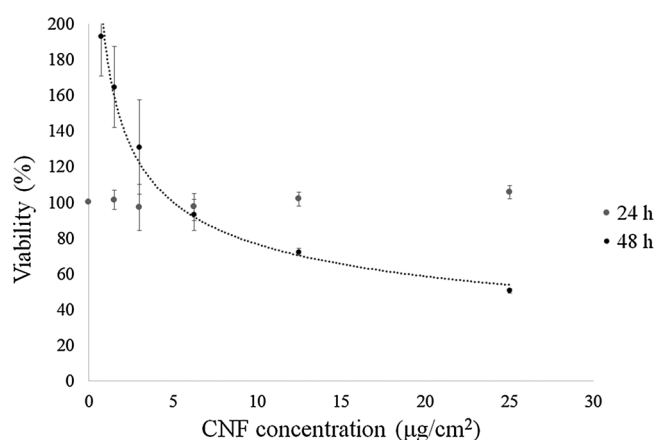


Fig. 3. Relative viability of A549 cells after exposure to different concentrations of CNF (24 h and 48 h) as assessed by the MTT assay. Results are expressed as $M \pm SD$ of 3 independent experiments.

following exposure to the highest concentration tested ($25 \mu\text{g}/\text{cm}^2$), as compared to controls ($p = 0.019$ one-way ANOVA, Tukey post-hoc test) (Fig. 6). However, even for this concentration, the level of DNA damage measured is quite low (6.68%) and may not have biological relevance. The DNA damage detected by the comet assay with FpG apart from DNA single- and double-strand breaks includes also oxidative lesions that are converted in DNA breaks. For CNF-treated cells the overall level of DNA breaks was not statistically different from that of control cells ($p > 0.05$, ANOVA). The comparison between the mean percentage of DNA in tail obtained with and without FpG treatment was only statistically significant for cells exposed to $12.5 \mu\text{g}/\text{cm}^2$ of CNF ($p < 0.05$) but still within very low levels. The mean percentage of DNA in tail obtained for EMS, the positive control, was 30.0% and 38.2%, without and with FpG treatment, respectively (Fig. 7).

The frequencies of MNBCs and the CBPI estimated following co-cultures exposure to CNF are presented in Fig. 8 (and Table 1 Supplementary material). Nanocellulose induced a statistically significant increase in the frequency of MNBCs at the two lowest concentrations (1.5 and $3 \mu\text{g}/\text{cm}^2$) tested ($p = 0.035$ and 0.001 , respectively); the frequency of nuclear buds was also significantly increased by $3 \mu\text{g}/\text{cm}^2$ of CNF ($p = 0.05$). No significant induction of nucleoplasmic bridges was

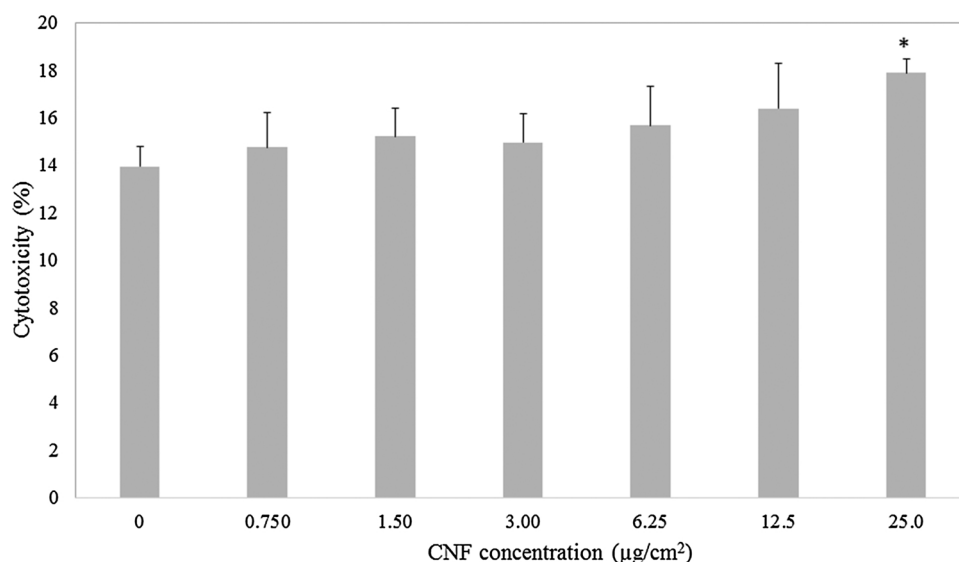


Fig. 4. Cytotoxicity results after a 48 h exposure of A549 cells to a concentration-range of CNF, as assessed by the LDH release assay. Results are expressed as $M \pm SD$. * $p < 0.05$.

observed in all CNF concentrations tested.

4. Discussion

The substantial number and variety of nanocellulose applications has raised the likelihood of human exposure in environmental and occupational settings, or as consumers and, consequently, has increased the concern about their potential adverse health effects. All high aspect-ratio nanomaterials, as nanofibrillated cellulose is, are recommended to be tested for their toxicity at the first phase of a flow chart developed by Dekkers et al. (2016) that attempts to prioritize the hazard assessment of nanomaterials and develop a nanospecific approach for their risk assessment. For this purpose, several complementary *in vitro* assays covering biological effects relevant for the occurrence of long-term effects, particularly cancer, are used. Compared with *in vivo* approaches, *in vitro* assays to characterize nanomaterials toxicity have shown to generate results in a simpler, faster and economic manner. Moreover, they can provide a basis for evaluating potential health risks of exposure and they can give insights into the mechanisms underlying the

effects of nanomaterials on cells (Collins et al., 2017). For example, measuring the levels of pro-inflammatory cytokines may give a first indication on the ability of the nanomaterials to cause immunotoxic effects *in vivo* whereas the cytotoxicity is central for a good interpretation of the results of the *in vitro* genotoxicity assays and can provide also mechanistic information about the interactions with the intracellular organelles, e.g., mitochondria or lysosomes. The strategy for *in vitro* genotoxicity testing of nanomaterials needs to include the detection of the most relevant events for the multistep process of malignancy, i.e., DNA damage, clastogenicity and aneugenicity, which are covered by the combination of the comet assay and the *in vitro* micronucleus assay (Louro et al., 2015).

In this study, a preliminary safety assessment of a CNF produced by TEMPO-mediated oxidation of an industrial bleached *Eucalyptus globulus* was conducted before its production is scaled-up. Following CNF production, its physicochemical characterisation showed that a high fibrillation degree (yield) was achieved, with 100% of the material in the nanoscale. In fact, with the pre-treatment, a high amount of carboxylic groups was introduced in the cellulose molecules, confirmed by

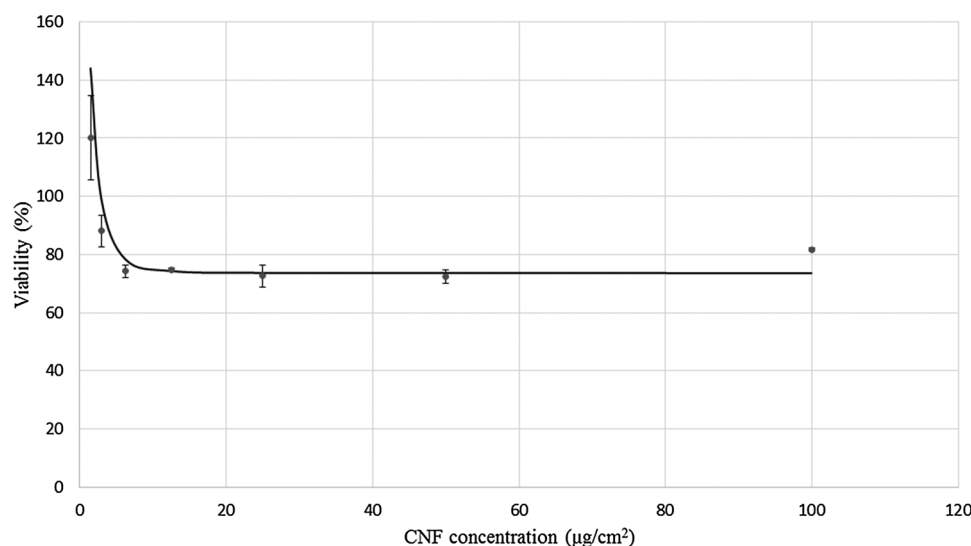


Fig. 5. Colony forming ability of A549 cells after 8 days exposure to different concentrations of CNF, as assessed by the clonogenic assay. Results are expressed as $M \pm SD$ of the cells surviving fraction relative to control.

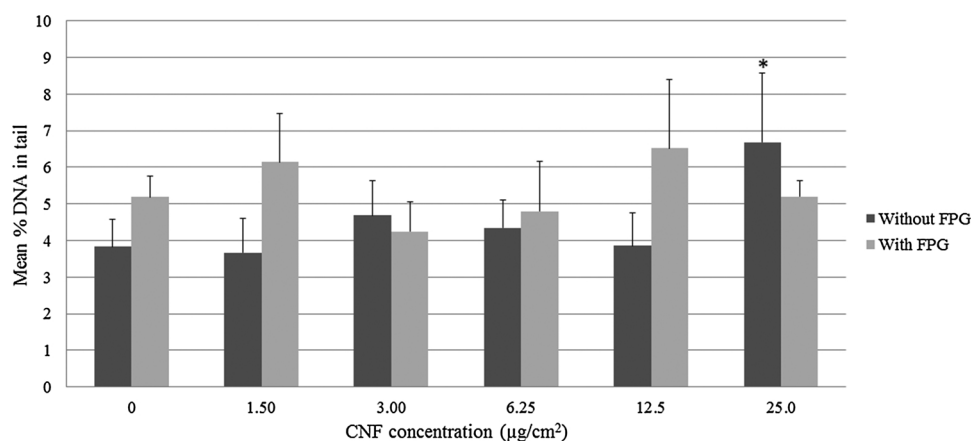


Fig. 6. Comet assay results obtained in the co-culture of A549 epithelial cells and THP-1 differentiated macrophages exposed to CNF, without and with FPG addition. Results are expressed as $M \pm SD$. * $p < 0.05$.

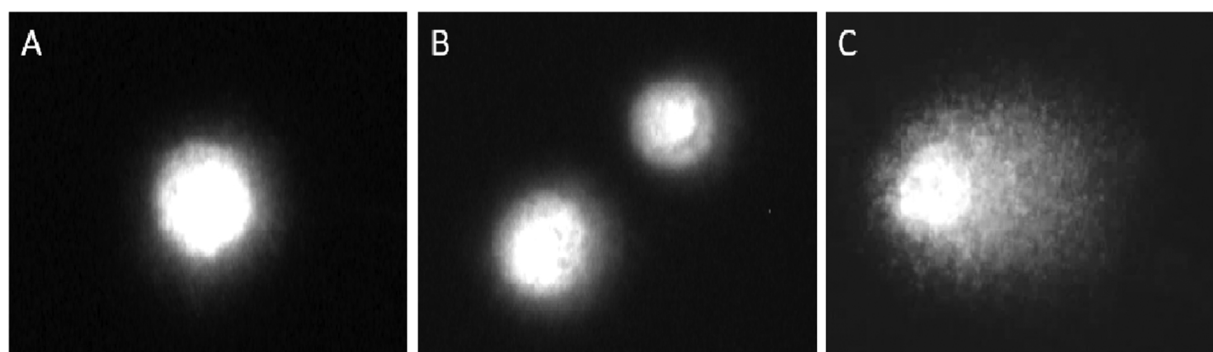


Fig. 7. A549 cell nucleoids observed under the fluorescence microscope in the comet assay with FPG addition. (A) Non-exposed cells control (B) A549 cells exposed to 12.5 µg/cm² of CNF (C) Positive EMS exposed cells control.

the degree of substitution close to 0.2. The high charge caused repulsion between the nanofibrils that compose the fibre wall. The subsequent high-pressure homogenization was therefore able to effectively separate and break the fibre chains, producing a nanocellulose sample with a small degree of polymerization. The results are in accordance with the literature for CNF produced by TEMPO-mediated oxidation applying ca. 5 mM NaClO/g of cellulose fibre (Jin et al., 2014; Lourenço et al., 2017; Saito and Isogai, 2007). As mentioned before, the diameter of the nanofibres was assessed by AFM and compared to that obtained from DLS measurements. The achieved mode of diameter is a common value for

this type of material (Gamelas et al., 2015; Hänninen et al., 2015; Lourenço et al., 2017), and the DLS result is of the same magnitude of those obtained for identical nanofibrils (Gamelas et al., 2015; Lourenço et al., 2017; Mandal and Chakrabarty, 2011).

The cytotoxicity of the CNF was assessed in A549 cells by three assays spanning different endpoints, from the alteration of cells metabolic activity (MTT assay) or loss of membrane integrity (LDH assay) to the cells proliferative ability in the presence of the nanofibres. All assays revealed the capacity of the highest CNF concentration (25 µg/cm²) to induce alveolar cells death, following a 48-h or 8 days exposure

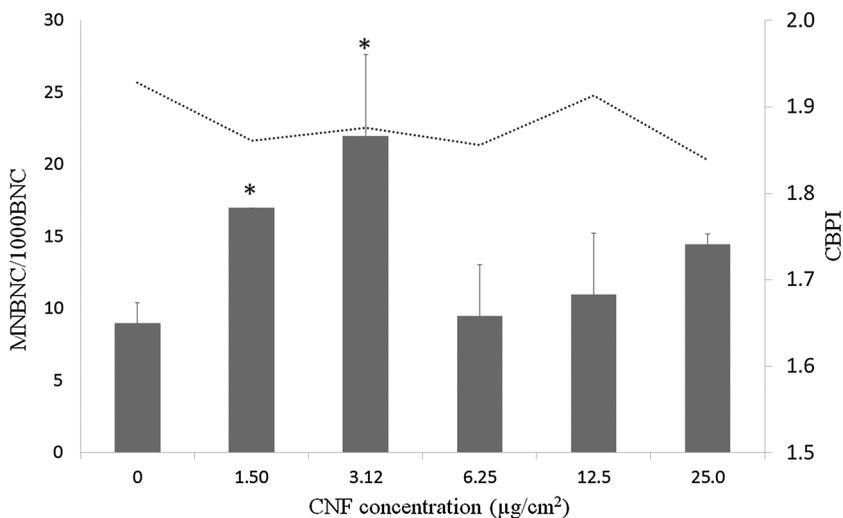


Fig. 8. Results of the micronucleus assay after A549 cells exposure to CNF. In columns, frequency of micronucleated binucleated cells (MNBCs) per 1000 binucleated cells (BNC); the dotted line represents the cytokinesis-blocked proliferation index (CBPI). Mitomycin C was used as a positive control and induced 54.5 MNBNC/1000BNC ($p = 0.000$). Results are expressed as $M \pm SD$. * $p < 0.05$.

(Figs. 3–5). In contrast, the 48 h of treatment with the lowest CNF concentration ($1.5 \mu\text{g}/\text{cm}^2$) resulted in a significant increase in cell viability (MTT assay) and the 8 days treatment stimulated cells proliferation and their capacity to form colonies (clonogenic assay). Thus, the results of the MTT and the clonogenic assays are in general agreement in that the effect of CNF on cell viability is concentration-dependent whereas the LDH assay revealed a lower sensitivity to detect CNF influence on cells viability. These findings agree with those reported by Colić et al. (2015), showing a dose-dependent decrease in L929 fibroblastic cell proliferation and metabolic activity after an incubation of 48 h with a high CNF concentration ($250 \mu\text{g}/\text{mL}$ – $1 \text{ mg}/\text{mL}$). However, as the cell proliferation inhibition was less than 30% and not associated with cell death or oxidative stress, the CNF was considered as non-cytotoxic (Colić et al., 2015). It should be noted, however, that the concentration-range tested in the referred work was much higher than that herein used and does not encompass the ones that increased cell proliferation. Other studies have addressed the cytotoxic potential of nanocelluloses in several cell lines and the majority showed non-toxic effects following a 24-h exposure, similarly to the data obtained in this study for the same exposure length. Kollar et al. (2011) observed no significant effect on THP-1 cell growth and viability after treatment with six variously modified types of non-nanosized cellulose after 24-h incubation, except for dialdehyde cellulose that significantly decreased cell viability. Likewise, Lopes et al. (2018) reported the absence of cytotoxic effects in THP-1 differentiated macrophages, HDF and MRC-5 cells exposed to three types of CNF for 24 h (Lopes et al., 2018). Pitkänen et al. (2014) reported no cytotoxic effect of a finest fraction of CNF in human cervix carcinoma (HeLa229) cells, as assessed by the highest tolerated dose (HTD) test. However, they reported the inhibition of cellular growth and viability decrease at the highest dose using the total protein content (TPC) test (24- and 72-h exposures). Hua et al. (2015) also reported the absence of toxicity in the indirect cytotoxicity test performed in THP-1 cells exposed for 24 h to the extract medium of three differently functionalized CNF films. No toxic effects in indirect cytotoxicity assays (crystal violet, MTT and LDH) were found in mouse fibroblasts incubated with the extracts of TEMPO-oxidized CNF and carboxymethylated CNF during 1, 4, and 7 days (Rashad et al., 2017). On the other hand, very high concentrations (2 – $5 \text{ mg}/\text{mL}$) of a needle-like cellulose nanowhisker from cotton cellulose were cytotoxic to bovine fibroblasts exposed for 24 h (Pereira et al., 2013); an upregulation of the expression of stress- and apoptosis-related genes (*HSP70.1*, *PRDX1* and *BAX*) was also identified.

None of those studies has reported a stimulation of cell metabolism upon nanocellulose exposure. A hypothesis for the effect herein observed is that CNF, at low concentrations, may stimulate alveolar cells to proliferate because they are biocompatible, and they mimic endogenous fibrous structures that may facilitate cell adhesion. Indeed, the observation under phase contrast microscopy of cells grown during 48 h in the presence of CNF confirmed that they were attached to CNF aggregates/agglomerates in the bottom of the culture well. At higher concentrations, however, CNF may slowdown cell proliferation due to increased mechanical stress, mimicking what has been observed in CNF hydrogels for 3D cell cultures (Nordli et al., 2016; Malinen et al., 2014). On the other hand, uncontrolled cell proliferation may also be a consequence of the nanofibre interaction with the mitotic spindle apparatus, as it has been described *in vitro* for asbestos fibres in various types of cells (Huang et al., 2011), for 1 to 4 nm width single-walled CNT in BEAS2B and SAEC cells (Sargent et al., 2009), for 10 to 20 nm thin multi-walled CNT in BEAS2B cells (Siegrist et al., 2014), and hypothesised for 13 and 14 nm multi-walled CNT in A549 and BEAS2B cells (Louro et al., 2016). These diameters are close to the ones of the CNF under study and thereby interference with the mitotic spindle can be also a plausible explanation for the observed increase in cell viability at low concentrations. At high concentrations agglomeration/aggregation occurs and the availability of single CNF to be uptaken by cells and interact with the spindle fibres greatly decreases. Interestingly, this

effect resembles the induction of fibroblasts proliferation *in vitro* following exposure to thin and curled dispersed single-walled CNT (Vietti et al., 2013; Wang et al., 2010) as this CNF is. The fibroblastic response to CNT is known to play a key role in tissue fibrosis that, in turn, may result in a carcinogenic effect on the long-term.

Overall, the referred studies evidence the gap that exists regarding long-term toxicity studies of CNF. Once we observed a significant cytotoxic effect only with an exposure length of 48 h or more, there is still a need of focusing the CNF toxicity studies on longer exposure times and encompassing the low-dose range. This is particularly important since low-dose chronic studies are nowadays considered more suitable experimental models for risk assessment than single acute exposure studies in that they better mimic human exposure (Oberdörster, 2010).

Immunotoxicity of CNF was assessed by determining the concentration of the proinflammatory cytokine IL-1 β in the A549 cell co-culture supernatant. Our finding of unchanged levels of IL-1 β in the co-culture of A549 and THP-1 is in agreement with the overall results from more comprehensive studies available in the literature that CNF has no proinflammatory effect (Basu et al., 2017; Colić et al., 2015; Hua et al., 2015; Mertaniemi et al., 2016; Nordli et al., 2016; Vartiainen et al., 2011). In addition, toxicological studies on the pulmonary toxicity of carbon nanotubes have suggested that when the nanofibre length exceeds the macrophages length, it triggers frustrated phagocytosis, which in turn stimulates a cytokine proinflammatory response (Brown et al., 2007; Murphy et al., 2012). However, Clift et al. (2011) reported that cellulose nanowhiskers from cotton, a nanocellulose that more resembles the needle-like structure of asbestos, did not cause any form of frustrated phagocytosis in macrophages, being instead internalized within vesicles. No signs of phagocytosis were also found in THP-1 macrophages exposed to three different modified CNF (Lopes et al., 2018). Nevertheless, Catalán et al. (2017) reported that CNF produced using TEMPO oxidation triggered the recruitment of neutrophils, macrophages, lymphocytes and eosinophils to the lungs of C57Bl/6 mice exposed by pharyngeal aspiration, indicating an acute inflammatory response. A significant dose-dependent increase in mRNA of the pro-inflammatory cytokines IL-1 β and IL-6, tumour necrosis factor α (TNF- α) and chemokine (C-X-C motif) ligand 5 (CXCL5) was detected in the lung tissue, but without an increase in their protein levels. Lopes et al. (2018) also reported increased levels of IL-1 β and TNF- α in THP-1 macrophages treated with 250 and 500 $\mu\text{g}/\text{mL}$, and 500 $\mu\text{g}/\text{mL}$, respectively, of unmodified CNF (Lopes et al., 2018). These CNF concentrations are in the range of those tested in the Colić et al. (2015) study that, conversely, reported no induction of those pro-inflammatory cytokines in peripheral blood mononuclear cells (PBMCs) cultures stimulated with phytohemagglutinin (31.25–1000 $\mu\text{g}/\text{mL}$). Still, the CNF concentrations herein used are below 31.25 $\mu\text{g}/\text{mL}$ and, therefore, a negative result was not unexpected. Non-nanometric cellulose fibres also trigger an inflammatory response in Wistar rats by inhalation, but it appears to be transient, declining in a 14-day period (Cullen et al., 2000).

Concerning the genotoxic effects of exposure to nanocellulose, the present results showed that the CNF under study induced a low but significant level of DNA damage in A549 cells in co-culture with THP-1 cells, at the $25 \mu\text{g}/\text{cm}^2$ concentration. In addition, two CNF concentrations (1.5 and $12.5 \mu\text{g}/\text{cm}^2$) caused a slight induction of the level of oxidative DNA lesions detected as FpG-sensitive sites, e.g., oxidised 8-oxoGua. It is known that oxidative stress can be rapidly repaired by the cell repair systems and thereby the 24-h timepoint might have been too long to allow the detection of this type of DNA damage in exposed cells. In fact, there are studies e.g., with TiO $_2$ nanomaterials, that showed an induction of FpG-sensitive sites in A549 cells at 2 or 3 h, which were not apparent at 24 h exposure (El Yamani et al., 2017; Ursini et al., 2014) indicating that from this study data the induction of oxidative DNA damage cannot be completely excluded. In the study by Stefaniak et al. (2014) nanocellulose, including CNF, induced significantly more free radicals than that of the essentially inert cellulose microcrystals, which

could lead to reactive oxygen species formation and DNA damage. Low, but significant values of DNA damage, detected by the comet assay, were also obtained *in vitro* in human lymphocytes exposed to brown cotton and curauá nanofibres (Lima et al., 2012). Regarding *in vivo* studies, Catalán et al. (2017) reported significant positive comet assay results ($p < 0.001$) in the lung cells of mice exposed to 10 and 40 µg/mouse of CNF by pharyngeal aspiration, but non-significant values of % DNA in tail compared to the zero dose for the highest concentrations tested, 80 and 200 µg/mouse. This observation agrees with the present *in vitro* results in that low CNF concentrations seem to induce more toxicity in lung cells than the higher ones, either *in vitro* or *in vivo*.

Interestingly, the two lowest CNF concentrations tested by the *in vitro* micronucleus assay were also able to increase significantly the frequency of chromosome numerical or structural anomalies in A549 cells, while for the highest does no effects were observed. On the other hand, the results of the CBPI did not show any significant decrease of A549 cells capacity to divide at those higher dose levels of CNF and thus an influence of toxicity on the micronucleus frequency is not likely. This result confirms the incidence of the CNF biological effects on the low-concentration range. A decrease in the genotoxic effect associated with a dosage increase has been reported for other nanomaterials, e.g. carbon nanotubes, and it is thought to be related with the aggregation or agglomeration of nanomaterials at the highest dose levels that decreases the bioavailability of nano-objects (Brown et al., 2007; Rittinghausen et al., 2014; Shvedova et al., 2005). A hypothesis associated with the decreased toxicity observed with functionalized carbon nanotubes is that their functionalization, with either carboxyl or amino groups, increase the adsorption of proteins in protein-rich biological media, which promotes their agglomeration (Allegrì et al., 2016). Cellulose nanofibres also show a strong tendency to agglomerate, especially after drying and in highly concentrated aqueous solutions due to strong inter- and intra-molecular hydrogen bonding; in nonpolar media they tend to form aggregates (Lima et al., 2012). These authors observed an inverse association between CNF aggregation and toxicity while Pereira et al. (2013) observed that high concentrations of cotton CNF resulted in large CNF aggregates and increased cytotoxicity. In the present study, an aggregation/agglomeration of CNF in the cell culture medium was clearly observed under the optical microscope (Fig. 1 Supplementary material) 24 h after cells treatment with the highest concentrations (25 µg/cm²), supporting the hypothesis that the decreased toxicity is related to a lower bioavailability of CNF in its nanosized form.

Catalán et al. (2017) reported no micronucleus induction in the bone marrow erythrocytes of mice exposed to CNF by pharyngeal aspiration, but the time between the exposure of mice to CNF and the bone marrow sampling might not have been sufficient to allow a systemic genotoxic effect (Catalán et al., 2017). Even though we observed micronuclei induction by the two lowest CNF concentrations tested, whether they were mediated by clastogenic or aneugenic mechanisms, both leading to irreversible chromosome damage linked to early events in carcinogenesis, was not investigated (Bonassi et al., 2011). Clastogenic events can often be associated to the formation of DNA adducts and to oxidative stress that result in DNA breakage that should have been distinguished by the comet assay. On the other hand, loss of chromosomes may be explained by a direct interaction of the CNF with tubulin from the mitotic spindle, or with proteins involved in the segregation of the chromosomes in metaphase, events that are not detected in the comet assay. Likewise, a significant disruption of the mitotic spindle by multi-walled CNT has been previously reported (Siegrist et al., 2014). Several studies have stated that the micronucleus assay is more sensitive to detect genotoxic effects of nanomaterials than the comet assay (Louro et al., 2016), but the type and repair capacities of target cells, the stage of cell cycle, and the time elapsed between exposure and analysis are additional factors that may contribute to the different sensitivities of these assays (Valentin-Severin et al., 2003).

5. Conclusions

Overall, the data of the present work suggests that CNF produced with an oxidative pre-treatment mediated by TEMPO is able to produce concentration-dependent effects in the viability and proliferation of human alveolar cells and genotoxic effects in these cells co-cultured with THP-1 macrophages, particularly at a low concentration-range. The results of cytotoxicity assessment also suggest that CNF exposures longer than 24 h are needed to yield detectable effects. The use of A549 cells co-cultured with THP-1 monocyte-derived macrophages allowed a preliminary assessment of CNF immunotoxicity that confirmed the absence of a proinflammatory effect at a low CNF concentration. Concerning CNF genotoxicity assessed in the same *in vitro* system, although no biologically relevant DNA damage was detected in A549 cells by the comet assay, the formation of micronuclei at the two lowest concentrations tested raised some concern about the safety of this nanofibre. Further studies should be performed to complement these findings, since they suggest that low CNF doses, which are the most realistic exposure doses to humans, may stimulate cell proliferation and induce aneugenic/clastogenic events in alveolar cells, representing a potential risk for human health. Given that this toxicity assessment of a newly produced CNF was conducted in an early phase of the nanofibre development, the present findings are expected to stimulate its modification towards a safer material.

Conflicts of interest

None.

Statement of author contributions

All authors contributed to the manuscript writing. In addition, Maria João Silva contributed to the study design and supervised the scientific work, Ana Filipa Lourenço and Paulo Ferreira produced and characterized the nanocellulose investigated in this study, and Célia Ventura performed the *in vitro* toxicological experiments, data analysis and discussion.

Acknowledgements

This research was co-funded through UID/BIM/00009/2013, Centre for Toxicogenomics and Human Health (ToxOmics), and SFRH/BDE/108095/2015, from the Foundation for Science and Technology, Portugal.

Appendix A. Supplementary data

Supplementary data associated with this article can be found, in the online version, at <https://doi.org/10.1016/j.toxlet.2018.04.013>.

References

- Abdul Khalil, H.P.S., Davoudpour, Y., Nazrul Islam, M., Mustapha, A., Sudesh, K., Dungan, R., Jawaid, M., 2014. Production and modification of nanofibrillated cellulose using various mechanical processes: a review. *Carbohydr. Polym.* 99, 649–665.
- Alexandrescu, L., Syverud, K., Gatti, A., Chinga-Carrasco, G., 2013. Cytotoxicity tests of cellulose nanofibril-based structures. *Cellulose* 20, 1765–1775.
- Allegrì, M., Perivoliotis, D.K., Bianchi, M.G., Chiu, M., Pagliaro, A., Koklioti, M.A., Trompeta, A.F.A., Bergamaschi, E., Bussolati, O., Charitidis, C.A., 2016. Toxicity determinants of multi-walled carbon nanotubes: the relationship between functionalization and agglomeration. *Toxicol. Rep.* 3, 230–243.
- Basu, A., Lindh, J., Alander, E., Strömme, M., Ferraz, N., 2017. On the use of ion-cross-linked nanocellulose hydrogels for wound healing solutions: physicochemical properties and application-oriented biocompatibility studies. *Carbohydr. Polym.* 174, 299–308.
- Bhattacharya, M., Malinen, M.M., Lauren, P., Lou, Y.-R., Kuisma, S.W., Kanninen, L., Lille, M., Corlu, A., Gu-Guen-Guillouzo, C., Ikkala, O., Laukkanen, A., Urtti, A., Yliperttula, M., 2012. Nanofibrillar cellulose hydrogel promotes three-dimensional liver cell culture. *J. Controlled Release* 164, 291–298.
- Bonassi, S., El-Zein, R., Bolognesi, C., Fenech, M., 2011. Micronuclei frequency in

- peripheral blood lymphocytes and cancer risk: evidence from human studies. *Mutagenesis* 26 (1), 93–100.
- Brown, D.M., Kinloch, I.A., Bangert, U., Windle, A.H., Walters, D.M., Walker, G.S., Scotchford, C.A., Donaldson, K., Stone, V., 2007. An in vitro study of the potential of carbon nanotubes and nanofibres to induce inflammation mediators and frustrated phagocytosis. *Carbon* 45, 1743–1756.
- Catalán, J., Ilves, M., Järventaus, H., Hannukainen, K.S., Kontturi, E., Vanhala, E., Alenius, H., Savolainen, K.M., Norppa, H., 2015. Genotoxic and immunotoxic effects of cellulose nanocrystals in vitro. *Environ. Mol. Mutagen.* 56, 171–182.
- Catalán, J., Rydman, E., Aimonen, K., Hannukainen, K.S., Suhonen, S., Vanhala, E., Moreno, C., Meyer, V., Perez, D.D., Sneek, A., Forsström, U., Højgaard, C., Willemoes, M., Winther, J.R., Vogel, U., Wolff, H., Alenius, H., Savolainen, K.M., Norppa, H., 2017. Genotoxic and inflammatory effects of nanofibrillated cellulose in murine lungs. *Mutagenesis* 32 (1), 23–31.
- Chinga-Carrasco, G., Miettinen, A., Luengo Hendriks, C.L., Kristofer Gamstedt, E., Kataja, M., 2011. Structural characterisation of wood pulp fibres and their nanofibrillated materials for biodegradable composite applications. In: Cuppoletti, J. (Ed.), *Nano Composites and Polymers with Analytical Methods – Book 3*. InTech, Rijeka ISBN 978-953-307-352-1.
- Clift, M.J., Foster, E.J., Vanhecke, D., Studer, D., Wick, P., Gehr, P., Rothen-Rutishauser, B., Weder, C., 2011. Investigating the interaction of cellulose nanofibers derived from cotton with a sophisticated 3D human lung cell coculture. *Biomacromolecules* 12, 3666–3673.
- Colić, M., Mihajlovic, D., Mathew, A., Naseri, N., Kokol, V., 2015. Cytocompatibility and immunomodulatory properties of wood based nanofibrillated cellulose. *Cellulose* 22, 763–778.
- Collins, A.R., Annangi, B., Rubio, L., Marcos, R., Dorn, M., Merker, C., Estrela-Lopis, I., Cimpan, M.R., Ibrahim, M., Cimpan, E., Ostermann, M., Sauter, A., Yamani, N.E., Shaposhnikov, S., Chevillard, S., Paget, V., Grall, R., Delic, J., de-Cerio, F.G., Suarez-Merino, B., Fessard, V., Hogeveen, K.N., Fjellsbø, L.M., Pran, E.R., Brzicova, T., Topinka, J., Silva, M.J., Leite, P.E., Ribeiro, A.R., Granjeiro, J.M., Grafrström, R., Prina-Mello, A., Dusinska, M., 2017. High throughput toxicity screening and intracellular detection of nanomaterials. *WIREs Nanomed. Nanobiotechnol.* 9, e1413. <http://dx.doi.org/10.1002/wnan.1413>.
- Cullen, R.T., Searl, A., Miller, B.G., Davis, J.M., Jones, A.D., 2000. Pulmonary and intra-peritoneal inflammation induced by cellulose fibres. *J. Appl. Toxicol.* 20, 49–60.
- Dekkers, S., Oomen, A.G., Bleeker, E.A.J., Vandebriel, R.J., Micheletti, C., Cabellos, J., Janer, G., Fuentes, N., Prina-mello, A., Movia, D., Nessler, F., Ribeiro, A.R., Emilio, P., Groenewold, M., Cassee, F.R., Sips, A.J.A.M., Dijkzeul, A., Van Teunenbroek, T., Wijnhoven, S.W.P., 2016. Towards a nanospecific approach for risk assessment. *Regul. Toxicol. Pharmacol.* 80, 46–59.
- Dong, S., Hirani, A.A., Colacino, K.R., Lee, Y.W., Roman, M., 2012. Cytotoxicity and cellular uptake of cellulose nanocrystals. *Nano Life* 2 (3), 1241006.
- Eichhorn, S.J., Dufresne, A., Aranguren, M., Marcovich, N.E., Capadona, J.R., Rowan, S.J., Weder, C., Thielemans, W., Roman, M., Renneckar, S., Gindl, W., Veigel, S., Keckes, J., Yano, H., Abe, K., Nogi, M., Nakagaito, A.N., Mangalam, A., Simonsen, J., Benight, A.S., Bismarck, A., Berglund, L.A., Peijs, T., 2010. Review: current international research into cellulose nanofibres and nanocomposites. *J. Mater. Sci.* 45, 1–33.
- El Yamani, N., Collins, A.R., Rundén-Pran, E., Fjellsbø, L.M., Shaposhnikov, S., Zienoldiny, S., Dusinska, M., 2017. In vitro genotoxicity testing of four reference metal nanomaterials, titanium dioxide, zinc oxide, cerium oxide and silver: towards reliable hazard assessment. *Mutagenesis* 32 (1), 117–126. <http://dx.doi.org/10.1093/mutage/gew060>.
- Fenech, M., 2007. Cytokinesis-block micronucleus cytome assay. *Nat. Protoc.* 2 (5), 1084–1104.
- Ferraz, N., Leschinskaya, A., Toomadj, F., Fellstrom, B., Strømme, M., Mhrianyan, A., 2013. Membrane characterization and solute diffusion in porous composite nanocellulose membranes for hemodialysis. *Cellulose* 20, 2959–2970.
- Gamelas, J.A.F., Pedrosa, J., Lourenço, A.F., Mutjé, P., González, I., Chinga-Carrasco, G., Singh, G., Ferreira, P.J.T., 2015. On the morphology of cellulose nanofibrils obtained by TEMPO-mediated oxidation and mechanical treatment. *Micron* 72, 28–33.
- Hänninen, T., Orelma, H., Laine, J., 2015. TEMPO oxidized cellulose thin films analysed by QCM-D and AFM. *Cellulose* 22, 165–171.
- Hakkara, T., Koivuniemi, R., Kosonen, M., Escobedo-Lucea, C., Sanz-Garcia, A., Vuola, J., Valtonen, J., Tammela, P., Mäkitie, A., Luukko, K., Yliperttula, M., Kavola, H., 2016. Nanofibrillar cellulose wound dressing in skin graft donor site treatment. *J. Controlled Release* 244, 292–301.
- Henriksson, M., 2008. Cellulose nanofibril networks and composites. Preparation, structure and properties. *KTH Chemical Science and Engineering*. p.61.
- Herzog, E., Casey, A., Lyng, F., Chambers, G., Byrne, H., Davoren, M., 2007. A new approach to the toxicity testing of carbon-based nanomaterials—the clonogenic assay. *Toxicol. Lett.* 174, 49–60.
- Hua, K., Ålander, E., Lindström, T., Mhrianyan, A., Strømme, M., Ferraz, N., 2015. Surface chemistry of nanocellulose fibers directs monocyte/macrophage response. *Biomacromolecules* 16, 2787–2795.
- Huang, S.X., Jaurand, M.C., Kamp, D.W., Whysner, J., Hei, T.K., 2011. Role of mutagenicity in asbestos fiber-induced carcinogenicity and other diseases. *J. Toxicol. Environ. Health B* 14, 179–245.
- Isogai, A., Saito, T., Fukuzumi, H., 2011. TEMPO-oxidized cellulose nanofibers. *Nanoscale* 3, 71–85.
- Jack, A.A., Nordli, H.R., Powell, L.C., Powell, K.A., Kishnani, H., Johnson, P.O., Pukstad, B., Thomas, D.W., Chinga-Carrasco, G., Hill, K.E., 2017. The interaction of wood nanocellulose dressings and wound pathogen *P aeruginosa*. *Carbohydr. Polym.* 157, 1955–1962.
- Jeong, S.I., Lee, S.E., Yang, H., Jin, Y.H., Park, C.S., Park, Y.S., 2010. Toxicologic evaluation of bacterial synthesized cellulose in endothelial cells and animals. *Mol. Cell. Toxicol.* 6, 373–380.
- Jia, B., Li, Y., Yang, B., Xiao, D., Zhang, S., Rajulu, A.V., Kondo, T., Zhang, L., Zhou, J., 2013. Effect of microcrystal cellulose and cellulose whisker on biocompatibility of cellulose based electrospun scaffolds. *Cellulose* 20, 1911–1923.
- Jin, L., Wei, Y., Xu, Q., Yao, W., Cheng, Z., 2014. Cellulose nanofibers prepared from TEMPO-oxidation of kraft pulp and its flocculation effect on kaolin clay. *J. Appl. Polym. Sci.* 131, 1–8.
- Kangas, H., Lahtinen, P., Sneek, A., Saariaho, A.-M., Laitinen, O., Hellén, E., 2014. Characterization of fibrillated celluloses. A short review and evaluation of characteristics with a combination of methods. *Nord. Pulp Pap. Res. J.* 29, 129–143.
- Kolakovic, R., Peltonen, L., Laukkanen, A., Hirvonen, J., Laaksonen, T., 2012. Nanofibrillar cellulose films for controlled drug delivery. *Eur. J. Pharm. Biopharm.* 82, 308–315.
- Kollar, P., Závalová, V., Hošek, J., Havelka, P., Sopuch, T., Karpíšek, M., Třetinová, D., Suchý, P. Jr., 2011. Cytotoxicity and effects on inflammatory response of modified types of cellulose in macrophage-like THP-1 cells. *Int. Immunopharmacol.* 11, 997–1001.
- Kovacs, T., Naish, V., O'Connor, B., Blaise, C., Gagné, F., Hall, L., Trudeau, V., Martel, P., 2010. An ecotoxicological characterization of nanocrystalline cellulose (NCC). *Nanotoxicology* 4, 255–270.
- Li, J., Wei, X., Wang, Q., Chen, J., Chang, G., Kong, L., Su, J., 2012. Homogeneous isolation of nanocellulose from sugarcane bagasse by high pressure homogenization. *Carbohydr. Polym.* 90, 1609–1613.
- Lima, R., Oliveira Feitosa, L., Rodrigues Maruyama, C., Abreu Barga, M., Yamawaki, P.C., Vieira, I.J., Teixeira, E.M., Corrêa, A.C., Caparelli Mattoso, L.H., Fernandes Fraceto, L., 2012. Evaluation of the genotoxicity of cellulose nanofibers. *Int. J. Nanomed.* 7, 3555–3565.
- Lin, N., Dufresne, A., 2014. Nanocellulose in biomedicine: current status and future prospect. *Eur. Polym. J.* 59, 302–325.
- Lopes, V.R., Sanchez-Martinez, C., Strømme, M., Ferraz, N., 2018. In vitro biological responses to nanofibrillated cellulose by human dermal, lung and immune cells: surface chemistry aspect. Part Fibre Toxicol. 14, 1.
- Lou, Y., Yan, R., Kanninen, L., Kuisma, T., Niklander, J., Noon, L.A., Burks, D., Urtti, A., Yliperttula, M., 2014. The use of nanofibrillar cellulose hydrogel as a flexible three-dimensional model to culture human pluripotent stem cells. *Stem Cell Dev.* 23 (4), 380–392.
- Lourenço, A.F., Gamelas, J.A.F., Nunes, T., Amaral, J., Mutjé, P., Ferreira, P.J., 2017. Influence of TEMPO-oxidized cellulose nanofibrils on the properties of filler-containing papers. *Cellulose* 24, 349–362.
- Louro, H., Bettencourt, A., Gonçalves, L.M., Almeida, A.J., Silva, M.J., 2015. Role of nanogenotoxicology studies in safety evaluation on nanomaterials. In: Thomas, S., Grohens, Y., Ninan, N. (Eds.), *Nanotechnology Applications for Tissue Engineering*. Elsevier, Waltham, pp. 263–287.
- Louro, H., Pinhão, M., Santos, J., Tavares, A., Vital, N., Silva, M.J., 2016. Evaluation of the cytotoxic and genotoxic effects of benchmark multi-walled carbon nanotubes in relation to their physicochemical properties. *Toxicol. Lett.* 262 (November (16)), 123–134.
- Malinen, M.M., Kanninen, L.K., Corlu, A., Isoniemi, H.M., Lou, Y.R., Yliperttula, M.L., Urtti, A.O., 2014. Differentiation of liver progenitor cell line to functional organotypic cultures in 3D nanofibrillar cellulose and hyaluronan-gelatin hydrogels. *Biomaterials* 35, 5110–5121.
- Mandal, A., Chakrabarty, D., 2011. Isolation of nanocellulose from waste sugarcane bagasse (SCB) and its characterization. *Carbohydr. Polym.* 86, 1291–1299.
- Mathew, A.P., Oksman, K., Pierron, D., Harmand, M.-F., 2012. Fibrous cellulose nanocomposite scaffolds prepared by partial dissolution for potential use as ligament or tendon substitutes. *Carbohydr. Polym.* 87, 2291–2298.
- Mathew, A.P., Oksman, K., Pierron, D., Harmand, M.F., 2013. Biocompatible fibrous networks of cellulose nanofibers and collagen crosslinked using genipin: potential as artificial ligament/tendons. *Macromol. Biosci.* 13, 289–298.
- Mertaniemi, H., Escobedo-Lucea, C., Sanz-Garcia, A., Gandía, G., Mäkitie, A., Partanen, J., Ikkala, O., Yliperttula, M., 2016. Human stem cell decorated nanocellulose threads for biomedical applications. *Biomaterials* 82, 208–220.
- Moreira, S., Silva, N.B., Almeida-Lima, J., Rocha, H.A., Medeiros, S.R., Alves Jr., C., Gama, F.M., 2009. BC nanofibers: in vitro study of genotoxicity and cell proliferation. *Toxicol. Lett.* 189, 235–241.
- Mossmann, T., 1983. Rapid colorimetric assay for cellular growth and survival: application to proliferation and cytotoxicity assays. *J. Immunol. Methods* 65, 53–63.
- Murphy, F.A., Schinwald, A., Poland, C.A., Donaldson, K., 2012. The mechanism of pleural inflammation by long carbon nanotubes: interaction of long fibres with macrophages stimulates them to amplify pro-inflammatory responses in mesothelial cells. *Part Fibre Toxicol.* 9, 8.
- Nechyporchuk, O., Belgacem, M.N., Bras, J., 2016. Production of cellulose nanofibrils: a review of recent advances. *Ind. Crops Prod.* 93, 2–25.
- Nordli, H.R., Chinga-Carrasco, G., Rokstad, A.M., Pukstad, B., 2016. Producing ultrapure wood cellulose nanofibrils and evaluating the cytotoxicity using human skin cells. *Carbohydr. Polym.* 150, 65–73.
- OECD – Organization for Economic Co-operation and Development, 2010. OECD Guideline for the Testing of Chemicals – In Vitro Mammalian Cell Micronucleus Test.
- Oberdörster, G., 2010. Safety assessment for nanotechnology and nanomedicine: concepts of nanotoxicology. *J. Intern. Med.* 267, 89–105.
- Osong, S.H., Norgren, S., Engstrand, P., 2016. Processing of wood-based microfibrillated cellulose and nanofibrillated cellulose and applications relating to papermaking: a review. *Cellulose* 23, 93–123.
- Park, E.K., Jung, H.S., Yang, H.I., Yoo, M.C., Kim, C., Kim, K.S., 2007. Optimized THP-1 differentiation is required for the detection of responses to weak stimuli. *Inflamm.*

- Res. 56 (1), 45–50. <http://dx.doi.org/10.1007/s00011-007-6115-5>.
- Pereira, M.M., Raposo, N.R.B., Brayner, R., Teixeira, E.M., Oliveira, V., Quintão, C.C.R., Camargo, L.S.A., Mattoso, L.H.C., Brandão, H.M., 2013. Cytotoxicity and expression of genes involved in the cellular stress response and apoptosis in mammalian fibroblast exposed to cotton cellulose nanofibres. *Nanotechnology* 24 (7), 075103.
- Pertile, R.A.N., Moreira, S., da Costa, R.M.G., Correia, A., Guardao, L., Gartner, F., Vilanova, M., Gama, M., 2012. Bacterial cellulose: long-term biocompatibility studies. *J. Biomater. Sci.* 23, 1339–1354.
- Pitkänen, M., Kangas, H., Laitinen, O., Sneek, A., Lahtinen, P., Peresin, M.S., Niinimäki, J., 2014. Characteristics and safety of nano-sized cellulose fibrils. *Cellulose* 21, 3871–3886.
- Rashad, A., Mustafa, K., Heggset, E.B., Syverud, K., 2017. Cytocompatibility of wood-derived cellulose nanofibril hydrogels with different surface chemistry. *Biomacromolecules* 18, 1238–1248.
- Rittinghausen, S., Hackbarth, A., Creutzenberg, O., Ernst, H., Heinrich, U., Leonhardt, A., Schaudien, D., 2014. The carcinogenic effect of various multi-walled carbon nanotubes (MWCNTs) after intraperitoneal injection in rats. *Part Fibre Toxicol.* 11, 59.
- Saito, T., Isogai, A., 2007. Wet strength improvement of TEMPO-oxidized cellulose sheets prepared with cationic polymers. *Ind. Eng. Chem. Res.* 46, 773–780.
- Sargent, L.M., Shvedova, A.A., Hubbs, A.F., Salisbury, J.L., Benkovic, S.A., Kashon, M.L., Lowry, D.T., Murray, A.R., Kisin, E.R., Friend, S., McKinstry, K.T., Battelli, L., Reynolds, S.H., 2009. Induction of aneuploidy by single-walled carbon nanotubes. *Environ. Mol. Mutagen.* 50, 708–717.
- Saska, S., Scarel-Caminaga, R.M., Teixeira, L.N., Franchi, L.P., dos Santos, R.A., Gaspar, A.M., de Oliveira, P.T., Rosa, A.L., Takahashi, C.S., Messaddeq, Y., Ribeiro, S.J., Marchetto, R., 2012. Characterization and in vitro evaluation of bacterial cellulose membranes functionalized with osteogenic growth peptide for bone tissue engineering. *J. Mater. Sci. Mater. Med.* 23, 2253–2266.
- Scarel-Caminaga, R.M., Saska, S., Franchi, L.P., Santos, R.A., Gaspar, A.M.M., Capote, T.S.O., Ribeiro, S.J.L., Messaddeq, Y., Marchetto, R., Takahashi, C.S., 2014. Nanocomposites based on bacterial cellulose in combination with osteogenic growth peptide for bone repair: cytotoxic, genotoxic and mutagenic evaluations. *J. Appl. Biol. Biotechnol.* 2, 1–8.
- Shvedova, A.A., Kisin, E.R., Mercer, R., Murray, A.R., Johnson, V.J., Potapovich, A.I., Tyurina, Y.Y., Gorelik, O., Arepalli, S., Schwegler-Berry, D., Hubbs, A.F., Antonini, J., Evans, D.E., Ku, B., Ramsey, D., Maynard, A., Kagan, V.E., Castranova, V., Baron, P., 2005. Unusual inflammatory and fibrogenic pulmonary responses to single-walled carbon nanotubes in mice. *Am. J. Physiol. Lung Cell. Mol. Physiol.* 289, L698–708.
- Shvedova, A.A., Kisin, E.R., Yanamala, N., Farcas, M.T., Menas, A.L., Williams, A., Fournier, P.M., Reynolds, J.S., Gutkin, D.W., Star, A., Reiner, R.S., Halappanavar, S., Kagan, V.E., 2016. Gender differences in murine pulmonary responses elicited by cellulose nanocrystals. *Part. Fibre Toxicol.* 13, 28.
- Siegrist, K.J., Reynolds, S.H., Kashon, M.L., Lowry, D.T., Dong, C., Hubbs, A.F., Young, S.H., Salisbury, J.L., Porter, D.W., Benkovic, S.A., McCawley, M., Keane, M.J., Mastovich, J.T., Bunker, K.L., Cena, L.G., Sparrow, M.C., Sturgeon, J.L., Dinu, C.Z., Sargent, L.M., 2014. Genotoxicity of multi-walled carbon nanotubes at occupationally relevant doses. *Part. Fibre Toxicol.* 11, 6.
- Siró, I., Plackett, D., 2010. Microfibrillated cellulose and new nanocomposite materials: a review. *Cellulose* 17, 459–494.
- Snyder-Talkington, B.N., Qian, Y., Castranova, V., Guo, N.L., 2012. New perspectives for in vitro risk assessment of multiwalled carbon nanotubes: application of coculture and bioinformatics. *J. Toxicol. Environ. Health B* 15, 468–492.
- Snyder-Talkington, B.N., Dong, C., Zhao, X., Dymacek, J., Porter, D.W., Wolfarth, M.G., Castranova, V., Qian, Y., Guo, N.L., 2015. Multi-walled carbon nanotube-induced gene expression in vitro: concordance with in vivo studies. *Toxicology* 328, 66–74.
- Stefaniak, A.B., Seehra, M.S., Fix, N.R., Leonard, S.S., 2014. Lung biodegradability and free radical production of cellulose nanomaterials. *Inhal. Toxicol.* 26 (12), 33–749.
- Sun, F., Nordli, H.R., Pukstad, B., Gamstedt, E.K., Chinga-Carrasco, G., 2017. Mechanical characteristics of nanocellulose-PEG bionanocomposite wound dressings in wet conditions. *J. Mech. Behav. Biomed. Mater.* 69, 377–384.
- Syverud, K., Kirsebom, H., Hajizadeh, S., Chinga-Carrasco, G., 2011. Cross-linking cellulose nanofibrils for potential elastic cryo-structured gels. *Nanoscale Res. Lett.* 6, 626.
- Ursini, C.L., Cavallo, D., Fresegna, A.M., Ciervo, A., Maiello, R., Tassone, P., Buresti, G., Casciardi, S., Iavicoli, S., 2014. Evaluation of cytotoxic, genotoxic and inflammatory response in human alveolar and bronchial epithelial cells exposed to titanium dioxide nanoparticles. *J. Appl. Toxicol.* 34, 1209–1219.
- Valentin-Severin, I., Le Hegarat, L., Lhuguenot, J.C., Le Bon, A.M., Chagnon, M.C., 2003. Use of HepG2 cell line for direct or indirect mutagens screening: comparative investigation between comet and micronucleus assays. *Mutat. Res.* 536 (1–2), 79–90.
- Vartiainen, J., Pöhler, T., Sirola, K., Pyllkänen, L., Alenius, H., Hokkinen, J., Tapper, U., Lahtinen, P., Kapanen, A., Putkisto, K., Hiekkataipale, P., Eronen, P., Ruokolainen, J., Laukkanen, A., 2011. Health and environmental safety aspects of friction grinding and spray drying of microfibrillated cellulose. *Cellulose* 18, 775–786.
- Vietti, G., Ibouaadaten, S., Palmi-Pallag, M., Yakoub, Y., Bailly, C., Fenoglio, I., Marbaix, E., Lison, D., van den Brule, S., 2013. Towards predicting the lung fibrogenic activity of nanomaterials: experimental validation of an in vitro fibroblast proliferation assay. *Part. Fibre Toxicol.* 10, 52. <http://dx.doi.org/10.1186/1743-8977-10-52>.
- Wang, L., Mercer, R.R., Rojanasakul, Y., Qiu, A., Lu, Y., Scabilloni, J.F., Wu, N., Castranova, V., 2010. Direct fibrogenic effects of dispersed single-walled carbon nanotubes on human lung fibroblasts. *J. Toxicol. Environ. Health A* 73, 410–422. <http://dx.doi.org/10.1080/15287390903486550>.
- Yanamala, N., Farcas, M.T., Hatfield, M.K., Kisin, E.R., Kagan, V.E., Geraci, C.L., Shvedova, A.A., 2014. In vivo evaluation of the pulmonary toxicity of cellulose nanocrystals: a renewable and sustainable nanomaterial of the future. *ACS Sustain. Chem. Eng.* 2, 1691–1698.

4. Cytotoxicity and genotoxicity of MWCNT-7 and crocidolite: assessment in alveolar epithelial cells versus their co-culture with monocyte-derived macrophages

Célia Ventura ^{a,b,c}, Joana FS Pereira ^{a,d}, Paulo Matos ^{a,d}, Bárbara Marques ^a, Peter Jordan ^{a,d}, António Sousa-Uva ^{b,d}, Maria João Silva ^{*a,c}

^a Department of Human Genetics, National Institute of Health Doutor Ricardo Jorge, Lisbon; ^b Department of Occupational and Environmental Health, National School of Public Health, NOVA University of Lisbon (UNL), Lisbon; ^c Center for Toxicogenomics and Human Health (ToxOmics), NOVA Medical School-FCM, UNL, Lisbon; ^d CISP – Public Health Research Center, Lisbon, Portugal. ^eBiolSI – Biosystems & Integrative Sciences Institute, Faculty of Sciences, University of Lisbon, Lisbon; Portugal.

The work included in this chapter is under review for publication in *Nanotoxicology*.

4.1. Abstract

In the past years, several *in vitro* studies have addressed the pulmonary toxicity of multi-walled carbon nanotubes (MWCNT) and compared it with that caused by asbestos fibers, but their conclusions have been somewhat inconsistent and difficult to extrapolate to *in vivo*. Since cell co-culture models were proposed to better represent the *in vivo* conditions than conventional monocultures, this work intended to compare the cytotoxicity and genotoxicity of MWCNT-7 (Mitsui-7) and crocidolite using A549 cells grown in a conventional monoculture or in co-culture with THP-1 macrophages. Although a decrease in A549 viability was noted following exposure to a concentration range of MWCNT-7 and crocidolite, no viability change occurred in similarly exposed co-cultures. Early events indicating epithelial to mesenchymal transition (EMT) were observed which could explain apoptosis resistance. The comet assay results were similar between the two models, being positive and negative for crocidolite and MWCNT-7, respectively. An increase in the micronucleus frequency was detected in the co-cultured A549-treated cells with both materials, but not in the monoculture. On the other hand, exposure of A549 monocultures to MWCNT-7 induced a highly significant increase in nucleoplasmic bridges in which those were found embedded. Our overall results demonstrate that (i) both materials are cytotoxic and genotoxic, (ii) the presence of THP-1 macrophages upholds the viability of A549 cells and increases the aneugenic/clastogenic effects of both materials probably through EMT and (iii) MWCNT-7 induces the formation of nucleoplasmic bridges in A549 cells.

4.2. Introduction

In the past years, several toxicological studies have addressed the hazard of multi-walled carbon nanotubes (MWCNT), a nanomaterial composed of multiple graphite sheets assembled in concentric layers, displaying various lengths and a diameter within the nanoscale. MWCNT applications are a fast-evolving field, with many different employments in industry and biomedicine¹. However, there is the concern that MWCNT inhalation may cause adverse pulmonary effects resulting from their physical properties and biopersistence, particularly when these are similar to asbestos fibers. Human exposure to asbestos fibres has been associated with the development of bronchogenic carcinoma, malignant mesothelioma, and interstitial pulmonary fibrosis (asbestosis)². In turn, rodents exposed to liquid suspensions of carbon nanotubes (CNT) by intratracheal instillation or pharyngeal aspiration developed acute or persistent pulmonary inflammation and persistent interstitial fibrosis with granuloma

formation, and bronchiolar or bronchioloalveolar hyperplasia^{1,3}. Moreover, the MWCNT-7 (Mitsui-7) induced malignant mesothelioma in mice^{4,5} and rats^{6,7,8,9}, and lung carcinomas in rats^{10,9}. Similarly to asbestos, MWCNT-7 injection in the peritoneal cavity of rats induced an early and selective sustained immunosuppressive response characterized by the accumulation of monocytic myeloid derived suppressor cells (CD11b/cint and His48hi) that possess the ability to suppress polyclonal activation of T lymphocytes¹¹. Besides, mesotheliomas induced by thin (diameter ~ 50 nm) and highly crystalline MWCNT present a homozygous deletion of the tumour suppressor genes *Cdkn2a/2b*, comparable to mesotheliomas induced by asbestos⁷. These evidences led the International Agency for Research on Cancer (IARC) to categorize the MWCNT-7 as possibly carcinogenic to humans (Group 2B)¹².

Concerning *in vitro* toxicological assays, divergent results have been reported. These can reflect different methodological approaches^{13,3}, different CNT physicochemical characteristics^{14,15,16,17,18} or even the use of different cell lines¹⁹. For instance, some MWCNT have been reported to induce DNA damage in A549 cells^{20,21} and in Met-5A cells, but not in BEAS 2B cells²² and to stimulate micronuclei formation in A549 cells²³ but not in the other two cell lines^{22,24}. Catalán et al. (2015) observed that straight MWCNT induced DNA strand breaks at low doses, while tangled MWCNT did so only at a higher dose²⁴. In an *in vitro* study of 15 different MWCNT, increased levels of DNA strand breaks were observed for treatments with thick and high Fe₂O₃ and Ni containing MWCNT, but overall MWCNT were weakly genotoxic and not cytotoxic²⁵. It has been recognized that the physicochemical characteristics of the MWCNT are major contributors for their toxicity. Pristine MWCNT are more cytotoxic than functionalized MWCNT, while functionalized MWCNT are more genotoxic compared to their pristine form²⁶. It has been proposed that the formation of larger agglomerates, dependent upon different protein coronae, contributes to mitigate the biological effects of functionalized MWCNT in protein-rich biological media²⁷.

Moreover, a modest correlation has been found between *in vitro* and *in vivo* toxicological studies that may be due to the use of conventional *in vitro* monocultures that do not mimic well the *in vivo* organization. Thus, it is expected that the simultaneous culture of cell types that co-exist in the organism will provide a more reliable toxicological information^{28,29}. For instance, a co-culture of human small airway epithelial cells (SAEC) and human microvascular endothelial cells (HMVEC) has correlated better with the *in vivo* mouse lung transcriptomic profile following MWCNT exposure than the two monocultures separately³⁰. Consequently, efforts are currently being made to implement co-culture models³¹.

In this study, we investigated the toxicity of the MWCNT-7 (Mitsui-7) and crocidolite asbestos, comparing the results obtained in a conventional A549 alveolar epithelial cell culture with those of a co-culture of the same cells with THP-1 differentiated macrophages. As already mentioned, MWCNT-7 and crocidolite share strong resemblances in their physical characteristics and a high biopersistence, as well. Moreover, crocidolite is a well-known cause of lung diseases², and consequently, a well-documented standard to compare the adverse effects of MWCNT-7. Alveolar macrophages are key cells in the immune response to CNT exposure. It has been proposed that macrophages try to degrade CNT. However, when the nanotube length exceeds that of the macrophage cell, they trigger frustrated phagocytosis^{32,33,3}, leading to the release of proinflammatory cytokines and chemokines (e.g., TNF α , IL-1 β , IL-6, IL-10 and MCP1) and activation of associated transcription factors (NF-kB and AP-1)^{34,35}. Inflammation can provide a tumour-promoting microenvironment crucial in the pulmonary outcome of exposure to both MWCNT-7 and crocidolite.

Here we report relevant toxicological findings in the monoculture and co-culture models *per se*, but also show that the results obtained in both cell cultures are not alike for the most part of the assays we performed. We suggest that toxicological outcomes may differ when different cell types are added into *in vitro* models, allowing further understanding of the complexity of the cell interplay.

4.3. Materials and Methods

4.3.1. Fiber characterization and preparation

The MWCNT-7, also known as Mitsui-7 (Mitsui & Co, Lda. Ibaraki, Japan), was provided as a sub-sample by the National Research Centre for the Working and Environment (NRCWE-006). Its physicochemical characteristics were described previously and are listed in table I.

Immediately before the experiments, a 2.56 mg/mL stock dispersion of the NRCWE-006 was prepared according to Jensen et al. (2011)³⁶. The hydrodynamic particle size-distribution (Z_{av} , nm) and the polydispersity index (PDI) of MWCNT-7 stock dispersion were measured shortly after sonication (Malvern Nano ZS, Malvern Inc., UK) by dynamic light scattering (DLS) and expressed as the mean of 10 consecutive measurements³⁷. Scanning electron microscopy (SEM) of the stock solution was also performed using a Phantom XL microscope.

Table I. Physicochemical characteristics of the MWCNT-7 (NRCWE-006, Mitsui-7).

Specific surface area (m ² /g) ^a	Thickness ± SD (nm) ^b	Geodesic length ± SD (nm) ^b	Aspect ratio ± SD ^b	Impurities % ^a	Minor Impurity phases ^c	Minor elements/coatings ^c
24-28	69.4 ± 1.4	4423.6 ± 2.3	63.7 ± 2.4	<1%	Fe ₂ O ₃	Na: 499 ± 103 µg/g Mg: 1 ± 1 µg/g Al: 66 ± 19 µg/g Fe: 355 ± 2 µg/g Ni: 1 µg/g

^a Information provided by manufacturer or the Joint Research Center (http://ihcp.jrc.ec.europa.eu/our_activities/nanotechnology/nanomaterials-repository/list_materials_JRC_rep_oct_2011.pdf).

^b Values reported by Tavares et al. 2014³⁷.

^c Values reported in the NANOGENOTOX Joint Action by Jensen 2013.

The crocidolite fibers are a standard reference mineral from the Union for International Cancer Control (UICC, Geneva, Switzerland) and were kindly provided by Dr. Fátima Aguiar from the Environmental Health Department of INSA. Their preparation and characterization have been described in detail^{38,39,40,41}. A stock solution was prepared at 1 mg/mL in phosphate buffer saline (PBS), pH 7.4 (Gibco). Prior to dilution in culture medium, fibers were passed through a syringe needle to ensure a better uniformity of the suspension.

4.3.2. Cell culture

The human alveolar epithelial cell line A549 (ATCC, Manassas, VA, USA, CCL-185) and the human monocytic leukaemia cell line THP-1 (ATCC, TIB-202) were both grown in RPMI 1640 medium (Gibco, Waltham, MA, USA) supplemented with 10% heat-inactivated foetal bovine serum (Gibco), 1% penicillin/streptomycin (10.000 U/mL, Gibco) and 1% fungizone (0.25 mg/mL, Gibco) at 37°C in 5% CO₂. THP-1 monocytes were grown on transwell inserts with a nominal pore size of 0.4 µm (Greiner Bio-One GmbH, Kremsmünster, Austria) at a density of 0.2×10⁵ cells/mL and differentiated into macrophages by a 48 h incubation with 100 ng/mL of 12-O-tetradecanoylphorbol-13-acetate (TPA, Sigma-Aldrich). The medium was substituted by serum-free medium for further 72 h to allow cells to recover from the TPA effect. In co-culture experiments, A549 cells were cultured in 12-well plates at a density of 0.5×10⁵ cells/mL and the inserts with differentiated THP-1 cells were placed directly on top. The resulting co-

culture presented a 1:5 proportion of THP-1:A549 cells based on Pinkerton KE et al. (1992)⁴², and was incubated for 24 h at 37° C and 5% CO₂. To ensure that THP-1 and A549 cells were exposed to the same concentrations of MWCNT-7 or crocidolite, the dispersions were added to the apical and basolateral sides of the insert.

4.3.3. MTT assay

A549 cells were exposed to 6.25, 12.5, 25, 50 and 100 µg/cm² of MWCNT-7, or 1.25, 2.5, 5, 10, 20 and 40 µg/cm² of crocidolite, for 24 h or 48 h. Co-cultures were exposed to 6.25, 25 and 100 µg/cm² of MWCNT-7, and 2.5, 10 or 40 µg/cm² of crocidolite, for 24 h or 48 h. SDS (0.1 µg/mL, Sigma) was used as a positive control with 1 h exposure. When studying the co-culture, the transwell inserts were separated from the plate, and the following steps of the assay performed independently in the A549 cells (plate) and in the THP-1 cells (inserts). After washing with PBS, cells were incubated for 2 h with fresh medium containing 10% of MTT solution (5 mg/mL, Calbiochem, Darmstadt, Germany). The medium was discharged and DMSO (Sigma) was added for 20 min under shaking. The absorbance was recorded at 570 nm against a reference filter set at 690 nm using a Multiscan Ascent spectrophotometer (Labsystems, Helsinki, Finland).

4.3.4. Determination of IL-1β

Cell culture supernatants were collected separately from the well plates and the corresponding inserts, after the 24 h and 48 h treatment of the comet and micronucleus assay, respectively, and stored at -80 °C until analysis. IL-1β concentrations were determined with the commercially available colorimetric sandwich ELISA – IL-1β-EASIA Kit KAP1211 (DIASource, Louvain-la-Neuve, Belgium), according to the manufacturer's protocol. A positive control was prepared adding 100 ng/µL of lipopolysaccharides (LPS; Sigma) and 5 mM adenosine 5'-triphosphate disodium salt (ATP; Sigma) to the cells cultured on the inserts⁴³.

4.3.5. SDS-PAGE and Western Blotting

Whole cell lysates from three different replicas of A549 cells grown in monoculture or co-culture with THP-1 macrophages and exposed to 25 µg/cm² of MWCNT-7 or 10 µg/cm² of crocidolite, for 24 h and 48 h, were analysed by western blotting. These concentrations were chosen because they had the highest change in cell viability

between the two cell culture models. Cells were lysed in SDS sample buffer, boiled for 10 min, centrifuged at 2,500 $\times g$ for 30 s, and proteins resolved in 12% SDS-PAGE mini-gels. Proteins were then transferred onto polyvinylidene difluoride (Bio-Rad) membranes using a Mini Trans-Blot cell (Bio-Rad). Membranes were probed using the indicated antibodies, and specific binding was detected via a secondary peroxidase-conjugated antibody (Bio-Rad) followed by chemiluminescence. Monoclonal anti-E cadherin was from BD transduction laboratories, anti-vimentin from Santa Cruz, polyclonal anti-GADPH from Abcam, and monoclonal anti-PCNA from Oncogene.

4.3.6. Evaluation of apoptosis

Apoptosis was evaluated after 48 h exposure to the lowest, medium and highest concentrations of crocidolite and MWCNT-7. For this purpose the activity of caspases 3/7 were measured using the Caspase-Glo® 3/7 Assay (Promega, Madison, USA) according to the manufacturer's instructions. The luminescence, proportional to the caspase activity, was measured using a Lucy2 microplate luminometer (Anthos Labtec Instruments GmbH, Austria). Background luminescence was determined in the culture medium and subtracted from all experimental values.

Apoptotic cells were also scored under bright field microscopy based on their typical morphologic features in Giemsa-stained slides prepared for the micronucleus assay from cultures exposed to 50 $\mu\text{g}/\text{cm}^2$ MWCNT-7.

4.3.7. Comet assay

Cells were exposed for 24 h to 6.25, 12.5, 25, 50 and 100 $\mu\text{g}/\text{cm}^2$ of MWCNT-7 or 1.56, 3,125, 6.25, 12.5, and 25 $\mu\text{g}/\text{cm}^2$ of crocidolite in 12-well plates. Ethyl methanesulphonate (EMS, 5mM, Sigma-Aldrich) was used as a positive control with 1-h exposure. The cells were washed with PBS, harvested after trypsinization and centrifuged, the pellets embedded in 0.8% low melting point agarose, then spread on 1% agarose-precoated microscope slides. Slides were immersed in lysis solution (2.5 M NaCl, 100 mM EDTA, 10 mM Tris, 10% DMSO, 1% Triton X-100, pH 10) for a minimum of 1 h and washed twice with enzyme buffer (40 mM HEPES, 100 mM KCl, 0.5 mM EDTA, 0.2 mg/mL BSA, pH 8). The agarose-embedded cells were treated with enzyme buffer or 50 μL of formamidopyrimidine DNA glycosylase (FpG, kindly provided by Dr. A. Collins, University of Oslo, Norway) for 30 min at 37°C. Apart from quantifying DNA single and double strand breaks, FpG allows the detection of oxidative DNA lesions. The slides were immersed into cold electrophoresis buffer (0.3 M NaOH, 1 mM

hydrated Na₂EDTA; pH 13) for 30 min, followed by a 25 min electrophoresis at 0.8 V/cm. Finally, after 10 min neutralization with PBS, slides were rinsed, dried and stained with ethidium bromide (0.125 µg/µL). Three independent experiments were carried out, each with two replicates per treatment condition. In each experiment, a total of 100 randomly selected nucleoids were analysed in FpG treated and untreated gels for each culture, using an Axioplan2 Imaging epifluorescence microscope equipped with a high resolution camera (Carl Zeiss Microscopy, Gottingen, Germany). Scoring was done with the Comet Imager 2.2 software (MetaSystems, Altlussheim, Germany), choosing the percentage of DNA in the tail as a measure of DNA damage. The results represent the mean (±SE) of three independent experiments.

4.3.8. Micronucleus assay

Following 6 h exposure to 6.25, 12.5, 25, 50 and 100 µg/cm² of MWCNT-7 or 2.5, 5, 10, 20, and 40 µg/cm² of crocidolite, cytochalasin B (Sigma) was added to the 12-well plates at a final concentration of 6 µg/mL. For each experiment, negative (non-treated cells) and positive (50 µg/mL mitomycin C, Sigma) controls were included. Briefly, at the end of the 48 h-treatment in the monoculture, cells were washed with PBS, detached with trypsin-EDTA, submitted to a hypotonic shock with a RPMI 1640:dH₂O:FBS (37.5:12.5:1) solution, centrifuged and the pellet spread onto microscope slides. In order to obtain binucleated cells after cytochalasin B addition, the exposure had to be prolonged for further 2 h in the co-culture. The slides were dried, fixed in absolute methanol (Sigma) and stained with 4% Giemsa (Merck, Darmstadt, Germany). Slides were scored under a bright field microscope for the presence of micronuclei using the criteria described by Thomas and Fenech (2011) in, at least, 2000 binucleated cells from two independent cultures⁴⁴. The proportion of mono-, bi- or multinucleate cells in 1000 cells per treatment was used to calculate the cytokinesis-blocked proliferation index (CBPI)⁴⁵.

4.3.9. Fluorescence in situ hybridization (FISH)

Additional glass slides prepared for the micronucleus assay of A549 cells exposed to 50 µg/cm² of MWCNT-7 were used for FISH using a biotin-labelled pan-centromeric probe and a FITC-labelled pan-telomeric probe (starFISH, Cambio, Cambridge, UK). Briefly, slides were treated with 0.1 mg/mL acid pepsin (0.01 N HCl), then fixed in 1% (wt/v) formaldehyde–PBS before dehydration through 5 min in ethanol series. Cellular DNA was denatured at 80°C for 2 min in 70% formamide (in 2xSSC), and dehydrated

through ethanol series. Probes were denatured 5 min at 37° C followed by 10 min at 85°C and hybridization was performed overnight at 37°C in a humid chamber. Post hybridization washes were performed at 37°C with 2xSSC (5 min), three times 0.5xSSC (3 min), two times 2xSSC (5 min, room temperature) and 0.45% BSA in a 0.15 M NaHCO₃ solution with 0.1% wt/vol Tween 20 (BT; 5 min). Cellular DNA were counterstained with 4',6-diamidino-2-phenylindole (DAPI; 0.5 g/mL) and mounted in Vectashield (Vector Laboratories, Burlingame, CA, USA). The hybridization signal of the telomeric probe was first analysed under a fluorescence microscope (Zeiss, Axioplan 2) using filters for DAPI and FICT. Then, the slides were incubated for 1 h at 40°C with Avid-Cy3 antibody (Amersham, Uppsala, Sweden), washed three times in BT at 40°C (5 min), re-mounted and analysed using filters for DAPI and Cy3. Hybridization signals were captured with a cooled charge-coupled device camera controlled by MacProbe software (PSI, Applied Imaging), processed using image analysis software, and overlaid electronically.

4.3.10. Immunofluorescence and confocal microscopy

For immunofluorescence analysis, cells were grown on coverslips, treated with 50 µg/cm² of MWCNT-7 as described for the micronucleus assay, fixed in ice-cold methanol at -20°C for 30 min, washed with PBS (Sigma-Aldrich), and incubated for 1 h with mouse anti-α-tubulin (clone B-5-1-2, Sigma-Aldrich). Cells were then thoroughly washed with PBS and incubated for 30 min with AlexaFluor488-conjugated secondary antibody (Life Technologies Invitrogen Corporation). Following thorough washing in PBS and DAPI staining of nuclei, coverslips were mounted on microscope slides with Vectashield (Vector Laboratories) and sealed with nail polish. Images were recorded and processed on a Leica TCS-SPE confocal microscope and assembled into figures with Adobe Photoshop software.

4.3.11. Statistical analysis

Statistical comparisons of the treated and control cells in the MTT and comet assays were evaluated through a one-way analysis of variance (ANOVA) followed by Tukey's multiple comparison test, after testing for normality. The two-tailed Student's t-test was used in the comet assay to compare results with and without FpG, and to compare the CBPI in treated and control cells. The 2-tailed Fisher's exact test was applied to analyse the results of the frequency of micronucleated cells. All analyses were

performed with the SPSS statistical package (version 25, SPSS Inc. Chicago, IL). The results are presented as the mean \pm standard deviation.

4.4. Results

4.4.1. MWCNT-7 characterization

The physicochemical properties of MWCNT-7 have been previously characterized, and are presented in the materials and methods section. Although some disagreement exists if DLS is applicable to non-spherical particles, the size distribution of the MWCNT was measured shortly after sonication in the stock solution, revealing a PDI of 0.381 ± 0.02 (mean \pm SD) and a Z_{av} of 1004 ± 34.03 (mean \pm SD).

4.4.2. Cytotoxicity

MWCNT-7 treatment of A549 cells in monoculture caused a significant and dose-dependent decrease in cell viability, being more pronounced at 48 h than at 24 h (figure 1). However, a similar treatment of A549 cells in co-culture with THP-1 macrophages induced a milder effect on A549 cell viability. The comparison of the viability measured at each concentration between both types of cultures revealed highly significant differences ($p < 0.001$ for all concentrations at 48 h; $p < 0.05$ for all concentrations at 24 h, t-test). These differences were supported by the results of the cytokinesis-block proliferation index (CBPI) derived from the micronucleus assay (figure 2A) in that a decrease in the cell proliferative capacity was observed in the monoculture at the highest MWCNT-7 concentration, while no effect was observed in the co-culture.

THP-1 cells were more sensitive to the cytotoxicity of MWCNT-7 than A549 cells, as can be observed in figure 1.

Regarding crocidolite cytotoxicity, A549 cell viability at 24 h decreased in a concentration-dependent and statistically significant manner for all concentrations tested ($p < 0.005$, Tukey test) except at the lowest one ($1.25 \mu\text{g}/\text{cm}^2$), reaching values below 70% viability at the highest concentrations tested. No significant differences were detected between the 24 h and 48 h exposure ($p > 0.05$) (figure 1). Although the co-culture exposure to crocidolite for 48 h resulted in a dose-dependent effect similar to that observed for the monoculture, the 24 h exposure retained or even increased significantly the A549 viability, at the two lowest concentrations tested ($p < 0.001$). CBPI analysis showed no signs of toxicity for both culture models (figure 2B).

As observed with the MWCNT-7 treatment, the crocidolite cytotoxicity was more pronounced in the THP-1 cells present in the co-culture, than in A549 cells, especially at 48 h exposure (figure 1).

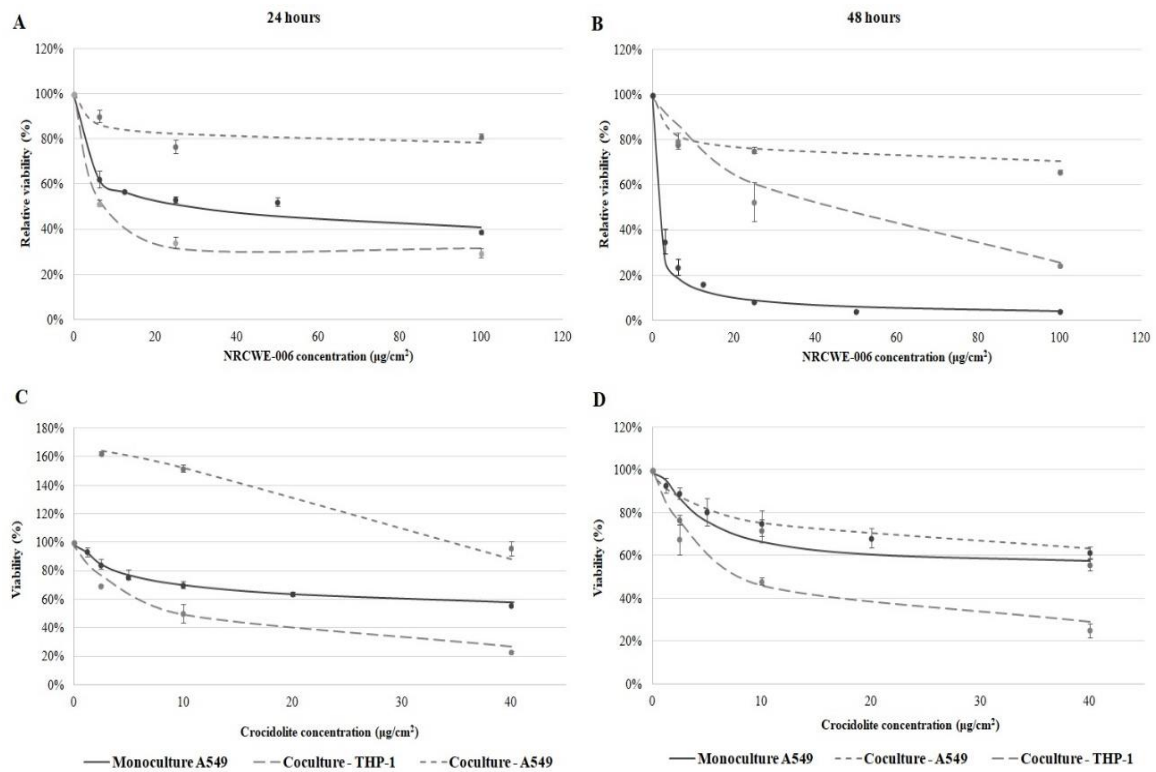


Figure 1. Relative viability of A549 cells in monoculture, and of A549 and THP-1 cells in co-culture, after exposure to different concentrations of MWCNT-7 for 24 h (A) and 48 h (B) and crocidolite for 24 h (C) and 48 h (D) as determined by the MTT assay.

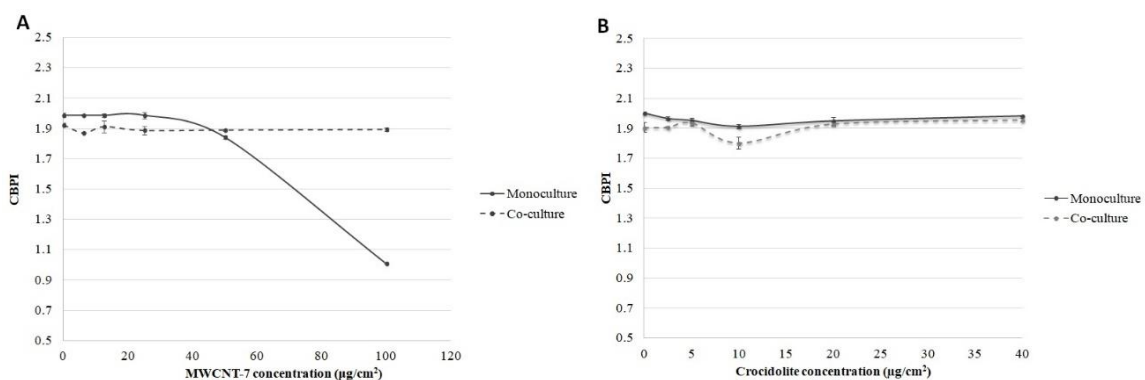


Figure 2. Cytokinesis-block proliferation index (CBPI) of A549 cells in monoculture and co-culture with THP-1 cells, after exposure to MWCNT-7 (A) or crocidolite (B) for 48 h (monoculture) or 50 h (co-culture).

4.4.3. Apoptosis and epithelial-mesenchymal transition (EMT)

In an attempt to elucidate how the presence of THP-1 cells in the co-culture influenced the viability of A549 cells exposed to both materials, we first investigated differences in apoptotic cell death by measuring caspase 3/7 activity.

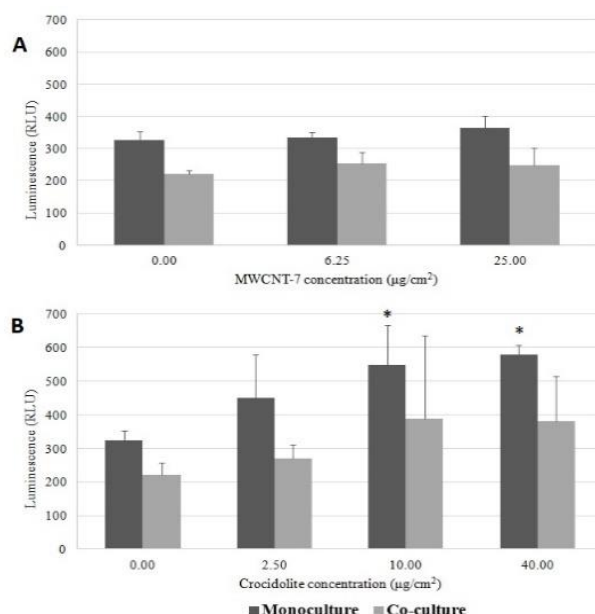


Figure 3. Caspase 3/7 activity in A549 cells in monoculture and co-culture with THP-1 cells, after exposure to MWCNT-7 (A) or crocidolite (B). RLU – Relative light units. * $p < 0.005$.

As shown in figure 3, the results obtained on the A549 cells exposed to MWCNT-7, either in monoculture or in co-culture, were not statistically significant from those of the controls, indicating that it does not induce apoptosis in the conditions tested. However, the result for the 100 µg/cm² concentration was not reliable, because at that concentration the interference from black MWCNT particle density is too high to allow a correct luminescence measurement, even with blank correction.

The exposure to several crocidolite concentrations increased apoptosis in a concentration-dependent manner reaching statistical significance at 10.0 µg/cm² and 40.0 µg/cm² of crocidolite comparatively to the non-exposed cells (ANOVA, $p < 0.005$; Tukey, $p = 0.01$ and $p = 0.005$, respectively). Although an increase of apoptosis was also observed in the co-cultured A549 cells after similar treatments, no statistically significant increase over the control value were found ($p > 0.05$, Kruskal-Wallis test).

The comparison of the results between the monoculture and the co-culture revealed a significant difference in the caspases 3/7 activity, both for the non-exposed cells and

for the cells exposed to all concentrations of MWCNT-7 and crocidolite (except for 10 $\mu\text{g}/\text{cm}^2$ crocidolite) ($p < 0.001$, t-test). These data suggest that macrophages protect A549 cell from death through apoptosis.

Second, the hypothesis that A549 cells may undergo EMT in the presence of THP-1 cells leading to growth arrest at G1/S phase and evasion from apoptosis was also explored. EMT of A549 cells in the presence of THP-1 cells was evaluated by western blotting through changes in the expression of the marker proteins E-cadherin, vimentin and proliferating cell nuclear antigen (PCNA) (figure 4). Upon the initiation of EMT, loss of cell-cell adhesion involves cleavage of epithelial cadherin (E-cadherin) at the plasma membrane and its subsequent degradation, and changes in the intermediate filament composition with the activation of vimentin expression⁴⁶. PCNA is a ring-shaped homotrimeric protein that acts as a cofactor of DNA polymerase delta in eukaryotic cells in both DNA replication and repair of excised damaged strands^{47,48}. Thus, it indicates if normal cell division is maintained or not in the exposed cell cultures.

The overall results are shown in figures 4 and 5. At 24 h exposure, the level of E-cadherin that is expressed in the A549 monoculture exposed to MWCNT-7 shows a slight but non-significant decrease. However, it is significantly lower in cells exposed to crocidolite comparatively to that of non-exposed cells. PCNA levels follow E-cadherin levels, suggesting that this decrease is a result of cell death. At 48 h exposure, PCNA also decreased compared to the non-exposed cells, particularly in the monoculture exposed to MWCNT-7, indicating, once again, cell death. Regarding the co-culture, there is no indication of PCNA loss, and E-cadherin is significantly lower in crocidolite-treated cells (t-test, $p < 0.05$) except at 48 h exposure to MWCNT-7, which seems to indicate an early EMT.

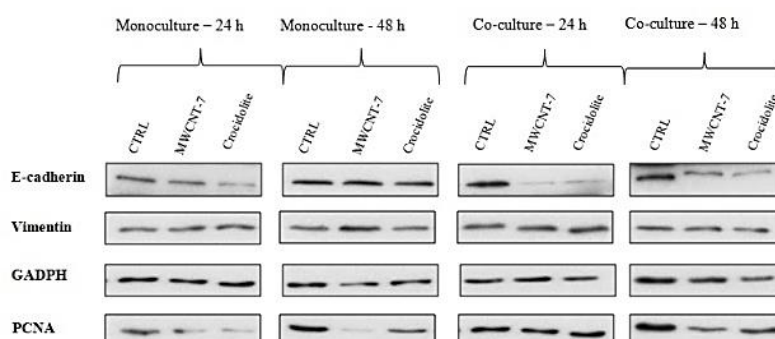


Figure 4. Expression levels of E-cadherin, vimentin, proliferating cell nuclear antigen (PCNA) and glyceraldehyde 3-phosphate dehydrogenase (GAPDH) in A549 cells by western blotting.

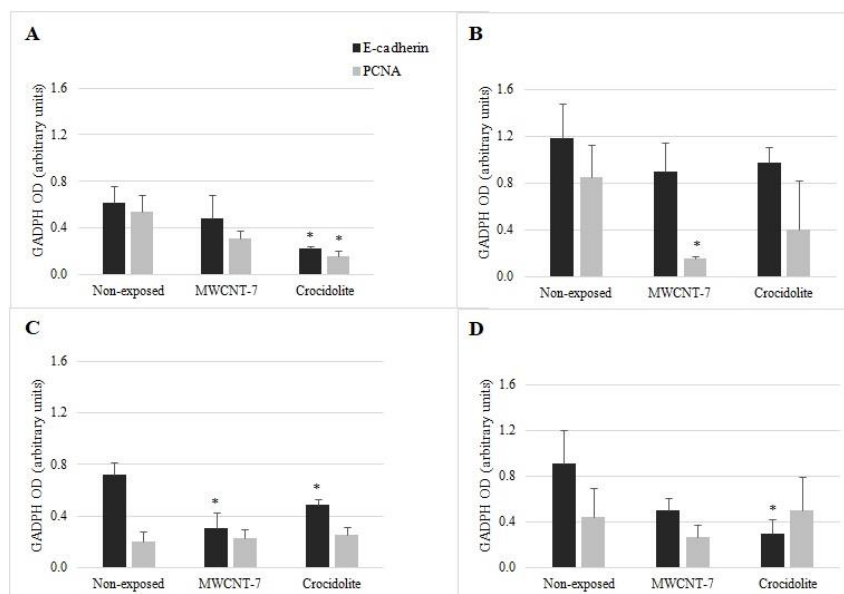


Figure 5. Mean levels of E-cadherin and PCNA in three replicates of A549 cells analysed by western blotting. Cells were cultured without (A and B) and with THP-1 macrophages (C and D) and exposed to 25 $\mu\text{g}/\text{cm}^2$ MWCNT-7 or 10 $\mu\text{g}/\text{cm}^2$ crocidolite for 24 h (A and C) and 48 h (B and D). * $p < 0.05$.

4.4.4. IL-1 β determination

In order to understand the differences in the cellular response between A549 cells in monoculture or in co-culture, we determined the levels of the cytokine IL-1 β , which is a key mediator of pro-inflammatory responses, in the conditioned culture media after exposure to MWCNT-7. IL-1 β concentration presented a potential dose-effect relationship following cells exposure to MWCNT-7 (comet assay supernatants), with higher IL-1 β concentrations in the inserts medium (THP-1 cells) than in the plate wells medium (A549 cells) (figure 6). IL-1 β was not detectable in the micronucleus assay supernatants.

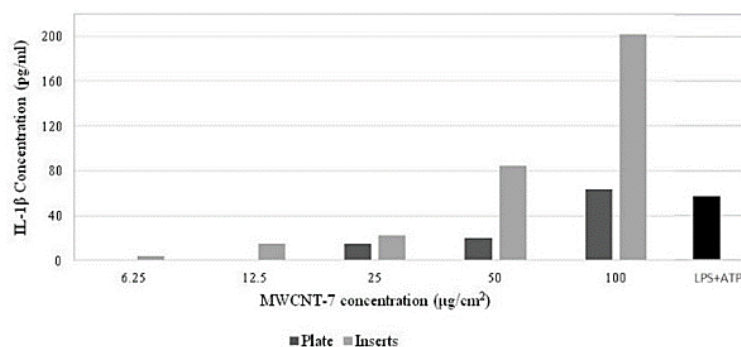


Figure 6. IL-1 β determination in the cell culture supernatants of A549 medium (dark grey) and THP-1 medium inserts (light grey) after exposure to a concentration range of MWCNT-7. 100 ng/ μl LPS with 5mM ATP was used as a positive control. Results are expressed as means of two independent determinations.

4.4.5. Genotoxicity

The genotoxicity of MWCNT-7 and crocidolite was investigated through the comet assay and the cytokinesis-block micronucleus assay, in both A549 monocultures and co-cultures with THP-1 cells. No DNA damage was induced in the monoculture of A549 cells exposed to MWCNT-7 (ANOVA, $p > 0.05$), and the differences in the mean level of DNA damage without and with FpG were not significant (t-test, $p > 0.05$), either in A549 cells cultured in monoculture or in co-culture. Moreover, when comparing the genotoxicity of both culture types, there was no significant difference for any concentration, without or with FpG (t-test, $p > 0.05$) (figure 7).

In contrast, crocidolite induced a concentration-dependent increase in the level of DNA lesions, both in the A549 monoculture and in the co-culture with THP-1 macrophages ($p < 0.001$, ANOVA). A significant increase in the percentage of DNA in tail was observed in the monoculture with FpG addition at the highest concentration tested ($p < 0.05$, t-test). The mean level of DNA damage in A549 cells was not altered between the monoculture and the co-culture, except for the lowest concentration (1.5 $\mu\text{g}/\text{cm}^2$ crocidolite) without FpG ($p = 0.01$, t-test), where more damage was induced in the co-culture than in the monoculture (figure 7).

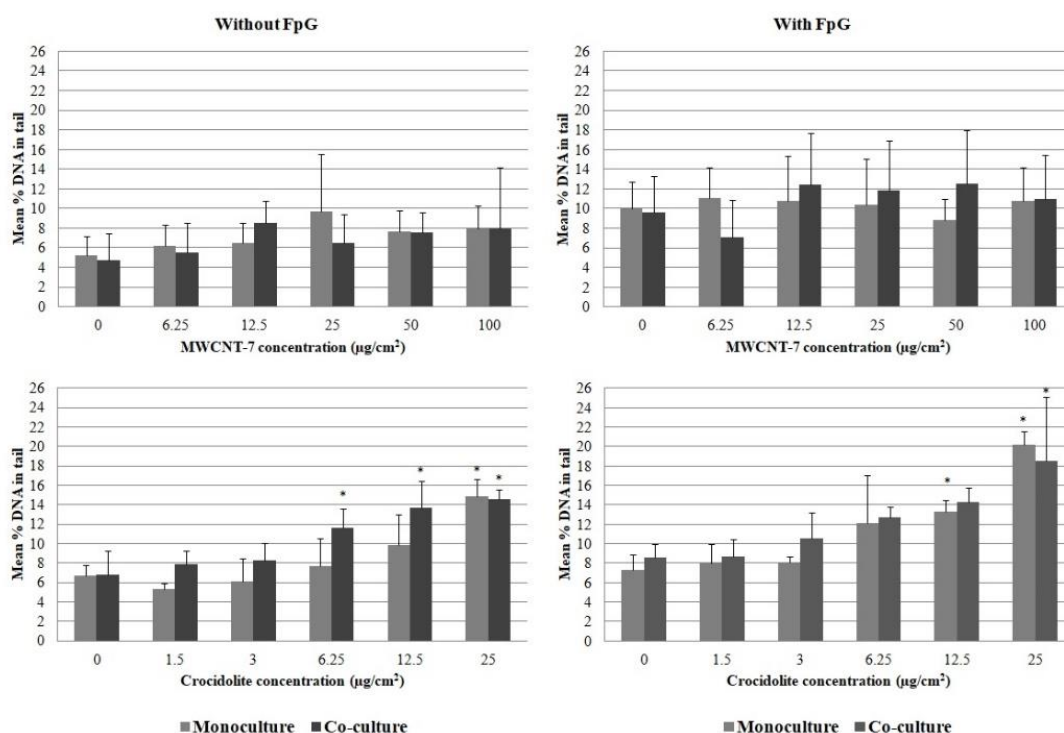


Figure 7. Comparison of the comet assay results in the A549 culture and co-culture with THP-1 cells exposed to a concentration-range of MWCNT-7 and crocidolite. * $p < 0.05$ for comparisons between treated and control cells in each culture model.

The results of the micronucleus assay show that neither MWCNT-7 nor crocidolite were able to induce micronucleus formation in A549 cells cultured under standard conditions (figure 8). Yet, in the co-culture with THP-1 cells, an increase of micronucleated binucleated cells (MNBC) frequency was observed for both materials. Concerning the MWCNT-7, this increase was significant at the two lowest concentrations ($p < 0.05$ for $6.25 \mu\text{g}/\text{cm}^2$ and $p < 0.005$ for $12.5 \mu\text{g}/\text{cm}^2$; Fisher's exact test), whereas for crocidolite, significance was reached for the three highest concentrations ($p < 0.005$ for $10 \mu\text{g}/\text{cm}^2$, $p < 0.05$ for $20 \mu\text{g}/\text{cm}^2$ and $p < 0.001$ for $40 \mu\text{g}/\text{cm}^2$; Fisher's exact test) (figure 8). At $100 \mu\text{g}/\text{cm}^2$ of MWCNT-7, micronuclei were not scored, since only mononucleated cells were present. In addition, in the co-culture after cytochalasin addition, A549 cells had to be incubated for 2 hours more to achieve binucleated cells, and a monoculture of A549 cells plated simultaneously with the co-culture presented a CPBI 13% higher, with 20% multinucleated cells compared with 7% in the co-culture.

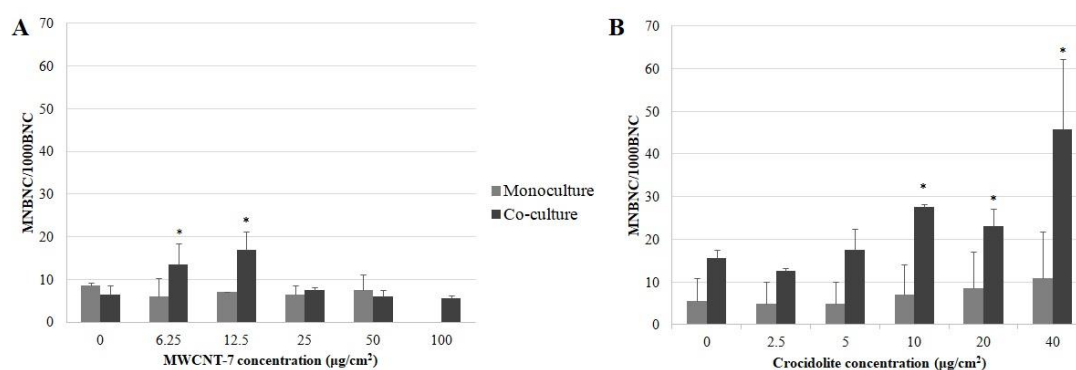


Figure 8. Frequency of micronucleated binucleated cells (MNBCs) per 1000 binucleated cells (BNC) in A549 cells in monoculture and co-culture with THP-1 cells, after exposure to MWCNT-7 (A) and crocidolite (B). Mitomycin (MMC) was used as a positive control, with a result of 40 and 48.5 MNBC/1000BNC in the monoculture and co-culture exposed to MWCNT-7, respectively ($p < 0.001$), and 39 and 44 MNBC/1000BNC in the monoculture and co-culture exposed to crocidolite, respectively ($p < 0.001$). * $p < 0.05$.

In addition, cells were scored for the presence of typical features of apoptosis after exposure to $50 \mu\text{g}/\text{cm}^2$ of MWCNT-7. The results showed a significant increase of apoptotic cells relatively to the normal controls ($p < 0.001$, Fisher's exact test).

4.4.6. Nucleoplasmic bridges characterization

During the above experiments, a distinct feature uniquely observed in the monoculture treated with 50 $\mu\text{g}/\text{cm}^2$ of MWCNT-7 was a significant increase in long and thin nucleoplasmic bridges (47 ± 1 in exposed cells vs 1 ± 0 in non-exposed cells, in 1000 BC, $p < 0.001$, Fisher's exact test) (figure 9).

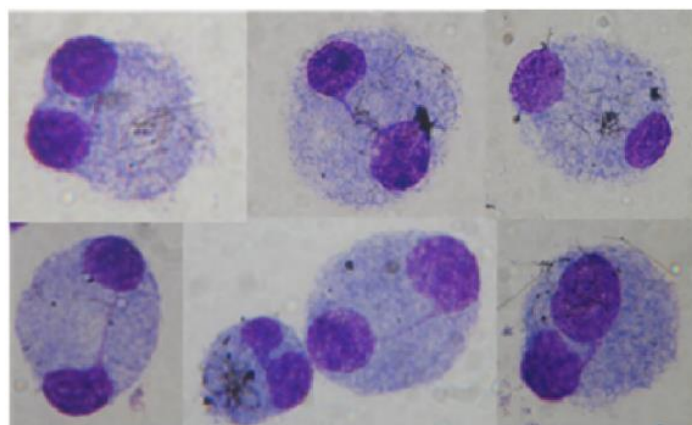


Figure 9. Optical microscopy photographs of A549 binucleated cells displaying nucleoplasmic bridges following exposure to 50 $\mu\text{g}/\text{cm}^2$ of MWCNT-7 (magnification 1000x).

To further investigate whether the origin of the nucleoplasmic bridges induced by MWCNT-7 were related to chromosomal fusion events, cells were analysed using FISH with pan-telomeric and pan-centromeric probes. The results showed the absence of centromeric signals in all nucleoplasmic bridges (80/80 bridges analysed), and a low frequency of telomeric signals (about 30% (16/23)), indicating that telomere end fusion is not the main origin of the nucleoplasmic bridges (figure 10).

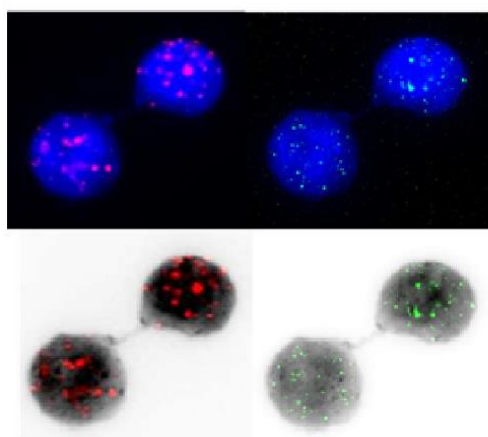


Figure 10. FISH investigation of the nucleoplasmic bridges detected in A549 cells exposed to 50 $\mu\text{g}/\text{cm}^2$ of MWCNT-7. Centromere and telomere probe signals are shown in red and in green, respectively. FISH images were also acquired as DAPI inverse counterstain to better distinguish the thin nucleoplasmic bridges (magnification 1000x).

Next, we used confocal microscopy analysis to study the morphology of these bridges. MWCNT were detected as black straight lines crossing or along the microtubule cytoskeleton and were localized in several intracellular focal planes, including the nuclei and nucleoplasmic bridges. All nucleoplasmic bridges analysed had one or more MWCNT either longitudinally or transversally embedded in the bridges (Figure 11).

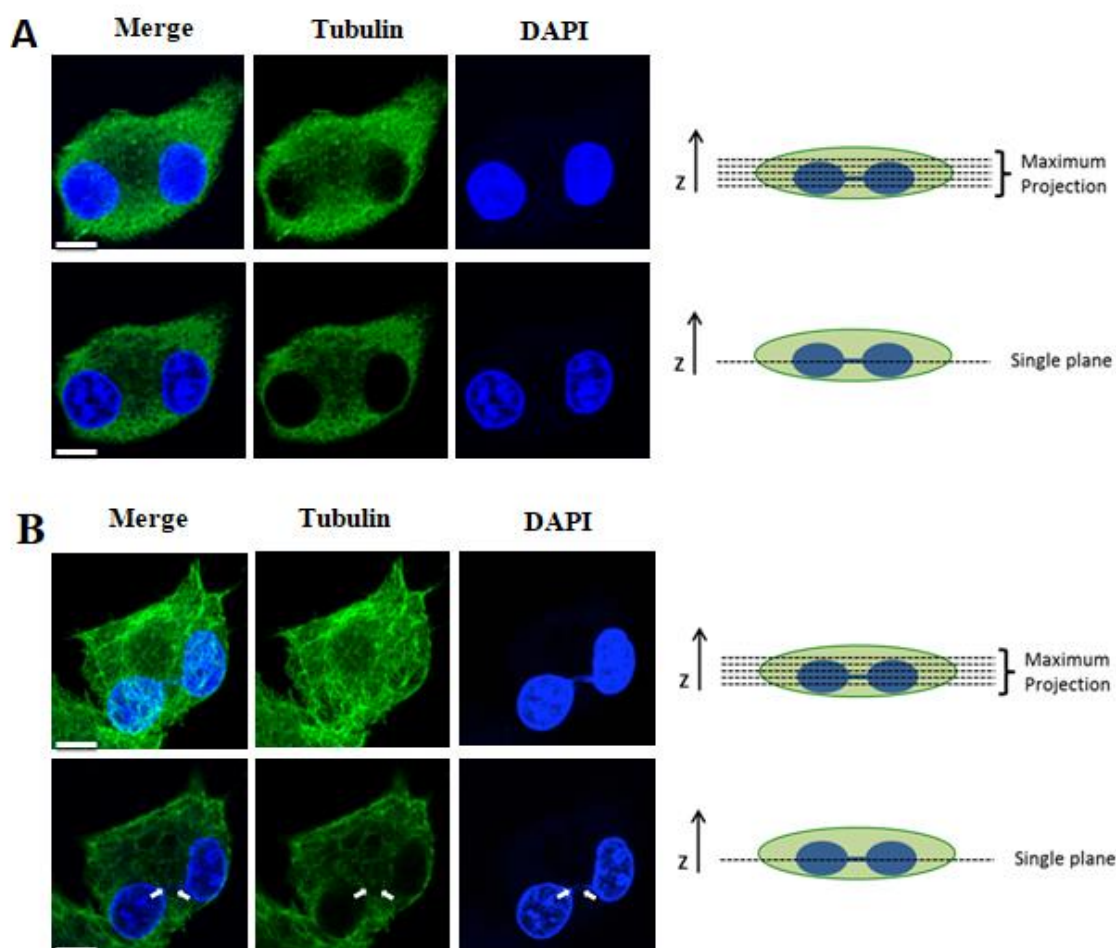


Figure 11. Confocal microscopy projection images of A549 cells after cytochalasin B treatment, incubated in the absence (A) or with 50 µg/cm² of MWCNT-7 (B). A nucleoplasmic bridge is distinguished between the two cell nuclei of the exposed cell. Tubulin is stained in green and DNA in blue. In (B), the presence of MWCNT crossing the nucleoplasmic bridges is shown with white arrows. Scale bars correspond to 10 µm.

4.5. Discussion

In this work, we characterized the cytotoxicity and genotoxicity of MWCNT-7 (Mitsui-7), a thick and long needle-like MWCNT, and compared it to that of crocidolite, a well-known carcinogenic asbestos fiber. In order to further increase the physiological

relevance of the study, we used a co-culture model of A549 alveolar cells and THP-1 macrophages to better approach the *in vivo* complexity of the pulmonary alveoli.

Our results confirm that both materials are toxic to A549 cells in conventional cultures, the MWCNT -7 being more cytotoxic than the crocidolite. Interestingly, the alveolar cells in co-culture with activated THP-1 showed a higher survival following treatment with both materials. This differential response was more pronounced after a 48 h exposure to MWCNT-7, which resulted in a 60% higher viability of co-cultured A549 cells than that of the monoculture. The CBPI values and the results of caspase 3/7 activity support that observation, in that the CBPI was not affected and the level of apoptosis was lower in A549 cells in co-culture than in the classic monoculture. Moreover, even though caspase 3/7 activity was not significantly different in cells exposed to 6.25 and 25 $\mu\text{g}/\text{cm}^2$ of MWCNT-7, a significant increase of cells with the typical features of apoptosis was microscopically observed in monocultures treated with 50 $\mu\text{g}/\text{cm}^2$ of MWCNT-7. This observation is in agreement with the CBPI results and indicates that, probably, apoptosis increases in MWCNT-7 concentrations higher than 25 $\mu\text{g}/\text{cm}^2$.

To explore whether the differences in cells fate following exposure to each material could be a consequence of EMT of A549 cells in the co-culture model, the expression of E-cadherin, vimentin and PCNA was analysed. EMT is a biologic process that drives an epithelial cell to assume a mesenchymal cell phenotype, with enhanced migratory capacity during embryonal development, but also as a stress response leading to invasiveness, elevated resistance to apoptosis, and greatly increased production of extra cellular matrix components during tumorigenesis⁴⁹. In the case of lung cancer, EMT is related to an increased metastatic ability⁵⁰ and an unfavourable prognosis for non-small cell lung cancer⁵¹ and other types of lung cancer⁵². It has been described that MWCNTs can directly promote EMT in rat alveolar type-II epithelial cells RLE-6TN through the activation of TGF- β /Smad2 signalling pathway⁵³, whereas the Akt/GSK-3 β /SNAIL-1 pathway is activated in BEAS-2B cells⁵⁴, contributing to the MWCNT-induced pulmonary fibrosis. Crocidolite fibers also induce EMT in mesothelial cells⁵⁵. In the monoculture, EMT was not visible by the E-cadherin and vimentin expression upon treatment with both materials for 24 h and 48 h; however, early EMT events, i.e., decrease in E-cadherin expression, was noticeable in the co-culture. Accordingly, Kawata et al. (2012) described that RAW 264.7 mouse macrophages induced EMT in A549 cells by TNF- α stimulation of transforming growth factor- β (TGF- β) expression, partially transduced by NF- κ β signalling⁵⁶. Wang et al. (2013) also described that long MWCNT stimulated alveolar macrophages to secrete TGF- β 1 that

activated TGF- β /Smad2 signalling in lung fibroblasts, leading to pulmonary fibrosis⁵³. TGF- β is involved in the regulation of both apoptosis and EMT, and its cellular effects are dependent on the cell cycle stage: apoptosis occurs mostly in the G2/M phase, whereas EMT is only induced in the G1/S phase⁵⁷. Our results suggest that most A549 cells in monoculture treated with MWCNT-7 were committed to apoptosis, given that both E-cadherin and PCNA levels decreased. By contrary, following co-culture treatment with MWCNT -7 or crocidolite, most A549 cells might have undergone early EMT, since E-cadherin expression decreased, vimentin remained constant and PCNA levels provided no evidence of cell death. This marked effect in the co-culture might be explained by growth arrest of A549 cells at G1/S triggered by TGF- β secreted by THP-1 macrophages, thus allowing maintenance of cell survival.

Regarding the genotoxicity assessment, MWCNT-7 failed to produce DNA damage detectable by comet assay but, interestingly, the two lowest concentrations (6.25 and 12.5 $\mu\text{g}/\text{cm}^2$) induced micronuclei in co-cultured A549 cells. Crocidolite exposure raised the micronucleus frequency in the same culture system, reaching a significant 2.29-fold increase at the highest concentration tested (40 $\mu\text{g}/\text{cm}^2$). In contrast with MWCNT-7, crocidolite was able to induce DNA lesions in the monocultured or co-cultured A549 cells.

In agreement with the results obtained, low levels, or no induction, of DNA strand breaks was reported in A549 cells, BEAS-2B cells and MeT-5A mesothelial cells after exposure to MWCNT-7 and other MWCNT^{22,19}. On the other hand, given that a crocidolite genotoxic mode of action is through ROS generation, mainly via the iron-catalysed reduction of oxygen (Fenton-like reaction), mitochondria-derived ROS, and ROS release from inflammatory cells^{58,59}, the positive comet assay results were expected. Moreover, the addition of FpG, a DNA repair enzyme that converts oxidative DNA lesions into DNA breaks, raised the level of DNA breaks in monocultured but not in co-cultured cells, which suggests that macrophages are not their main contributors. This finding agrees with previous reports that the long length of crocidolite fibers results in the secretion of inflammatory cytokines, but not in a strong ROS production by the macrophages⁶⁰.

On the other hand, MWCNT-7-induced micronuclei in A549 cells in the presence of THP-1 cells were not presumably produced by ROS-mediated DNA and subsequent chromosome breakage, since the FpG-comet assay yielded a negative result. Previous studies have reported that long CNT induce NLRP3 inflammasome activation⁶¹ and macrophage secretion of IL-1 β , IL-6 and IL-8 as a consequence of frustrated phagocytosis³³. Indeed, we found increased levels of IL-1 β in the supernatant of the co-

culture exposed to the MWCNT, especially in the THP-1 supernatant, indicating a differentiation towards the pro-inflammatory M1 phenotype. However, IL-1 β was not detected in the co-cultures used for the micronucleus assay, probably because cytochalasin B is an inhibitor of actin polymerization and inhibits phagocytosis by macrophages. Consequently, micronuclei are probably not caused by an inflammatory effect. In alternative, micronuclei might be related to the suggested EMT of A549 cells as above discussed. It is likely that the higher survival rate of mesenchymal cells may lead to an enrichment of a cell population with chromosomal alterations, which may be translated into an increased micronucleus frequency. For instance, Kajita et al. (2004) reported that Snail and Slug, two transcriptional repressors involved in the regulation of EMT, may promote cell survival after genotoxic stress through direct transcriptional repression of genes involved in many aspects of programmed cell death, as TP53⁶².

Micronucleus increase has been related to an increased risk of cancer⁴⁴. The micronucleus induction by the two lowest concentrations of MWCNT-7, allied to its possible contribution to stimulate EMT of alveolar cells, raises some concern about the carcinogenic potential of this CNT. It should be noted that this is the only CNT categorized by IARC as possibly carcinogenic to humans (Group 2B) due to evidences of carcinogenicity in rodents¹². Crocidolite is a well-known cause of mesothelioma and, like all other forms of asbestos, it is classified as carcinogenic to humans (group 1; IARC 2012).

Noteworthy, a pronounced increase in nucleoplasmic bridges ($p < 0.001$), without a corresponding micronucleus increase was observed in A549 cells exposed to 50 $\mu\text{g}/\text{cm}^2$ MWCNT-7, but only in the monoculture. These bridges that are formed between the two nuclei of a binucleated cell have been deemed to be originated from dicentric chromosomes and have been found associated to the formation of micronuclei with acentric chromosome fragments, which result from asymmetrical chromosome exchanges^{63,64}. In this work, the absence of micronuclei in the binucleated cells with nucleoplasmic bridges suggested a mechanism other than clastogenesis. FISH telomeric probes were used to evaluate if they were caused by telomere end fusions due to telomere shortening, loss of telomere capping proteins or defects in telomere cohesion⁶⁵. The results indicated that telomeric end fusions could not explain the formation of those bridges, since telomeric probe signals were not visualized in most of them. On the other hand, by confocal microscopy, the presence of MWCNT-7 embedded or intruding the nucleoplasmic bridges were clearly observed that might suggest a physical interference with chromatin. It is known that A549 cells can internalize single-walled CNT (SWCNT) that accumulate in the perinuclear

region⁶⁶. Although Kang et al. (2010) reported that MWCNT of 10-30 nm diameter and 1-2 μm or 0.5-1 μm length were excluded from the Hep G2 cells⁶⁷, intracellular trafficking of individual or small bundles of functionalized MWCNT towards the perinuclear region was observed by Kostarelos et al. (2007) in several cell types, even under endocytosis-inhibiting conditions⁶⁸. In A549 cells, a contribution of direct translocation through the plasma membrane into the cytoplasm (the “nanoneedle” activity) and a mix of energy-dependent mechanisms (endocytosis and macropinocytosis) are possible ways of internalisation of functionalized MWCNT that were found free in the cytoplasm or wrapped into endosome-like structures⁶⁶. Once inside the cell, there is evidence that CNT may interact with or interfere with the organization of DNA, actin, microtubules and, probably, with intermediate filaments such as the nuclear laminas⁶⁹. A biomimetic microtubule model was proposed where bundles of MWCNT longitudinally associate with microtubules, or one or more of the 13 microtubule protofilaments is substituted by a MWCNT, ultimately leading to cell division arrest and apoptosis⁶⁹. A dose-related increase in the frequency of disrupted centrosomes and abnormal mitotic spindles was observed in BEAS-2B cells exposed to MWCNT⁷⁰, and in SAEC and BEAS-2B cells exposed to SWCNT⁷¹. SWCNT were observed in association with mitotic spindle microtubules, within the centrosome structure and in condensed chromatin, leading to fragmented centrosomes, disrupted mitoses, and an aneuploid chromosome number⁷¹. Previously, Muller et al. (2008) had found that MWCNT induced both centromere-positive and -negative micronuclei in MCF-7 cells⁷². Although the presence of nucleoplasmic bridges could be related to chromosomal mis-segregation caused by mitotic spindle aberrations, our observation that MWCNT can intersect the bridges indicates a mechanism based on direct mechanical interference of CNT with the chromosomes during their segregation. It might happen that these cells lose the ability to divide, and, thus, be over-represented in the binucleated cell population. On the other hand, the absence of a significant number of nucleoplasmic bridges in the co-cultured binucleated cells may be related to the nuclear division delay estimated by the CBPI, which might be a consequence of A549 G1/S phase arrest.

4.6. Conclusions

CNT toxicity has been intensively investigated and several studies have highlighted their potential for causing adverse effects in lung cells similarly to asbestos. In this study, using a monoculture of A549 epithelial alveolar cells and a co-culture of those cells with THP-1 macrophages, we show that MWCNT-7, also known as Mitsui-7, is

toxic to A549 cells and to THP-1 macrophages, and induces chromosome alterations (micronucleus assay) in co-cultured A549 cells, as does crocidolite. However, the capacity of crocidolite to induce DNA lesions in A549 cells (comet assay) was not observed for MWCNT-7. On the other hand, the comparison of these endpoints in a co-culture model vs the classical monoculture of A549 cells, provided evidence for some dissimilar responses between MWCNT-7 and crocidolite exposure that were further explored. A plausible explanation for the higher A549 cell survival observed in the co-culture after exposure to both materials may be that the presence of THP-1 macrophages induces epithelial to mesenchymal transition of the alveolar cells, with mesenchymal cells being more resistant to cell death. This hypothesis was supported by the expression of E-cadherin, vimentin and PCNA in unexposed and exposed cells in monoculture and co-culture, which were compatible with apoptosis preferentially occurring in treated (24 h and 48 h) monocultures and EMT occurring in co-cultured A549 cells. In addition, the higher survival rate of A549 cells in co-culture with THP-1 macrophages is likely to result in an enrichment of cells with DNA or chromosome damage, which may explain the induction of micronuclei by both materials exclusively in co-cultured alveolar cells. Moreover, the origin of the nucleoplasmic bridges induced by a single concentration of Mitsui-7 in A549 cells monocultures (without concomitant micronucleus formation) was suggested to derive from a direct interference of the CNT with chromatin or cytoskeletal filaments during mitosis, as visualized under confocal microscopy. Taken together, our *in vitro* findings using the co-culture of A549 cells and macrophages highlight some important effects of MWCNT-7, including its potential to increase cell survival by induction of epithelial to mesenchymal transition, and accumulation of chromosome damage that may lead to chromosome instability, two hallmarks of cancer cells. Given that macrophages have an important role in the alveoli defence against biopersistent particles, and that inflammation can provide a tumour-promoting microenvironment, these co-cultures are likely to better mimic the *in vivo* outcomes associated to CNT exposure, e.g., lung fibrosis and carcinogenesis, indicating that the use of co-cultures can provide critical toxicological information that will be missed when using the classic lung cells monocultures.

Acknowledgements

The authors acknowledge Carmo Proença and Fátima Aguiar, Environmental Health Department of INSA for the kind gift of the crocidolite used in this work, and to Henriqueta Louro, Human Genetics Department of INSA for the DLS analysis of Mitsui-7. This research was supported by the Foundation for Science and Technology, Centre for Toxicogenomics and Human Health (ToxOmics) under grant (UID/BIM/00009/2013) and by ToxApp4NanoCELF (PTDC/SAU-PUB/32587/2017).

4.7. References

1. NIOSH. Occupational Exposure to Carbon Nanotubes and Nanofibers. 2013.
2. Mossman BT, Lippmann M, Hesterberg TW, Kelsey KT, Barchowsky A, Bonner JC. Pulmonary endpoints (lung carcinomas and asbestosis) following inhalation exposure to asbestos. *J Toxicol Environ Health B Crit Rev.* 2011;14 (1–4):76–121.
3. Landsiedel R, Sauer UG, Ma-hock L, Schnekenburger J, Wiemann M. Pulmonary toxicity of nanomaterials : a critical comparison of published *in vitro* assays and *in vivo* inhalation or instillation studies. *Nanomedicine (Lond).* 2014;9:2557–85.
4. Takagi A, Hirose A, Nishimura T, Fukumori N, Ogata A, Ohashi N, et al. Induction of mesothelioma in p53 + / – mouse by intraperitoneal application of multi-wall carbon nanotube. *J Toxicol Sci.* 2008;33(1):105–16.
5. Takagi A, Hirose A, Futakuchi M, Tsuda H, Kanno J. Dose-dependent mesothelioma induction by intraperitoneal administration of multi-wall carbon nanotubes in p53 heterozygous mice. *Cancer Sci.* 2012;103(8):1440–4.
6. Sakamoto Y, Nakae D, Fukumori N, Tayama K. Induction of mesothelioma by a single intrascrotal administration of multi-wall carbon nanotube in intact male Fischer 344 rats. *J Toxicol Sci.* 2009;34(1):65–76.
7. Nagai H, Okazaki Y, Chew S, Misawa N, Yamashita Y, Akatsuka S, et al. Diameter and rigidity of multiwalled carbon nanotubes are critical factors in mesothelial injury and carcinogenesis. *Proc Natl Acad Sci U S A.* 2011;108 (49):E1330-8.
8. Rittinghausen S, Hackbarth A, Creutzenberg O, Ernst H, Heinrich U, Leonhardt A, et al. The carcinogenic effect of various multi-walled carbon nanotubes (MWCNTs) after intraperitoneal injection in rats. *Part Fibre Toxicol.* 2014;11:59–77.

9. Suzui M, Futakuchi M, Fukamachi K, Numano T, Abdelgied M, Takahashi S, et al. Multiwalled carbon nanotubes intratracheally instilled into the rat lung induce development of pleural malignant mesothelioma and lung tumors. *Cancer Sci.* 2016;107(7):924–35.
10. Kasai T, Umeda Y, Ohnishi M, Mine T, Kondo H, Takeuchi T. Lung carcinogenicity of inhaled multi-walled carbon nanotube in rats. *Part Fibre Toxicol.* 2016;13:53.
11. Huaux F, d'Ursel de Bousies V, Parent M-A, Orsi M, Uwambayinema F, Devosse R, et al. Mesothelioma response to carbon nanotubes is associated with an early and selective accumulation of immunosuppressive monocytic cells. *Part Fibre Toxicol.* 2015;13(1):46.
12. Grosse Y, Loomis D, Guyton KZ, Lauby-Secretan B, El Guissassi F, Bouvard V, et al. Carcinogenicity of fluoro-edenite, silicon carbide fibres and whiskers, and carbon nanotubes. *Lancet Oncol.* 2015;8(1):24–5.
13. Casey A, Herzog E, Lyng FM, Byrne HJ, Chambers G, Davoren M. Single walled carbon nanotubes induce indirect cytotoxicity by medium depletion in A549 lung cells. *Toxicol Lett.* 2008;179:78–84.
14. Oberdörster G, Maynard A, Donaldson K, Castranova V, Fitzpatrick J, Ausman K, et al. Principles for characterizing the potential human health effects from exposure to nanomaterials: elements of a screening strategy. *Part Fibre Toxicol.* 2005;2:8.
15. Kim J, Lim H, Minai-tehrani A, Kwon J, Woo C, Choi M, et al. Toxicity and Clearance of Intratracheally Administered Multiwalled Carbon Nanotubes from Murine Lung. *J Toxicol Environ Heal Part A.* 2010;73(21–22):1530–43.
16. Yu K, Kim JE, Seo HW, Chae C. Differential Toxic Responses Between Pristine and Functionalized Multiwall Nanotubes Involve Induction of Autophagy Accumulation in Murine Lung. *J Toxicol Environ Heal Part A.* 2013;76:1282–92.
17. Chatterjee N, Yang J, Kim H, Jo E, Kim P, Choi K, et al. Potential Toxicity of Differential Functionalized Multiwalled Carbon Nanotubes (MWCNT) in Human Cell Line (BEAS2B) and *Caenorhabditis elegans*. *J Toxicol Environ Heal Part A.* 2014;77:1399–408.
18. Taylor AJ, McClure CD, Shipkowski KA, Thompson EA, Hussain S, Garantziotis S, et al. Atomic Layer Deposition Coating of Carbon Nanotubes with Aluminum Oxide Alters Pro-Fibrogenic Cytokine Expression by Human Mononuclear Phagocytes *In Vitro* and Reduces Lung Fibrosis in Mice *In Vivo*. *PLoS One.* 2014;9(9):e106870.

19. Louro H, Pinhão M, Santos J, Tavares A, Vital N, Silva MJ. Evaluation of the cytotoxic and genotoxic effects of benchmark multi-walled carbon nanotubes in relation to their physicochemical properties. *Toxicol Lett.* 2016;262:123–34.
20. Cavallo D, Fanizza C, Ursini CL, Casciardi S, Paba E, Ciervo A, et al. Multi-walled carbon nanotubes induce cytotoxicity and genotoxicity in human lung epithelial cells. *J Appl Toxicol.* 2012;32(6):454–64.
21. Karlsson HL, Cronholm P, Gustafsson J, Mo L. Copper Oxide Nanoparticles Are Highly Toxic. A Comparison between Metal Oxide Nanoparticles and Carbon Nanotubes - Chemical Research in Toxicology (ACS Publications). 2008;1726–32.
22. Lindberg HK, Falck GC-M, Singh R, Suhonen S, Järventaus H, Vanhala E, et al. Genotoxicity of short single-wall and multi-wall carbon nanotubes in human bronchial epithelial and mesothelial cells *in vitro*. 2013;313(1):24–37
23. Kato T, Totsuka Y, Ishino K, Matsumoto Y, Tada Y, Nakae D, et al. Genotoxicity of multi-walled carbon nanotubes in both *in vitro* and *in vivo* assay systems. *Nanotoxicology.* 2013;7(4):452–61.
24. Catalán J, Siivola KM, Nymark P, Lindberg H, Suhonen S, Järventaus H, et al. *In vitro* and *in vivo* genotoxic effects of straight versus tangled multi-walled carbon nanotubes. *Nanotoxicology.* 2015;10(6):794–806.
25. Jackson P, Kling K, Jensen KA, Clausen PA, Madsen AM, Wallin H, et al. Characterization of Genotoxic Response to 15 Multiwalled Carbon Nanotubes with Variable Physicochemical properties Including Surface Functionalizations in the FE1-Muta(TM) Mouse Lung Epithelial Cell Line. *Environ Mol Mutagen.* 2015;56:183–203.
26. Zhou L, Forman HJ, Ge Y, Lunec J. Multi-walled carbon nanotubes: A cytotoxicity study in relation to functionalization, dose and dispersion. *Toxicol Vitro.* 2017;42(April):292–8.
27. Allegri M, Perivoliotis DK, Bianchi MG, Chiu M, Pagliaro A, Koklioti MA, et al. Toxicity determinants of multi-walled carbon nanotubes: The relationship between functionalization and agglomeration. *Toxicol Reports.* 2016;3:230–43.
28. Snyder-Talkington BN, Qian Y, Castranova V, Guo NL. New perspectives for *in vitro* risk assessment of multiwalled carbon nanotubes: application of coculture and bioinformatics. *J Toxicol Environ Health B Crit Rev.* 2012;15(7):468–92.
29. Dymacek J, Snyder-Talkington BN, Porter DW, Mercer RR, Wolfarth MG, Castranova V, et al. mRNA and miRNA Regulatory Networks Reflective of Multi-Walled Carbon Nanotube-Induced Lung Inflammatory and Fibrotic Pathologies in Mice. *Toxicol Sci.* 2015;144(1):51–64.

30. Snyder-talkington BN, Dong C, Zhao X, Dymacek J, Porter DW, Wolfarth MG, et al. Multi-walled carbon nanotube-induced gene expression *in vitro*: Concordance with *in vivo* studies. *Toxicology* 2015;328:66–74.
31. Shamir ER, Ewald AJ. Three-dimensional organotypic culture: experimental models of mammalian biology and disease. *Nat Rev Mol Cell Biol.* 2014 Sep 17;15:647–64.
32. Brown DM, Kinloch IA, Bangert U, Windle AH, Walter DM, Walker GS, et al. An *in vitro* study of the potential of carbon nanotubes and nanofibres to induce inflammatory mediators and frustrated phagocytosis. *Carbon N Y.* 2007;45(9):1743–56.
33. Murphy FA, Schinwald A, Poland CA, Donaldson K. The mechanism of pleural inflammation by long carbon nanotubes: interaction of long fibres with macrophages stimulates them to amplify pro-inflammatory responses in mesothelial cells. *Part Fibre Toxicol.* 2012;9(1):8.
34. He X, Young S-H, Fernback JE, Ma Q. Single-Walled Carbon Nanotubes Induce Fibrogenic Effect by Disturbing Mitochondrial Oxidative Stress and Activating NF- κ B Signaling. *J Clin Toxicol.* 2012;suppl 5.
35. Oberdörster G, Maynard AA, Donaldson K, Castranova V, Fitzpatrick J, Ausman KK, et al. Principles for characterizing the potential human health effects from exposure to nanomaterials: elements of a screening strategy. *Part Fibre Toxicol.* 2005;2(1):8.
36. Tavares AM, Louro H, Antunes S, Quarré S, Simar S, Temmerman P De, et al. Genotoxicity evaluation of nanosized titanium dioxide, synthetic amorphous silica and multi-walled carbon nanotubes in human lymphocytes. *Toxicol Vitro.* 2014;28:60–9.
37. Jensen KA, Yahia K, Christiansen E, Jacobsen NR, Wallin H, Guiot C, et al. Towards a method for detecting the potential genotoxicity of nanomaterials. Final protocol for producing suitable manufactured nanomaterial exposure media. Copenhagen; 2011.
38. Timbrell V, Rendall R. Preparation of the UICC* Standard Reference Samples of Asbestos. *Powder Technol.* 1972;5:279–87.
39. Rendall R. The data sheets on the chemical and physical properties of the UICC standard reference samples. In: Shapiro H., editor. Pneumoconiosis proceedings of the international conference, 1969, Johannesburg. Oxford: Oxford University Press; 1970. p. 23–7.
40. Timbrell V. Characteristics of the International Union Against Cancer standard reference samples of asbestos. In: Shapiro H., editor. Pneumoconiosis

- proceedings of the international conference, 1969, Johannesburg. Oxford: Oxford University Press; 1970. p. 28–36.
41. Kohyama N, Shinohara Y, Suzuki Y. Mineral phases and some reexamined characteristics of the International Union against cancer standard asbestos samples. *Am J Ind Med*. 1996;30(5):515–28.
 42. Pinkerton K, Gehn P, Crapo J. Comparative Biology of Normal Lung. Treatise on Pulmonary Toxicology, Volume 1. Boca raton, FL: CRC Press; 1992.
 43. Park EK, Jung HS, Yang HI, Yoo MC, Kim C, Kim KS. Optimized THP-1 differentiation is required for the detection of responses to weak stimuli. *Inflamm Res*. 2007;56(1):45–50.
 44. Thomas P, Fenech M. Cytokinesis-block micronucleus cytome assay in lymphocytes. *Methods Mol Biol*. 2011;682:217–34.
 45. OECD guideline for the testing of chemicals. 2014. Report No.: TG 487.
 46. Lamouille S, Xu J, Derynck R. Molecular mechanisms of epithelial-mesenchymal transition. *Nat Rev Mol Cell Biol*. 2014;15(3):178–96.
 47. Essers J, Theil AF, Céline B, van Cappellen WA, Houtsmuller AB, Kanaar R, et al. Nuclear Dynamics of PCNA in DNA Replication and Repair. *Mol Cell Biol* 2005;25(21):9350–9
 48. Moldovan GL, Pfander B, Jentsch S. PCNA, the Maestro of the Replication Fork. *Cell*. 2007;129(4):665–79.
 49. Kalluri R, Weinberg RA. The basics of epithelial-mesenchymal transition. *J Clin Invest*. 2009;119(6).
 50. Chaffer CL, Weinberg RA. A perspective on cancer cell metastasis. *Science*. 2011;331(6024):1559–64.
 51. Bremnes RM, Veve R, Hirsch FR, Franklin WA. The E-cadherin cell – cell adhesion complex and lung cancer invasion, metastasis, and prognosis. *Lung Cancer* 2002;36:115–24.
 52. Mizutani H, Okano T, Minegishi Y, Matsuda K. HSP27 modulates epithelial to mesenchymal transition of lung cancer cells in a Smad-independent manner. *Oncol Letters*. 2010;1:1011–16.
 53. Wang P, Wang Y, Nie X, Braïni C, Bai R, Chen C. Multiwall Carbon Nanotubes Directly Promote Fibroblast – Myofibroblast and Epithelial – Mesenchymal Transitions through the Activation of the TGF- β / Smad Signaling Pathway. *Small*. 2015;11(4):446–55.
 54. Polimeni M, Gulino GR, Gazzano E, Kopecka J, Marucco A, Fenoglio I, et al. Multi-walled carbon nanotubes directly induce epithelial-mesenchymal transition

- in human bronchial epithelial cells via the TGF- β -mediated Akt/GSK-3 β /SNAIL-1 signalling pathway. *Part Fibre Toxicol.* 2016;13:27.
55. Qi F, Okimoto G, Jube S, Napolitano A, Pass HI, Laczko R, et al. Continuous exposure to chrysotile asbestos can cause transformation of human mesothelial cells via HMGB1 and TNF- α signaling. *Am J Pathol.* 2013;183(5):1654–66.
 56. Kawata M, Koinuma D, Ogami T, Umezawa K, Iwata C, Watabe T, et al. TGF- β -induced epithelial-mesenchymal transition of A549 lung adenocarcinoma cells is enhanced by pro-inflammatory cytokines derived from RAW 264.7 macrophage cells. *J Biochem.* 2012;151(2):205–16.
 57. Song Y, Li X, Du X. Exposure to nanoparticles is related to pleural effusion, pulmonary fibrosis and granuloma. *Eur Respir J.* 2009;34(3):559–67.
 58. Ritesh Kumar Srivastava, Lohani M, Aditya Bhushan Pant, Rahman Q. Cytogenotoxicity of amphibole asbestos fibers in cultured human lung epithelial cell line: Role of surface iron. *Toxicol Ind Health.* 2010;26(9):575–82.
 59. Liu W, Ernst JD, Broaddus VC. Phagocytosis of crocidolite asbestos induces oxidative stress, DNA damage, and apoptosis in mesothelial cells. *Am J Respir Cell Mol Biol.* 2000;23:371–8.
 60. Padmore T, Stark C, Turkevich LA, Champion JA. Quantitative analysis of the role of fiber length on phagocytosis and inflammatory response by alveolar macrophages. *Biochem Biophys Acta.* 2017;1861(2):58–67.
 61. Hussain S, Sangtian S, Anderson SM, Snyder RJ, Marshburn JD, Rice AB, et al. Inflammasome activation in airway epithelial cells after multi-walled carbon nanotube exposure mediates a profibrotic response in lung fibroblasts. *Part Fibre Toxicol.* 2014;11(1):28.
 62. Kajita M, McClinic KN, Wade PA. Aberrant Expression of the Transcription Factors Snail and Slug Alters the Response to Genotoxic Stress. *Mol Cell Biol.* 2004;24(17):7559–66.
 63. Thomas P, Umegaki K, Fenech M. Nucleoplasmic bridges are a sensitive measure of chromosome rearrangement in the cytokinesis-block micronucleus assay. *Mutagenesis.* 2003;18(2):187–94.
 64. Cheong HSJ, Seth I, Joiner MC, Tucker JD. Relationships among micronuclei, nucleoplasmic bridges and nuclear buds within individual cells in the cytokinesis-block micronucleus assay. *Mutagenesis.* 2013;28(4):433–40.
 65. Fenech M. Cytokinesis-block micronucleus cytome assay. *Nat Protoc.* 2007;2(5):1084–104.

66. Lacerda L, Pastorin G, Gathercole D, Buddle J, Prato M, Bianco A, et al. Intracellular trafficking of carbon nanotubes by confocal laser scanning microscopy. *Adv Mater.* 2007;19(11):1480–4.
67. Kang B, Chang S, Dai Y, Yu D, Chen D. Cell response to carbon nanotubes: Size-dependent intracellular uptake mechanism and subcellular fate. *Small.* 2010;6(21):2362–6.
68. Kostarelos K, Lacerda L, Pastorin G, Wu W, Wieckowski S, Luangsivilay J, et al. Cellular uptake of functionalized carbon nanotubes is independent of functional group and cell type. *Nat Nanotechnol.* 2007;2(2):108–13.
69. Rodriguez-Fernandez, L., Valiente, R., Gonzalez J, Villegas JC, Fanarraga ML. Multiwalled carbon nanotubes display microtubule biomimetic properties *in vivo*, enhancing microtubule assembly and stabilization. *ACS Nano.* 2012;6(8):6614–25.
70. Siegrist KJ, Reynolds SH, Kashon ML, Lowry DT, Dong C, Hubbs AF, et al. Genotoxicity of multi-walled carbon nanotubes at occupationally relevant doses. *Part Fibre Toxicol.* 2014;11:6–21.
71. Sargent LM, Hubbs AF, Young S-H, Kashona ML, Dinu CZ, Salisbury JL, et al. Single-walled carbon nanotube-induced mitotic disruption. *Mutat Res.* 2012;745(0):28–37.
72. Muller J, Decordier I, Hoet PH, Thomassen L, Lison D, Kirsch-volders M. Clastogenic and aneugenic effects of multi-wall carbon nanotubes in epithelial cells. *Carcinogenesis.* 2008;29(2):427–33.

5. Functional effects of differentially expressed microRNAs in alveolar epithelial cells exposed to MWCNT-7 or crocidolite

Célia Ventura^{1,2,3}, Luís Vieira^{1,3}, Catarina Silva³, António Sousa-Uva^{2,4}, Maria João Silva^{1,3}

¹ Department of Human Genetics, National Institute of Health Doutor Ricardo Jorge, Lisbon; ² Department of Occupational and Environmental Health, National School of Public Health, NOVA University of Lisbon (UNL), Lisbon; ³ Center for Toxicogenomics and Human Health (ToxOmics), NOVA Medical School-FCM, UNL, Lisbon; ⁴ CISP – Public Health Research Center, Lisbon, Portugal.

The work included in this chapter is submitted for publication in *Archives of Toxicology*.

5.1. Abstract

Multi-walled carbon nanotubes (MWCNT) are widely used engineered nanomaterials in industrial and biomedical applications. Yet, several studies have demonstrated that MWCNT inhalation may induce pulmonary adverse effects, and one of these, the MWCNT-7 (Mitsui-7), has been classified as possibly carcinogenic to humans. However, its molecular mechanisms of action are poorly understood and there are no known biomarkers of exposure or effect for occupational monitoring. More recently, several pulmonary diseases, including lung cancer, have been associated with alterations in microRNA expression that are considered useful to detect or evaluate disease progression. Differentially-expressed microRNAs (DE miRNAs) also allow understanding the molecular effects induced by a toxicant. In this study, we describe the identification of a set of DE miRNAs in A549 epithelial alveolar cells, following 24 hours exposure to an occupationally relevant dose of MWCNT-7 (0.25 $\mu\text{g}/\text{cm}^2$) or an equivalent dose of crocidolite. The functional pathways enriched with genes targeted by these DE miRNAs indicate that exposed cells change their survival, differentiation and proliferative properties under the influence of the AMPK, FoxO, TGF- β and Hippo pathways, as well as their metabolic activity and cell-to-cell communication. In addition, MWCNT-7 affects the actin cytoskeleton regulation, ubiquitin mediated proteolysis, and extracellular matrix-receptor interactions. In turn, crocidolite more intensely affects the PI3K-Akt and mTOR pathways, endocytosis, and central carbon metabolism. Since deregulation of these pathways is related to carcinogenesis, an interaction network of DE miRNAs and corresponding target cancer-related genes was constructed, highlighting the carcinogenic potential of both materials, even at low dose and short-term exposure.

5.2. Introduction

Carbon nanotubes (CNT) are one of the most promising products of nanotechnology with an extensive variety of applications in industry and biomedicine¹. Multi-walled carbon nanotubes (MWCNT) consist of multiple cylindrical graphite sheets assembled in concentric layers with nanoscale diameter (less than 100 nm). They can be functionalized by the introduction of specific elements on the original pristine form, and display unique physicochemical properties, e.g., are mechanically strong, flexible, lightweight, heat resistant, and high electrical conductors.

Several toxicological studies have demonstrated that exposure to some MWCNT can induce immunotoxic, cytotoxic and genotoxic effects, and nowadays they are

considered an occupational hazard². In rodents, exposure to MWCNT have caused acute or persistent pulmonary inflammation, persistent interstitial fibrosis, granuloma formation, and bronchiolar or bronchioloalveolar hyperplasia^{1,3}. These adverse pulmonary effects are associated with the intrinsic physicochemical properties and biopersistence of MWCNT^{4,3}. Particularly, those that have similarity with the fiber-like shape of asbestos have raised a strong concern about their carcinogenic potential⁵. The discordant carcinogenic evidence obtained for different carbon nanotubes led the International Agency for Research on Cancer (IARC) to categorize them as not classifiable as to their carcinogenicity to humans (Group 3), with the exception of the MWCNT-7 (Mitsui-7) that was classified as a possibly human carcinogenic (Group 2B)⁶. This MWCNT induced peritoneal mesothelioma after a single intraperitoneal injection in mice (0.003–3 mg/animal)^{7,8}, two intraperitoneal injections with a one-week interval in rats (0.5-5 mg/animal)⁹, intrascrotal injection (1 mg/animal) in rats¹⁰ and promoted lung carcinomas after whole-body inhalation exposure of male (0.2 and 2 mg/m³) and female rats (2 mg/m³)¹¹. Moreover, it promoted growth and neoplastic progression of mice lung cells previously exposed to methylcholanthrene, causing lung bronchioloalveolar adenomas and adenocarcinomas at doses similar to the ones that can be achieved in human occupational exposures¹². Like asbestos, Mitsui-7 injection in the peritoneal cavity of rats induced an early and selective sustained immunosuppressive response characterized by the accumulation of monocytic Myeloid Derived Suppressor Cells that possess the ability to suppress polyclonal activation of T lymphocytes¹³. Interestingly, mesotheliomas induced by thin (diameter ~ 50 nm) and highly crystalline MWCNT share a homozygous deletion of the tumour suppressor genes *Cdkn2a/2b*, similar to mesotheliomas induced by asbestos⁹. In the Nagai et al. (2011) study, it was proposed that thin and crystalline MWCNT might have a piercing effect in the mesothelial cell membrane, but aggregative and thick MWCNT do not cause direct injury in mesothelial cells, the carcinogenicity of those being mediated by indirect effects.

In the last years, genomic approaches have been applied to study CNT toxicity with the aim of obtaining insightful information on the genes and corresponding functional pathways that they affect. Toxicogenomics expects to find unique transcriptional profiles that, besides providing evidence of the cellular mechanistic mode of action of CNT, may also be used as biomarkers for biomonitoring purposes^{14,15}. Some of the most frequently disturbed biological processes following cell or animal exposure to CNT include apoptosis, inflammation, oxidative stress, fibrosis, cell cycle and proliferation, among others¹⁶.

Moreover, several nanomaterials have been associated with epigenetic alterations, i.e., changes in the regulation of gene expression caused by DNA methylation, histone tail alterations and differential microRNA (miRNA) expression^{17,18}. miRNAs are small 19 to 25 nucleotides-long non-coding RNAs usually acting as endogenous repressors of gene activity via post-transcriptional binding to a “seed” sequence in the 3′ untranslated region (3′-UTR) of mRNA¹⁹. Lung cells have a specific miRNA profile, and several pulmonary diseases, such as chronic obstructive pulmonary disease, asthma, cystic fibrosis, pulmonary hypertension and lung cancer, have been associated with alterations in miRNA expression^{20,21,22}. Several under- or over-expressed miRNAs have been reported in malignant mesothelioma tumours, and some have been suggested as potential biomarkers for histopathological subtyping of tumours^{23,24,25} or as potential regulators of the adenoma to adenocarcinoma transition²⁶. Moreover, cell-free circulating miRNAs in plasma are highly sensitive, reproducible, specific and stable^{27,28}. In addition to be promising biomarkers for tumour classification and staging^{29,30}, they are considered potential blood biomarkers for monitoring human exposure, especially in occupational settings.

In rodents exposed to MWCNT, miRNA analysis in whole blood correlated *FCRL5*/miR-122-5p to the presence of hyperplasia, *MTHFD2*/miR-206-3p to fibrosis, *FAM178A*/miR-130a-3p to bronchiolo-alveolar adenoma, and *IL7R*/miR-210-3p to bronchiolo-alveolar adenocarcinoma, among others²⁶. In two other studies, one identified the altered miRNAs and the corresponding pathways in mouse embryo-derived NIH/3T3 cells using a high-throughput deep sequencing method³¹, and other identified global lung miRNA/mRNA regulatory relationships associated with inflammation and fibrosis using a microarray³². Nymark et al. (2011), also using microarray technology, studied mRNA and miRNA expression changes associated with mitochondrial dysfunction in human bronchial epithelial cells exposed to MWCNT-7 and found a 330-gene miRNA signature, of which four miRNAs were associated with decreased mitochondrial membrane potential³³.

Asbestos exposure was also associated with changes in miRNA expression in patient's tumours and normal lung tissues, with 13 asbestos-related differentially expressed (DE) miRNAs, including over-expression of the squamous cell carcinoma-associated miR-205, linked to down-regulation of the *DOK4* gene, an insulin receptor substrate gene involved in cellular growth, signalling, and survival³⁴.

In this study, we used next-generation sequencing (NGS) technology to sequence miRNAs in A549 epithelial alveolar cells exposed to MWCNT-7 (Mitsui-7) or crocidolite asbestos during 24 hours, and bioinformatics tools to identify DE miRNAs, their

corresponding target genes and deregulated cellular pathways. Since much criticism has emerged from the high carbon nanotube mass doses commonly used in *in vitro* toxicity studies, as it can take a long time to reach them in the human airways in real life^{35,3}, we used a dose of MWCNT-7 (0.25 µg/cm²) that has been considered as occupationally relevant³⁶. Crocidolite was used to compare the miRNA profile and molecular pathways with MWCNT-7 exposure, due to their strong similarity in terms of physical characteristics and high biopersistence, and because of the well-known lung adverse effects of crocidolite, namely, asbestosis, lung cancer and mesothelioma³⁷. This methodology allowed to identify a set of miRNAs associated to the exposure to MWCNT-7 or crocidolite, and to deepen the knowledge on its molecular modes of action at occupational relevant doses, their similarities and differences. Our results also point towards possible future targets for mechanistic research on the toxicity of these materials.

5.3 Materials and Methods

5.3.1 Fibre characterization and preparation

The MWCNT-7, also known as Mitsui-7 (Mitsui and Co, Lda. Ibaraki, Japan), was provided as a sub-sample by the National Research Centre for the Working and Environment (NRCWE-006). Its physicochemical characteristics were described previously and are listed in table I.

Table I. Physicochemical characteristics of the MWCNT-7 (NRCWE-006, Mitsui-7).

Specific surface area (m ² /g)	Thickness ± SD (nm)	Geodesic length ± SD (nm)	Aspect ratio ± SD ^b	Impurities %	Minor Impurity phases ^c	Minor elements/coatings ^c
24-28 ^a 22 ^c	69.4 ± 1.4 ^b 74 ± 28 ^c 49 – 100 ^d	4423.6 ± 2.3 ^b 5730 ± 3674 ^c 3000 – 5000 ^d	63.7 ± 2.4	<1% ^a < 0.5% ^d	Fe ₂ O ₃	Na: 499 ± 103 µg/g Mg: 1 ± 1 µg/g Al: 66 ± 19 µg/g Fe: 355 ± 2 µg/g Ni: 1 µg/g

^aInformation provided by manufacturer or the Joint Research Center (http://ihcp.jrc.ec.europa.eu/our_activities/nanotechnology/nanomaterials-repository/list_materials_JRC_rep_oct_2011.pdf).

^b Values reported by Tavares et al. 2014³⁸

^cValues reported in the NANOGENOTOX Joint Action by Jensen 2013³⁹.

^d Values reported by Poulsen et al. 2013⁴⁰.

Immediately before the experiments, a 2.56 mg/mL stock dispersion of the NRCWE-006 was prepared according to⁴¹. The hydrodynamic particle size-distribution (Z_{av} , nm) and the polydispersity index (PDI) of MWCNT-7 stock dispersion were measured shortly after sonication (Malvern Nano ZS, Malvern Inc., UK) by dynamic light scattering (DLS) and expressed as the mean of 10 consecutive measurements³⁸. Scanning electron microscopy (SEM) of the stock solution was also performed using a Phantom XL microscope.

The crocidolite fibres are a standard reference mineral from the Union for International Cancer Control (UICC, Geneva, Switzerland) and were kindly provided by Dr. Fátima Aguiar from the Environmental Health Department of INSA. Their preparation and characterization have been described in detail^{42,43,44,45}. A stock solution was prepared at 1 mg/mL in phosphate buffer saline (PBS), pH 7.4 (Gibco, Waltham, MA, USA). Prior to dilution in culture medium, fibres were passed through a syringe needle to ensure a better uniformity of the suspension.

5.3.2. Cell culture

The A549 cell line was obtained from the American Type Culture Collection (ATCC® Manassas, VA, USA, CCL-185™) and grown in RPMI 1640 medium (Gibco) supplemented with 10% heat-inactivated fetal bovine serum (FBSi) (Gibco), 1% penicillin/streptomycin (1.000 U/mL penicillin and 10 mg/mL streptomycin, Gibco) and 1 % fungizone (0.25 mg/mL, Gibco) at 37 °C in an atmosphere of 5% CO₂. The cells were cultured on 6–well plates at a density of 1 x 10⁵ cells/mL in a total volume of 2 mL/well and exposed to 0.25 µg/cm² of MWCNT-7 or crocidolite during 24 h. Non-exposed cells were used as controls.

5.3.3. RNA extraction

Total RNA was isolated from non-exposed A549 cells, and A549 cells exposed to MWCNT-7 or crocidolite, using the miRNeasy Mini Kit (Qiagen) according to the manufacturer's protocol. Total RNA was eluted in RNase-free water and stored at -80°C until use. RNA concentration and purity was determined using a NanoViewPlus Spectrophotometer (General Electric, Boston, Massachusetts, USA). RNA quality was assessed using the Fragment Analyser (Advanced Analytical Technologies, Santa Clara, California, USA) and the HS RNA kit. All samples showed an RNA quality number ≥ 9. Samples were diluted to a final concentration of 1 µg of RNA in 5 µL nuclease-free water.

5.3.4. Library preparation and sequencing

Three RNA samples and a control sample (Human Brain Total RNA, Thermo Fisher Scientific) were used to generate indexed cDNA libraries with the TruSeq Small RNA Library Prep kit (Illumina, San Diego, California, USA) with minor protocol adaptations as follows. Library amplification was performed using 18 cycles to increase the yield of miRNA fragments. The purification of the amplified cDNA constructs was carried out using a 4% agarose gel. Product recovery was made by immersing the gel slices in 200 µl ultrapure water followed by incubation at 300 rpm for 2 hours at room temperature and overnight at 4°C in a Thermomixer Compact (Eppendorf). The eluate was then transferred to a QIAshredder column (Qiagen) and centrifuged at 10.000 rpm for 1 minute. Purified libraries were quantified using Qubit (Thermo Fisher Scientific) and their sizes were quality checked using the Fragment Analyzer with the HS NGS Fragment kit and 2% agarose gel electrophoresis. After normalization, libraries were pooled, denatured and diluted according to standard procedures for the MiSeq instrument (Illumina). Two sequencing runs of 1x75 bp read length were performed using the Small RNA workflow with loading library concentrations of 10 pM and 20 pM. The control sample was included in the first sequencing run.

5.3.5. Sequencing data analysis

Sequencing raw data was processed using the built-in Small RNA analysis workflow of the MiSeq instrument (Illumina). In brief, sequencing reads were aligned to 2578 human mature miRNA sequences obtained from miRBase v20 database⁴⁶ using bowtie⁴⁷. A matrix containing raw counts of reads per mature miRNA sequence in each sample (supplementary files 1 and 2) was obtained for each sequencing run.

5.3.6. Differential expression analysis

Raw counts were used to perform differential expression analysis of miRNAs between non-exposed cells and cells exposed to MWCNT-7 or crocidolite. All analyses were conducted using R v3.4.2⁴⁸ and RStudio v1.0.143⁴⁹. Two R software packages, DESeq2 v1.18.1⁵⁰ and RNASeqGUI v1.1.2⁵¹, were used for differential expression analysis. The latter was used for performing differential expression with the EdgeR Exact Test⁵². A p-adjusted (padj) value of 0.1 and a false discovery rate (FDR) of 0.1 were used in DESeq2 and EdgeR, respectively. Two independent matrix files were constructed containing only the replicate counts for non-exposed and MWCNT-7-exposed cells, and for non-exposed and crocidolite-exposed cells, using the original

raw counts. The miRNAs with low counts were filtered prior to differential expression analysis from each matrix using the Filtering Interface of RNASeqGUI. The 'counts per million' (CPM) was chosen as the filtering method with parameter values $\text{cpm} = 20$ and $\text{cv.cutoff} = 25$. The filtered count matrices (supplementary files 3 and 4) were used as direct input in DESeq2 using the script described in supplementary file 5. In the case of EdgeR Exact Test, the raw counts in the filtered matrices were further normalized according to the trimmed mean of M values method⁵³ in the Normalization Interface of RNASeqGUI (supplementary files 6 and 7). The set of miRNAs identified by DESeq2 and EdgeR are described in supplementary files 8-11. Selected sets of differentially-expressed (DE) miRNAs in MWCNT-7- and crocidolite-exposed cells were subsequently defined according to the following criteria:

1. $\text{padj} < 0.05$ in DESeq2 or $\text{FDR} < 0.05$ in EdgeR Exact Test
and
2. $\log_2 \text{fold-change} > |0.5|$ in DESeq2 or $\log_2 \text{fold-change} > |0.75|$ in EdgeR

The \log_2 fold-change cut-off was set higher in EdgeR than in DESeq2 because EdgeR showed a larger distribution of fold-change values.

5.3.7. Pathway analysis of miRNA target genes

The DIANA-miRPath v3.0 web server⁵⁴ was used for the identification of miRNA target genes, Kyoto Encyclopedia of Genes and Genomes (KEGG) pathways⁵⁵ and GO terms^{56,57}. miRNA target genes were initially identified using experimentally-supported interactions contained in Tarbase v7.0⁵⁸ or, in its absence, of predicted interactions available in TargetScan 6.2⁵⁹. The “Genes intersection” method was used for pathway analysis. An intersection set composed of 3 miRNAs was used, i.e., all genes targeted by at least 3 miRNAs contained in the selected set was used for enrichment analysis. The p -value threshold was of 0.05. Advanced statistic options included “FDR Correction” and “Conservative Stats” (which penalizes pathways with very few target gene nodes). The resulting list of KEGG affected pathways was manually filtered according to the main categories “metabolism”, “genetic information processing”, “environmental processing” and “cellular processes”. The category “organismal systems” was removed from the analysis since it does not cover biological systems related to the lung function. In addition, only the pathways related to lung pathology in the category “human diseases” were retained.

5.3.8. miRNA - target gene network analysis

DE miRNAs in crocidolite- or MWCNT-7-exposed cells for which target genes were identified in KEGG's 'Pathways in Cancer' (hsa05200) were loaded into Cytoscape version 3.7.0⁶⁰ for network extension using CyTargetLinker 4.0.1⁶¹. miRBase accession numbers were retrieved for each of the miRNA names (miRBase v.20) using miRNAmeConverter web interface⁶². miRTarBase⁶³ miRNA-target gene validated interactions (release 7.0) were used as the link set in CyTargetLinker. The extended networks were filtered using a text file containing a list of the 'Pathways in Cancer' target genes detected in pathway analysis (Supplementary files 12 and 13). Log₂-fold change values and corresponding FDR obtained with EdgeR Exact Test for each of the miRNAs were uploaded in filtered networks to visualize the over- or under-expression of miRNAs and their FDR, respectively.

5.4. Results

5.4.1. miRNA differential expression analysis

Several under- and over-expressed miRNAs were identified in the A549 cell cultures after exposure to MWCNT-7 or crocidolite. The total number of DE miRNAs was dependent on the tool used to assess differential expression, with DESeq2 identifying a lower number of DE miRNAs comparatively to EdgeR. Thus, the total number of DE miRNAs in MWCNT-7- and crocidolite-exposed cells identified with DESeq2 and EdgeR was of 49 and 48, and of 85 and 86, respectively. All the miRNAs identified as DE in DESeq2 were also found using EdgeR. After filtering the above-mentioned miRNAs according to the criteria previously described, a total of 17 and 21 miRNAs were DE in cells following 24 h exposure to MWCNT-7 or crocidolite, respectively (Table 2).

5.4.2. Functional pathways and gene ontology analyses

The prediction of the molecular KEGG pathways that were affected by the under- or over-expression of the miRNAs listed in Table 1 is represented in figures 1 and 2. These functional pathways were grouped according to the KEGG subcategories and represented as pie charts (figure 3).

Table 2. Differentially expressed miRNAs in A549 cells after 24 hours exposure to MWCNT-7 or crocidolite, comparatively to non-exposed cells. miRNA names shown in bold represent under- or over-expressed miRNAs found by both DESeq2 and EdgeR Exact Test.

DESeq2		miRNA name	log ₂ -fold change	padj/FDR
MWCNT-7	under-expressed	hsa-miR-1910-5p	-1.271318978	0.009759099
		hsa-miR-99b-3p	-0.798281222	0.028683657
		hsa-miR-423-5p	-0.763078633	3.10E-16
		hsa-miR-1180-3p	-0.735194908	1.59E-06
		hsa-miR-744-5p	-0.65453858	0.0021697
		hsa-miR-181b-5p	-0.590474101	3.32E-12
		hsa-miR-28-3p	-0.58369319	2.65E-28
		hsa-miR-423-3p	-0.580059647	9.12E-25
	hsa-miR-181a-3p	-0.553571253	4.24E-06	
	over-expressed	hsa-miR-27a-3p	0.59466829	2.60E-06
		hsa-miR-15b-5p	0.619551169	0.000271135
		hsa-miR-30c-5p	0.674722475	0.034758839
		hsa-miR-23a-3p	0.688561186	0.002886279
		hsa-miR-222-3p	0.889045128	0.037397783
crocidolite	under-expressed	hsa-miR-24-3p	-0.73414992	0.034786063
		hsa-miR-101-3p	-0.713150785	0.004304365
		hsa-miR-340-5p	-0.582456605	0.008301919
		hsa-miR-1180-3p	-0.547168087	0.00139618
		hsa-miR-28-3p	-0.542911017	5.28E-21
		hsa-miR-409-3p	-0.530453512	0.002514626
	over-expressed	hsa-miR-27a-3p	0.505266368	0.000380578
		hsa-miR-15b-5p	0.66820634	0.000380578
		hsa-miR-30c-5p	0.798185792	0.011901228
		hsa-miR-23a-3p	0.842683962	0.000380578
EdgeR Exact Test		miRNA name	log ₂ -fold change	padj/FDR
MWCNT-7	under-expressed	hsa-miR-654-5p	-1.845844483	0.007762024
		hsa-miR-1908-3p	-1.487354661	0.041120488
		hsa-miR-1910-5p	-1.168992982	0.000451106
		hsa-let-7d-3p	-0.789489298	0.003483815
	over-expressed	hsa-miR-23a-3p	0.747148058	1.70E-07
		hsa-miR-222-3p	0.951838697	0.000112017
crocidolite	under-expressed	hsa-miR-654-5p	-2.211630362	0.003227417
		hsa-miR-1908-3p	-1.626975718	0.049569238
		hsa-miR-382-5p	-1.49883479	0.039304006
		hsa-miR-193a-5p	-1.021835193	0.010603353
		hsa-miR-210-5p	-0.886993244	0.041209528
	over-expressed	hsa-miR-134-5p	0.777447093	0.011187302
		hsa-miR-30c-5p	0.823403475	1.32E-06
		hsa-miR-23a-3p	0.873117105	7.84E-12
		hsa-miR-758-3p	0.9645798	0.019932114
		hsa-miR-548o-3p	0.987369546	0.040452333
		hsa-miR-215-5p	1.174234661	0.040628046
		hsa-miR-130b-5p	1.324235257	0.035406988
		hsa-miR-422a	1.333924898	0.001101338

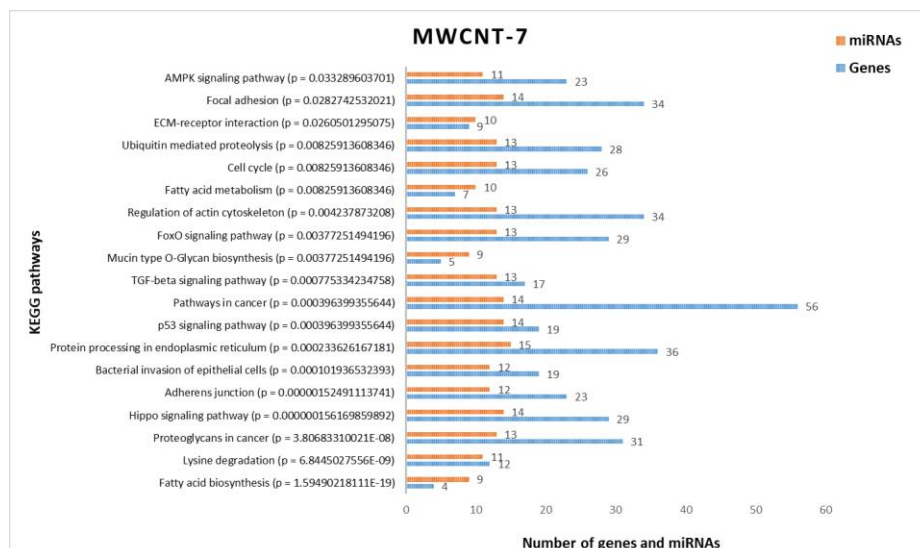


Figure 1. KEGG pathways enriched with genes targeted by the differentially expressed miRNAs in A549 cells exposed to MWCNT-7, ordered by decreasing p-value.

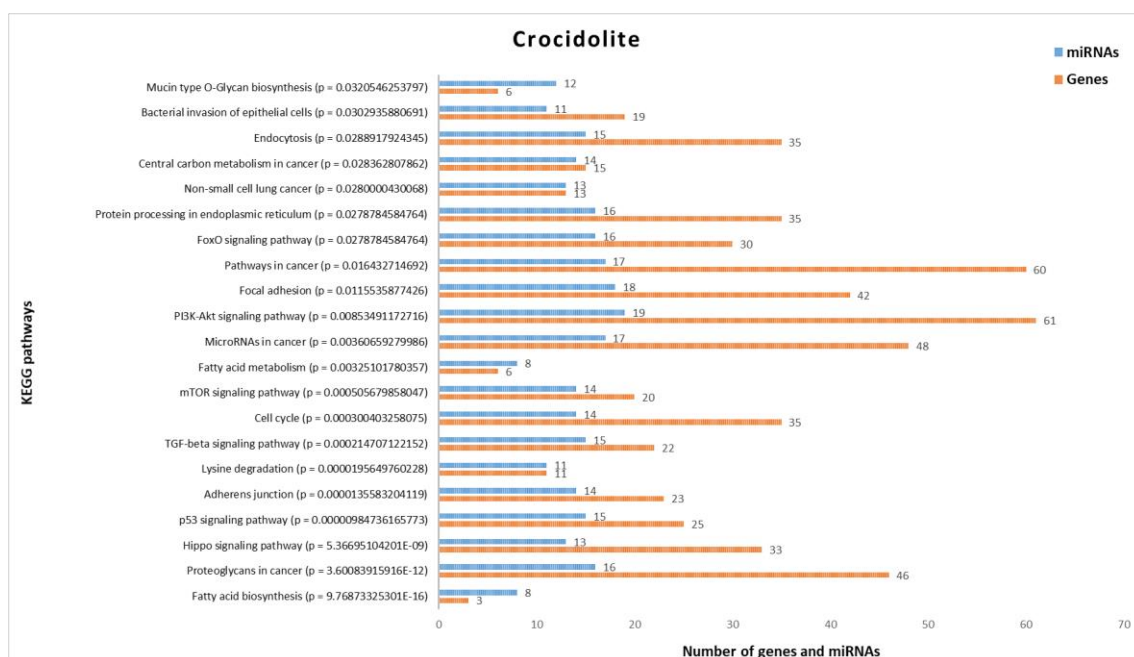


Figure 2. KEGG pathways enriched with genes targeted by the differentially expressed miRNAs in A549 cells exposed to crocidolite, ordered by decreasing p-value.

The main enriched KEGG categories are environmental information processing (encompassing the subcategories “signal transduction” and “signalling molecules and interaction”), and cellular processes (encompassing the subcategories “transport and catabolism”, “cell growth and death” and “cellular community”). As shown in figure 3, most of the enriched cellular pathways are shared between MWCNT-7 and crocidolite and are related to cell metabolism, processes of cell growth and death, cell-to-cell

communication, protein processing in the endoplasmatic reticulum, and signal transduction. Furthermore, other molecular pathways are enriched for each exposure, namely, “regulation of actin cytoskeleton”, “ubiquitin mediated proteolysis” and “ECM-receptor interaction” in cells exposed to MWCNT-7, and “endocytosis”, “central carbon metabolism in cancer”, “microRNAs in cancer”, “non-small cell lung cancer”, “P13K-Akt signalling pathway” and “mTOR signalling pathway” in cells exposed to crocidolite.

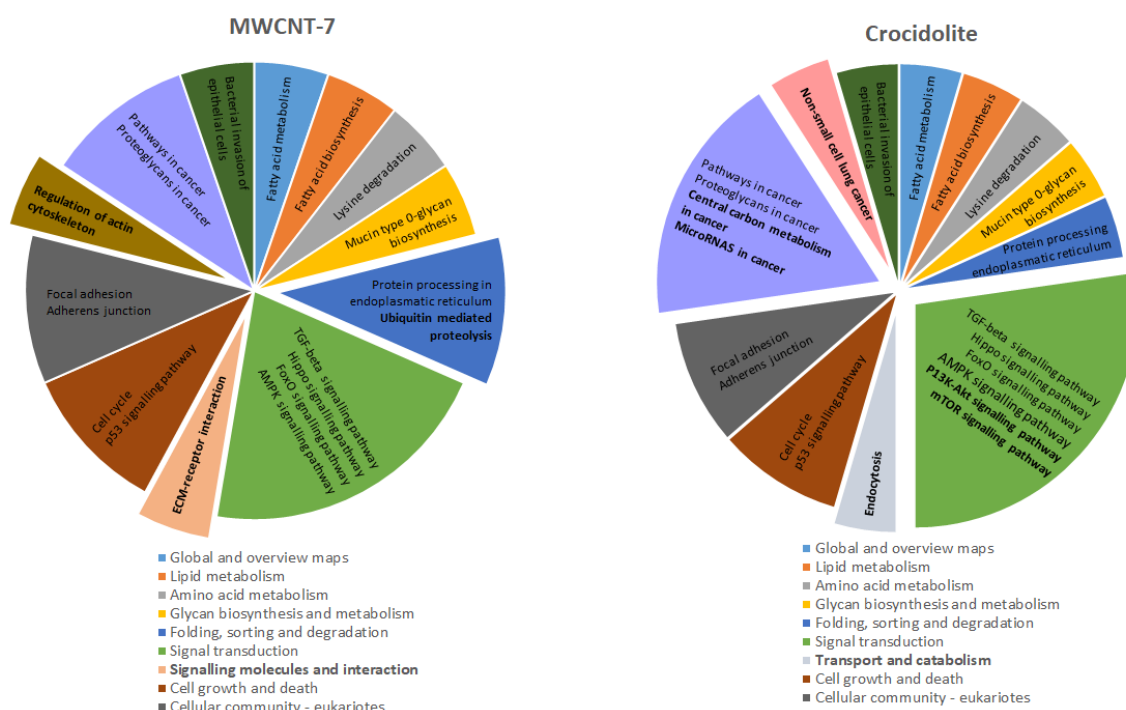


Figure 3. Pie charts of the proportion of enriched pathways in A549 cells after 24 h exposure to MWCNT-7 or crocidolite, organized according to KEGG sub-categories. In bold, unique pathways and subcategories found in MWCNT-7 or crocidolite exposed cells.

Pathway analysis identified miRNA target genes in 'Pathways in Cancer' for 14 out of 17 DE miRNAs in MWCNT-7-exposed cells. miRNAs with no target genes in this pathway included hsa-miR-1180-3p, hsa-miR-1910-5p and hsa-miR-654-5p. Likewise, 17 out of 21 miRNAs had 'Pathways in Cancer' target genes in crocidolite-exposed cells. miRNAs hsa-miR-1180-3p, hsa-miR-215-5p, hsa-miR-134-5p and hsa-miR-654-5p had no target genes in this pathway. The number of target cancer genes was of 56 and 60 in MWCNT-7-exposed and crocidolite-exposed-cells, respectively.

Ontology analysis showed that four molecular functions (RNA binding, poly(A) RNA binding, ion binding, enzyme binding) and four cellular components (organelle, cytosol,

protein complex and micro-ribonucleoprotein complex) were enriched in both MWCNT-7 and crocidolite exposures. Exposure to the latter included three other cellular components (nucleoplasm, RISC complex and cytoplasmic mRNA processing body). The enriched GO biological processes for each material are shown in figures 5 and 6, and the majority are associated to regulation of gene expression, e.g., positive regulation of nuclear-transcribed mRNA catabolic process - deadenylation-dependent decay, positive regulation of nuclear-transcribed mRNA poly(A) tail shortening, negative regulation of translation involved in gene silencing by miRNA, and nucleobase-containing compound catabolic process, among others. Of special interest, we found enrichment of the fibroblast growth factor receptor, epidermal growth factor receptor, and Notch signalling pathways in cells exposed to either MWCNT-7 or crocidolite.

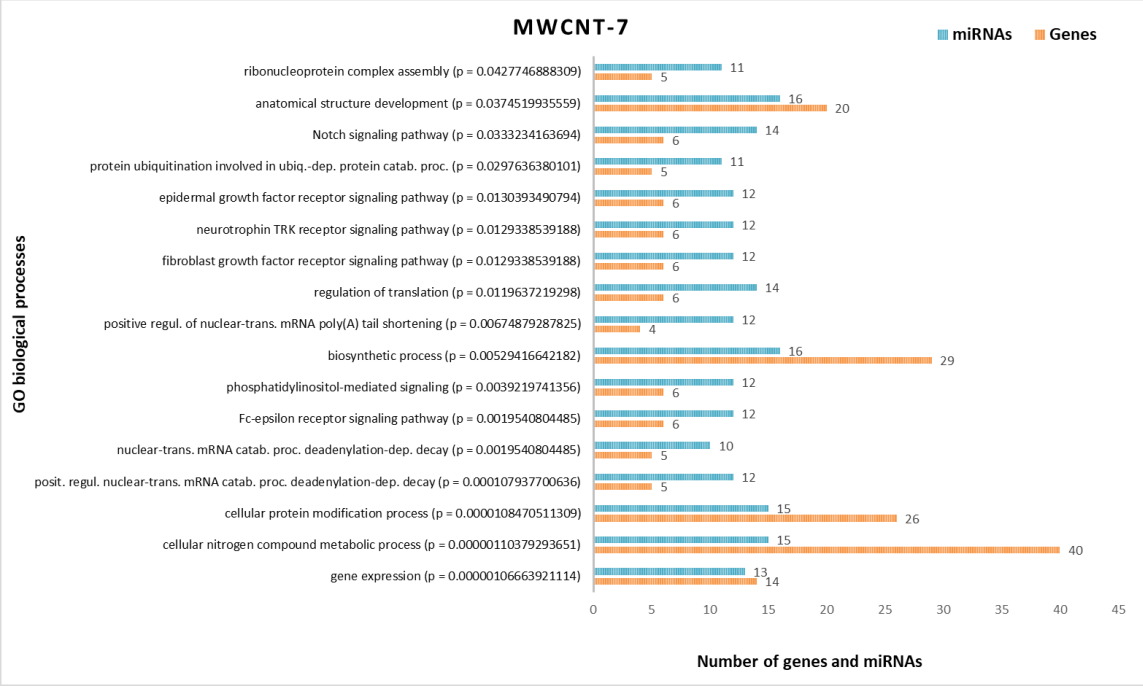


Figure 4. GO terms enriched with target genes of the differentially expressed miRNAs in A549 cells exposed to MWCNT-7, ordered by decreasing p-value.

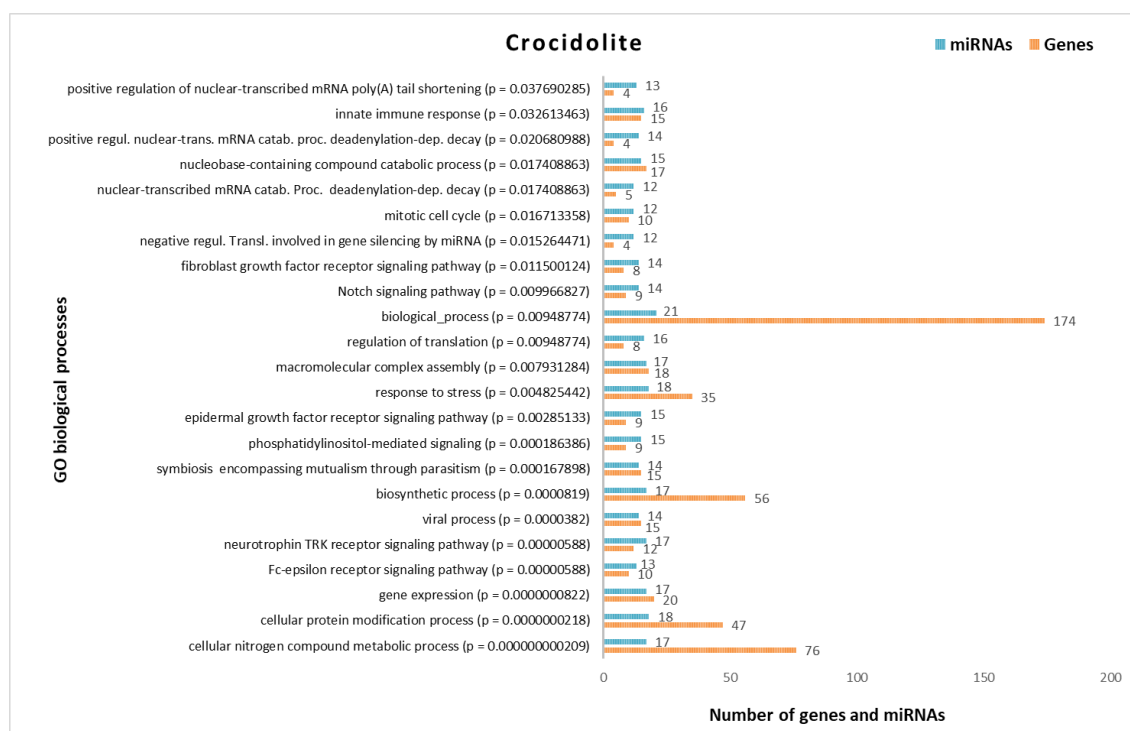


Figure 5. GO terms enriched with target genes of the differentially expressed miRNAs in A549 cells exposed to crocidolite, ordered by decreasing p-value.

5.4.3. miRNA - target cancer genes interaction network

We performed a network analysis of the DE miRNAs and their target genes included in the KEGG subcategory “pathways in cancer” because of the over-representation of cancer-related molecular pathways in cells exposed to MWCNT-7 or crocidolite. “Pathways in cancer” is a global KEGG subcategory, i.e., it includes many pathways of other subcategories that are related to cancer, for instance, many signal transduction or metabolic pathways. Thus, it allows an overview of many linked pathways that determine cell survival, differentiation and proliferation. In this analysis, only a part of the possible miRNA-target gene interactions were represented since for some miRNAs and some target genes no interactions are described in mirTarBase. These included 3 out of 14 miRNAs (hsa-miR-1908-3p, hsa-let-7d-3p and hsa-miR-181a-3p) and 20 out of 56 target genes in MWCNT-7-exposed cells and 4 out of 17 miRNAs (hsa-miR-548o-3p, hsa-miR-210-5p, hsa-miR-422a and hsa-miR-1908-3p) and 9 out of 60 target genes in crocidolite-exposed cells. However, several oncogenes including *CCND1*, *EGFR*, *MDM2* and *MYC*, and several tumour suppressor genes including *PTEN*, *RUNX1* or *SMAD2* are included in the networks. The comparison of both networks suggests that crocidolite has a higher impact than MWCNT-7 in the A549 cell pathways related to cancer (figure 6).

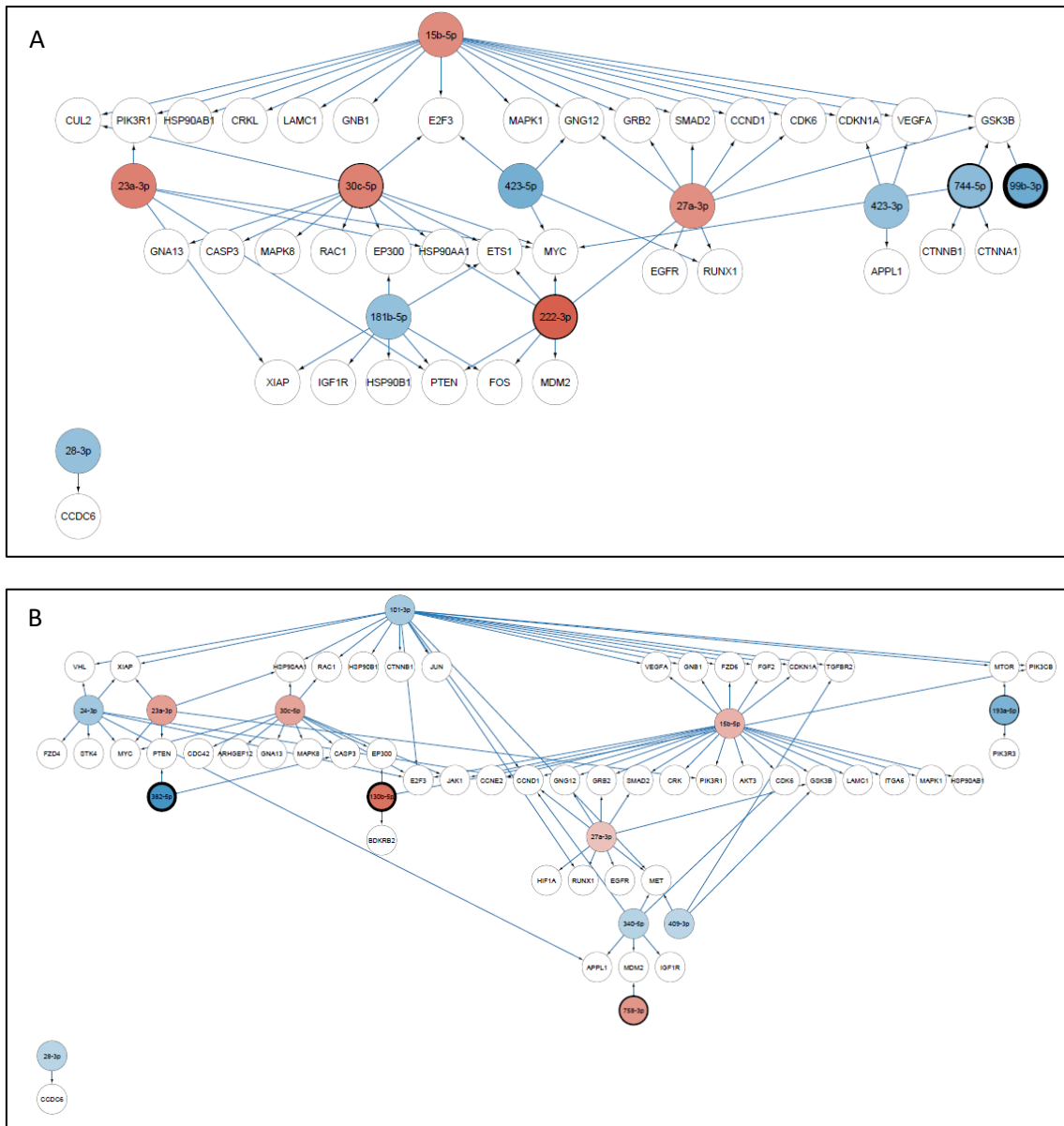


Fig 6. Networks of miRNA-target gene interactions in MWCNT-7- (A) and crocidolite- (B) exposed A549 cells. The yFiles Tree Layout version 1.0.1 (yWorks, Germany) was used as the algorithm to visualize the networks. Nodes colored blue indicate lower expression in exposed cells whereas nodes colored red indicate higher expression, relatively to non-exposed cells. miRNA nodes with thicker borders indicate higher FDR values whereas those with thinner borders indicate lower FDR values. Thus, network nodes with darker blue or red circles and thinner borders represent miRNAs with potential higher impact in the network. Gene nodes are shown in white. The "hsa-miR-" prefix of miRNA names was omitted for a better visualization.

5.5. Discussion

In this study, using alveolar epithelial cells exposed to a low concentration of MWCNT-7 or crocidolite we identified sets of miRNAs associated with the exposure to each material. Some of those miRNAs have been reported as regulators of cellular pathways

related to control of cell growth, proliferation, differentiation and survival. For both materials, signal transduction was the main enriched cellular process, and several well-known pathways such as the transforming growth factor- β (TGF- β), the mammalian target of rapamycin (mTOR), and the Forkhead box O (FoxO) pathways were enriched in the functional pathway analysis.

The AMP-activated protein kinase (AMPK) pathway and the FoxO pathway are commonly deregulated in cells exposed to MWCNT-7 and crocidolite. AMPK is a highly conserved metabolic sensor of intracellular adenosine nucleotide levels that is activated when ATP production decreases, resulting in relative increases in AMP or ADP⁶⁴. This cell signalling pathway plays critical roles in regulating growth and reprogramming metabolism, and other cellular processes including autophagy and cell polarity⁶⁴. AMPK, upon oxidative and nutrient stress, e.g., low glucose or oxygen levels, leads to a concomitant inhibition of anabolic pathways, such as protein, fatty acid and glycogen synthesis, and activation of catabolic pathways, such as fatty acid oxidation and glycolysis. One of its downstream effects is the activation of FoxO transcription factors, increasing the expression of its target genes that regulate cellular differentiation, growth, survival, cell cycle, metabolism, stress and tumour suppression pathways⁶⁵. By contrary, phosphorylation by the phosphatidylinositol 3-kinase/serine-threonine kinase (PI3K/Akt) pathway, that was found to be enriched in cells exposed to crocidolite, inactivates FoxO proteins decreasing gene expression of negative cell cycle regulators and promoting cell survival, growth and proliferation⁶⁵. In addition, the PI3K/Akt pathway positively regulates the mTOR pathway, which was also enriched upon crocidolite exposure, while the AMPK pathway acts as a negative regulator of the mTOR pathway. The mTOR pathway regulates cell metabolism, growth, proliferation and survival through several cellular processes, including lipid metabolism, autophagy, protein synthesis and ribosome biogenesis, and is deregulated in human diseases such as cancer and type 2 diabetes^{66,67}. This is in line with the metabolic pathways that were identified as being affected in cells exposed to each of the materials, i.e., fatty acid biosynthesis, lysine degradation and mucin type O-glycan biosynthesis in KEGG analysis, or biosynthetic processes, cellular nitrogen compound metabolic process, nucleobase-containing compound deadenylation and several other catabolic processes involved in regulation of transcription and translation in GO analysis. It is known that cancer cells show alterations in mucin-type O-glycosylation, which is a widespread post-translational modification of proteins involved in a variety of important biological processes in eukaryotes⁶⁸. Moreover, proteoglycans in cancer is the second major enriched KEGG pathway. Proteoglycans are proteins with one or more covalently

bound glycosaminoglycan chain that are constituents of the extracellular matrix (ECM) or are located in the basement membrane or plasma membranes of cells, either directly via an intercalated protein core or via a glycosyl-phosphatidyl-inositol anchor^{69,70}. ECM proteins and structures can determine cell behaviour, polarity, migration, differentiation, proliferation and survival by communicating with the intracellular cytoskeleton and transmitting growth factor signals⁷¹. Hence, alterations in the EMC proteoglycans can interfere with these cell functions, and ECM-receptor interaction is one enriched KEGG subcategory, as well as adherens junction and focal adhesion. Another commonly affected pathway, the Hippo pathway, is regulated by cell-cell contact, cell polarity and actin cytoskeleton, among other signals, like the cell state of energy and hormonal⁷². Hippo major functions are restricting tissue growth in adults and modulating cell proliferation, differentiation, and migration in developing organs⁷². Many upstream regulators for the Hippo pathway are components of tight junctions and adherens junctions.

A pathway differentially enriched in cells exposed to MWCNT-7, also enriched in GO analysis, is the ubiquitin proteolytic system. The ubiquitin proteolytic system has influence on a broad spectrum of cellular processes, e.g., regulation of cell cycle, differentiation and development, response to extracellular effectors and stress, modulation of cell surface receptors and ion channels, DNA repair, regulation of the immune and inflammatory responses and biogenesis of organelles⁷³. One of the cellular pathways this system tightly regulates is the TGF- β signalling pathway, another enriched pathway. The TGF- β is a superfamily of cytokines crucial in regulating cell growth, differentiation, apoptosis, motility, invasion, extracellular matrix production, angiogenesis, and immune response⁷⁴. In the early stages of cancer development, TGF- β acts as a tumour suppressor, whereas in later stages, supports invasion and metastasis by modulating the immune system and tumour microenvironment⁷⁴. The main signal transducers for TGF- β signalling are the Smads, a family of structurally related proteins⁷⁵. Smad2, which is represented in the gene networks of figure 6, is one of these essential mediators. Its possible down-regulation through the overexpression of the miRNAs hsa-miR-15b-5p and hsa-miR-27a-3p can reduce the inhibitory response of TGF- β , thus causing dysregulation of cell growth.

GO analysis has also highlighted the involvement of the epidermal growth factor receptor (EGFR) and Notch signalling pathways in the molecular effects of MWCNT-7 and crocidolite. EGFR and Notch signalling are essential in cell proliferation, differentiation, and apoptosis^{76,77}. Their deregulation is a common event in cancer, including in non-small-cell lung cancer (NSCLC), and EGF and Notch receptors are

widely used targets of cancer therapy^{78,79}. Overexpression of EGFR was detected in more than half cases of NSCLC, most frequently in squamous cells, associated with a poor prognosis and chemoresistance. As to the Notch signalling, its role in NSCLC is more complex, but there are several theories trying to explain the crosstalk between Notch and EGFR⁸⁰.

Since the deregulation of the above-mentioned pathways, in which the well-known p53 pathway can be included, are related to malignancy and tumorigenesis, cell cycle regulation is an affected function in cells exposed to MWCNT-7 and crocidolite. In fact, “pathways in cancer” is altered in the KEGG category human diseases. This pathway was also found enriched in the analysis of the mRNA targets of upregulated miRNA in the whole blood of 8 workers with no less than 6 months exposure to MWCNTs by inhalation⁸¹, confirming its *in vivo* relevance. The richness of interconnections between the cancer related genes depicted in figure 6 suggests that cancer is an important outcome of MWCNT-7 and crocidolite exposures.

Non-small cell lung cancer is significantly enriched in crocidolite exposure, although from the 40 and 28 miRNAs found differently expressed, respectively, in tumour samples of stage I squamous cell carcinoma and adenocarcinoma, only the hsa-miR-758-3p, associated to squamous cell carcinoma, is upregulated in crocidolite exposure⁸². MicroRNAs in cancer and central metabolism in cancer are also specific crocidolite-enriched pathways, which may suggest that crocidolite is more carcinogenic than MWCNT-7. However, miR-hsa-222-3p is upregulated in cells exposed to MWCNT-7, but not to crocidolite. The miR-hsa-222 regulates the expression of a potent inhibitor of cell cycle and tumour suppressor protein, p27, and is overexpressed in NSCLC, indicating poor prognostic factors and poor survival^{83,84,85}. The miR-hsa-222-3p has been found in exosomes released from epithelial ovarian cancer cells that are transferred to macrophages causing their polarization towards the M2 phenotype, further enhancing tumour progression⁸⁶. Moreover, it was present in patient serum exosomes and proposed as a biomarker of epithelial ovarian cancer. Furthermore, exosomal miR-hsa-222-3p seems to play a critical role in gemcitabine resistance in NSCLC chemotherapy. Exosomes rich in miR-222-3p, transferred from gemcitabine resistant A549 cells to recipient A549 cells via caveolin- and lipid raft-dependent endocytosis, have enhanced their proliferation, gemcitabine resistance, migration, invasion, and anti-apoptosis by directly targeting the promoter of *SOCS3*⁸⁷. In addition, a higher level of exosomal miR-222-3p in patient's sera predicted worse prognosis in NSCLC following gemcitabine therapy. Let-7d is another miRNA down-regulated in MWCNT-7 exposure. It belongs to the Let-7 family, a group of miRNAs that act as a

tumour suppressor miRNAs and regulate the expression of oncogenes in several types of human cancers, including lung cancer⁸⁸. A549 cells express high levels of Let-7d and its down-regulation has been associated to the development of idiopathic pulmonary fibrosis⁸⁹ and non-small cell lung cancer (NSCLC), being also related to a shortened postoperative survival⁹⁰.

The regulation of cell actin cytoskeleton pathway is also affected after exposure to MWCNT-7, but not to crocidolite. It is thought that MWCNT may interact with or interfere with actin, microtubules and probably with intermediate filaments such as the nuclear laminas⁹¹. A biomimetic microtubule model was proposed, where bundles of MWCNT are longitudinally associated with microtubules or where one or more of the 13 microtubule protofilaments is substituted by a MWCNT, ultimately leading to cell division arrest and apoptosis⁹¹. Consequently, a dose-related increase in the frequency of disrupted centrosomes and abnormal mitotic spindles was observed in human bronchial epithelial cells exposed to MWCNT⁹².

Finally, endocytosis was affected in cells exposed to crocidolite, suggesting a more significant role of this mode of cell entry for crocidolite fibres than for MWCNT-7 nanofibres. MWCNT can have a piercing effect in the plasma membrane and directly translocate into the cytoplasm due to their needle-like structure.⁹³ observed intracellular trafficking of MWCNT towards the perinuclear region in several cell types, even under endocytosis-inhibiting conditions. Moreover, MWCNT were found free in the A549 cell cytoplasm or wrapped into endosome-like structures, possibly due to the contribution of direct translocation, endocytosis and micropinocytosis⁹⁴.

Overall, we identified several functional pathways in epithelial cells that are affected by MWCNT-7 or crocidolite exposure, which is one great advantage of using NGS. This sequencing technique detects all cellular miRNAs, and not only the ones predefined by microarrays, allowing a complete profile of the gene regulation changes occurring through miRNA expression. It should not be forgotten that, as in all *in vitro* studies using representative established cell lines, as the A549 human alveolar type II epithelial cells^{95,96}, we cannot exclude that other functional pathways would be significantly affected in normal primary epithelial lung cells.

5.6 Conclusion

The role of miRNAs in regulating gene expression is being increasingly understood, either promoting or suppressing biological pathways. Consequently, the identification of the differently expressed miRNAs in cells or tissues after exposure to a toxic can allow

the recognition of its possible mechanisms of action. Our results strongly indicate that A549 cells exposed to an occupationally relevant dose of MWCNT-7, and an identical dose of crocidolite, are changing their survival, differentiation and proliferative capabilities under the major influence of the AMPK, FoxO, TGF- β and Hippo pathways, thus influencing cell-to-cell communication and their metabolic activity. A gene network analysis of pathways related to cancer showed the involvement of several oncogenes and tumour suppressor genes in the alveolar cell response to exposure to MWCNT-7 and crocidolite that can represent future targets of research on its molecular effects. Moreover, the overall results suggest that crocidolite has a greater impact than MWCNT-7 in cell survival, differentiation and proliferation. Furthermore, MWCNT-7 seems to affect the regulation of the actin cytoskeleton, the ubiquitin mediated proteolysis system, and ECM-receptor interactions. In turn, crocidolite more profoundly affects the P13K-Akt and mTOR signalling pathways, endocytosis, and central carbon metabolism in cancer.

Acknowledgements

The authors are grateful to Carmo Proença and Fátima Aguiar from the Environmental Health Department of INSA, for the kind gift of crocidolite used in this work, and to Henriqueta Louro from the Department of Human Genetics of INSA for DLS analysis of Mitsui-7. This work was supported by the Foundation for Science and Technology, Centre for Toxicogenomics and Human Health (ToxOmics) under grant UID/BIM/00009/2013 and by ToxApp4NanoCELF (grant PTDC/SAU-PUB/32587/2017). This work is a result of the GenomePT project (POCI-01-0145-FEDER-022184), supported by COMPETE 2020 - Operational Programme for Competitiveness and Internationalisation (POCI), Lisboa Portugal Regional Operational Programme (Lisboa2020), Algarve Portugal Regional Operational Programme (CRESC Algarve2020), under the PORTUGAL 2020 Partnership Agreement, through the European Regional Development Fund (ERDF), and by Fundação para a Ciência e a Tecnologia (FCT).

(Due to the high number of pages of the supplementary material, these files are only available in the digital version of this thesis).

Manuscript supplementary material

The contents of each supplementary file are the following:

Supplementary_file_1.txt: Output file ('Hits.txt') of the Small RNA analysis workflow of the MiSeq instrument corresponding to the first sequencing run. The file presents the number of miRNA hits in each library according to miRBase version 20 database. The correspondence between the libraries and column labels is the following:

S1: non-exposed cells

S2: MWCNT-7-exposed cells

S3: crocidolite-exposed cells

S7: human brain total RNA (control)

Supplementary_file_2.txt: Output file ('Hits.txt') of the Small RNA analysis workflow of the MiSeq instrument corresponding to the second sequencing run. The file presents the number of miRNA hits in each library according to miRBase version 20 database. The correspondence between the libraries and column labels is the following:

S1: non-exposed cells

S2: MWCNT-7-exposed cells

S3: crocidolite-exposed cells

Supplementary_file_3.csv: Matrix containing the replicate counts corresponding to the non-exposed and MWCNT-7-exposed cells after filtering. The correspondence between the libraries and column labels is the following:

Exp1_0_1d_A: non-exposed cells (first run)

Exp1_0_1d_B: non-exposed cells (second run)

Exp1_CNT_1d_A: MWCNT-7-exposed cells (first run)

Exp1_CNT_1d_B: MWCNT-7-exposed cells (second run)

Supplementary_file_4.csv: Matrix containing the replicate counts corresponding to the non-exposed and crocidolite-exposed cells after filtering. The correspondence between the libraries and column labels is the following:

Exp1_0_1d_A: non-exposed cells (first run)

Exp1_0_1d_B: non-exposed cells (second run)

Exp1_ASB_1d_A: crocidolite-exposed cells (first run)

Exp1_ASB_1d_B: crocidolite-exposed cells (second run)

Supplementary_file_5.doc: Template R script used for the analysis of differential expression of miRNAs between non-exposed cells and cells exposed to MWCNT-7 or crocidolite in DESeq2. The 'filtered.csv' file corresponds to the filtered counts file and the 'conditions.csv' file was used as the design file for the analysis. A 'conditions.csv' design file for the comparison between non-exposed and MWCNT-7-exposed cells was constructed.

Supplementary_file_6.csv: Normalized counts file corresponding to the non-exposed and MWCNT-7-exposed cells. The correspondence between the libraries and column labels is the same as in 'supplementary_file_3.csv'.

Supplementary_file_7.csv: Normalized counts file corresponding to the non-exposed and crocidolite-exposed cells. The correspondence between the libraries and column labels is the same as in 'supplementary_file_4.csv'.

Supplementary_file_8: Results file for DESeq2 differential expression analysis between non-exposed and MWCNT-7-exposed cells.

Supplementary_file_9: Results file for DESeq2 differential expression analysis between non-exposed and crocidolite-exposed cells.

Supplementary_file_10.tsv: Results file for EdgeR Exact Test differential expression analysis between non-exposed and MWCNT-7-exposed cells.

Supplementary_file_11.tsv: Results file for EdgeR Exact Test differential expression analysis between non-exposed and crocidolite-exposed cells.

Supplementary_file_12.xlsx: List of 'Pathways in Cancer' (hsa05200) target genes and number of target genes per differentially-expressed miRNA in MWCNT-7-exposed cells.

Supplementary_file_13.xlsx: List of 'Pathways in Cancer' (hsa05200) target genes and number of target genes per differentially-expressed miRNA in crocidolite-exposed cells.

5.7. References

1. NIOSH. Occupational Exposure to Carbon Nanotubes and Nanofibers. 2013.
2. Trout DB, Schulte PA. Medical surveillance, exposure registries, and epidemiologic research for workers exposed to nanomaterials. *Toxicology*. 2010;269(2–3):128–35.

3. Landsiedel R, Sauer UG, Ma-hock L, Schnekenburger J, Wiemann M. Pulmonary toxicity of nanomaterials : a critical comparison of published in vitro assays and in vivo inhalation or instillation studies. *Nanomedicine* (Lond). 2014;9:2557–85.
4. Lanone S, Andujar P, Kermanizadeh A, Boczkowski J. Determinants of carbon nanotube toxicity. *Adv Drug Deliv Rev.* 2013;65(15):2063–9.
5. Pacurari M, Castranova V, Vallyathan V. Single- and Multi-Wall Carbon Nanotubes Versus Asbestos: Are the Carbon Nanotubes a New Health Risk to Humans ? *J Toxicol Environ Heal Part A.* 2010;73:378–95.
6. IARC working group on the Evaluation of Carcinogenic Risks to Humans. Some Nanomaterials and Some Fibres To Humans Some Nanomaterials and Some Fibres. Lyon, France: World Health Organization; 2017. p. 325.
7. Takagi A, Hirose A, Nishimura T, Fukumori N, Ogata A, Ohashi N, et al. Induction of mesothelioma in p53 + / – mouse by intraperitoneal application of multi-wall carbon nanotube. *J Toxicol Sci.* 2008;33(1):105–16.
8. Takagi A, Hirose A, Futakuchi M, Tsuda H, Kanno J. Dose-dependent mesothelioma induction by intraperitoneal administration of multi-wall carbon nanotubes in p53 heterozygous mice. *Cancer Sci.* 2012;103(8):1440–4.
9. Nagai H, Okazaki Y, Chew S, Misawa N, Yamashita Y, Akatsuka S, et al. Diameter and rigidity of multiwalled carbon nanotubes are critical factors in mesothelial injury and carcinogenesis. *Proc Natl Acad Sci USA.* 2011 Dec 6;108(49):E1330-8
10. Sakamoto Y, Nakae D, Fukumori N, Tayama K. Induction of mesothelioma by a single intrascrotal administration of multi-wall carbon nanotube in intact male Fischer 344 rats. *J Toxicol Sci.* 2009;34(1):65–76.
11. Kasai T, Umeda Y, Ohnishi M, Mine T, Kondo H, Takeuchi T. Lung carcinogenicity of inhaled multi- walled carbon nanotube in rats. *Part Fibre Toxicol.* 2016;1–19.
12. Sargent LM, Porter DW, Staska LM, Hubbs AF, Lowry DT, Battelli L, et al. Promotion of lung adenocarcinoma following inhalation exposure to multi-walled carbon nanotubes. *Part Fibre Toxicol.* 2014;11(3):1–18.
13. Huaux F, d'Ursel de Bousies V, Parent M-A, Orsi M, Uwambayinema F, Devosse R, et al. Mesothelioma response to carbon nanotubes is associated with an early and selective accumulation of immunosuppressive monocytic cells. *Part Fibre Toxicol.* 2015;13(1):46.

14. Aardema MJ, Macgregor JT. Toxicology and genetic toxicology in the new era of “toxicogenomics”: impact of “-omics” technologies. *Mutat Res.* 2002;499:13–25.
15. Ellinger-ziegelbauer H, Aubrecht J, Kleinjans JC, Ahr H, Ag BH, Toxicology S. Application of toxicogenomics to study mechanisms of genotoxicity and carcinogenicity. *Toxicol Lett.* 2009;186:36–44.
16. Ventura C, Sousa-Uva A, Lavinha J, Silva MJ. Conventional and novel “omics”-based approaches to the study of carbon nanotubes pulmonary toxicity. *Environ Mol Mutagen.* 2018;59(4):334-62.
17. Stoccoro A, Karlsson HL, Coppedè F, Migliore L. Epigenetic effects of nano-sized materials. *Toxicology.* 2013;313(1):3–14.
18. Lu X, Miousse IR, Pirela S V., Melnyk S, Koturbash I, Demokritou P. Short-term exposure to engineered nanomaterials affects cellular epigenome. *Nanotoxicology.* 2016;10(2):140–50.
19. Ha M, Kim VN. Regulation of microRNA biogenesis. *Nat Rev Mol Cell Biol.* 2014;15:509–24.
20. Yanaihara N, Caplen N, Bowman E, Seike M, Kumamoto K, Yi M, et al. Unique microRNA molecular profiles in lung cancer diagnosis and prognosis. *Cancer Cell.* 2006;9(3):189–98.
21. Rupani H, Sanchez-elsner T, Howarth P. microRNAs and respiratory diseases. *Eur Respir J.* 2013;41:695–705.
22. Sessa R, Hata A. Role of microRNAs in lung development and pulmonary diseases. *Pulm Circ.* 2013;3(2):315–28.
23. Guled M, Lahti L, Lindholm PM, Salmenkivi K, Bagwan I. CDKN2A , NF2 , and JUN are dysregulated among other genes by miRNAs in malignant mesothelioma — A miRNA microarray analysis. *Genes Chromosomes Cancer.* 2009;48:615–23.
24. Busacca S, Germano S, Cecco L De, Rinaldi M, Comoglio F, Favero F, et al. microRNA signature of malignant mesothelioma with potential diagnostic and prognostic implications. *Am J Respir Cell Mol Biol.* 2010;42:312–9.
25. Ak G, Tomaszek SC, Kosari F, Metintas M, Jett JR, Metintas S, et al. microRNA and mRNA features of malignant pleural mesothelioma and benign asbestos-related pleural effusion. *Biomed Res Int.* 2015;635748:1–8.
26. Snyder-talkington BN, Dong C, Sargent LM, Porter DW, Staska LM, Hubbs AF, et al. mRNAs and miRNAs in whole blood associated with lung hyperplasia, fibrosis,

and bronchiolo-alveolar adenoma and adenocarcinoma after multi-walled carbon nanotube inhalation exposure in mice. *J Appl Toxicol*. 2016;36(1):161–74.

27. Chen X, Ba Y, Ma L, Cai X, Yin Y, Wang K, et al. Characterization of microRNAs in serum: a novel class of biomarkers for diagnosis of cancer and other diseases. *Cell Reseach*. 2008;18:997–1006.

28. Schwarzenbach H, Nishida N, Calin GA, Pantel K. Clinical relevance of circulating cell-free microRNAs in cancer. *Nat Rev Clin Oncol*. 2014 Feb 4;11:145.

29. Bru T, Weber DG, Johnen G, Bryk O, Jo K. Identification of miRNA-103 in the cellular fraction of human peripheral blood as a potential biomarker for malignant mesothelioma – A pilot study. *PLoS One*. 2012;7(1):1–9.

30. Pu Q, Huang Y, Lu Y, Peng Y, Zhang J, Feng G. Tissue-specific and plasma microRNA profiles could be promising biomarkers of histological classification and TNM stage in non-small cell lung cancer. *Thorac Cancer*. 2016;7:348–54.

31. Li S, Wang H, Qi Y, Tu J, Bai Y, Tian T, et al. Biomaterials assessment of nanomaterial cytotoxicity with SOLiD sequencing-based microRNA expression profiling. *Biomaterials*. 2011;32(34):9021–30.

32. Dymacek J, Snyder-Talkington BN, Porter DW, Mercer RR, Wolfarth MG, Castranova V, et al. mRNA and miRNA regulatory networks reflective of multi-walled carbon nanotube-induced lung inflammatory and fibrotic pathologies in mice. *Toxicol Sci*. 2015;144(1):51–64.

33. Nymark P, Wijshoff P, Cavill R, van Herwijnen M, Coonen MLJJ, Claessen S, et al. Extensive temporal transcriptome and microRNA analyses identify molecular mechanisms underlying mitochondrial dysfunction induced by multi-walled carbon nanotubes in human lung cells. *Nanotoxicology*. 2015;9(September):624–35.

34. Nymark P, Guled M, Borze I, Faisal A, Lahti L, Salmenkivi K. Integrative analysis of microRNA, mRNA and aCGH data reveals asbestos- and histology-related changes in lung cancer. *Genes Chromosomes Cancer*. 2011;50:585–97.

35. Oberdörster G. Safety assessment for nanotechnology and nanomedicine: Concepts of nanotoxicology. *J Intern Med*. 2010;267(1):89–105.

36. Porter DW, Hubbs AF, Mercer RR, Wu N, Wolfarth MG, Sriram K, et al. Mouse pulmonary dose- and time course-responses induced by exposure to multi-walled carbon nanotubes. *Toxicology*. 2010;269(2–3):136–47.

37. Mossman BT, Lippmann M, Hesterberg TW, Kelsey KT, Barchowsky A, Bonner JC. Pulmonary endpoints (lung carcinomas and asbestosis) following inhalation exposure to asbestos. *J Toxicol Environ Health B Crit Rev.* 2011;14(1–4):76–121.
38. Tavares AM, Louro H, Antunes S, Quarré S, Simar S, Temmerman P De, et al. Genotoxicity evaluation of nanosized titanium dioxide, synthetic amorphous silica and multi-walled carbon nanotubes in human lymphocytes. *Toxicol Vitro.* 2014;28:60–9.
39. Jensen KA. deliverable 4.1: Summary report on the primary physicochemical properties of manufactured nanomaterials used in NANOGENOTOX. Copenhagen; 2013.
40. Poulsen SS, Jacobsen NR, Labib S, Wu D, Husain M, Bøgelund JP, et al. Transcriptomic analysis reveals novel mechanistic insight into murine biological responses to multi-walled carbon nanotubes in lungs and cultured lung epithelial cells. *PLoS One.* 2013;8(11):1–25.
41. Jensen KA, Yahia K, Christiansen E, Jacobsen NR, Wallin H, Guiot C, et al. Towards a method for detecting the potential genotoxicity of nanomaterials. Final protocol for producing suitable manufactured nanomaterial exposure media. Copenhagen; 2011.
42. Timbrell V, Rendall R. Preparation of the UICC* Standard Reference Samples of Asbestos. *Powder Technol.* 1972;5:279–87.
43. Rendall R. The data sheets on the chemical and physical properties of the UICC standard reference samples. In: Shapiro H., editor. Pneumoconiosis proceedings of the international conference, 1969, Johannesburg. Oxford: Oxford University Press; 1970. p. 23–7.
44. Timbrell V. Characteristics of the International Union Against Cancer standard reference samples of asbestos. In: Shapiro H., editor. Pneumoconiosis proceedings of the international conference, 1969, Johannesburg. Oxford: Oxford University Press; 1970. p. 28–36.
45. Kohyama N, Shinohara Y, Suzuki Y. Mineral phases and some reexamined characteristics of the International Union against cancer standard asbestos samples. *Am J Ind Med.* 1996;30(5):515–28.
46. Kozomara A, Griffiths-jones S. miRBase: annotating high confidence microRNAs using deep sequencing data. *Nucleic Acids Res.* 2014;42:68–73.

47. Langmead B, Trapnell C, Pop M, Salzberg SL. Ultrafast and memory-efficient alignment of short DNA sequences to the human genome. *Genome Biol.* 2009;10(3):R25.
48. R Core Team. R: A language and environment for statistical computing. Vienna, Austria: R Foundation for Statistical Computing; 2017.
49. RStudio Team. RStudio: Integrated development for R [Internet]. Boston, MA: RStudio, Inc.; 2016. Available from: <http://www.rstudio.com/>
50. Love MI, Huber W, Anders S. Moderated estimation of fold change and dispersion for RNA-seq data with DESeq2. *Genome Biol.* 2014;15:550.
51. Russo F, Angelini C. RNASeqGUI: a GUI for analysing RNA-Seq data. *Bioinformatics.* 2014;30(17):2514–6.
52. Robinson MD, McCarthy DJ, Smyth GK. edgeR: a Bioconductor package for differential expression analysis of digital gene expression data. *Bioinformatics.* 2010;26(1):139–40.
53. Robinson MD, Oshlack A. A scaling normalization method for differential expression analysis of RNA-seq data. *Genome Biol.* 2010;11:R25.
54. Vlachos IS, Zagganas K, Paraskevopoulou MD, Georgakilas G, Karagkouni D, Vergoulis T, et al. DIANA-miRPath v3.0: deciphering microRNA function with experimental support. *Nucleic Acids Res.* 2015;43(May):W460–W466.
55. Kanehisa M, Sato Y, Furumichi M, Morishima K, Tanabe M. New approach for understanding genome variations in KEGG. *Nucleic Acids Res.* 2019;47(D1):D590–5.
56. Ashburner M, Ball CA, Blake JA, Botstein D, Butler H, et al. Gene Ontology: tool for the unification of biology. *Nat Genet.* 2000;25(1):25–9.
57. The Gene Ontology Consortium. The Gene Ontology Resource: 20 years and still GOing strong. *Nucleic Acids Res.* 2019;47(November 2018):330–8.
58. Vlachos IS, Paraskevopoulou MD, Karagkouni D, Georgakilas G, Vergoulis T, Kanellos I, et al. DIANA-TarBase v7.0: indexing more than half a million experimentally supported miRNA:mRNA interactions. *Nucleic Acids Res.* 2015;43:153–9.
59. Garcia DM, Baek D, Shin C, Bell GW, Grimson A, Bartel D. Weak seed-pairing stability and high target-site abundance decrease the proficiency of Isy-6 and other miRNAs. *Nat Struct Mol Biol.* 2012;18(10):1139–46.

60. Shannon P, Markiel A, Ozier O, Baliga NS, Wang JT, Ramage D, et al. Cytoscape : A software environment for integrated models of biomolecular interaction networks. *Genome Res.* 2003;13:2498–504.
61. Kutmon M, Evelo CT, Ehrhart F, Coort SL, Willighagen EL, Morris JH. CyTargetLinker app update : A flexible solution for network extension in Cytoscape. *F1000Research.* 2019;7:743–54.
62. Haunsberger SJ, Connolly NMC, Prehn JHM. Gene expression miRNAConverter : an R/bioconductor package for translating mature miRNA names to different miRBase versions. *Bioinformatics.* 2017;33(4):592–3.
63. Hsu S, Lin F, Wu W, Liang C, Huang W, Chan W, et al. miRTarBase : a database curates experimentally validated microRNA – target interactions. *Nucleic Acids Res.* 2011;39(November 2010):163–9.
64. Mihaylova MM, Shaw RJ. The AMP-activated protein kinase (AMPK) signaling pathway coordinates cell growth, autophagy, & metabolism. *Nat Cell Biol.* 2012;13(9):1016–23.
65. Zhang X, Tang N, Hadden TJ, Rishi AK. Akt , FoxO and regulation of apoptosis. *Biochim Biophys Acta* 2011;1813(11):1978–86.
66. Laplante M, David M. mTOR signaling at a glance. *J Cell Sci.* 2009;122:3589–94.
67. Saxton RA, Sabatini DM. mTOR Signaling in Growth, Metabolism, and Disease. *Cell* 2017;168(6):960–76.
68. Tian E, Hagen KG Ten. Recent insights into the biological roles of mucin-type O-glycosylation. *Glycoconj J.* 2009;26:325–34.
69. Kjellén L, Lindahl U. Proteoglycans: structures and interactions. *Annu Rev Biochem.* 1991;60(1):443–75.
70. Iozzo R V, Schaefer L. Proteoglycan form and function : A comprehensive nomenclature of proteoglycans. *Matrix Biol.* 2015;42:11–55.
71. Kim S, Turnbull J, Guimond S. Extracellular matrix and cell signalling : the dynamic cooperation of integrin, proteoglycan and growth factor receptor. *J Endocrinol.* 2011;209:139–51.
72. Meng Z, Moroishi T, Guan K. Mechanisms of Hippo pathway regulation. *Genes Dev.* 2016;1–17.

73. Ciechanover A, Orian A, Schwartz AL. Ubiquitin-mediated proteolysis : biological regulation via destruction. *BioEssays*. 2000;22:442–51.
74. Syed V. TGF- b signaling in cancer. *J Cell Biochem*. 2016;1287:1279–87.
75. Samanta D, Datta PK. Alterations in the Smad pathway in human cancers. *Front Biosci*. 2015;17:1281–93.
76. Wee P, Wang Z. Epidermal growth factor receptor cell proliferation. *Cancers (Basel)*. 2017;9(52):1–45.
77. Bray SJ. Notch signalling in context. *Nat Rev Mol Cell Biol*. 2016;17:722–5.
78. Seshacharyulu, Parthasarathy Ponnusamy MP, Haridas D, Jain M, Ganti A, Batra SK. Targeting the EGFR signaling pathway in cancer therapy. *Expert Opin Ther Targets*. 2012;16(1):15–31.
79. Yuan X, Wu H, Xu H, Xiong H, Chu Q, Yu S. Notch signaling : An emerging therapeutic target for cancer treatment. *Cancer Lett*. 2015;369(1):20–7.
80. Pancewicz-wojtkiewicz J. Epidermal growth factor receptor and notch signaling in non- small- cell lung cancer. *Cancer Med*. 2016;5(12):3572–8.
81. Shvedova AA, Yanamala N, Kisin ER, Khailulli TO, Birch ME, Fatkhutdinova LM. Integrated analysis of dysregulated ncRNA and mRNA expression profiles in humans exposed to carbon nanotubes. *PLoS One*. 2016;11(3):1–32.
82. Ma J, Mannoer K, Gao L, Tan A, Guarnera MA, Zhan M, et al. Characterization of microRNA transcriptome in lung cancer by next-generation deep sequencing. *Mol Oncol*. 2014;8(7):1208–19.
83. Sage C, Nagel R, David A, Schrier M, Mesman E, Mangiola A, et al. Regulation of the p27 tumor suppressor by miR-221 and miR-222 promotes cancer cell proliferation. *EMBO J*. 2007;26(15):3699–708.
84. Mao K, Zhang W, Liang X, Ma Y. microRNA-222 expression and its prognostic potential in non-small cell lung cancer. *Sci world J*. 2014;ID 908326.
85. Zhong C, Ding S, Xu Y, Huang H. microRNA-222 promotes human non-small cell lung cancer H460 growth by targeting p27. *Int J Clin Exp Med*. 2015;8(4):5534–40.
86. Ying X, Wu Q, Wu X, Zhu Q, Wang X, Jiang L. Epithelial ovarian cancer-secreted exosomal miR-222-3p induces polarization of tumor-associated macrophages. *Oncotarget*. 2016;7(28):43076–87.

87. Wei F, Ma C, Zhou T, Dong X, Luo Q, Geng L, et al. Exosomes derived from gemcitabine-resistant cells transfer malignant phenotypic traits via delivery of miRNA-222-3p. *Mol Cancer*. 2017;16:132–46.
88. Kolenda T, Przybyła W, Teresiak A, Mackiewicz A, Lamperska KM. The mystery of let-7d – a small RNA with great power. *Contemp Oncol (Pozn)*. 2014;18(5):293–301.
89. Pandit K V, Corcoran D, Yousef H, Yarlagadda M, Tzouvelekis A, Gibson KF, et al. Inhibition and role of let-7d in idiopathic pulmonary fibrosis. *Am J Respir Crit Care Med*. 2010;182:220–9.
90. Takamizawa J, Konishi H, Yanagisawa K, Tomida S, Osada H, Endoh H, et al. Advances in brief reduced expression of the let-7 microRNAs in human lung cancers in association with shortened postoperative survival. *Cancer Res*. 2004;64:3753–6.
91. Rodriguez-Fernandez, L., Valiente, R., Gonzalez J, Villegas JC, Fanarraga ML. Multiwalled carbon nanotubes display microtubule biomimetic properties *in vivo*, enhancing microtubule assembly and stabilization. *ACS Nano*. 2012;6(8):6614–25.
92. Siegrist KJ, Reynolds SH, Kashon ML, Lowry DT, Dong C, Hubbs AF, et al. Genotoxicity of multi-walled carbon nanotubes at occupationally relevant doses. *Part Fibre Toxicol* 2014;11:6–21.
93. Kostarelos K, Lacerda L, Pastorin G, Wu W, Wieckowski S, Luangsivilay J, et al. Cellular uptake of functionalized carbon nanotubes is independent of functional group and cell type. *Nat Nanotechnol*. 2007;2(2):108–13.
94. Lacerda L, Pastorin G, Gathercole D, Buddle J, Prato M, Bianco A, et al. Intracellular trafficking of carbon nanotubes by confocal laser scanning microscopy. *Adv Mater*. 2007;19(11):1480–4.
95. Giard DJ, Aaronson SA, Todaro GJ, Arnstein P, Kersey JH, Dosik H, et al. *In vitro* cultivation of human tumors: establishment of cell lines derived from a series of solid tumors. *J Natl Cancer Inst*. 1973;51(5):1417–1423.
96. Foster KA, Oster CG, Mayer MM, Avery ML, Audus KL. Characterization of the A549 cell line as a type ii pulmonary epithelial cell model for drug metabolism. *Exp Cell Res* 1998;243(2):359–66.

6. Final Conclusions

Nanotechnologies have a great potential for advancing society, as nanomaterials applications expand throughout hundreds of consumers products, ranging from industrial to biomedical purposes. However, assessing their safety should keep pace with their development, to the best use of their benefits without the costs of their potential human adverse effects. This responsible development and innovation of nanotechnologies includes research efforts to predict the possible occupational health hazards that can result from workers' exposure to these new materials, in order to prevent occupational diseases, particularly, on the long term. In this context, apart from the exposure evaluation, *in vitro* toxicological studies to assess their potential hazard are crucial to contribute for the risk assessment framework. Nowadays, although there are some data about MWCNT pulmonary effects, the mechanisms underlying those effects are still under debate. As to CNF, this data is still missing due to its more recent applications.

In this study, the toxicity of two nanofibres, MWCNT-7 (Mitsui-7) and a CNF produced by TEMPO-mediated oxidation of an industrial bleached *Eucalyptus globulus* kraft pulp, was characterized, and insights on the Mitsui-7 mechanism of action were obtained. For this purpose, several *in vitro* complementary approaches were used, encompassing a wide spectrum of methodologies from well-established cytotoxicity and genotoxicity assays to a forefront epigenotoxic approach using high throughput sequencing technology. Moreover, a co-culture of A549 epithelial alveolar cells with THP-1 macrophages was implemented, in an attempt to better resemble the *in vivo* situation, since macrophages have an important role in the alveoli defence against biopersistent particles. Crocidolite was used as a positive control material, due to its similarity with nanofibres, particularly, its shape and high biopersistence, and the well-known professional diseases induced in exposed workers, namely, asbestosis, mesothelioma and lung cancer.

Overall, the present findings demonstrate that the tested CNF stimulate alveolar cell proliferation at low concentrations, whereas higher concentrations are moderately toxic. Although no relevant DNA damage was detected in these epithelial cells by the comet assay, the formation of micronuclei was observed at low CNF concentrations, which are the ones more realistic and relevant for human exposure in occupational settings. Moreover, no immunotoxic effects were detected.

MWCNT-7 (Mitsui-7) is cytotoxic and genotoxic to alveolar cells. Moreover, the comparison of results obtained for MWCNT-7 and crocidolite toxicities using a conventional A549 cell culture and a co-culture with macrophages evidenced some dissimilarities in toxicity between both *in vitro* models that were further explored. An

important one is that, after exposure to each of the materials, A549 cells in co-culture exhibit a higher survival ability than in monoculture. This may happen because THP-1 macrophages induce epithelial to mesenchymal transition in A549 cells, with mesenchymal cells being more resistant to cell death. Such transformation may result in the enrichment of DNA damaged cells, explaining the induction of micronuclei by both materials observed exclusively in co-cultured alveolar cells. Remarkably, a single MWCNT-7 concentration induced a high frequency of nucleoplasmic bridges in monocultured A549 cells, probably through a direct interference of the rigid nanofibres with chromatin or cytoskeletal filaments during mitosis.

In addition, a unique set of DE miRNAs was identified in response to A549 cells exposure to a MWCNT-7 dose that has been considered occupationally relevant. These DE miRNAs indicate some of the molecular mechanisms of action of this nanomaterial through the analysis of the cellular pathways that were enriched in genes regulated by these miRNA. Furthermore, their comparison with crocidolite DE miRNAs shows that each material can affect different cellular functional pathways, e.g., the mTOR or the ubiquitin-mediated proteolysis pathways, but they also share high similarity in respect to the deregulation of cell survival, differentiation and proliferation, namely, through the AMPK, FoxO, TGF- β and Hippo pathways. Additionally, the potential carcinogenic effects of MWCNT-7 were highlighted not only by its similarity with crocidolite, but also by the creation of a well-linked network of genes related to cancer that are up- or down-regulated by the DE miRNAs in alveolar cells.

Overall, this research contributed to the risk assessment of nanofibres to which man is, or will likely be, exposed in environmental, including occupational, settings. In addition, a miRNA signature of the MWCNT-7 exposure was identified in alveolar cells, which may be further explored as a future molecular biomarker for monitoring occupational exposure to this nanofibre. Furthermore, some molecular and cellular mechanism underlying the toxicity of MWCNT-7 were investigated in comparison to those of crocidolite, pointing to a similar outcome, i.e., lung disease. Ultimately, these findings are expected to contribute to healthy and safer workplaces, by excluding or reducing the handling of hazardous nanomaterials in the workplace and supporting the implementation of regulation to protect workers health.

7. Future Perspectives

Nowadays, there are still several scientific knowledge gaps concerning the health protection of workers that may be exposed to nanofibres and subjected to its resulting potential health adverse effects. An increased understanding of the hazard of these nanomaterials, such as MWCNT-7 and CNF, is needed to develop effective risk management practices. Although the potential toxicity of these two nanofibres has been demonstrated in this work, and a miRNA profile suggested as a possible biomarker of occupational exposure, several aspects should be further developed in order to translate research into practice and fill those gaps.

The DE miRNA here identified should be confirmed using a different methodology, e.g., reverse transcription – quantitative polymerase chain reaction (RT-qPCR). Moreover, it would be important to experimentally test if the cellular functional pathways, identified by bioinformatics tools as being enriched in genes regulated by these DE miRNAs, are effectively being activated or repressed in cells exposed to MWCNT-7 or crocidolite. For that purpose, additional studies of gene expression should be performed. On the other hand, key events of these materials mode of action were identified and can be further explored from a mechanistic point of view.

Furthermore, following in vitro studies, the miRNA expression should be investigated in vivo, in order to identify the ones that are concomitantly differentially expressed as cell-free circulating miRNAs. If some or all of these miRNAs are simultaneously altered in blood circulation, then they could effectively be useful in the biomonitoring of human respiratory exposure to MWCNT-7, crocidolite or, possibly, other nanofibres.

Noteworthy, all technical procedures for miRNA analysis are now implemented in the Department of Human Genetics of the National Institute of Health Doutor Ricardo Jorge, allowing their application to a multitude of new epigenomic and toxicological research. Several different nanomaterials, as well as other chemicals, can be tested through the exposure of target cells to the agent under study, miRNA extraction of these cells, next-generation sequencing and bioinformatics analysis of the DE miRNAs and functional pathway enrichment analysis. With this technological improvement, it is expected to deepen the study of the toxicological adverse effects of nanomaterials and contribute to the implementation of preventive strategies of human exposure to their hazards.

Ultimately, the data here presented can be one more contribution to develop recommendations for the manufacturing and handling of these nanofibres from a health and safety perspective, and to integrate more knowledge into regulatory frameworks of Occupational Health and Safety.